ISSN 2307-8960 (online)

World Journal of *Clinical Cases*

World J Clin Cases 2024 February 16; 12(5): 872-1038

Published by Baishideng Publishing Group Inc

World Journal of Clinical Cases

Contents

Thrice Monthly Volume 12 Number 5 February 16, 2024

EDITORIAL

ORIGINAL ARTICLE

Clinical and Translational Research

Retrospective Cohort Study

Retrospective Study

Observational Study

CASE REPORT

LETTER TO THE EDITOR

World Journal of Clinical Cases

Thrice Monthly Volume 12 Number 5 February 16, 2024

Contents

ABOUT COVER

AIMS AND SCOPE

The primary aim of *World Journal of Clinical Cases* (*WJCC*, *World J Clin Cases*) is to provide scholars and readers from various fields of clinical medicine with a platform to publish high-quality clinical research articles and communicate their research findings online.

WJCC mainly publishes articles reporting research results and findings obtained in the field of clinical medicine and covering a wide range of topics, including case control studies, retrospective cohort studies, retrospective studies, clinical trials studies, observational studies, prospective studies, randomized controlled trials, randomized clinical trials, systematic reviews, meta-analysis, and case reports.

INDEXING/ABSTRACTING

The *WJCC* is now abstracted and indexed in Science Citation Index Expanded (SCIE, also known as SciSearch®), Journal Citation Reports/Science Edition, Current Contents®/Clinical Medicine, PubMed, PubMed Central, Reference Citation Analysis, China Science and Technology Journal Database, and Superstar Journals Database. The 2023 Edition of Journal Citation Reports® cites the 2022 impact factor (IF) for *WJCC* as 1.1; IF without journal self cites: 1.1; 5-year IF: 1.3; Journal Citation Indicator: 0.26; Ranking: 133 among 167 journals in medicine, general and internal; and Quartile category: Q4.

RESPONSIBLE EDITORS FOR THIS ISSUE

NAME OF JOURNAL
World Journal of Clinical Cases

ISSN
ISSN 2307-8960 (online)

LAUNCH DATE
April 16, 2013

FREQUENCY
Thrice Monthly

PUBLICATION DATE
February 16, 2024

World Journal of Clinical Cases

Submit a Manuscript: https://www.f6publishing.com

World J Clin Cases 2024 February 16; 12(5): 872-874

DOI: 10.12998/wjcc.v12.i5.872

ISSN 2307-8960 (online)

EDITORIAL

Is it possible to anchor a tooth with photobiomodulation?

Angela Dominguez

Specialty type: Dentistry, oral surgery and medicine

Provenance and peer review: Invited article; Externally peer reviewed.

Peer-review model: Single blind

Peer-review report's scientific quality classification

Grade A (Excellent): 0
Grade B (Very good): B
Grade C (Good): 0
Grade D (Fair): 0
Grade E (Poor): 0

P-Reviewer: Sekhar P, India

Received: November 20, 2023
Peer-review started: November 20, 2023
First decision: December 27, 2023
Revised: January 4, 2024
Accepted: January 22, 2024
Article in press: January 22, 2024
Published online: February 16, 2024

Angela Dominguez, Department of Orthodontics, Faculty of Dentistry, Benemerita Universidad Autónoma de Puebla, Zaragoza de Puebla Calle 4 Sur 104, Puebla, Mexico

Corresponding author: Angela Dominguez, DDS, Researcher, Department of Orthodontics, Faculty of Dentistry, Benemerita Universidad Autónoma de Puebla, Calle 4 Sur 104, Edificio Carolino, Col. Centro, C.P. 72000, Puebla, Mexico. angela.dominguezc@gmail.com

Abstract

During orthodontic treatment, we can achieve differential movements by using photobiomodulation (PBM) as an adjuvant before applying force. We can expect a greater bone density that initially resists movement while applying PBM to the other teeth to achieve an accelerating effect. The proposed protocol is to use an 810 nm laser at 0.1W power, applying between 4 and 6J per tooth for 22 s on the vestibular and lingual root surfaces, following the axial axis of the tooth. The energy density depends on the tip selected in the instrument. Normal bone remodeling cannot be avoided by applying high doses of PBM. PBM should be applied before orthodontic force to reduce tooth movement. In addition, PBM can be used during force application to teeth that require acceleration to achieve differential movement in orthodontic treatments. The protocol is the same in both scenarios.

Key Words: Photobiomodulation; Orthodontic movement; Diode laser; PBM; Anchorage in orthodontics

Core Tip: During orthodontic treatment, we can obtain differential movements by using photobiomodulation as an adjuvant before applying force to the teeth we want to use for anchoring, and photobiomodulation-assisted orthodontics to accelerate the movements when force is applied.

Citation: Dominguez A. Is it possible to anchor a tooth with photobiomodulation? *World J Clin Cases* 2024; 12(5): 872-874
URL: https://www.wjgnet.com/2307-8960/full/v12/i5/872.htm
DOI: https://dx.doi.org/10.12998/wjcc.v12.i5.872

INTRODUCTION

Anchorage in orthodontics, refers to the ability to prevent movement of one or more teeth while another tooth or group of teeth is being moved. To be successful in space closure orthodontic treatment, it's a must to plan the anchorage system protocol. According to this protocol, teeth can be classified as active or reactive/passive units based on their distinct functions during space closure. The active component typically experiences more movement, while the other component provides resistance (anchorage)[1]. To serve as an anchorage unit, PBM can be used as a preparatory therapy in the affected tooth(s).

Photobiomodulation (PBM) using specific wavelengths and parameters is effective for accelerating dental movement[2-5]. However, the application confused the achievement of anchorage or retention of teeth with inhibiting movement through high dosage. This misconception originates from the relationship illustrated in the Arndt-Schulz curve.

The Arndt-Schulz curve is often used to describe the biphasic dose response of PBM. Research reports a biphasic dose response, indicating that lower levels of laser light result in better tissue stimulation and repair than higher levels of laser light[6].

Bone undergoes constant turnover throughout life *via* bone remodeling, which maintains the structural integrity of the skeletal system and contributes metabolically to the body's calcium and phosphorus balance. Remodeling involves resorbing old or damaged bone and depositing new bone material. Two main cell types, osteoclasts and osteoblasts, along with osteocytes, are involved in bone remodeling[7].

An increased number of osteoblasts is necessary to improve bone density. PBM results in a statistically significant increase in osteoblasts as early as 5 d[8].

PBM has been used for retention phases[9], bone regeneration after rapid palatal expansion[10], and to improve implant stability[11].

PBM applied to bone results in increased osteoblasts, newly formed matrix, collagen synthesis, and microvascular reestablishment[12], suggesting positive effects on implant treatment.

It is possible to use PBM during the retention stage, increasing bone density, and decreasing the possibility that the tooth will move because no force is applied.

In this case, it should be applied every week for a month and repeat an application every 3 months. The parameters are the same, the difference is that when no force is applied, no pre-osteoclasts are recruited and the effect of acceleration of movement is not generated.

Considering all the above principles, it can be concluded that PBM cannot be used to achieve absolute anchorage of a tooth[1]; bone remodeling is a dynamic process involving both apposition and resorption. When a laser is applied, it increases osteoblast proliferation without being cytotoxic to preosteoclasts[13]. During orthodontic treatment, we can achieve differential movements by using PBM as an adjuvant before applying force. We can expect greater bone density, which initially resists movement, while PBM is applied to the other teeth to achieve an acceleration effect.

High doses aimed at inhibiting osteoblast proliferation should never be administered during treatment, as this would not inhibit movement, but rather reduce bone density. The claim that high doses of PBM inhibit tooth movement ignores the biology of permanent bone remodeling.

If the treatment plan is well designed and the anchor teeth are identified, PBM should be applied weekly for one month before braces. This protocol should be followed for teeth with inadequate bone support during periodontal therapy before orthodontic treatment to increase bone density and minimize the response to force on the targeted teeth. During treatment, PBM is applied only to the teeth we want to accelerate, not to the teeth we want to move less. Technical abbreviations will be explained the first time they are used. This creates a differential movement and helps reduce the reaction that can occur when relying on teeth or segments with a larger root area to move other teeth.

PROTOCOL

The protocol for preparing a tooth and improving periapical bone density before orthodontic treatment is the same as that used to accelerate tooth movement. The difference between the two scenarios is the stimulus provided by the application of force, which recruits pre-osteoclasts and leads to an increase in osteoclastogenesis[13]. When applied prior to movement (without force), osteoblast proliferation increases, improving the bone density of the anchoring unit. It is not necessary to completely anchor the tooth or group of teeth, as there is always permanent bone remodeling that allows homeostasis.

The proposed protocol involves the use of an 810 nm laser at 0.1W power, delivering between 4 and 6J per tooth for 22 s to the vestibular and lingual root surfaces following the axial axis of the tooth[14]. The energy density depends on the tip selected in the instrument.

CONCLUSION

Normal bone remodeling cannot be avoided by using high doses of PBM. PBM should be applied prior to orthodontic force to reduce tooth movement. PBM can also be used during the application of force to teeth that require acceleration to achieve differential movement in orthodontic treatment. The protocol is the same in both scenarios.

ACKNOWLEDGEMENTS

To my long-time co-author, my husband Sergio A. Velasquez, for the English revision of this manuscript.

FOOTNOTES

Author contributions: Dominguez A contributed to writing, editing, and reviewing the manuscript.

Conflict-of-interest statement: Angela Dominguez declare that I have no conflicts of interest.

Country/Territory of origin: Colombia

ORCID number: Angela Dominguez 0000-0002-6434-1969.

S-Editor: Liu JH
L-Editor: A
P-Editor: Yu HG

REFERENCES

1 **Ribeiro GL**, Jacob HB. Understanding the basis of space closure in Orthodontics for a more efficient orthodontic treatment. *Dental Press J Orthod* 2016; **21**: 115-125 [PMID: 27275623 DOI: 10.1590/2177-6709.21.2.115-125.sar]
2 **Cruz DR**, Kohara EK, Ribeiro MS, Wetter NU. Effects of low-intensity laser therapy on the orthodontic movement velocity of human teeth: a preliminary study. *Lasers Surg Med* 2004; **35**: 117-120 [PMID: 15334614 DOI: 10.1002/lsm.20076]
3 **Sousa MV**, Pinzan A, Consolaro A, Henriques JF, de Freitas MR. Systematic literature review: influence of low-level laser on orthodontic movement and pain control in humans. *Photomed Laser Surg* 2014; **32**: 592-599 [PMID: 25335088 DOI: 10.1089/pho.2014.3789]
4 **Domínguez Camacho A**, Montoya Guzmán D, Velásquez Cujar SA. Effective Wavelength Range in Photobiomodulation for Tooth Movement Acceleration in Orthodontics: A Systematic Review. *Photobiomodul Photomed Laser Surg* 2020; **38**: 581-590 [PMID: 32609566 DOI: 10.1089/photob.2020.4814]
5 **Siddiqui JA**, Partridge NC. Physiological Bone Remodeling: Systemic Regulation and Growth Factor Involvement. *Physiology (Bethesda)* 2016; **31**: 233-245 [PMID: 27053737 DOI: 10.1152/physiol.00061.2014]
6 **Huang YY**, Chen AC, Carroll JD, Hamblin MR. Biphasic dose response in low level light therapy. *Dose Response* 2009; **7**: 358-383 [PMID: 20011653 DOI: 10.2203/dose-response.09-027.Hamblin]
7 **Grajales M**, Ríos-Osorio N, Jimenez-Peña O, Mendez-Sanchez J, Sanchez-Fajardo K, García-Perdomo HA. Effectiveness of photobiomodulation with low-level lasers on the acceleration of orthodontic tooth movement: a systematic review and meta-analysis of split-mouth randomized clinical trials. *Lasers Med Sci* 2023; **38**: 200 [PMID: 37667064 DOI: 10.1007/s10103-023-03870-7]
8 **Dominguez A**, Bayona G, Casas A. In vitro response of Human Pre-Osteoclasts to low intensity Laser irradiation. *Journal of Research in Biology* 2012; **2**: 733-741 [DOI: 10.1063/1.4757823]
9 **Mirzaei R**, Arash V, Rahmati-Kamel M, Abesi F, Bijani A. Evaluation of the Effects of Low-Level Laser Therapy on the Rate of Relapse of Mandibular Incisors after Fixed Orthodontic Treatment: A Randomized Controlled Trial. *JBUMS* 2023; **25**: 152-159 [DOI: 10.5114/jos.2021.108838]
10 **Cepera F**, Torres FC, Scanavini MA, Paranhos LR, Capelozza Filho L, Cardoso MA, Siqueira DC, Siqueira DF. Effect of a low-level laser on bone regeneration after rapid maxillary expansion. *Am J Orthod Dentofacial Orthop* 2012; **141**: 444-450 [PMID: 22464526 DOI: 10.1016/j.ajodo.2011.10.023]
11 **Costa ACF**, Maia TAC, de Barros Silva PG, Abreu LG, Gondim DV, Santos PCF. Effects of low-level laser therapy on the orthodontic mini-implants stability: a systematic review and meta-analysis. *Prog Orthod* 2021; **22**: 6 [PMID: 33586080 DOI: 10.1186/s40510-021-00350-y]
12 **Amaroli A**, Colombo E, Zekiy A, Aicardi S, Benedicenti S, De Angelis N. Interaction between Laser Light and Osteoblasts: Photobiomodulation as a Trend in the Management of Socket Bone Preservation-A Review. *Biology (Basel)* 2020; **9** [PMID: 33238412 DOI: 10.3390/biology9110409]
13 **Dominguez A**, León P, Aristizabal JF. Effect of Low Level Laser Therapy on Local Bone Resorption During Orthodontic Treatment: A Randomized Controlled Trial. *Int J Odontostomat* 2016; **10**: 483-490 [DOI: 10.4067/S0718-381X2016000300016]
14 **Domínguez A**, Velásquez S. Acceleration Effect of Orthodontic Movement by Application of Low-intensity Laser. *J Oral Laser Appl* 2010; **2**: 99-105

World Journal of Clinical Cases

Submit a Manuscript: https://www.f6publishing.com

World J Clin Cases 2024 February 16; 12(5): 875-879

DOI: 10.12998/wjcc.v12.i5.875

ISSN 2307-8960 (online)

EDITORIAL

Strengthening pharmacotherapy research for COVID-19-induced pulmonary fibrosis

Yan-Miao Liu, Jing Zhang, Jing-Jing Wu, Wei-Wei Guo, Fu-Shan Tang

Specialty type: Pharmacology and pharmacy

Provenance and peer review: Invited article; Externally peer reviewed.

Peer-review model: Single blind

Peer-review report's scientific quality classification

Grade A (Excellent): 0
Grade B (Very good): 0
Grade C (Good): C
Grade D (Fair): D
Grade E (Poor): 0

P-Reviewer: Casu C, Italy; Löffler-Stastka H, Austria

Received: December 7, 2023
Peer-review started: December 7, 2023
First decision: December 17, 2023
Revised: December 26, 2023
Accepted: January 15, 2024
Article in press: January 15, 2024
Published online: February 16, 2024

Yan-Miao Liu, The First Clinical Institute, Zunyi Medical University, Zunyi 563006, Guizhou Province, China

Yan-Miao Liu, Jing-Jing Wu, Wei-Wei Guo, Fu-Shan Tang, Key Laboratory of Clinical Pharmacy in Zunyi City, Zunyi Medical University, Zunyi 563006, Guizhou Province, China

Jing Zhang, Department of Respiratory Medicine, Central Hospital in Jinchang City, Jinchang 737102, Gansu Province, China

Jing-Jing Wu, Wei-Wei Guo, Fu-Shan Tang, Department of Clinical Pharmacy, Key Laboratory of Basic Pharmacology of Guizhou Province and School of Pharmacy, Zunyi Medical University, Zunyi 563006, Guizhou Province, China

Jing-Jing Wu, Wei-Wei Guo, Fu-Shan Tang, Key Laboratory of Basic Pharmacology of Ministry of Education and Joint International Research Laboratory of Ethnomedicine of Ministry of Education, Zunyi Medical University, Zunyi 563006, Guizhou Province, China

Corresponding author: Fu-Shan Tang, PhD, Professor, Department of Clinical Pharmacy, Key Laboratory of Basic Pharmacology of Guizhou Province and School of Pharmacy, Zunyi Medical University, No. 6 Xuefu West Road, Xinpu New District, Zunyi 563006, Guizhou Province, China. fstang@vip.163.com

Abstract

The global spread of severe acute respiratory syndrome coronavirus 2 has resulted in a significant number of individuals developing pulmonary fibrosis (PF), an irreversible lung injury. This condition can manifest within a short interval following the onset of pneumonia symptoms, sometimes even within a few days. While lung transplantation is a potentially lifesaving procedure, its limited availability, high costs, intricate surgeries, and risk of immunological rejection present significant drawbacks. The optimal timing of medication administration for coronavirus disease 2019 (COVID-19)-induced PF remains controversial. Despite this, it is crucial to explore pharmacotherapy interventions, involving early and preventative treatment as well as pharmacotherapy options for advanced-stage PF. Additionally, studies have demonstrated disparities in anti-fibrotic treatment based on race and gender factors. Genetic mutations may also impact therapeutic efficacy. Enhancing research efforts on pharmacotherapy interventions, while considering relevant pharmacological factors and optimizing the timing and dosage of medication administration, will lead to enhanced, personalized, and fair treatment for individuals impacted by COVID-19-related

PF. These measures are crucial in lessening the burden of the disease on healthcare systems and improving patients' quality of life.

Key Words: COVID-19; Pulmonary fibrosis; Pharmacotherapy intervention; Medication administration; Timing; Dosage

Core Tip: Pulmonary fibrosis (PF) induced by coronavirus disease 2019 (COVID-19) represents a significant and serious complication of the disease. When PF advances to a critical stage, lung transplantation becomes the sole life-saving option. Our call is for an intensified focus on researching pharmacotherapy interventions for COVID-19-induced PF, aimed at identifying potential medication options.

Citation: Liu YM, Zhang J, Wu JJ, Guo WW, Tang FS. Strengthening pharmacotherapy research for COVID-19-induced pulmonary fibrosis. *World J Clin Cases* 2024; 12(5): 875-879
URL: https://www.wjgnet.com/2307-8960/full/v12/i5/875.htm
DOI: https://dx.doi.org/10.12998/wjcc.v12.i5.875

INTRODUCTION

Coronavirus disease 2019 (COVID-19) is a respiratory illness caused by the severe acute respiratory syndrome coronavirus 2. It has been observed that COVID-19 patients may develop pulmonary fibrosis (PF), a serious complication that affects their quality of life even after recovery[1]. PF is characterized by damage to the lung tissue, excessive scarring, and impaired lung function[2]. This often leads to respiratory failure and can be fatal[3]. It is important to explore pharmacotherapy interventions that can prevent or reduce fibrosis damage in COVID-19 patients[4].

PATHOGENESIS OF COVID-19-INDUCED PF

The pathogenesis of COVID-19-induced PF is complex and involves various molecular mechanisms. Transforming growth factor-β and PI3K/AKT signaling pathways play important roles in the development of PF[5]. The activation of these pathways leads to fibroblast proliferation, migration, and conversion into myofibroblasts, resulting in excessive scarring[6]. Cytokine storm, and the resulting overactive inflammation, are also tightly interconnected with the activation, proliferation, and migration of fibroblasts[7]. Additionally, the EGFR pathway has been implicated in COVID-19-related PF[8].

PHARMACOTHERAPY INTERVENTIONS

Medication commonly used in clinical treatment

Pirfenidone and nintedanib are currently approved for the treatment of idiopathic PF and have shown efficacy in COVID-19-induced PF[4,9-11]. Pirfenidone inhibits fibroblast proliferation and extracellular matrix deposition, while nintedanib slows down the development of fibrosis[6,10]. Both medications have similar efficacy in reducing lung function decline [12,13]. However, pirfenidone may cause liver injury, and nintedanib is not recommended for patients with moderate or severe liver injury[14,15].

Medications less commonly used in clinical treatment

N-acetylcysteine (NAC) and mesenchymal stem cell (MSC) therapy have shown potential as adjuvant treatments for COVID-19-induced PF. NAC replenishes glutathione levels and MSCs have anti-inflammatory and regenerative properties[16,17]. DPP-4 inhibitors and statins, commonly used for diabetes and cholesterol management, respectively, may also prevent fibrosis[7,18]. Anakinra, Xuanfei Baidu Decoction (a traditional Chinese medicine), nimotuzumab, and vitamin D supplementation have shown promising results in treating COVID-19-induced PF[19-22].

Potential medication therapies with limited evidence

Several medications, such as natural polysaccharides, baicalin, the endocannabinoid system, dihydroartemisinin and (-)-Epigallocatechin-3-gallate, have shown anti-fibrotic effects in preclinical trials but lack clinical trial date[23-27]. Tocilizumab and baricitinib combination therapy has shown effectiveness but has controversial safety concerns[21,28]. PI3K inhibitors hold promise but require further exploration for safe use[29].

Table 1 The recommended dosages in literatures for some medications in use

Medications	Recommended dosages
Pirfenidone	2400 mg/d for 12-24 wk[6]
Nintedanib	150 mg or 100 mg (for patients with mild hepatic impairment) twice daily[10]
N-acetyl-cysteine	Oral 600 mg every 8 h, oral 600 mg twice daily for 14 d, or intravenous 40 mg/(kg × d) for 3 d[16]
Anakinra	A total dose of 600 mg (a loading dose of 200 mg twice daily, followed by 100 mg once daily for 2 d)[19]
Nimotuzumab	Intravenous administration: 2-3 times with an interval of 72 h, including a loading dose of 200 mg, followed by 100 mg[21]
Vitamin D	COVID-19 patients with 25-hydrodroxyvitamin D serum levels under 20 ng/mL: 6000-7000 oral IU/d for the first 6-8 wk for correction of deficiency and 2000 to 3000 oral IU/d for maintenance[22]

COVID-19: Coronavirus disease 2019.

PHARMACOLOGICAL CONSIDERATIONS ON ANTI-FIBROSIS TREATMENT FOR COVID-19-INDUCED PF

When testing the effects of pharmacotherapy for COVID-19-induced PF, it is crucial to consider pharmacological factors. Studies have demonstrated that nintedanib exhibits comparable therapeutic effects across various ethnic groups, including Asian and White patients[15,30]. Additionally, the literature finding also confirms that the gender has no noticeable effect on nintedanib pharmacokinetics[15]. In terms of the utilization of anti-fibrotic treatment, Black patients are 40% less likely than their White counterparts to receive such treatment, and similarly, female patients are 59% less likely than their male counterparts[31].

These findings offer valuable insights into potential disparities in the administration of anti-fibrotic treatment, highlighting the importance and potential significance of race and gender factors. Further research in this area holds great promise for exploring and understanding these disparities in greater detail, which can contribute to the development of more personalized and equitable treatment approaches. Additionally, investigating the influence of race and gender on the effectiveness and safety profiles of anti-fibrotic therapies can provide a deeper understanding of their impact on different patient populations, ultimately leading to improved healthcare outcomes for all individuals.

In individuals with telomerase reverse transcriptase (TERT) mutations, there may be an increased risk of developing COVID-19-induced PF[32]. It has also been observed that TERT/TERC mutations are resistant to pirfenidone therapy [33]. Additionally, other genetic variants such as MUC5B, DPP9, and ATP11A have been associated with COVID-19-induced PF[34]. Exploring the role of genetics in this condition may pave the way for the development of novel agents for targeted therapy and personalized treatment.

TIMING AND DOSAGES OF MEDICATIONS PROPOSED FOR COVID-19-INDUCED PF

The optimal timing of medication administration for COVID-19-induced PF remains a topic of ongoing debate, with advocates for early and preventative approaches as well as those in favor of using anti-fibrotic drugs only when clear signs of PF with progressive exacerbations are present[7,10,35]. Each perspective is grounded in its own reasoning. Supporters of early intervention argue that COVID-19-induced PF might constitute an irreversible process, while those who are cautious about early treatment weigh the cost of anti-fibrosis treatment against the potential inevitability of COVID-19-induced PF. The nuances of these contrasting views underscore the complexity surrounding the optimal timing for administering anti-fibrotic drugs in the context of COVID-19-related complications. Further research on the timing of anti-fibrotic medication for PF caused by COVID-19 from both basic and clinical perspectives is necessary.

In order to achieve successful pharmacotherapy, proper dosages of promising drugs for anti-fibrosis treatment should be investigated. Table 1 summarizes the recommended dosages for some medications currently in use. Additionally, the development of novel drug delivery systems, such as inhalable systems including lipid-based nanocarriers, nanovesicles, polymeric nanocarriers, protein nanocarriers, nanosuspensions, nanoparticles, gold nanoparticles, and hydrogel, could prove to be a promising area for the treatment of PF caused by COVID-19[36].

CONCLUSION

COVID-19-induced PF has emerged as a challenging problem with no known cure. Pharmacotherapy interventions aimed at delaying disease progression and improving quality of life are crucial. Pirfenidone and nintedanib are currently the mainstay of treatment, while other medications serve as potential adjuvant therapies. Rational use of DPP-4 inhibitors, statins, NAC, anakinra, vitamin D, and nimotuzumab may prevent or control the progression of COVID-19-induced PF. Traditional Chinese medicine and other experimental medications require further research and clinical trials to evaluate their efficacy and safety. Additional research is necessary to strengthen pharmacotherapy interventions aimed

at managing COVID-19-induced PF, while taking into account relevant pharmacological factors and optimizing the timing and dosage of medication administration. Such efforts will lead to the development of enhanced, equitable, and personalized approaches to managing this condition.

FOOTNOTES

Author contributions: Liu YM contributed to the manuscript outline and composed the paper; Wu JJ and Guo WW were responsible for sourcing and organizing relevant literature, as well as discussing the importance of the pharmacotherapy research; Zhang J and Tang FS originated the concept for this manuscript; Tang FS provided supervision, reviewed the paper, and finalized the manuscript; All authors have read and approved the final manuscript.

Supported by the Project of Special Funds for Science and Technology Cooperation in Guizhou Provinces and Zunyi City, No. Shengshikehe(2015)53.

Conflict-of-interest statement: All the authors have nothing to disclose.

Country/Territory of origin: China

ORCID number: Yan-Miao Liu 0009-0004-4553-8127; Jing Zhang 0009-0003-2899-8474; Jing-Jing Wu 0009-0008-1713-7624; Wei-Wei Guo 0009-0001-0687-0934; Fu-Shan Tang 0000-0001-8779-1041.

S-Editor: Zhang H
L-Editor: A
P-Editor: Yu HG

REFERENCES

1 **Wang J**, Wang BJ, Yang JC, Wang MY, Chen C, Luo GX, He WF. [Research advances in the mechanism of pulmonary fibrosis induced by coronavirus disease 2019 and the corresponding therapeutic measures]. *Zhonghua Shao Shang Za Zhi* 2020; **36**: 691-697 [PMID: 32174095 DOI: 10.3760/cma.j.cn501120-20200307-00132]

2 **Zhan X**, Liu B, Tong ZH. [Postinflammatroy pulmonary fibrosis of COVID-19: the current status and perspective]. *Zhonghua Jie He He Hu Xi Za Zhi* 2020; **43**: 728-732 [PMID: 32894907 DOI: 10.3760/cma.j.cn112147-20200317-00359]

3 **George PM**, Patterson CM, Reed AK, Thillai M. Lung transplantation for idiopathic pulmonary fibrosis. *Lancet Respir Med* 2019; **7**: 271-282 [PMID: 30738856 DOI: 10.1016/S2213-2600(18)30502-2]

4 **Ferrara F**, Granata G, Pelliccia C, La Porta R, Vitiello A. The added value of pirfenidone to fight inflammation and fibrotic state induced by SARS-CoV-2: Anti-inflammatory and anti-fibrotic therapy could solve the lung complications of the infection? *Eur J Clin Pharmacol* 2020; **76**: 1615-1618 [PMID: 32594204 DOI: 10.1007/s00228-020-02947-4]

5 **Wu N**, Li Z, Wang J, Geng L, Yue Y, Deng Z, Wang Q, Zhang Q. Low molecular weight fucoidan attenuating pulmonary fibrosis by relieving inflammatory reaction and progression of epithelial-mesenchymal transition. *Carbohydr Polym* 2021; **273**: 118567 [PMID: 34560978 DOI: 10.1016/j.carbpol.2021.118567]

6 **Al-Kuraishy HM**, Batiha GE, Faidah H, Al-Gareeb AI, Saad HM, Simal-Gandara J. Pirfenidone and post-Covid-19 pulmonary fibrosis: invoked again for realistic goals. *Inflammopharmacology* 2022; **30**: 2017-2026 [PMID: 36044102 DOI: 10.1007/s10787-022-01027-6]

7 **Smelcerovic A**, Kocic G, Gajic M, Tomovic K, Djordjevic V, Stankovic-Djordjevic D, Anderluh M. DPP-4 Inhibitors in the Prevention/Treatment of Pulmonary Fibrosis, Heart and Kidney Injury Caused by COVID-19-A Therapeutic Approach of Choice in Type 2 Diabetic Patients? *Front Pharmacol* 2020; **11**: 1185 [PMID: 32848788 DOI: 10.3389/fphar.2020.01185]

8 **Abdo Cuza AA**, Ávila JP, Martínez RM, González JJ, Aspuro GP, Gutiérrez Martínez JA, Suzarte MR, Hernández DS, Añé-Kouri AL, Ramos TC. Nimotuzumab for COVID-19: case series. *Immunotherapy* 2021 [PMID: 34806405 DOI: 10.2217/imt-2021-0269]

9 **Medical Panel of Severe/Critical COVID-19**, The Third Affiliated Hospital of Sun Yat-sen University. Management of severe/critical novel COVID-19: recommendations of the third affiliated hospital of Sun Yat-sen University. *Zhongshan Daxue Xuebao* 2020; **41**: 345351

10 **Hashemian SM**, Farhadi T, Varahram M, Velayati AA. Nintedanib: a review of the properties, function, and usefulness to minimize COVID-19-induced lung injury. *Expert Rev Anti Infect Ther* 2023; **21**: 7-14 [PMID: 36440472 DOI: 10.1080/14787210.2023.2153116]

11 **Choudhary R**, Kumar A, Ali O, Pervez A. Effectiveness and Safety of Pirfenidone and Nintedanib for Pulmonary Fibrosis in COVID-19-Induced Severe Pneumonia: An Interventional Study. *Cureus* 2022; **14**: e29435 [PMID: 36299940 DOI: 10.7759/cureus.29435]

12 **Vancheri C**, Kreuter M, Richeldi L, Ryerson CJ, Valeyre D, Grutters JC, Wiebe S, Stansen W, Quaresma M, Stowasser S, Wuyts WA; INJOURNEY Trial Investigators. Nintedanib with Add-on Pirfenidone in Idiopathic Pulmonary Fibrosis. Results of the INJOURNEY Trial. *Am J Respir Crit Care Med* 2018; **197**: 356-363 [PMID: 28889759 DOI: 10.1164/rccm.201706-1301OC]

13 **George PM**, Wells AU, Jenkins RG. Pulmonary fibrosis and COVID-19: the potential role for antifibrotic therapy. *Lancet Respir Med* 2020; **8**: 807-815 [PMID: 32422178 DOI: 10.1016/S2213-2600(20)30225-3]

14 **Sakızcı Uyar B**, Ensarioğlu K, Kurt EB, Özkan D, Özbal Güneş S. Anti-fibrotic Treatment for Pulmonary Fibrosis Induced by COVID-19: A Case Presentation. *Turk J Anaesthesiol Reanim* 2022; **50**: 228-231 [PMID: 35801331 DOI: 10.5152/TJAR.2021.20450]

15 **Wind S**, Schmid U, Freiwald M, Marzin K, Lotz R, Ebner T, Stopfer P, Dallinger C. Clinical Pharmacokinetics and Pharmacodynamics of Nintedanib. *Clin Pharmacokinet* 2019; **58**: 1131-1147 [PMID: 31016670 DOI: 10.1007/s40262-019-00766-0]

16 **Micheletto C**, Izquierdo JL, Avdeev SN, Rada Escobar RA, Pacheco Gallego MC. N-acetylcysteine as a therapeutic approach to post-COVID-19 pulmonary fibrosis adjunctive treatment. *Eur Rev Med Pharmacol Sci* 2022; **26**: 4872-4880 [PMID: 35856379 DOI: 10.26355/eurrev_202207_29212]

17 **Chen L**, Qu J, Kalyani FS, Zhang Q, Fan L, Fang Y, Li Y, Xiang C. Mesenchymal stem cell-based treatments for COVID-19: status and future perspectives for clinical applications. *Cell Mol Life Sci* 2022; **79**: 142 [PMID: 35187617 DOI: 10.1007/s00018-021-04096-y]

18 **Sadeghdoust M**, Aligolighasemabadi F, Dehesh T, Taefehshokr N, Sadeghdoust A, Kotfis K, Hashemiattar A, Ravandi A, Aligolighasemabadi N, Vakili O, Grabarek B, Staszkiewicz R, Łos MJ, Mokarram P, Ghavami S. The Effects of Statins on Respiratory Symptoms and Pulmonary Fibrosis in COVID-19 Patients with Diabetes Mellitus: A Longitudinal Multicenter Study. *Arch Immunol Ther Exp (Warsz)* 2023; **71**: 8 [PMID: 36853269 DOI: 10.1007/s00005-023-00672-1]

19 **Nan D**, Abraira-Meriel C, de la Roz-Fernández S, Maestre-Orozco T, Hernandez JL, Fernandez-Ayala M. Delayed Use of the Recombinant Human IL-1 Receptor Antagonist Anakinra in Five COVID-19 Patients with Pulmonary Fibrosis and Persistent Hypoxaemia: A Preliminary Report. *Eur J Case Rep Intern Med* 2021; **8**: 002821 [PMID: 34790623 DOI: 10.12890/2021_002821]

20 **Wang Y**, Sang X, Shao R, Qin H, Chen X, Xue Z, Li L, Wang Y, Zhu Y, Chang Y, Gao X, Zhang B, Zhang H, Yang J. Xuanfei Baidu Decoction protects against macrophages induced inflammation and pulmonary fibrosis *via* inhibiting IL-6/STAT3 signaling pathway. *J Ethnopharmacol* 2022; **283**: 114701 [PMID: 34606948 DOI: 10.1016/j.jep.2021.114701]

21 **Londres HD**, Armada JJ, Martínez AH, Abdo Cuza AA, Sánchez YH, Rodríguez AG, Figueroa SS, Llanez Gregorich EM, Torres Lahera ML, Peire FG, González TM, González YZ, Añé Kouri AL, Palomo AG, Concepción MT, Pérez LM, Luaces-Alvarez PL, Iglesias DE, Hernández DS, Suzarte MR, Ramos TC. Blocking EGFR with nimotuzumab: a novel strategy for COVID-19 treatment. *Immunotherapy* 2022; **14**: 521-530 [PMID: 35306855 DOI: 10.2217/imt-2022-0027]

22 **Cutolo M**, Paolino S, Smith V. Evidences for a protective role of vitamin D in COVID-19. *RMD Open* 2020; **6** [PMID: 33372031 DOI: 10.1136/rmdopen-2020-001454]

23 **Chen RR**, Li YJ, Chen JJ, Lu CL. A review for natural polysaccharides with anti-pulmonary fibrosis properties, which may benefit to patients infected by 2019-nCoV. *Carbohydr Polym* 2020; **247**: 116740 [PMID: 32829859 DOI: 10.1016/j.carbpol.2020.116740]

24 **Song S**, Ding L, Liu G, Chen T, Zhao M, Li X, Li M, Qi H, Chen J, Wang Z, Wang Y, Ma J, Wang Q. The protective effects of baicalin for respiratory diseases: an update and future perspectives. *Front Pharmacol* 2023; **14**: 1129817 [PMID: 37007037 DOI: 10.3389/fphar.2023.1129817]

25 **Lucaciu O**, Aghiorghiesei O, Petrescu NB, Mirica IC, Benea HRC, Apostu D. In quest of a new therapeutic approach in COVID-19: the endocannabinoid system. *Drug Metab Rev* 2021; **53**: 478-490 [PMID: 33683968 DOI: 10.1080/03602532.2021.1895204]

26 **You X**, Jiang X, Zhang C, Jiang K, Zhao X, Guo T, Zhu X, Bao J, Dou H. Dihydroartemisinin attenuates pulmonary inflammation and fibrosis in rats by suppressing JAK2/STAT3 signaling. *Aging (Albany NY)* 2022; **14**: 1110-1127 [PMID: 35120332 DOI: 10.18632/aging.203874]

27 **Liu J**, Bodnar BH, Meng F, Khan AI, Wang X, Saribas S, Wang T, Lohani SC, Wang P, Wei Z, Luo J, Zhou L, Wu J, Luo G, Li Q, Hu W, Ho W. Epigallocatechin gallate from green tea effectively blocks infection of SARS-CoV-2 and new variants by inhibiting spike binding to ACE2 receptor. *Cell Biosci* 2021; **11**: 168 [PMID: 34461999 DOI: 10.1186/s13578-021-00680-8]

28 **Kai Y**, Matsuda M, Suzuki K, Kasamatsu T, Kajita A, Uno K, Muro S. Tocilizumab and Baricitinib for Recovery From Acute Exacerbation of Combined Pulmonary Fibrosis and Emphysema Secondary to COVID-19 Infection: A Case Report. *Cureus* 2022; **14**: e23411 [PMID: 35481309 DOI: 10.7759/cureus.23411]

29 **Margaria JP**, Moretta L, Alves-Filho JC, Hirsch E. PI3K Signaling in Mechanisms and Treatments of Pulmonary Fibrosis Following Sepsis and Acute Lung Injury. *Biomedicines* 2022; **10** [PMID: 35453505 DOI: 10.3390/biomedicines10040756]

30 **Taniguchi H**, Xu Z, Azuma A, Inoue Y, Li H, Fujimoto T, Bailes Z, Schlenker-Herceg R, Kim DS. Subgroup analysis of Asian patients in the INPULSIS(®) trials of nintedanib in idiopathic pulmonary fibrosis. *Respirology* 2016; **21**: 1425-1430 [PMID: 27399197 DOI: 10.1111/resp.12852]

31 **Kaul B**, Lee JS, Petersen LA, McCulloch C, Rosas IO, Bandi VD, Zhang N, DeDent AM, Collard HR, Whooley MA. Disparities in Antifibrotic Medication Utilization Among Veterans With Idiopathic Pulmonary Fibrosis. *Chest* 2023; **164**: 441-449 [PMID: 36801465 DOI: 10.1016/j.chest.2023.02.027]

32 **Yetkin NA**, Kiraz A, Baran Ketencioğlu B, Bol C, Tutar N. Are MUC5B and TERT mutations genetic risk factors for pulmonary fibrosis in individuals with severe COVID-19? *Tuberk Toraks* 2023; **71**: 34-40 [PMID: 36912407 DOI: 10.5578/tt.20239905]

33 **Ma H**, Wu X, Li Y, Xia Y. Research Progress in the Molecular Mechanisms, Therapeutic Targets, and Drug Development of Idiopathic Pulmonary Fibrosis. *Front Pharmacol* 2022; **13**: 963054 [PMID: 35935869 DOI: 10.3389/fphar.2022.963054]

34 **Patrucco F**, Solidoro P, Gavelli F, Apostolo D, Bellan M. Idiopathic Pulmonary Fibrosis and Post-COVID-19 Lung Fibrosis: Links and Risks. *Microorganisms* 2023; **11** [PMID: 37110318 DOI: 10.3390/microorganisms11040895]

35 **Chinese Research Hospital Association**; Respiratory Council. [Expert recommendations for the diagnosis and treatment of interstitial lung disease caused by novel coronavirus pneumonia]. *Zhonghua Jie He He Hu Xi Za Zhi* 2020; **43**: 827-833 [PMID: 32992435 DOI: 10.3760/cma.j.cn112147-20200326-00419]

36 **Wan Q**, Zhang X, Zhou D, Xie R, Cai Y, Zhang K, Sun X. Inhaled nano-based therapeutics for pulmonary fibrosis: recent advances and future prospects. *J Nanobiotechnology* 2023; **21**: 215 [PMID: 37422665 DOI: 10.1186/s12951-023-01971-7]

World Journal of Clinical Cases

Submit a Manuscript: https://www.f6publishing.com

World J Clin Cases 2024 February 16; 12(5): 880-890

DOI: 10.12998/wjcc.v12.i5.880

ISSN 2307-8960 (online)

ORIGINAL ARTICLE

Clinical and Translational Research

Causal associations between gastroesophageal reflux disease and essential hypertension: A bidirectional Mendelian randomization study

Ning Wei, Ming-Hui Liu, Yu-Hu Song

Specialty type: Medicine, research and experimental

Provenance and peer review: Unsolicited article; Externally peer reviewed.

Peer-review model: Single blind

Peer-review report's scientific quality classification

Grade A (Excellent): 0
Grade B (Very good): B
Grade C (Good): C
Grade D (Fair): 0
Grade E (Poor): 0

P-Reviewer: Kreisel W, Germany; Skrypnyk I, Ukraine

Received: October 16, 2023
Peer-review started: October 16, 2023
First decision: November 28, 2023
Revised: December 12, 2023
Accepted: January 16, 2024
Article in press: January 16, 2024
Published online: February 16, 2024

Ning Wei, Ming-Hui Liu, Yu-Hu Song, Department of Gastroenterology, Union Hospital, Tongji Medical College, Huazhong University of Science and Technology, Wuhan 430022, Hubei Province, China

Corresponding author: Yu-Hu Song, MD, PhD, Professor, Department of Gastroenterology, Union Hospital, Tongji Medical College, Huazhong University of Science and Technology, No. 1277 Jiefang Avenue, Wuhan 430022, Hubei Province, China. yuhusong@163.com

Abstract

BACKGROUND

Clinical studies have reported that patients with gastroesophageal reflux disease (GERD) have a higher prevalence of hypertension.

AIM

To performed a bidirectional Mendelian randomization (MR) analysis to investigate the causal link between GERD and essential hypertension.

METHODS

Eligible single nucleotide polymorphisms (SNPs) were selected, and weighted median, inverse variance weighted (IVW) as well as MR egger (MR-Egger) regression were used to examine the potential causal association between GERD and hypertension. The MR-Pleiotropy RESidual Sum and Outlier analysis was used to detect and attempt to reduce horizontal pleiotropy by removing outliers SNPs. The MR-Egger intercept test, Cochran's *Q* test and "leave-one-out" sensitivity analysis were performed to evaluate the horizontal pleiotropy, heterogeneities, and stability of single instrumental variable.

RESULTS

IVW analysis exhibited an increased risk of hypertension (OR = 1.46, 95%CI: 1.33-1.59, *P* = 2.14E-16) in GERD patients. And the same result was obtained in replication practice (OR = 1.002, 95%CI: 1.0008-1.003, *P* = 0.000498). Meanwhile, the IVW analysis showed an increased risk of systolic blood pressure (β = 0.78, 95%CI: 0.11-1.44, *P* = 0.021) and hypertensive heart disease (OR = 1.68, 95%CI: 1.36-2.08, *P* = 0.0000016) in GERD patients. Moreover, we found an decreased risk of Barrett's esophagus (OR = 0.91, 95%CI: 0.83-0.99, *P* = 0.043) in essential hypertension patients.

CONCLUSION
We found that GERD would increase the risk of essential hypertension, which provided a novel prevent and therapeutic perspectives of essential hypertension.

Key Words: Gastroesophageal reflux disease; Essential hypertension; Hypertensive heart disease; Mendelian randomization study

Core Tip: This study used a method of bidirectional Mendelian randomization, and its results highlighted that gastroesophageal reflux disease (GERD) was positively associated with the risk of essential hypertension, suggesting a new prevent strategy and therapeutic perspectives of essential hypertension in patients with GERD.

Citation: Wei N, Liu MH, Song YH. Causal associations between gastroesophageal reflux disease and essential hypertension: A bidirectional Mendelian randomization study. *World J Clin Cases* 2024; 12(5): 880-890
URL: https://www.wjgnet.com/2307-8960/full/v12/i5/880.htm
DOI: https://dx.doi.org/10.12998/wjcc.v12.i5.880

INTRODUCTION

Gastroesophageal reflux disease (GERD) is a disease in which gastric acid, bile acids and other gastric contents reflux into the esophagus for etiologies like hiatal hernia or abnormal movement of the lower esophagus[1,2]. Even in East Asia, where the prevalence is relatively low, GERD has an prevalence of 5%-10%, while in Europe and the United States, that could be as high as 15%-30%[3-5]. Gastroesophageal reflux can not only lead to esophagitis, Barrett's esophagus (BE), but also a risk factor for esophageal cancer. GERD is also closely linked to heart disease[6]. A Mendelian randomized study showed that GERD can lead to heart diseases such as myocardial infarction and atrial fibrillation[7]. As another common disease, essential hypertension can damage the heart, kidneys, and increase the risk of cerebral hemorrhage, but the cause of essential hypertension remains unclear[8].

Previous clinical studies showed that patients with GERD may have a higher prevalence of essential hypertension, but the results might be influenced by sample size and potentially confounding factors such as lifestyle, socioeconomic status, and underlying medical conditions, and that conclusions may not be accurate[9-11]. There were a few studies on this topic and little attention was paid. Mendelian randomization (MR) is an increasingly popular clinical research method that applies instrumental variable (IV) techniques to assess causal relationships between risk factors and complex human characteristics[12,13]. For exposed IV randomly assigned during conception and was not affected by disease state, MR studies can rule out the influence of confounding factors and reverse causation on causation between exposure and outcome[14].

Our study used the MR method to investigate the causal role of GERD and BE in the development of essential hypertension, and then studied the relationship between GERD and hypertensive heart failure, and further explored the protective effect of gastroesophageal reflux treatment on essential hypertension.

MATERIALS AND METHODS

Data sources

In order to examine the causal connection between GERD/BE and essential hypertension, we used data from two different genome-wide association studies (GWAS) to perform this MR analysis. Data of GERD and BE were obtained from the largest and latest GWAS conducted by Ong *et al*[15]. They applied multitrait GWAS models combining 129080 cases and 473524 controls to identify risk loci of GERD and BE. GERD and BE cases were defined through the International Classification of Disease, tenth version code [for GERD Multi-trait Analysis of GWAS (MTAG)] and confirmed BE diagnosis pathologically (for BE MTAG).

GWAS of essential hypertension (55917 cases and 162837 controls), hypertensive heart disease (3938 cases and 162837 controls), and hypertensive heart and/or renal disease (4363 cases and 162837 controls) were obtained from FinnGen R7 study. Summary statistics for replication practice of essential hypertension (1237 cases and 359957 controls) and diastolic blood pressure (436424 individuals) were obtained from the United Kingdom Biobank. Summary statistics for systolic blood pressure (97656 individuals) were obtained from the IEU study in 2022.

Procedures of MR analysis

Schematic diagram of the bidirectional MR study on the causal relationship between GERD and hypertension was shown in Figure 1. In our study, we firstly performed MR analysis with all eligible single nucleotide polymorphisms (SNPs). The

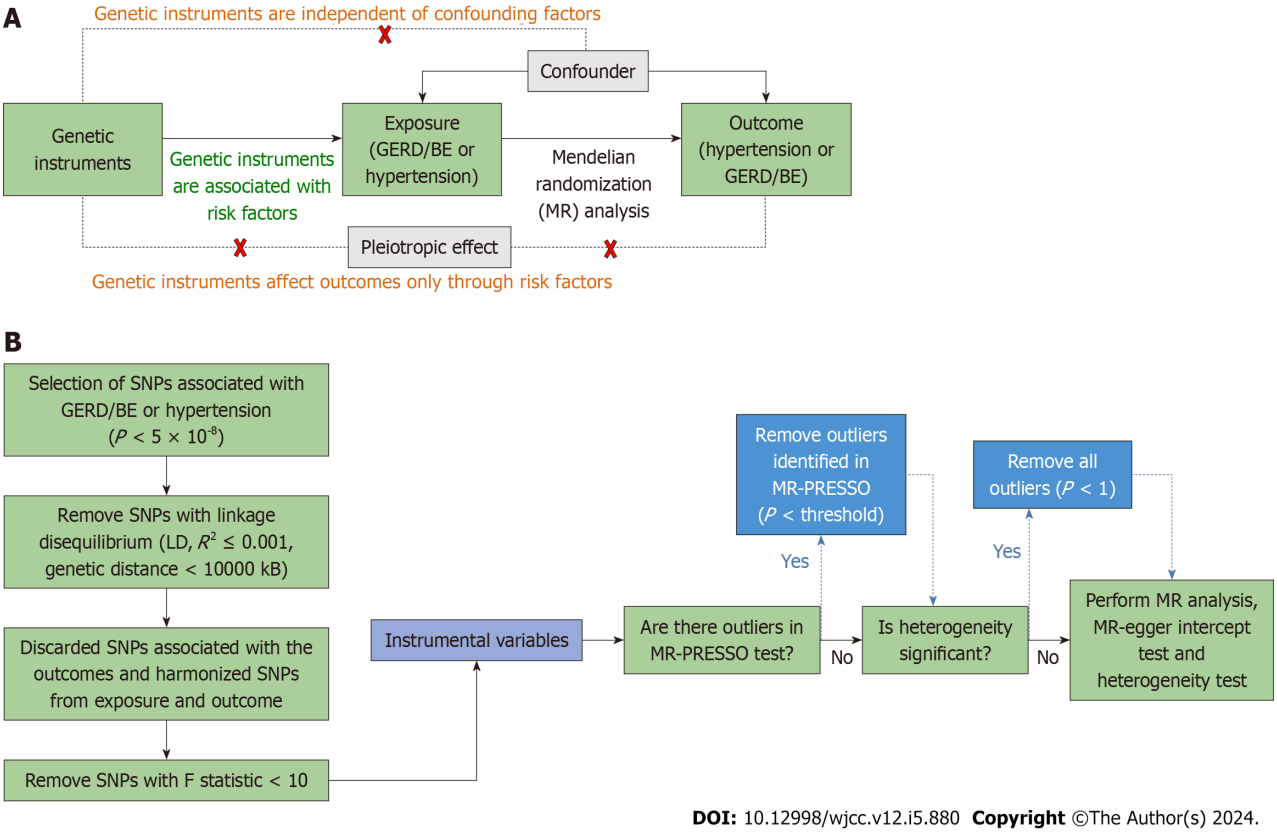

DOI: 10.12998/wjcc.v12.i5.880

Figure 1 Schematic representation of the bidirectional Mendelian randomization study on the causal relationship between gastroesophageal reflux disease and hypertension. A: Schematic diagram showing the design of the bidirectional Mendelian randomization (MR) analysis; B: Flow chart of the MR analysis. MR: Mendelian randomization; GERD: Gastroesophageal reflux disease; SNPs: Single nucleotide polymorphism; MR-PRESSO: MR-Pleiotropy RESidual Sum and Outlier; BE: Barret's esophagus.

outlier variants were eliminated if the MR-Pleiotropy RESidual Sum and Outlier (MR-PRESSO) analysis identified a significant horizontal pleiotropy (with a P value smaller than the cutoff in the MR-PRESSO outlier test). After detecting heterogeneity with Cochran's *Q* test, we eliminated all the SNPs whose P value in the MR-PRESSO outlier test was less than 1 if the heterogeneity was still significant. At last, we performed MR PRESSO and Cochran's *Q* test again, MR analysis, "leave-one-out" sensitivity analysis and MR-Egger intercept test to draw the conclusion with caution.

IVs

SNPs are used in MR analyses to assess the causal relationship; the SNPs chosen should meet three key assumptions: (1) Genetic instruments predict the exposure ($P < 5 \times 10^{-8}$); (2) genetic instruments are not associated with potential confounders; and (3) genetic instruments affect the outcome only through the exposure[16]. We undertook a number of procedures to choose eligible SNPs.

First, $P < 5 \times 10^{-8}$, linkage disequilibrium ($R^2 \leq 0.001$), Hardy-Weinberg equilibrium, and genetic distance 10000 kB were necessary for SNPs related with GERD/BE. The effect alleles, allele frequencies, *P* values, SEs, and *P* values for each SNP were then gathered. The exposure SNPs were then retrieved from the selected outcome data, and SNPs that were substantially ($P < 5 \times 10^{-8}$) linked with the outcomes were excluded. Thirdly, the palindromic and incompatible SNPs were deleted while harmonizing the exposure and result SNPs to maintain the concordance of the effect alleles. The *F*-statistic was determined in order to avoid bias brought on by weak proxies, although no IV had a *F* statistic of less than 10[17].

Statistical analysis

In this investigation, various techniques were utilized to determine whether there was a causal relationship between GERD/BE and essential hypertension. These techniques included inverse variance weighted (IVW), weighted median (WM), and MR-Egger regression. For SNPs, which showed the greatest power but was subject to biases, IVW computed a weighted average of the Wald ratio on the premise that all the instruments were valid[18]. Because the random-effect model maintains conservative estimates even when heterogeneity is identified, it was used in this work for IVW. When at least half of the IVs were valid, WM investigated the median effects of all instrumental SNPs, which made it harder to create biases[19]. Independent of the validity of IVs, the MR-Egger regression model yielded a reasonably reliable estimate. But the MR-Egger approach was susceptible to being influenced by outliers[20].

In this study, the Cochran's *Q* test *P* value was utilized to determine whether there was heterogeneity in the MR analysis. When $P \geq 0.05$, it was decided that there was no heterogeneity in the analysis. A symmetry plot showed that

there was no heterogeneity, and the funnel plot was also utilized to find it.

Pleiotropy was discovered using the intercept term in MR-Egger regression and MR-PRESSO[21]. The MR-Egger intercept test with $P < 0.05$ indicated the existence of directional horizontal pleiotropy[22]. The MR-PRESSO analysis detected and attempted to reduce horizontal pleiotropy by removing significant outliers. Global test in MR-PRESSO with $P < 0.05$ indicated the existence of horizontal pleiotropy and outlier test P value was used to correct the results, which can eliminate horizontal pleiotropy by removing outlier SNPs. The total effect of each remaining SNP was also estimated using the leave-one-out method in order to evaluate the impact of each SNP. All statistical tests were performed by the "TwoSampleMR" package for the R program (version 4.2.1).

Ethics

We used publicly accessible GWAS summary data or published trial data for our analyses. For this manuscript, no original data were gathered, and no ethics committee permission was needed. The institutional ethics review committees for each of the included studies gave their approval, and all participants gave their written informed permission.

RESULTS

MR analysis for causal link between GERD and hypertension

As shown in Table 1, the result of IVW demonstrated that the strong causal link of GERD and essential hypertension (OR = 1.46, 95%CI: 1.33-1.59, P = 2.14E-16). However, heterogeneity and horizontal pleiotropy were detected (Supplementary Figure 1), so we repeated the validation by changing data of hypertension. In replication practice of GERD on essential hypertension, after MR-PRESSO test and heterogeneity analysis, there were no outliers SNPs or heterogeneity or horizontal pleiotropy (Supplementary Table 1), and the IVW analysis also exhibited an increased risk of essential hypertension (OR = 1.002, 95%CI: 1.0008-1.003, P = 0.000498) in GERD patients.

Moreover, we assessed causal relationship of GERD and blood pressure. The IVW analysis exhibited an increased risk of systolic blood pressure in GWRD patients (β = 0.78, 95%CI: 0.11-1.44, P = 0.021) and an increased risk of diastolic blood pressure in GWRD patients (β = 0.09, 95%CI: 0.08-0.12, P = 1.2E-17), but heterogeneity and horizontal pleiotropy were detected in diastolic blood pressure, making the result doubtful. Meanwhile, the IVW analysis exhibited an increased risk of hypertensive heart disease (OR = 1.68, 95%CI: 1.36-2.08, P = 0.0000016) in GERD patients and an increased risk of hypertensive heart and/or renal disease in GERD patients (OR = 1.61, 95%CI: 1.33-1.94, P = 0.000001), indicating a strong causal relationship between GERD and hypertensive heart/renal disease.

As the results mentioned above, we could conclude the causal effect of genetically predicted GERD on hypertension, hypertensive heart/renal disease, and systolic blood pressure.

MR analysis for causal link of BE with hypertension

The results of Table 1 showed no causal link of BE and essential hypertension (OR = 1.000058, 95%CI: 0.9993-1.00079, P = 0.88). However, in replication practice, there was strong causal link of BE and essential hypertension (OR = 1.054, 95%CI: 1.00035-1.1097, P = 0.048). There were no heterogeneity or horizontal pleiotropy in the MR analysis of BE on essential hypertensive in both practices. Therefore, the causal link of BE and essential hypertension need more study to prove.

MR analysis for causal link between hypertension and GERD/BE

Scatter plots were used to display the individual SNP effects and combined effects from each MR approach for each outcome database (Figures 2-5).

In Table 2, we displayed the relationship between hypertension and GERD/BE and the credibility of results was judged using heterogeneity test and pleiotropy test (Supplementary Table 2). There was no causal relationship between essential hypertension and GERD (OR = 1.02, 95%CI: 0.98-1.05, P = 0.344) (Figure 6). Similarly, diastolic blood pressure and systolic blood pressure are not related to the prevalence rate of GERD, with IVW as (β = 0.04, 95%CI: -0.02-0.1, P = 0.179) and (β = -0.003, 95%CI: -0.009-0.003, P = 0.311) respectively (Figure 7). However, we found an decreased risk of BE (OR = 0.91, 95%CI: 0.83-0.99, P = 0.043) in essential hypertension patients, and there were no heterogeneity or horizontal pleiotropy, proving the reliability of this result.

Funnel plots indicated the locations of each outcome's heterogeneity, and leave-one-out plots revealed that the relationships were unlikely to be caused by specific extreme SNPs (Supplementary Figures 1-4).

DISCUSSION

Clinical and mendelian randomized studies had shown that gastroesophageal reflux was a risk factor for heart diseases such as atrial fibrillation and coronary heart disease[9,23-25]. Proton-pump inhibitors (PPI) used to treat gastroesophageal reflux may also relieve pain due to cardiovascular disease[26,27]. The β-blockers used to treat hypertension can also reduce the tone of the lower esophageal sphincter while lowering blood pressure, resulting in aggravation of gastroesophageal reflux symptoms in some hypertensive patients at the beginning of medication[28].

The prevalence of GERD in East Asia is low, ranging from 5 to 10 percent[29]. However, after studying some populations in central China, Li *et al*[27] found that 44.2% (38/86) of essential hypertensive patients had gastroesophageal reflux. Suyu *et al*[11] also found that the proportion of patients with hypertension with GERD was as high as 31.4% (137/

Table 1 Mendelian randomization estimates from different methods of assessing the causal effect between gastroesophageal reflux disease/Barret's esophagus and essential hypertension

Exposure	Outcome	Step	Nsnp	IVW			WM			MR-Egger		
				OR or beta	95%CI	*P* value	OR or beta	95%CI	*P* value	OR or beta	95%CI	*P* value
Gastroesophageal reflux disease	Essential hypertension	3	69	1.46	1.33, 1.59	2.14E-16	1.34	1.19, 1.50	6.80E-07	2.073	1.23, 3.50	0.0082
	Duplicate essential hypertension	1	77	1.002	1.0008, 1.003	4.98E-04	1.0013	0.9998, 1.0028	0.084	1.0018	0.996, 1.0076	0.54
	Diastolic blood pressure[1]	3	58	0.09	0.08, 0.12	1.2E-17	0.095	0.066, 0.12	7.8E-11	0.034	-0.12, 0.19	0.66
	Systolic blood pressure[1]	3	61	0.78	0.11, 1.44	0.021	0.59	-0.36, 1.53	0.23	4.42	0.28, 8.55	0.04
	Hypertensive heart disease	1	75	1.68	1.36, 2.08	1.60E-06	1.82	1.38, 2.42	2.90E-05	2.99	0.85, 10.48	0.09
	Hypertensive heart and/or renal disease	2	73	1.61	1.33, 1.94	1.00E-06	1.72	1.31, 2.26	8.91772E-05	2.89	0.96, 8.75	0.064
Barret's esophagus	Essential hypertension	1	16	1.00006	0.9993, 1.0008	0.88	1.000033	0.999, 1.001	0.95	1.002	0.997, 1.0067	0.4
	Duplicate essentialhy-pertension	1	16	1.05	1.0004, 1.11	0.048	1.078	1.001, 1.16	0.046	1.1	0.75, 1.61	0.62

[1]Except that the results of diastolic blood pressure and diastolic blood pressure were expressed in beta, other results were expressed in OR. Step: (1) Mendelian randomization (MR) analysis without removing single nucleotide polymorphisms (SNPs); (2) MR analysis after removing the SNPs [with *P* value less than threshold in MR-Pleiotropy RESidual Sum and Outlier (MR-PRESSO) test]; and (3) MR analysis after removing all the SNPs (with *P* value less than 1 in MR-PRESSO outlier test). N snp: Number of single nucleotide polymorphisms; IVW: Inverse variance weighted; WM: Weighted median; MR-Egger: Mendelian randomization egger.

Table 2 Mendelian randomization estimates from different methods of assessing the causal effect between essential hypertension and gastroesophageal reflux disease/Barret's esophagus

Exposure	Outcome	Step	Nsnp	IVW			WM			MR-Egger		
				OR or beta	95%CI	*P* value	OR or beta	95%CI	*P* value	OR or beta	95%CI	*P* value
Duplicate essential hypertension	Gastroesophageal reflux disease	3	31	1.015	0.98, 1.05	0.344	1.027	0.99, 1.07	0.202	1.038	0.94, 1.15	0.471
Diastolic blood pressure[1]		3	154	0.042	-0.02, 0.104	0.179	0.026	-0.05, 0.103	0.518	-0.194	-0.39, 0.003	0.056
Systolic blood pressure[1]		3	11	-0.003	-0.009, 0.003	0.311	-0.004	-0.01, 0.003	0.274	-0.031	-0.07, 0.007	0.148
essentialhypertension	Barret's esophagus	3	31	0.911	0.83, 0.997	0.043	0.929	0.82, 1.05	0.254	0.869	0.65, 1.16	0.345

[1]Except that the results of diastolic blood pressure and diastolic blood pressure were expressed in beta, other results were expressed in OR. Step: (1) Mendelian randomization (MR) analysis without removing single nucleotide polymorphisms (SNPs); (2) MR analysis after removing the SNPs [with *P* value less than threshold in MR-Pleiotropy RESidual Sum and Outlier (MR-PRESSO) test]; and (3) MR analysis after removing all the SNPs (with *P* value less than 1 in MR-PRESSO outlier test). N snp: Number of single nucleotide polymorphisms; IVW: Inverse variance weighted; WM: Weighted median; MR-Egger: Mendelian randomization egger.

436). Our findings clearly suggest that gastroesophageal reflux can lead to elevated blood pressure and essential hypertension.

Gudlaugsdottir *et al*[30] concluded that hypertension was more prevalent in patients with BE (OR = 5.1, $P < 0.0001$) and also had a higher prevalence in patients with reflux esophagitis (OR = 3.8, $P < 0.001$). But our study did not clarify the role of BE in hypertension. PPI therapy, anti-reflux mucosectomy (ARMS), and fundoplication are other treatments for gastroesophageal reflux, which may play a protective role against hypertension by relieving gastroesophageal reflux[31]. Some clinical studies have found that the hypertension was well controlled in some patients after the treatment of gastroesophageal reflux by fundoplication[10]. We were failed to determine the possible protective effects of PPI/ARMS/

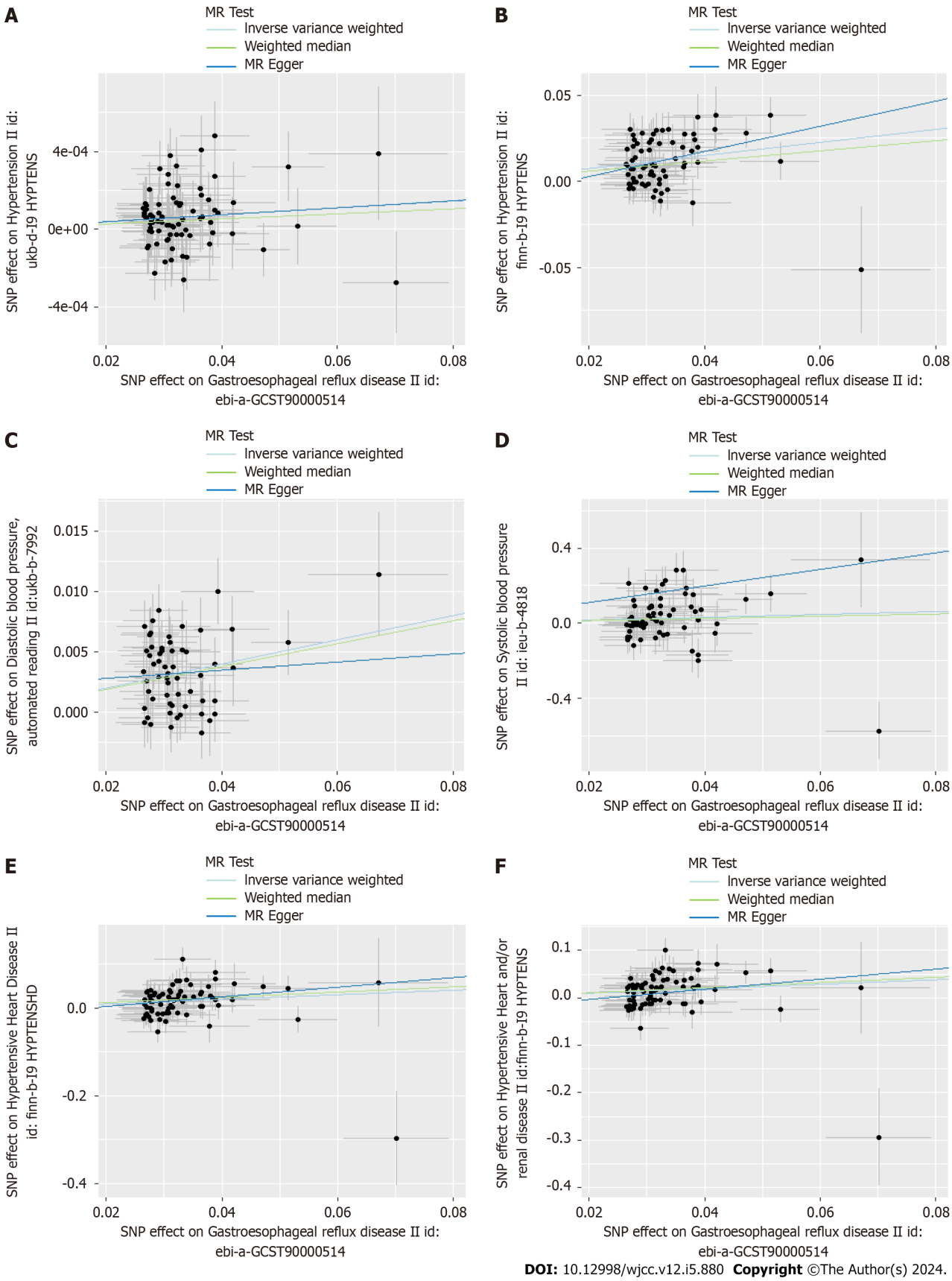

DOI: 10.12998/wjcc.v12.i5.880

Figure 2 Scatter plots for the causal association between gastroesophageal reflux disease and hypertension. A: Gastroesophageal reflux disease (GERD) on essential hypertension; B: Replication practice for GERD on essential hypertension; C: GERD on diastolic blood pressure; D: GERD on systolic blood pressure; E: GERD on hypertensive heart disease; F: GERD on hypertensive heart and/or renal disease. MR: Mendelian randomization; SNPs: Single nucleotide polymorphism.

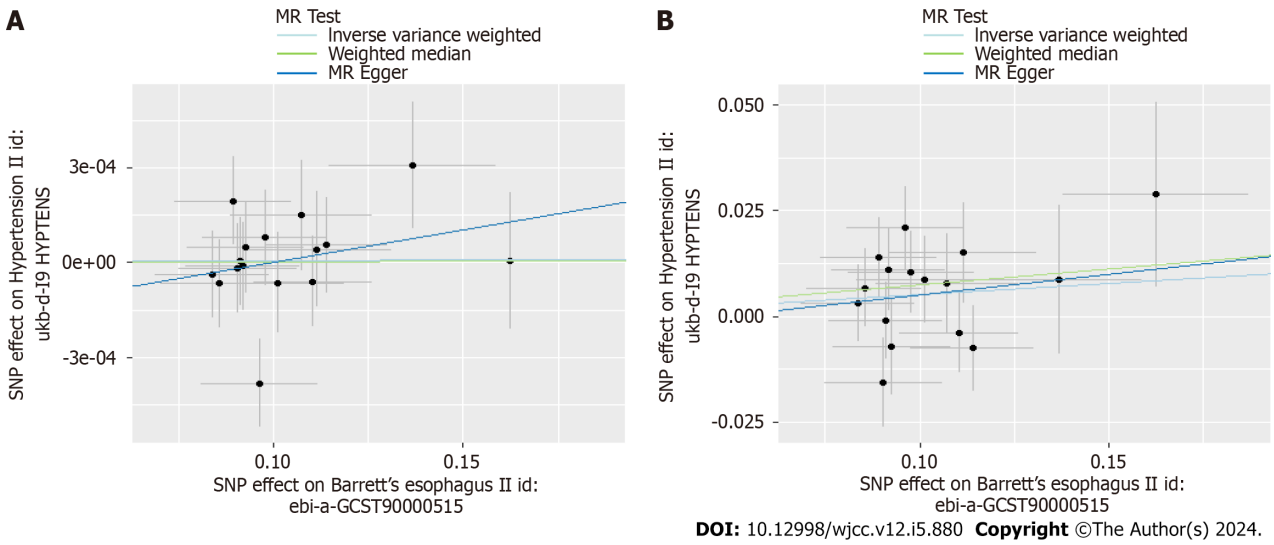

DOI: 10.12998/wjcc.v12.i5.880

Figure 3 Scatter plots for the causal association between Barret's esophagus and hypertension. A: Barret's esophagus (BE) on essential hypertension; B: Replication practice for BE on essential hypertension. MR: Mendelian randomization; SNPs: Single nucleotide polymorphism.

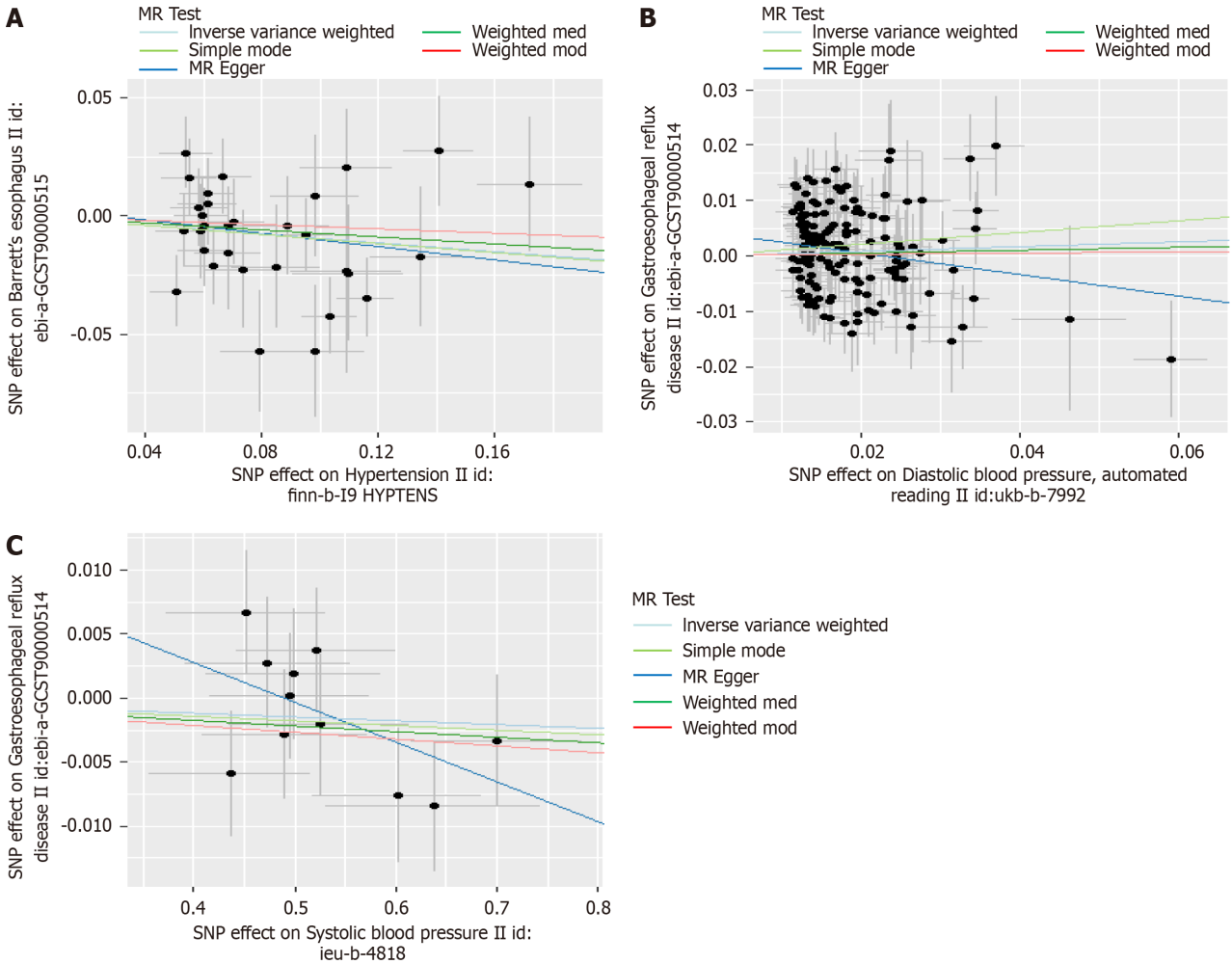

DOI: 10.12998/wjcc.v12.i5.880

Figure 4 Scatter plots for the causal association between hypertension and Gastroesophageal reflux disease. A: Duplicate essential hypertension on Gastroesophageal reflux disease (GERD); B: Diastolic blood pressure and GERD; C: Systolic blood pressure and GERD. MR: Mendelian randomization; SNPs: Single nucleotide polymorphism.

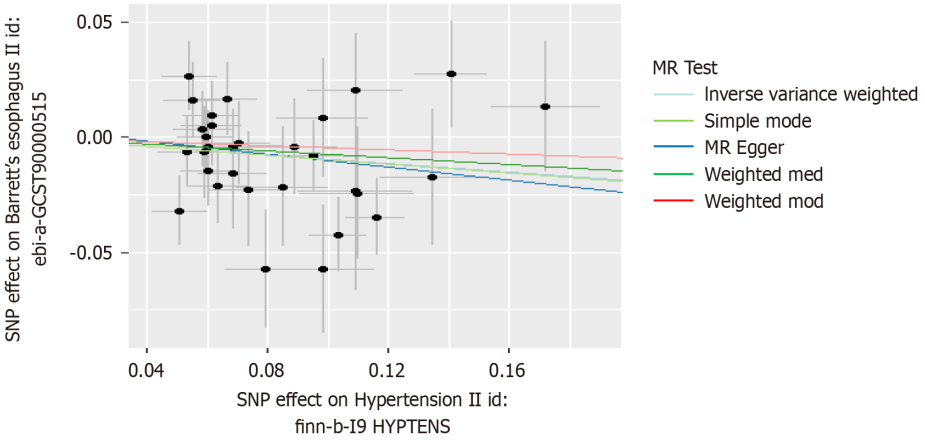

DOI: 10.12998/wjcc.v12.i5.880

Figure 5 Scatter plots for the causal association between hypertension and Barret's esophagus: Duplicate essential hypertension on Barret's esophagus. MR: Mendelian randomization; SNPs: Single nucleotide polymorphism.

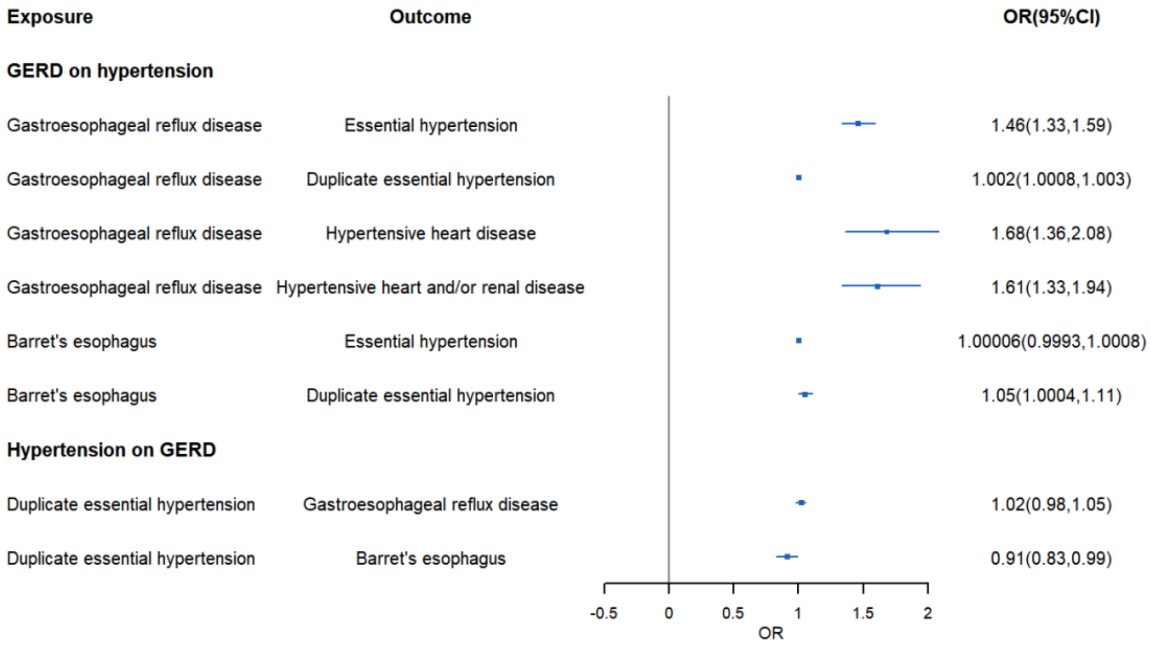

DOI: 10.12998/wjcc.v12.i5.880

Figure 6 Forest plot for the causal association between hypertension and Gastroesophageal reflux disease. GERD: Gastroesophageal reflux disease.

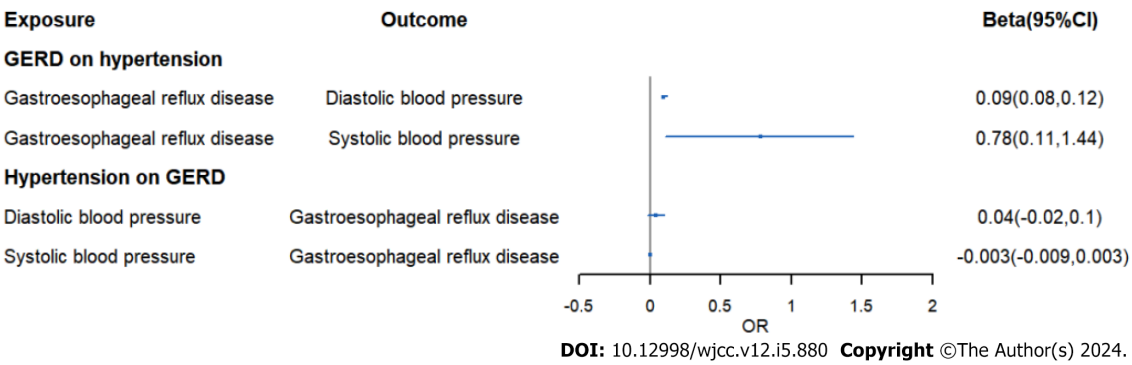

DOI: 10.12998/wjcc.v12.i5.880

Figure 7 Forest plot for the causal association between hypertension and Barret's esophagus. GERD: Gastroesophageal reflux disease.

fundoplication on hypertension due to insufficient SNP/databases. In addition, our study suggested that gastroesophageal reflux can also lead to hypertensive heart failure.

The anterior wall of the esophagus is closely adjacent to the posterior wall of the heart, and the autonomic nerves of the esophagus and heart also overlap and cross[32,33]. Some studies believe that the presence of gastroesophageal reflux is often accompanied by pain, which would stimulate the patient's sympathetic nerve excitation, resulting in increased blood pressure[34]. In addition, gastroesophageal reflux can lead to arrhythmias, and arrhythmias such as bradycardia can also lead to hypertension[35,36]. Gastroesophageal reflux may also cause hypertension by affecting the level of mediators in plasma that regulate hypertension. Some studies found that plasma concentrations of nitric oxide metabolites increased significantly after 8 wk of inhibition of gastric acid secretion[37,38].

Several limitations should be considered in our MR analysis. Firstly, the summary GWAS data only concern individuals of European, so results may not be representative of the whole population. Secondly, although we took steps to exclude outlier SNPs, horizontal pleiotropy and heterogeneity still exited in our analysis. However, we used different methods to draw a conclusion to eliminate the impact of pleiotropy and heterogeneity.

CONCLUSION

Gastroesophageal reflux can lead to increased blood pressure, hypertension, and hypertensive heart failure. Patients with essential hypertension should be examined and treated for gastroesophageal reflux, and patients with gastroesophageal reflux should also be monitored for hypertension.

ARTICLE HIGHLIGHTS

Research background

Some clinical studies have suggested that gastroesophageal reflux disease (GERD) may have a causal relationship with essential hypertension, but the relevant conclusions may be affected by confounding factors and small sample sizes.

Research motivation

Determining the causal relationship between GERD and essential hypertension could provide new perspectives for the treatment of patients with GERD and hypertension.

Research objectives

We would perform a bidirectional Mendelian randomization (MR) analysis to investigate the causal link between GERD and essential hypertension.

Research methods

A series of steps were conducted to select eligible single nucleotide polymorphisms, and inverse variance weighted (IVW), weighted median and MR egger regression were used to examine whether there was a causal association between GERD and hypertension.

Research results

IVW analysis exhibited an increased risk of hypertension (OR = 1.46, 95%CI: 1.33-1.59, P = 2.14E-16) in GERD patients. Meanwhile, the IVW analysis showed an increased risk of systolic blood pressure and hypertensive heart disease in GERD patients.

Research conclusions

GERD was positively associated with the risk of essential hypertension, suggesting a new prevent strategy and therapeutic perspectives of essential hypertension in patients with GERD.

Research perspectives

The specific mechanisms associated with GERD and essential hypertension need to be further clarified.

FOOTNOTES

Author contributions: Song YH and Wei N concept of the study and grant obtain; Liu MH data analysis; Liu MH and Wei H preparation of manuscript; Song YH and Wei N administrative, technical, or material support; study supervision; all the authors read and approved the paper.

Supported by National Natural Science Foundation of China (General Program), No. 82070631.

Institutional review board statement: We used publicly accessible GWAS summary data or published trial data for our analyses. For this

manuscript, no original data were gathered, and no ethics committee permission was needed.

Clinical trial registration statement: We used publicly accessible GWAS summary data or published trial data for our analyses. For this manuscript, no original data were gathered, and no ethics committee permission was needed. The institutional ethics review committees for each of the included studies gave their approval, and all participants gave their written informed permission.

Informed consent statement: We used publicly accessible GWAS summary data or published trial data for our analyses. For this manuscript, no original data were gathered, and no ethics committee permission was needed. The institutional ethics review committees for each of the included studies gave their approval, and all participants gave their written informed permission.

Conflict-of-interest statement: There are no conflicts of interest to report.

Data sharing statement: No additional data are available.

Country/Territory of origin: China

ORCID number: Ning Wei 0000-0001-8931-8995; Yu-Hu Song 0000-0003- 4178-4916.

S-Editor: Qu XL
L-Editor: A
P-Editor: Zheng XM

REFERENCES

1 **Mikami DJ**, Murayama KM. Physiology and pathogenesis of gastroesophageal reflux disease. *Surg Clin North Am* 2015; **95**: 515-525 [PMID: 25965127 DOI: 10.1016/j.suc.2015.02.006]
2 **Zheng Z**, Shang Y, Wang N, Liu X, Xin C, Yan X, Zhai Y, Yin J, Zhang J, Zhang Z. Current Advancement on the Dynamic Mechanism of Gastroesophageal Reflux Disease. *Int J Biol Sci* 2021; **17**: 4154-4164 [PMID: 34803489 DOI: 10.7150/ijbs.65066]
3 **Maret-Ouda J**, Markar SR, Lagergren J. Gastroesophageal Reflux Disease. *JAMA* 2020; **324**: 2565 [PMID: 33351044 DOI: 10.1001/jama.2020.21573]
4 **Sandhu DS**, Fass R. Current Trends in the Management of Gastroesophageal Reflux Disease. *Gut Liver* 2018; **12**: 7-16 [PMID: 28427116 DOI: 10.5009/gnl16615]
5 **El-Serag HB**, Sweet S, Winchester CC, Dent J. Update on the epidemiology of gastro-oesophageal reflux disease: a systematic review. *Gut* 2014; **63**: 871-880 [PMID: 23853213 DOI: 10.1136/gutjnl-2012-304269]
6 **Clarrett DM**, Hachem C. Gastroesophageal Reflux Disease (GERD). *Mo Med* 2018; **115**: 214-218 [PMID: 30228725]
7 **Sun X**, Chen L, Zheng L. A Mendelian randomization study to assess the genetic liability of gastroesophageal reflux disease for cardiovascular diseases and risk factors. *Hum Mol Genet* 2022; **31**: 4275-4285 [PMID: 35861629 DOI: 10.1093/hmg/ddac162]
8 **Elliott WJ**. Systemic hypertension. *Curr Probl Cardiol* 2007; **32**: 201-259 [PMID: 17398315 DOI: 10.1016/j.cpcardiol.2007.01.002]
9 **Chen CH**, Lin CL, Kao CH. Association between gastroesophageal reflux disease and coronary heart disease: A nationwide population-based analysis. *Medicine (Baltimore)* 2016; **95**: e4089 [PMID: 27399102 DOI: 10.1097/MD.0000000000004089]
10 **Hu Z**, Chen M, Wu J, Song Q, Yan C, Du X, Wang Z. Improved control of hypertension following laparoscopic fundoplication for gastroesophageal reflux disease. *Front Med* 2017; **11**: 68-73 [PMID: 28213877 DOI: 10.1007/s11684-016-0490-7]
11 **Suyu H**, Liu Y, Jianyu X, Luo G, Cao L, Long X. Prevalence and Predictors of Silent Gastroesophageal Reflux Disease in Patients with Hypertension. *Gastroenterol Res Pract* 2018; **2018**: 7242917 [PMID: 29849598 DOI: 10.1155/2018/7242917]
12 **Davey Smith G**, Hemani G. Mendelian randomization: genetic anchors for causal inference in epidemiological studies. *Hum Mol Genet* 2014; **23**: R89-R98 [PMID: 25064373 DOI: 10.1093/hmg/ddu328]
13 **Birney E**. Mendelian Randomization. *Cold Spring Harb Perspect Med* 2022; **12** [PMID: 34872952 DOI: 10.1101/cshperspect.a041302]
14 **Sekula P**, Del Greco M F, Pattaro C, Köttgen A. Mendelian Randomization as an Approach to Assess Causality Using Observational Data. *J Am Soc Nephrol* 2016; **27**: 3253-3265 [PMID: 27486138 DOI: 10.1681/ASN.2016010098]
15 **Ong JS**, An J, Han X, Law MH, Nandakumar P; 23andMe Research team; Esophageal cancer consortium, Schumacher J, Gockel I, Bohmer A, Jankowski J, Palles C, Olsen CM, Neale RE, Fitzgerald R, Thrift AP, Vaughan TL, Buas MF, Hinds DA, Gharahkhani P, Kendall BJ, MacGregor S. Multitrait genetic association analysis identifies 50 new risk loci for gastro-oesophageal reflux, seven new loci for Barrett's oesophagus and provides insights into clinical heterogeneity in reflux diagnosis. *Gut* 2022; **71**: 1053-1061 [PMID: 34187846 DOI: 10.1136/gutjnl-2020-323906]
16 **Boef AG**, Dekkers OM, le Cessie S. Mendelian randomization studies: a review of the approaches used and the quality of reporting. *Int J Epidemiol* 2015; **44**: 496-511 [PMID: 25953784 DOI: 10.1093/ije/dyv071]
17 **Burgess S**, Thompson SG; CRP CHD Genetics Collaboration. Avoiding bias from weak instruments in Mendelian randomization studies. *Int J Epidemiol* 2011; **40**: 755-764 [PMID: 21414999 DOI: 10.1093/ije/dyr036]
18 **Burgess S**, Butterworth A, Thompson SG. Mendelian randomization analysis with multiple genetic variants using summarized data. *Genet Epidemiol* 2013; **37**: 658-665 [PMID: 24114802 DOI: 10.1002/gepi.21758]

19 **Bowden J**, Davey Smith G, Haycock PC, Burgess S. Consistent Estimation in Mendelian Randomization with Some Invalid Instruments Using a Weighted Median Estimator. *Genet Epidemiol* 2016; **40**: 304-314 [PMID: 27061298 DOI: 10.1002/gepi.21965]

20 **Burgess S**, Thompson SG. Interpreting findings from Mendelian randomization using the MR-Egger method. *Eur J Epidemiol* 2017; **32**: 377-389 [PMID: 28527048 DOI: 10.1007/s10654-017-0255-x]

21 **Verbanck M**, Chen CY, Neale B, Do R. Publisher Correction: Detection of widespread horizontal pleiotropy in causal relationships inferred from Mendelian randomization between complex traits and diseases. *Nat Genet* 2018; **50**: 1196 [PMID: 29967445 DOI: 10.1038/s41588-018-0164-2]

22 **Burgess S**, Thompson SG. Erratum to: Interpreting findings from Mendelian randomization using the MR-Egger method. *Eur J Epidemiol* 2017; **32**: 391-392 [PMID: 28664250 DOI: 10.1007/s10654-017-0276-5]

23 **Mohamed A**, Ochoa Crespo D, Kaur G, Ashraf I, Peck MM, Maram R, Malik BH. Gastroesophageal Reflux and Its Association With Atrial Fibrillation: A Traditional Review. *Cureus* 2020; **12**: e10387 [PMID: 33062508 DOI: 10.7759/cureus.10387]

24 **Maruyama T**, Fukata M, Akashi K. Association of atrial fibrillation and gastroesophageal reflux disease: Natural and therapeutic linkage of the two common diseases. *J Arrhythm* 2019; **35**: 43-51 [PMID: 30805043 DOI: 10.1002/joa3.12125]

25 **Chang CS**, Chen HJ, Liao CH. Patients with Cerebral Stroke Have an Increased Risk of Gastroesophageal Reflux Disease: A Population-Based Cohort Study. *J Stroke Cerebrovasc Dis* 2018; **27**: 1267-1274 [PMID: 29325919 DOI: 10.1016/j.jstrokecerebrovasdis.2017.12.001]

26 **Dong H**, Li X, Cai M, Zhang C, Mao W, Wang Y, Xu Q, Chen M, Wang L, Huang X. Integrated bioinformatic analysis reveals the underlying molecular mechanism of and potential drugs for pulmonary arterial hypertension. *Aging (Albany NY)* 2021; **13**: 14234-14257 [PMID: 34016786 DOI: 10.18632/aging.203040]

27 **Li ZT**, Ji F, Han XW, Wang L, Yue YQ, Wang ZG. The Role of Gastroesophageal Reflux in Provoking High Blood Pressure Episodes in Patients With Hypertension. *J Clin Gastroenterol* 2018; **52**: 685-690 [PMID: 28961574 DOI: 10.1097/MCG.0000000000000933]

28 **Lazebnik LB**, Komissarenko IA, Mikheeva OM. [Cardiovascular pathology associated with digestive system diseases]. *Eksp Klin Gastroenterol* 2011; 69-74 [PMID: 21919242]

29 **Zhang D**, Liu S, Li Z, Wang R. Global, regional and national burden of gastroesophageal reflux disease, 1990-2019: update from the GBD 2019 study. *Ann Med* 2022; **54**: 1372-1384 [PMID: 35579516 DOI: 10.1080/07853890.2022.2074535]

30 **Gudlaugsdottir S**, Verschuren W, Dees J, Stijnen T, Wilson J. Hypertension is frequently present in patients with reflux esophagitis or Barrett's esophagus but not in those with non-ulcer dyspepsia. *Eur J Intern Med* 2002; **13**: 369 [PMID: 12225781 DOI: 10.1016/s0953-6205(02)00090-0]

31 **Katzka DA**, Kahrilas PJ. Advances in the diagnosis and management of gastroesophageal reflux disease. *BMJ* 2020; **371**: m3786 [PMID: 33229333 DOI: 10.1136/bmj.m3786]

32 **Sánchez-Quintana D**, Cabrera JA, Climent V, Farré J, Mendonça MC, Ho SY. Anatomic relations between the esophagus and left atrium and relevance for ablation of atrial fibrillation. *Circulation* 2005; **112**: 1400-1405 [PMID: 16129790 DOI: 10.1161/CIRCULATIONAHA.105.551291]

33 **Celebi OO**, Celebi S, Aydogdu S. A dangerous and risky relationship: Esophagus and left atrium. *Pacing Clin Electrophysiol* 2019; **42**: 568-569 [PMID: 30758845 DOI: 10.1111/pace.13630]

34 **Blackshaw LA**, Haupt JA, Omari T, Dent J. Vagal and sympathetic influences on the ferret lower oesophageal sphincter. *J Auton Nerv Syst* 1997; **66**: 179-188 [PMID: 9406123 DOI: 10.1016/s0165-1838(97)00082-9]

35 **Bayés-Genís A**, Guindo J, Viñolas X, Tomás L, Elosua R, Duran I, Bayés de Luna A. Cardiac arrhythmias and left ventricular hypertrophy in systemic hypertension and their influences on prognosis. *Am J Cardiol* 1995; **76**: 54D-59D [PMID: 7495219 DOI: 10.1016/s0002-9149(99)80493-7]

36 **Afzal MR**, Savona S, Mohamed O, Mohamed-Osman A, Kalbfleisch SJ. Hypertension and Arrhythmias. *Heart Fail Clin* 2019; **15**: 543-550 [PMID: 31472889 DOI: 10.1016/j.hfc.2019.06.011]

37 **Kato S**, Kitamura M, Korolkiewicz RP, Takeuchi K. Role of nitric oxide in regulation of gastric acid secretion in rats: effects of NO donors and NO synthase inhibitor. *Br J Pharmacol* 1998; **123**: 839-846 [PMID: 9535011 DOI: 10.1038/sj.bjp.0701691]

38 **Takeuchi K**, Sugamoto S, Yamamoto H, Kawauchi S, Tashima K. Interactive roles of endogenous prostaglandin and nitric oxide in regulation of acid secretion by damaged rat stomachs. *Aliment Pharmacol Ther* 2000; **14** Suppl 1: 125-134 [PMID: 10807414 DOI: 10.1046/j.1365-2036.2000.014s1125.x]

World Journal of Clinical Cases

Submit a Manuscript: https://www.f6publishing.com

World J Clin Cases 2024 February 16; 12(5): 891-902

DOI: 10.12998/wjcc.v12.i5.891

ISSN 2307-8960 (online)

ORIGINAL ARTICLE

Clinical and Translational Research

Serum urate is associated with an increased risk of inflammatory bowel disease: A bidirectional Mendelian randomization study

Song Zhang, Xue Fang, Le Kang, Xiang-Yu Sui, Miao Liu, Yu-Jia Luo, Shuo Fu, Zhao-Shen Li, Sheng-Bing Zhao, Yu Bai

Specialty type: Medicine, research and experimental

Provenance and peer review: Invited article; Externally peer reviewed.

Peer-review model: Single blind

Peer-review report's scientific quality classification

Grade A (Excellent): 0
Grade B (Very good): 0
Grade C (Good): C
Grade D (Fair): 0
Grade E (Poor): 0

P-Reviewer: Vaishalli PM, India

Received: December 9, 2023
Peer-review started: December 9, 2023
First decision: December 14, 2023
Revised: January 1, 2024
Accepted: January 23, 2024
Article in press: January 23, 2024
Published online: February 16, 2024

Song Zhang, Xue Fang, Le Kang, Xiang-Yu Sui, Miao Liu, Yu-Jia Luo, Shuo Fu, Yu Bai, Department of Gastroenterology, Changhai Hospital, Shanghai 200433, China

Zhao-Shen Li, Sheng-Bing Zhao, Department of Gastroenterology, Changhai Hospital, Second Military Medical University/Naval Medical University, Shanghai 200433, China

Zhao-Shen Li, Sheng-Bing Zhao, Digestive Endoscopy Center, Changhai Hospital, Naval/Second Military Medical University, Shanghai 200433, China

Zhao-Shen Li, Sheng-Bing Zhao, National Clinical Research Center for Digestive Diseases, Shanghai 200433, China

Corresponding author: Yu Bai, MD, PhD, Academic Research, Associate Professor, Researcher, Department of Gastroenterology, Changhai Hospital, No. 168 Changhai Road, Yangpu District, Shanghai 200433, China. changhaibaiyu@smmu.edu.cn

Abstract

BACKGROUND

Previous studies have indicated bidirectional associations between urate levels and inflammatory bowel disease (IBD), including ulcerative colitis (UC) and Crohn's disease (CD). However, it remains unclear whether the observations are causal because of confounding factors.

AIM

To investigate the causal associations between urate levels and IBD using bidirectional Mendelian randomization (MR).

METHODS

Independent genetic variants for urate levels and IBD were selected as instrumental variables from published genome-wide association studies (GWASs). Summary statistics for instrument-outcome associations were retrieved from three separate databases for IBD (the UK Biobank, the FinnGen database and a large GWAS meta-analysis) and one for urate levels (a large GWAS meta-analysis). MR analyses included the inverse-variance-weighted method, weighted-median estimator, MR-Egger and sensitivity analyses (MR-PRESSO). A meta-analysis was also conducted to merge the data from separate outcome databases using a fixed-effects model.

RESULTS
Genetically higher serum urate levels were strongly associated with an increased risk of UC [odds ratio (OR): 1.95, 95% confidence interval (CI): 1.86-2.05] after outlier correction, and the ORs (95%CIs) for IBD and CD were 0.94 (95%CI: 0.86-1.03) and 0.91 (95%CI: 0.80-1.04), respectively. Animal studies have confirmed the positive association between urate levels and UC. Moreover, genetically predicted IBD was inversely related to urate levels (OR: 0.97, 95%CI: 0.94-0.99). However, no association was observed between genetically influenced UC or CD and urate levels.

CONCLUSION
Urate levels might be risk factors for UC, whereas genetically predicted IBD was inversely associated with urate levels. These findings provide essential new insight for treating and preventing IBD.

Key Words: Inflammatory bowel disease; Urate levels; Antioxidant; Mendelian randomization; Single nucleotide polymorphism

Core Tip: Previous observational studies have indicated the association between urate levels and inflammatory bowel disease (IBD) (including ulcerative colitis (UC) and Crohn's disease). To overcome the limitations of conventional observational studies and investigate the causal association between urate levels and IBD, we conducted a bidirectional Mendelian randomization (MR) study. MR analysis revealed that higher urate levels may be risk factors for UC, and genetically predicted IBD was inversely associated with urate levels.

Citation: Zhang S, Fang X, Kang L, Sui XY, Liu M, Luo YJ, Fu S, Li ZS, Zhao SB, Bai Y. Serum urate is associated with an increased risk of inflammatory bowel disease: A bidirectional Mendelian randomization study. *World J Clin Cases* 2024; 12(5): 891-902
URL: https://www.wjgnet.com/2307-8960/full/v12/i5/891.htm
DOI: https://dx.doi.org/10.12998/wjcc.v12.i5.891

INTRODUCTION

Inflammatory bowel disease (IBD), comprising ulcerative colitis (UC) and Crohn's disease (CD), is characterized by chronic inflammation and a prolonged duration in the gastrointestinal tract[1]. Epidemiological studies have confirmed that the incidence of IBD in developing countries has exceeded 0.3% with the rapid adoption of the Western lifestyle[1,2]. Specifically, there are 322 and 214 cases per 100000 for CD and 505 and 214 cases per 100000 for UC in Europe and the United States, respectively. The long course of IBD lasts throughout the patient's life, and the risk of colorectal cancer is much greater than that in the general population[3,4]. The pathogenesis of IBD involves interplay between environmental risk factors (not limited to smoking, unfavorable lifestyles and diets) and genetic variants, resulting in inadequate intestinal immune activation and dysbiosis of the gut microbiota[5,6]. Previous studies demonstrated that depleted mucosal antioxidant defense was common in IBD and thus may impede mucosal repair and compromise the inflamed mucosa[7]. Over the past decade, the association between antioxidants and IBD has attracted considerable interest[7-10] in light of the strong association between antioxidant capacity and the severity and disease activity of IBD.

Urate is vital as an antioxidant for neutralizing hydroxyl, superoxide and peroxynitrite radicals, which can decrease oxidative stress *in vivo*[11,12]. Previous studies have indicated that the serum uric acid-to-creatinine ratio is positively correlated with disease activity in CD patients[13]. Increased urate levels were positively correlated with an increased risk of UC[14]. Moreover, the use of a clinical drug (allopurinol) improved the severity of colitis by reducing urate levels[15]. An animal study by Rahimian *et al*[9] further demonstrated that uric acid mediated the protective effects of inosine against colitis. Overall, the relationship between urate levels and IBD (including UC and CD) has not been well established. A recent Mendelian randomization (MR) study by Chen *et al*[16] did not support the causal effect of serum urate levels on UC or CD incidence. However, the causal effect of these polymorphisms remains elusive because of the limited number of single-nucleotide polymorphisms (SNPs) used as instrumental variables (IVs). However, the causal effect of IBD (including UC and CD) on urate levels remains unclear.

Using genetic variants identified through genome-wide association studies (GWAS), MR is a popular approach for investigating the causal relationship between exposures and outcomes[17]. Therefore, to overcome the limitations of conventional observational studies, we aimed to examine the potential bidirectional relationship between IBD (including UC and CD) and serum urate levels in the present MR study. In addition, we conducted *in vivo* animal studies to verify the association between urate levels and IBD. This study provides reliable insight into the causal associations between urate levels and IBD.

MATERIALS AND METHODS

Study design

A bidirectional two-sample MR analysis was performed to assess the causal relationship between IBD and urate levels (Figure 1). SNPs associated with risk factors were selected as IVs. The MR study was based on three assumptions: (1) The SNPs used as IVs are strongly associated with exposure (urate level or IBD); (2) The SNPs are not associated with any confounder of exposure–outcome associations; and (3) The SNPs exert effects through exposure only. In combination with the three principles mentioned above, palindromic SNPs were identified and excluded in IV selection. All the data used in the current study were publicly available GWAS summary statistics; therefore, no additional ethical approval or informed consent was needed. GWAS summary statistics were searched to extract leading SNPs related to urate levels and IBD (including UC and CD) as IVs. Gene-outcome associations were retrieved from three databases: (1) A large-scale GWAS meta-analysis; (2) The Finngen database (version 7, https://r7.finngen.fi/); and (3) The UK Biobank (UKB).

Selection of the instrumental genetic variables

SNPs related to urate levels were selected as IVs from a GWAS (Köttgen *et al*[18]), which included a total sample size of 110347 European individuals with various serum urate levels[18]. SNPs that were significantly associated with urate levels ($P < 5 \times 10^{-8}$) were extracted. A linkage disequilibrium (LD)-based clumping procedure was performed using the 1000 Genomes EUR reference panel ($r^2 < 0.01$ and clump distance > 10000 kb) to ensure that each IV was independent. When SNPs related to exposure were absent in the outcome GWAS statistics, the proxy SNPs significantly associated with the variants of interest were selected ($r^2 > 0.8$).

Summary statistics for IBD were obtained from the GWAS meta-analysis (Liu *et al*[19]), which included a total of 34652 participants of European ancestry (cases/controls for IBD: 12882/21770; UCs: 6968/20464; CDs: 5956/14927). Nearly 12 million SNPs were included in all three GWAS summary statistics. SNPs ($P < 5 \times 10^{-8}$) were selected and used for LD-based clumping. The proxy SNPs were extracted when SNPs related to exposure were absent. The IV selection procedure for IBD was the same as that for urate levels (described in the previous paragraph).

F-statistics, calculated as $(\text{beta}/\text{SE})^2$, were used to quantify the strength of each IV, and a value > 10 was considered sufficient[20]. In the present study, all F-statistics were greater than 10, indicating that there is little possibility of weak instrument bias based on summary statistics.

SNP-outcome data sources

Summary-level data for urate levels were obtained from GWAS statistics (Köttgen *et al*[18]), as described in section 2.2. Gene-environment associations for IBD were obtained from three separate databases: (1) The GWAS meta-analysis from Liu *et al*[19]; (2) The Finngen database; and (3) The UKB (for UC data only). The Liu *et al*'s study has been described previously[19]. In the Finngen study, CD and UC were defined by their ICD codes, while IBD was a term consisting of CD, UC and indeterminate colitis. Among the patients and controls, 8966/312336 had IBD, 3243/318059 had CD, and 6803/314499 had UC. The UKB data for UC were extracted from a GWAS meta-analysis by Jiang *et al*[21], which included 2569 patients and 453779 controls. GWASs on IBD and CD were not available in the UKB.

Statistical analysis of primary MR

The primary analysis method employed was the inverse-variance weighted (IVW) method, which assumes that all SNPs are valid and yields the most precise estimates[22]. In the presence of a sufficient sample size and absence of the pleiotropic effect of IVs, the IVW estimate is robust to confounding factors and approximates the true value[23]. A multiplicative random effect IVW model was applied when the heterogeneity significantly differed ($P < 0.05$).

Supplementary and sensitivity analysis

In addition to the IVW method, other robust methods (weighted median, MR-Egger and MR-PRESSO) were used to ensure the consistency and efficiency of the MR results. The weighted-median method could provide consistent causal estimates even when more than half of the IVs were invalid[23]. The MR-Egger estimates allowed the included IVs to demonstrate unbalanced pleiotropy[24]. The MR-PRESSO approach was used to detect horizontal pleiotropic outliers [25], and IVW estimates were performed to further investigate the causal relationship between exposure and outcome through outlier removal. Cochran's Q test was applied to further examine the heterogeneity among all SNPs within each database. Leave-one-out analyses and scatter plots describing the causal relationship between serum urate levels and IBD were also generated.

Animal studies

All animal experimental procedures were approved and conducted in accordance with the guidelines of the Animal Care Committee of Navy Medical University. C57BL/6 mice were kept under a 12-h light/dark cycle with free access to water and a standard rodent diet. Cohoused, seven-week-old male C57BL/6 mice ($n = 5$) were administered 2% dextran sulfate sodium (DSS) (36–50 kDa; MP Biomedicals) in their drinking water ad libitum for 7 consecutive days, followed by 2 d of normal water.

Disease activity score and histological analysis in mice

Body weight, the presence of occult bacteria per rectum, stool consistency, and colon length were documented. A scoring system was used to assess diarrhea and the presence of occult or overt blood in the stool. Changes in body weight are

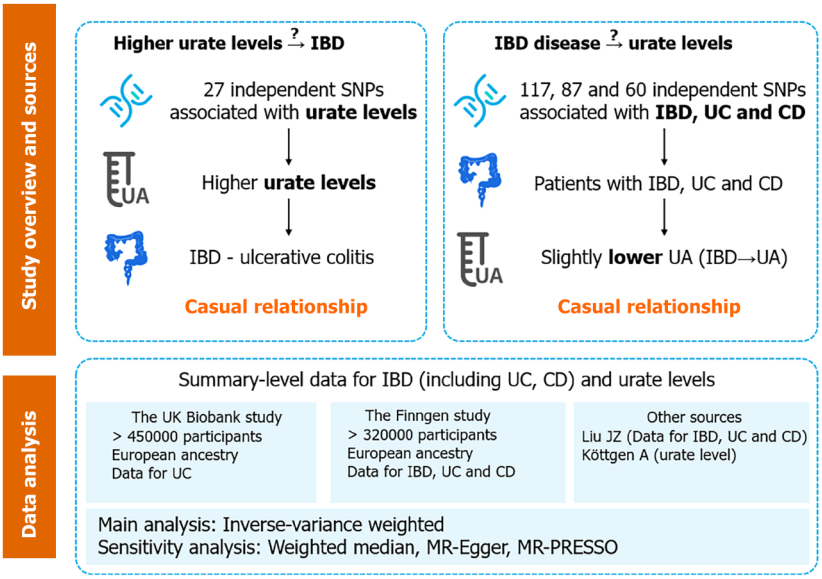

DOI: 10.12998/wjcc.v12.i5.891

Figure 1 Overview of study design. IBD: Inflammatory bowel disease; SNP: Single-nucleotide polymorphisms; UC: Ulcerative colitis; CD: Crohn's disease; UA: Ursolic acid; MR: Mendelian randomization.

reported as the percentage loss of baseline body weight[26]. The ring of the rectum was harvested postmortem, fixed in 4% buffered formalin, and embedded in paraffin for subsequent HE staining.

Enzyme-linked immunosorbent assay

Interleukin (IL)-6, IL-1β, tumor necrosis factor (TNF)-α and urate levels in the serum were quantified using commercial Enzyme-linked immunosorbent assay (ELISA) kits in accordance with the manufacturer's instructions (Multi Sciences Ltd., Hangzhou, China).

MR results are presented as odds ratios (ORs) with 95% confidence intervals (CIs) of the outcome risk of a unit change in exposure. A two-sided *P* value < 0.05 was considered to indicate statistical significance. All the statistical analyses were performed mainly with R software (version 4.2.0, The R Foundation for Statistical Computing; TwoSampleMR and MR-PRESSO package) and SPSS 26.0.

RESULTS

Urate levels to IBD

Twenty-seven independent SNPs were identified as genetic IVs for urate levels, and the median (minimum, maximum) F statistic was 63.4 (35.4-1406.3) (Supplementary Table 1). Detailed information for urate-related SNPs is listed in Supplementary Table 2.

According to the meta-analysis of IVW estimates, the pooled ORs for IBD, UC and CD that were genetically predicted per log-OR increase in urate levels were 0.94 (95%CI: 0.86-1.03), 0.97 (95%CI: 0.89-1.07) and 0.91 (95%CI: 0.80-1.04), respectively (Figure 2).

According to the sensitivity analysis (Supplementary Table 3), the three results were similar for the weighted-median estimator (Supplementary Figure 1). No pleiotropic effects were detected in any of the databases by MR-Egger estimation. Different outliers were identified by MR-PRESSO for IBD (n = 4), UC (n = 5) and CD (n = 5) in the GWAS meta-analysis by Liu *et al*[19] and UC (n = 3) in the UKB database, which resulted in potential pleiotropy assessed by global testing. Most of the results remained similar after outlier exclusion correction, except for IVs of urate levels on UC (UKB database) (before correction: OR = 0.93, 95%CI: 0.75-1.17; after correction: OR = 2.70, 95%CI: 2.54-2.87). Cochran's Q test was performed after outlier exclusion to test heterogeneity. Among the urate level-related genetic IVs affecting IBD and CD identified by Liu *et al*[19] and UC (from the UKB database), a multiplicative random effect IVW model was used to evaluate the genetic estimate after heterogeneity was detected. A strongly positive causal relationship was detected between urate levels and UC after outlier exclusion and between urate levels and UC incidence according to a multiplicative random effects IVW estimate (OR = 1.95, 95%CI: 1.86-2.05). A scatter plot was generated to visualize the effect size of each MR method (Figure 3). Leave-one-out analysis indicated that the associations between urate levels and IBD incidence were unlikely to be driven by certain specific SNPs (Supplementary Figure 2).

IBD-to-urate levels

A total of 117, 87, and 60 SNPs reached a genome-wide level of significance with IBD, UC and CD, respectively. A summary and detailed description of the variants are presented in Supplementary Tables 1 and 4.

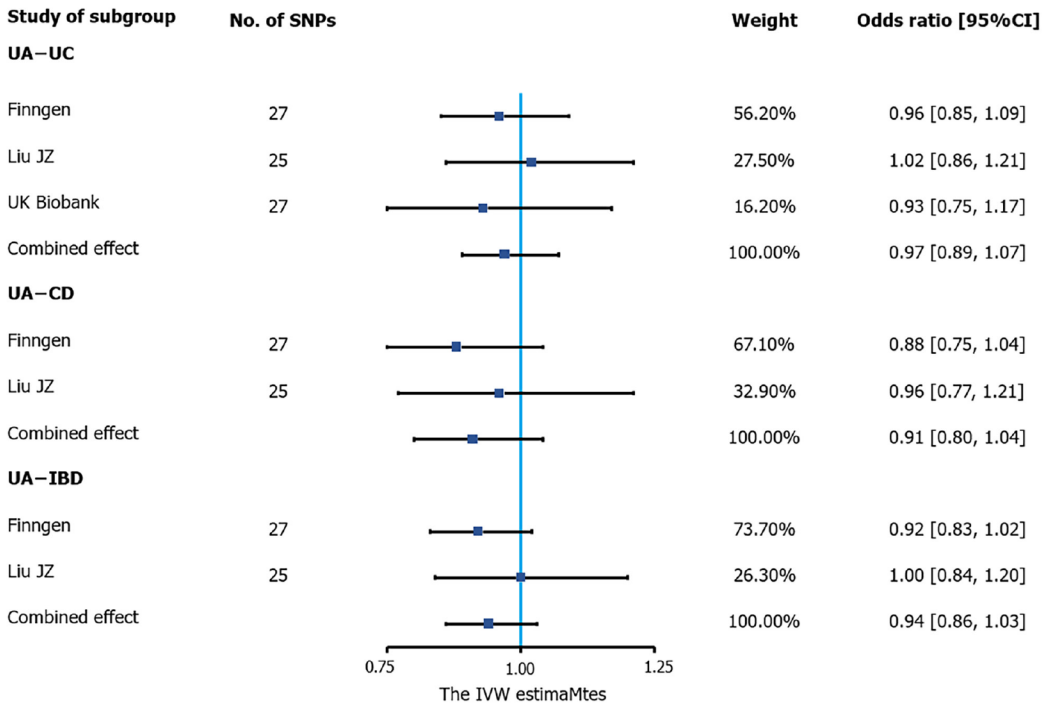

DOI: 10.12998/wjcc.v12.i5.891

Figure 2 Association of urate levels and inflammatory bowel disease in Mendelian randomization analyses (inverse-variance weighted estimate). Estimated odds ratios (OR) represent the effect of per log-OR increase in urate levels on inflammatory bowel disease (IBD), using inverse-variance weighted analysis, per outcome database separately. The meta-analyses combined the three databases (genome-wide association studies meta-analysis by Liu *et al* [19] and the FinnGen and UK Biobank databases) for UC and the former two databases for IBD and Crohn's disease (UK Biobank data were not available) using a fixed-effects model. IBD: Inflammatory bowel disease; UA: Ursolic acid; UC: Ulcerative colitis; SNP: Single-nucleotide polymorphisms; CD: Crohn's disease; CI: Confidence interval; IVW: Inverse-variance weighted.

The results of IVW analysis demonstrated that IBD was negatively correlated with urate levels (OR = 0.97, 95%CI: 0.94-0.99) (Figure 4). However, no association between UC (or CD) and urate levels was observed. The combined ORs of UC and CD on urate levels were 0.99 (95%CI: 0.97-1.01) and 1.00 (95%CI: 0.99-1.02), respectively.

According to the sensitivity analysis (Supplementary Table 5), the weighted-median estimator showed comparable results to the estimates from the IVW analysis (Supplementary Figure 3). MR-Egger analysis demonstrated no evidence of pleiotropy, while the MR-PRESSO global test indicated that there were 7 outliers from the association between IBD and urate levels (P = 0.02) and 2 statistically nonsignificant outliers from the association between CD and urate levels (P = 0.006). Heterogeneity was detected from the association between IBD and urate levels after outlier correction by Cochran's Q statistics. However, the results remained similar after correction for outliers and after the application of the multiplicative random effects IVW estimate (OR = 0.97, 95%CI: 0.94-0.99). A scatter plot was generated to visualize the effect size of each MR method (Figure 5). The results remained consistent in the leave-one-out analysis (Supplementary Figure 4), indicating that the results of the current analyses were stable and reliable.

Results of animal studies, HE staining and ELISA

To validate the positive association between serum urate levels and UC, 2% DSS was used to induce experimental colitis (n = 5 per group). The effects of these treatments included a decrease in body weight (Figure 6A), an increase in the disease activity index (Figure 6B), a decrease in colon length (Figure 6C), and increased inflammatory infiltration according to HE staining (Figure 6D). The expression levels of proinflammatory factors, including IL-6, IL-1β and TNF-α, in the serum were significantly elevated in IBD mice (Figure 6E). Additionally, the serum urate level was also increased in IBD mice (Figure 6F). Together, these results provide evidence that there is a positive association between urate levels and IBD.

DISCUSSION

In the current study, we evaluated the causal relationship between IBD and urate levels. We found evidence that genetic liability to urate levels was strongly associated with a higher risk of UC after outlier correction, and genetic liability to IBD was slightly anticorrelated to urate levels. Animal studies have confirmed the association between high urate levels and IBD. However, our study did not observe a causal relationship between CD and urate levels.

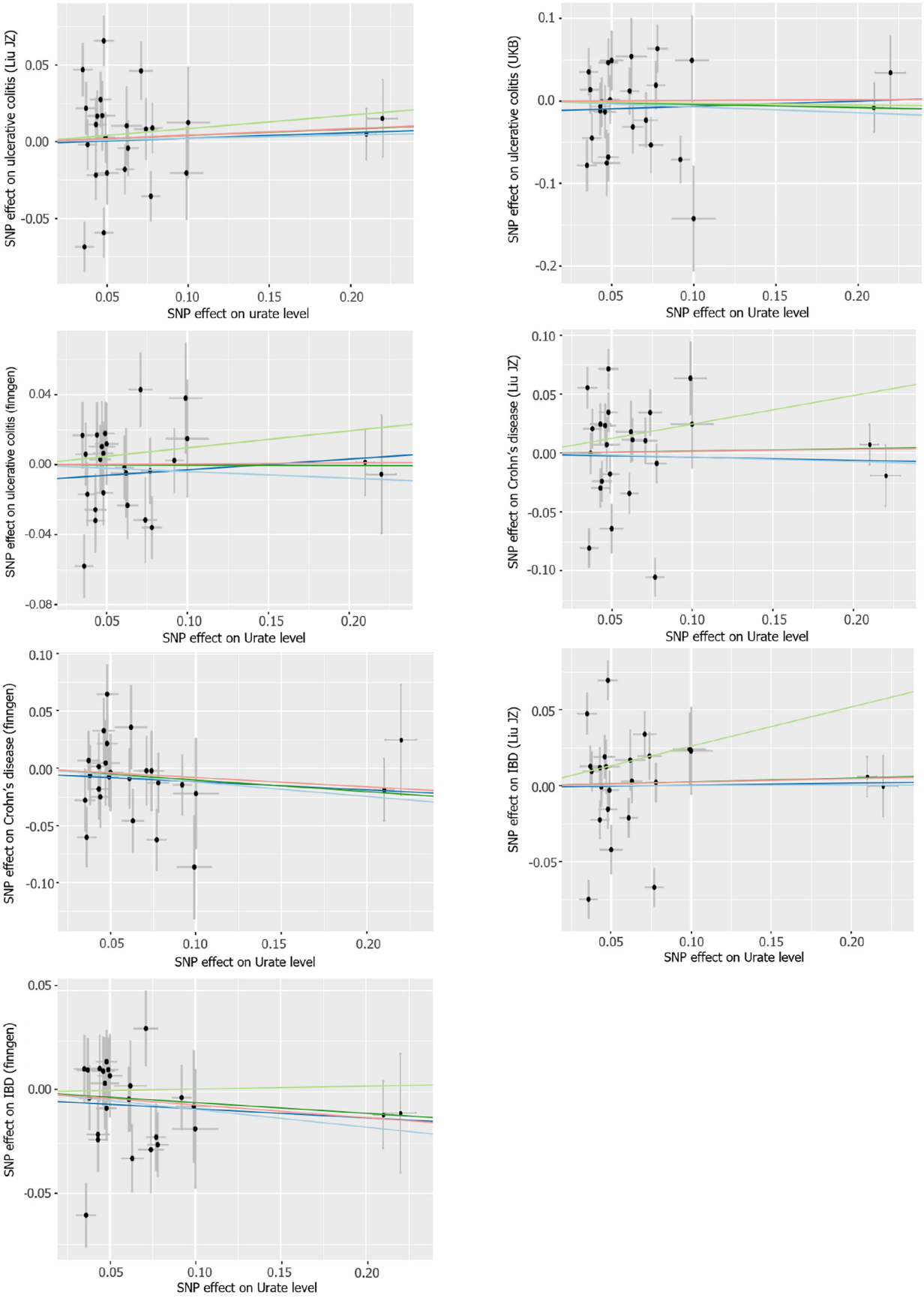

DOI: 10.12998/wjcc.v12.i5.891

Figure 3 Scatter plot of Mendelian randomization analyses from urate levels to inflammatory bowel disease in each database. The X-axes indicate the single-nucleotide polymorphisms (SNPs) of urate levels, while the Y-axes indicate the SNPs of inflammatory bowel disease from different outcome databases. The black dots represent the genetic instruments included in the current Mendelian randomization (MR) analyses. The five colors represent five different

genetic estimates: Red: Inverse-variance weighted; Blue: Weighted-median estimator; Green: MR Egger. IBD: Inflammatory bowel disease; SNP: Single-nucleotide polymorphisms.

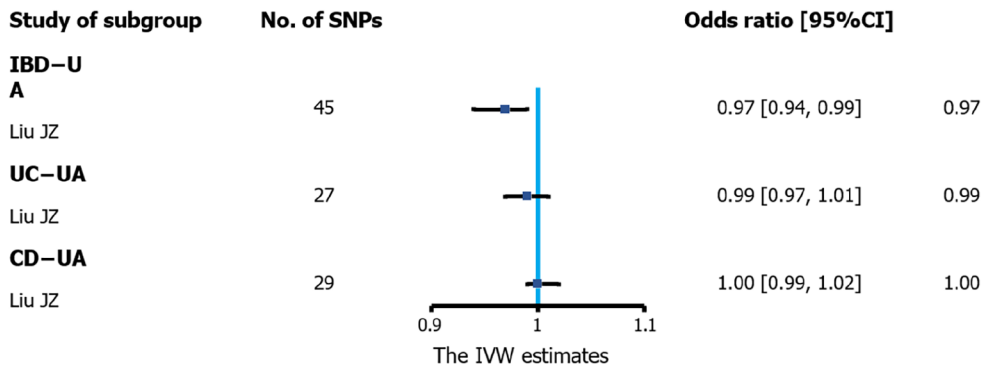

DOI: 10.12998/wjcc.v12.i5.891

Figure 4 Association of inflammatory bowel disease and urate levels in Mendelian randomization analyses (inverse-variance weighted estimate). Estimated odds ratio (OR) represent the effect of per log-OR increase in inflammatory bowel disease on urate levels, using inverse-variance weighted analysis with a fixed-effects model. IBD: Inflammatory bowel disease; UC: Ulcerative colitis; CD: Crohn's disease; CI: Confidence interval; SNP: Single-nucleotide polymorphisms; UA: Ursolic acid; IVW: Inverse-variance weighted.

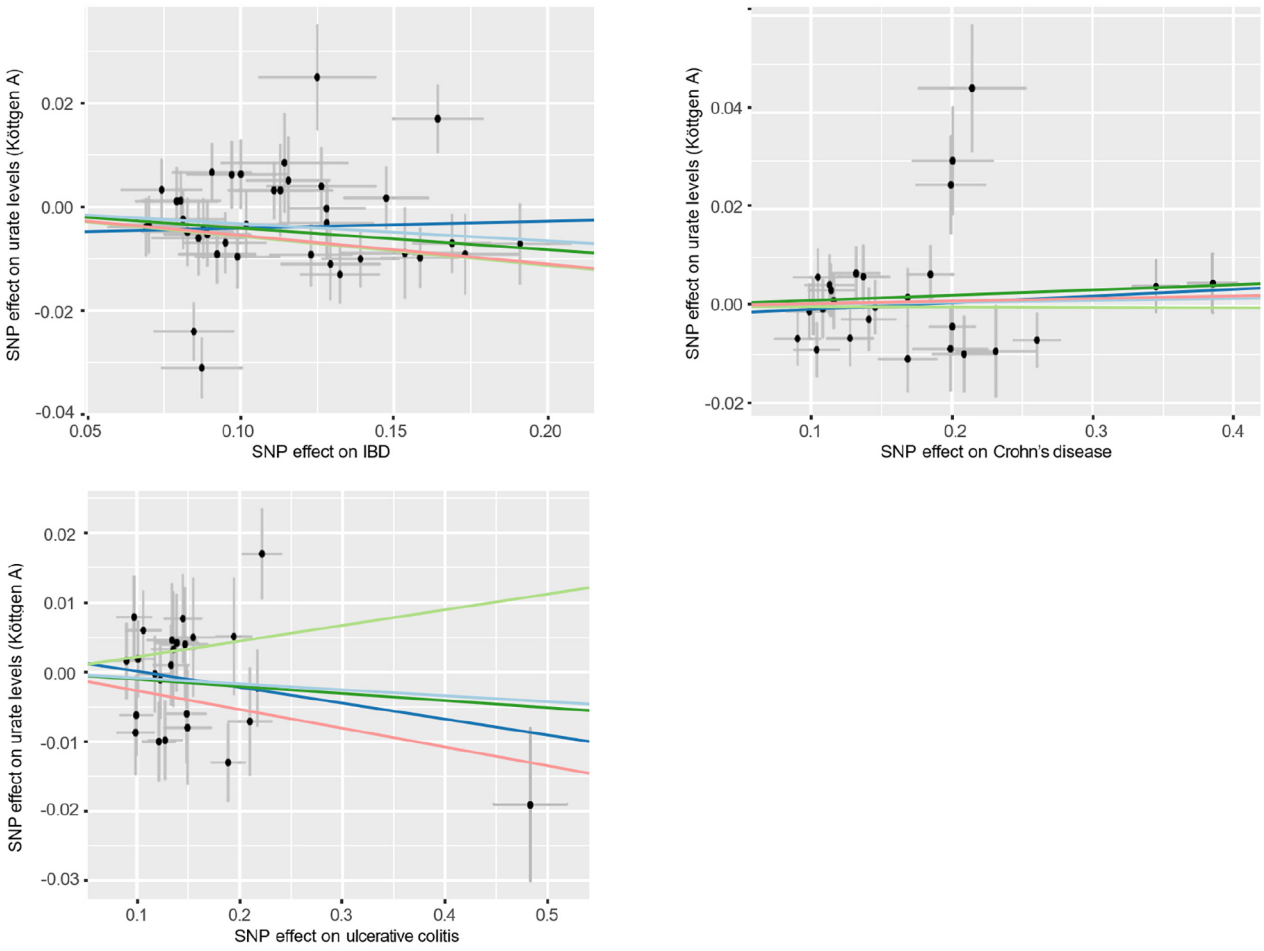

DOI: 10.12998/wjcc.v12.i5.891

Figure 5 Scatter plot of the association of inflammatory bowel disease with urate levels. The detailed description is the same as in Figure 3. IBD: Inflammatory bowel disease; SNP: Single-nucleotide polymorphisms.

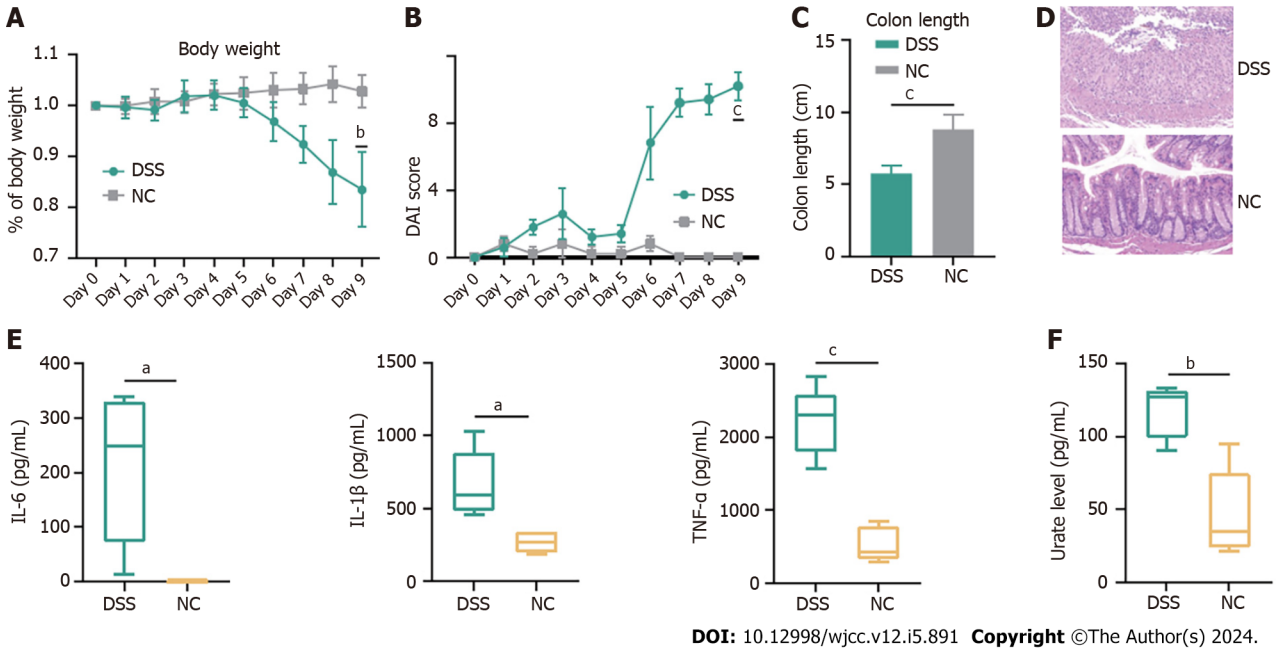

DOI: 10.12998/wjcc.v12.i5.891

Figure 6 Dextran sulfate sodium contributed to increase of inflammation in inflammatory bowel disease mice. C57BL/6 mice were administered dextran sulfate sodium (DSS) (2%) for 7 d (and a control group was provided with water only for comparison) and 2 d for water. A-E: DSS group (n = 5) exhibited a significant aggravation of inflammatory bowel disease-associated changes in of body weight (A), disease activity index (B), colon length (C), inflammatory infiltration (D) and increased levels of interleukin (IL)-6, IL-1β and tumor necrosis factor-α (E); F: Compared with control group (n = 5), DSS group demonstrated increased levels of urate levels. DSS: Dextran sulfate sodium; NC: Control group; IL: Interleukin; TNF: Tumor necrosis factor; DAI: Disease activity index. $^{a}P < 0.05$; $^{b}P < 0.01$; $^{c}P < 0.001$.

Previous observational studies have suggested that urate levels might be a risk factor for IBD. Zhu *et al*[13] included more than four hundred IBD patients and 51 non-IBD controls and reported that urate levels were significantly greater in IBD patients. Similarly, Tian *et al*[14] reported that increased urate levels were associated with UC in a retrospective case-control study. Moreover, IBD patients have an increased incidence of nephrolithiasis as well as urolithiasis[27]. To date, the only MR analysis conducted to investigate the causal relationship of urate levels with IBD has demonstrated that genetically predicted urate levels are not associated with the risk of CD or UC. In part, our study was consistent with previous reports in that we found a strong positive association between urate levels and UC but not with CD or IBD. Animal studies further demonstrated a positive association between urate levels and colitis incidence. In addition, IBD but not UC or CD was inversely correlated with urate levels.

The biological connection between IBD and urate levels has not been fully elucidated. Current studies suggest that intestinal inflammation (including oxidative stress) and dysbiosis of the gut microbiota are the main etiologies of IBD[6]. Increased urate levels mediate the exacerbation of mucosal colitis induced by DSS by enhancing intestinal permeability [15]. Treatment with allopurinol *via* gavage alleviated the pathogenic increase in proinflammatory cytokines and reduced oxidative stress biomarkers in patients with colitis[15,28]. A recent study reported that rhein significantly alleviated DSS-induced colitis and led to decreased urate levels, while the probiotic Lactobacillus was involved in regulating host metabolism[29]. These results support the idea of a relationship between serum urate levels and intestinal inflammation, suggesting that urate levels might be a therapeutic target for IBD. Our results supported previous results that urate levels were positively associated with an increased risk of UC but not with IBD or CD. One of the reasons could be the lack of association between urate levels and CD (a major subtype of IBD). Our results also confirmed that there was no bidirectional causal relationship between urate levels and CD incidence. Furthermore, we considered only the dichotomous IBD diagnosis rather than the IBD course or severity, which greatly influenced patients' clinical manifestations. Further MR analysis should be conducted to investigate the causal relationship between urate levels and disease activity and course of IBD, as relevant GWAS data are available. Moreover, we found a slight inverse association between IBD incidence and urate levels. One possible explanation could be that including summary statistics from only one GWAS increased the heterogeneity and reduced the credibility of our results. A meta-analysis should be conducted once multiple data sources for urate levels are available.

There are three major strengths in the current study. First, the MR design is suitable for causal inference. As an alternative to randomized controlled trials, the MR method can partly avoid bias from confounding factors and reverse causation, which might increase the reliability of the results compared with those of observational studies. To our knowledge, this is the first bidirectional MR analysis investigating the causal relationship between IBD (and its subtypes) and urate levels. Second, we obtained summary-level data from large genetic consortia and GWASs, which included large sample sizes, with 110347 participants for urate levels, 355952 (21846 patients) for IBD, 805082 (16340 patients) for UC and 342185 (9199 patients) for CD. Third, population stratification bias was minimized because all GWAS summary statistics data in the current study were generated from the European population.

Nevertheless, potential limitations in our MR study should be considered. First, MR design can be biased by pleiotropic effects. The current study involved the implementation of various sensitivity analyses, which were performed based on distinct assumptions regarding the fundamental characteristics of pleiotropy, and most of the analyses showed stable results. Moreover, MR-Egger tests and MR-PRESSO analyses were conducted to explore horizontal pleiotropy[24, 25]. After removing potential outlier SNPs, we observed a strong positive causal relationship between urate levels and UC, and most of the results were robust. Second, all participants included in the current study were European, which may limit the generalizability of our findings to other populations. Further MR analyses should be conducted to verify our findings in individuals of non-European descent. Third, in our present research, summary statistics for IBD were obtained from three databases, while data on urate levels were sourced solely from one large GWAS meta-analysis (Köttgen *et al*[18]). The utilization of data from a single source may compromise the reliability of the results. Therefore, once GWAS summary statistics from diverse sources become available, meta-analyses should be conducted to further verify our findings on the inverse association between IBD and urate levels.

The findings that serum urate levels increase the risk of UC add to the evidence from another MR analysis demonstrating a new risk factor for IBD. Recently, a meta-analysis based on large-scale cohorts demonstrated that the consumption of several types of food and drinks, for example, beer, wine, and beef, was associated with increased serum urate levels[30]; however, we are unaware of the risk related to the foods mentioned above. Moreover, many dietary approaches have been developed to reduce inflammation, prevent relapse, and manage the disease severity of IBD[31]. Our current study indicated that monitoring and managing urate levels in patients with IBD and accounting for diets that are associated with elevated urate levels in dietary therapy may provide additional benefits.

CONCLUSION

In summary, we systemically evaluated the potential causal relationship between IBD and urate levels. Our current MR analysis demonstrated that genetically predicted urate levels are causally associated with an elevated risk of UC, while IBD was inversely correlated with urate levels. Considering the close relationship between diet and urate levels, our study provides crucial new insight into treating and preventing IBD. These findings indicate that IBD patients may benefit from monitoring and reducing their serum urate levels.

ARTICLE HIGHLIGHTS

Research background

Inflammatory bowel disease (IBD), mainly consisted of Crohn's disease (CD) and ulcerative colitis (UC), is a chronic inflammatory disease. As a vital antioxidant, urate can decrease oxidative stress *in vivo*, which may be associated with IBD state. However, the causality between IBD and urate levels has not been investigated.

Research motivation

Previous studies indicated uric acid-to-creatinine ratio and urate were positively correlated with the disease activity of CD and UC. Despite the existing findings demonstrated the bidirectional associations between urate levels and IBD, including UC and CD, the causality association between them remains unclear. This study seeks to investigate the causal association between IBD and urate through Mendelian randomization (MR) study, which may shed crucial new insight into treating and preventing IBD. In specific, IBD patients may benefit from monitoring and reducing serum urate levels.

Research objectives

The study aims to investigate the bidirectional causal relationship between urate levels and IBD by performing MR analysis, to better understand the gene susceptibility of urate levels and IBD.

Research methods

Single nucleotide polymorphisms retrieved from genome-wide association studies (GWASs) was selected as instrument variants. Summary GWAS statistics for instrument-outcome associations were retrieved from three separate databases for IBD (UK Biobank, FinnGen database and a large GWAS meta-analysis) and one for urate levels (a large GWAS meta-analysis). Inverse-variance-weighted was performed to investigate the bidirectional causal relationship, and other sensitivity analysis were conducted to strengthen the results. Meta-analysis was conducted to merge the data from separate outcome databases using a fixed-effects model.

Research results

The current study found that the genetic susceptibility to urate levels was associated with increased UC risk [odds ratio (OR): 1.95, 95% confidence interval (CI): 1.86-2.05], and animal studies confirmed the positive association between urate levels and UC. Additionally, genetically predicted IBD was inversely related to urate levels (OR: 0.97, 95%CI: 0.94-0.99). However, no association was observed between genetically influenced UC or CD and urate levels.

Research conclusions

This study identified urate levels might be risk factors for UC, whereas genetically predicted IBD was inversely associated with urate levels. The current results shed new insight into prevention and treatment of IBD.

Research perspectives

Although the current study investigated the causal relationship between urate levels and UC, which was further verified by animal studies, the precise mechanism by which high urate levels affects the development of UC remains unknown. More basic and clinical studies should be conducted for identification of key regulators and molecules during the process.

ACKNOWLEDGEMENTS

We thank the UKB, the Finngen database and the IEU OpenGWAS project for sharing the summary-level data and all efforts from the researchers.

FOOTNOTES

Co-first authors: Song Zhang and Xue Fang.

Co-corresponding authors: Sheng-Bing Zhao and Yu Bai.

Author contributions: Zhang S, Zhao SB and Bai Y designed the research; Zhang S, Kang L and Luo YJ performed the research; Zhang S, Fang X, Kang L and Luo YJ analyzed the data; Sui XY, Liu M and Fu S visualized the data; Zhang S, Fang X, Kang L, Sui XY, Zhao SB and Bai Y wrote the paper; Fang X, Zhao S and Bai Y received the funding; Li ZS, Zhao SB and Bai Y supervised the research.

Supported by National Natural Science Foundation of China, No. 82170567, No. 81873546, No. 82170568, and No. 82300627; Program of Shanghai Academic/Technology Research Leader, No. 22XD1425000; The "Shu Guang" project of Shanghai Municipal Education Commission and Shanghai Education Development Foundation, No. 19SG30, China; Deep Blue Project of Naval Medical University (Pilot Talent Plan); The Chenguang Program of Shanghai Education Development Foundation and Shanghai Municipal Education Commission, No. 22CGA42; The Shanghai Sailing Program, No. 23YF1458600; and Shanghai Natural Science Foundation, No. 23ZR1478700.

Institutional review board statement: The study did not include human trials.

Institutional animal care and use committee statement: All animal experimental procedures were approved and conducted in accordance with the guidelines of the Animal Care Committee of Navy Medical University (CHEC(A.E.)2023-046).

Informed consent statement: All data used in the current manuscript was available online, thus the Signed Informed Consent Form(s) or Document(s) was not applied for the current manuscript.

Conflict-of-interest statement: The authors declare no conflicts of interest.

Data sharing statement: The data underlying this article are available in individual referenced papers, the Finngen database (https://r7.finngen.fi/) and the IEU OpenGWAS project (https://gwas.mrcieu.ac.uk/).

ARRIVE guidelines statement: The authors have read the ARRIVE guidelines, and the manuscript was prepared and revised according to the ARRIVE guidelines.

Country/Territory of origin: China

ORCID number: Song Zhang 0000-0002-8192-8462; Zhao-Shen Li 0000-0003-0404-242X; Sheng-Bing Zhao 0000-0002-1922-451X; Yu Bai 0000-0002-7577-6001.

S-Editor: Fan JR
L-Editor: A
P-Editor: Yu HG

REFERENCES

1 **Khalili H**, Chan SSM, Lochhead P, Ananthakrishnan AN, Hart AR, Chan AT. The role of diet in the aetiopathogenesis of inflammatory bowel disease. *Nat Rev Gastroenterol Hepatol* 2018; **15**: 525-535 [PMID: 29789682 DOI: 10.1038/s41575-018-0022-9]

2 **Ng SC**, Shi HY, Hamidi N, Underwood FE, Tang W, Benchimol EI, Panaccione R, Ghosh S, Wu JCY, Chan FKL, Sung JJY, Kaplan GG. Worldwide incidence and prevalence of inflammatory bowel disease in the 21st century: a systematic review of population-based studies. *Lancet* 2017; **390**: 2769-2778 [PMID: 29050646 DOI: 10.1016/S0140-6736(17)32448-0]

3 **Benchimol EI**, Guttmann A, Griffiths AM, Rabeneck L, Mack DR, Brill H, Howard J, Guan J, To T. Increasing incidence of paediatric inflammatory bowel disease in Ontario, Canada: evidence from health administrative data. *Gut* 2009; **58**: 1490-1497 [PMID: 19651626 DOI: 10.1136/gut.2009.188383]

4 **Frolkis AD**, Dykeman J, Negrón ME, Debruyn J, Jette N, Fiest KM, Frolkis T, Barkema HW, Rioux KP, Panaccione R, Ghosh S, Wiebe S, Kaplan GG. Risk of surgery for inflammatory bowel diseases has decreased over time: a systematic review and meta-analysis of population-based studies. *Gastroenterology* 2013; **145**: 996-1006 [PMID: 23896172 DOI: 10.1053/j.gastro.2013.07.041]

5 **Huang H**, Fang M, Jostins L, Umićević Mirkov M, Boucher G, Anderson CA, Andersen V, Cleynen I, Cortes A, Crins F, D'Amato M, Deffontaine V, Dmitrieva J, Docampo E, Elansary M, Farh KK, Franke A, Gori AS, Goyette P, Halfvarson J, Haritunians T, Knight J, Lawrance IC, Lees CW, Louis E, Mariman R, Meuwissen T, Mni M, Momozawa Y, Parkes M, Spain SL, Théâtre E, Trynka G, Satsangi J, van Sommeren S, Vermeire S, Xavier RJ; International Inflammatory Bowel Disease Genetics Consortium, Weersma RK, Duerr RH, Mathew CG, Rioux JD, McGovern DPB, Cho JH, Georges M, Daly MJ, Barrett JC. Fine-mapping inflammatory bowel disease loci to single-variant resolution. *Nature* 2017; **547**: 173-178 [PMID: 28658209 DOI: 10.1038/nature22969]

6 **Ni J**, Wu GD, Albenberg L, Tomov VT. Gut microbiota and IBD: causation or correlation? *Nat Rev Gastroenterol Hepatol* 2017; **14**: 573-584 [PMID: 28743984 DOI: 10.1038/nrgastro.2017.88]

7 **Buffinton GD**, Doe WF. Depleted mucosal antioxidant defences in inflammatory bowel disease. *Free Radic Biol Med* 1995; **19**: 911-918 [PMID: 8582668 DOI: 10.1016/0891-5849(95)94362-h]

8 **Koutroubakis IE**, Malliaraki N, Dimoulios PD, Karmiris K, Castanas E, Kouroumalis EA. Decreased total and corrected antioxidant capacity in patients with inflammatory bowel disease. *Dig Dis Sci* 2004; **49**: 1433-1437 [PMID: 15481315 DOI: 10.1023/b:ddas.0000042242.22898.d9]

9 **Rahimian R**, Fakhfouri G, Daneshmand A, Mohammadi H, Bahremand A, Rasouli MR, Mousavizadeh K, Dehpour AR. Adenosine A2A receptors and uric acid mediate protective effects of inosine against TNBS-induced colitis in rats. *Eur J Pharmacol* 2010; **649**: 376-381 [PMID: 20868668 DOI: 10.1016/j.ejphar.2010.09.044]

10 **Bourgonje AR**, Feelisch M, Faber KN, Pasch A, Dijkstra G, van Goor H. Oxidative Stress and Redox-Modulating Therapeutics in Inflammatory Bowel Disease. *Trends Mol Med* 2020; **26**: 1034-1046 [PMID: 32620502 DOI: 10.1016/j.molmed.2020.06.006]

11 **Krishnan E**. Inflammation, oxidative stress and lipids: the risk triad for atherosclerosis in gout. *Rheumatology (Oxford)* 2010; **49**: 1229-1238 [PMID: 20202928 DOI: 10.1093/rheumatology/keq037]

12 **Waring WS**. Uric acid: an important antioxidant in acute ischaemic stroke. *QJM* 2002; **95**: 691-693 [PMID: 12324642 DOI: 10.1093/qjmed/95.10.691]

13 **Zhu F**, Feng D, Zhang T, Gu L, Zhu W, Guo Z, Li Y, Lu N, Gong J, Li N. Altered uric acid metabolism in isolated colonic Crohn's disease but not ulcerative colitis. *J Gastroenterol Hepatol* 2019; **34**: 154-161 [PMID: 29926959 DOI: 10.1111/jgh.14356]

14 **Tian S**, Li J, Li R, Liu Z, Dong W. Decreased Serum Bilirubin Levels and Increased Uric Acid Levels are Associated with Ulcerative Colitis. *Med Sci Monit* 2018; **24**: 6298-6304 [PMID: 30196310 DOI: 10.12659/MSM.909692]

15 **Chiaro TR**, Soto R, Zac Stephens W, Kubinak JL, Petersen C, Gogokhia L, Bell R, Delgado JC, Cox J, Voth W, Brown J, Stillman DJ, O'Connell RM, Tebo AE, Round JL. A member of the gut mycobiota modulates host purine metabolism exacerbating colitis in mice. *Sci Transl Med* 2017; **9** [PMID: 28275154 DOI: 10.1126/scitranslmed.aaf9044]

16 **Chen J**, Ruan X, Yuan S, Deng M, Zhang H, Sun J, Yu L, Satsangi J, Larsson SC, Therdoratou E, Wang X, Li X. Antioxidants, minerals and vitamins in relation to Crohn's disease and ulcerative colitis: A Mendelian randomization study. *Aliment Pharmacol Ther* 2023; **57**: 399-408 [PMID: 36645152 DOI: 10.1111/apt.17392]

17 **Lawlor DA**, Harbord RM, Sterne JA, Timpson N, Davey Smith G. Mendelian randomization: using genes as instruments for making causal inferences in epidemiology. *Stat Med* 2008; **27**: 1133-1163 [PMID: 17886233 DOI: 10.1002/sim.3034]

18 **Köttgen A**, Albrecht E, Teumer A, Vitart V, Krumsiek J, Hundertmark C, Pistis G, Ruggiero D, O'Seaghdha CM, Haller T, Yang Q, Tanaka T, Johnson AD, Kutalik Z, Smith AV, Shi J, Struchalin M, Middelberg RP, Brown MJ, Gaffo AL, Pirastu N, Li G, Hayward C, Zemunik T, Huffman J, Yengo L, Zhao JH, Demirkan A, Feitosa MF, Liu X, Malerba G, Lopez LM, van der Harst P, Li X, Kleber ME, Hicks AA, Nolte IM, Johansson A, Murgia F, Wild SH, Bakker SJ, Peden JF, Dehghan A, Steri M, Tenesa A, Lagou V, Salo P, Mangino M, Rose LM, Lehtimäki T, Woodward OM, Okada Y, Tin A, Müller C, Oldmeadow C, Putku M, Czamara D, Kraft P, Frogheri L, Thun GA, Grotevendt A, Gislason GK, Harris TB, Launer LJ, McArdle P, Shuldiner AR, Boerwinkle E, Coresh J, Schmidt H, Schallert M, Martin NG, Montgomery GW, Kubo M, Nakamura Y, Munroe PB, Samani NJ, Jacobs DR Jr, Liu K, D'Adamo P, Ulivi S, Rotter JI, Psaty BM, Vollenweider P, Waeber G, Campbell S, Devuyst O, Navarro P, Kolcic I, Hastie N, Balkau B, Froguel P, Esko T, Salumets A, Khaw KT, Langenberg C, Wareham NJ, Isaacs A, Kraja A, Zhang Q, Wild PS, Scott RJ, Holliday EG, Org E, Viigimaa M, Bandinelli S, Metter JE, Lupo A, Trabetti E, Sorice R, Döring A, Lattka E, Strauch K, Theis F, Waldenberger M, Wichmann HE, Davies G, Gow AJ, Bruinenberg M; LifeLines Cohort Study, Stolk RP, Kooner JS, Zhang W, Winkelmann BR, Boehm BO, Lucae S, Penninx BW, Smit JH, Curhan G, Mudgal P, Plenge RM, Portas L, Persico I, Kirin M, Wilson JF, Mateo Leach I, van Gilst WH, Goel A, Ongen H, Hofman A, Rivadeneira F, Uitterlinden AG, Imboden M, von Eckardstein A, Cucca F, Nagaraja R, Piras MG, Nauck M, Schurmann C, Budde K, Ernst F, Farrington SM, Theodoratou E, Prokopenko I, Stumvoll M, Jula A, Perola M, Salomaa V, Shin SY, Spector TD, Sala C, Ridker PM, Kähönen M, Viikari J, Hengstenberg C, Nelson CP; CARDIoGRAM Consortium; DIAGRAM Consortium; ICBP Consortium; MAGIC Consortium, Meschia JF, Nalls MA, Sharma P, Singleton AB, Kamatani N, Zeller T, Burnier M, Attia J, Laan M, Klopp N, Hillege HL, Kloiber S, Choi H, Pirastu M, Tore S, Probst-Hensch NM, Völzke H, Gudnason V, Parsa A, Schmidt R, Whitfield JB, Fornage M, Gasparini P, Siscovick DS, Polašek O, Campbell H, Rudan I, Bouatia-Naji N, Metspalu A, Loos RJ, van Duijn CM, Borecki IB, Ferrucci L, Gambaro G, Deary IJ, Wolffenbuttel BH, Chambers JC, März W, Pramstaller PP, Snieder H, Gyllensten U, Wright AF, Navis G, Watkins H, Witteman JC, Sanna S, Schipf S, Dunlop MG, Tönjes A, Ripatti S, Soranzo N, Toniolo D, Chasman DI, Raitakari O, Kao WH, Ciullo M, Fox CS, Caulfield M, Bochud M, Gieger C. Genome-wide association analyses identify 18 new loci associated with serum urate concentrations. *Nat Genet* 2013; **45**: 145-154 [PMID: 23263486 DOI: 10.1038/ng.2500]

19 **Liu JZ**, van Sommeren S, Huang H, Ng SC, Alberts R, Takahashi A, Ripke S, Lee JC, Jostins L, Shah T, Abedian S, Cheon JH, Cho J, Dayani

NE, Franke L, Fuyuno Y, Hart A, Juyal RC, Juyal G, Kim WH, Morris AP, Poustchi H, Newman WG, Midha V, Orchard TR, Vahedi H, Sood A, Sung JY, Malekzadeh R, Westra HJ, Yamazaki K, Yang SK; International Multiple Sclerosis Genetics Consortium; International IBD Genetics Consortium, Barrett JC, Alizadeh BZ, Parkes M, Bk T, Daly MJ, Kubo M, Anderson CA, Weersma RK. Association analyses identify 38 susceptibility loci for inflammatory bowel disease and highlight shared genetic risk across populations. *Nat Genet* 2015; **47**: 979-986 [PMID: 26192919 DOI: 10.1038/ng.3359]

20 **Luo J**, Xu Z, Noordam R, van Heemst D, Li-Gao R. Depression and Inflammatory Bowel Disease: A Bidirectional Two-sample Mendelian Randomization Study. *J Crohns Colitis* 2022; **16**: 633-642 [PMID: 34739073 DOI: 10.1093/ecco-jcc/jjab191]

21 **Jiang L**, Zheng Z, Fang H, Yang J. A generalized linear mixed model association tool for biobank-scale data. *Nat Genet* 2021; **53**: 1616-1621 [PMID: 34737426 DOI: 10.1038/s41588-021-00954-4]

22 **Burgess S**, Butterworth A, Thompson SG. Mendelian randomization analysis with multiple genetic variants using summarized data. *Genet Epidemiol* 2013; **37**: 658-665 [PMID: 24114802 DOI: 10.1002/gepi.21758]

23 **Bowden J**, Davey Smith G, Haycock PC, Burgess S. Consistent Estimation in Mendelian Randomization with Some Invalid Instruments Using a Weighted Median Estimator. *Genet Epidemiol* 2016; **40**: 304-314 [PMID: 27061298 DOI: 10.1002/gepi.21965]

24 **Bowden J**, Davey Smith G, Burgess S. Mendelian randomization with invalid instruments: effect estimation and bias detection through Egger regression. *Int J Epidemiol* 2015; **44**: 512-525 [PMID: 26050253 DOI: 10.1093/ije/dyv080]

25 **Verbanck M**, Chen CY, Neale B, Do R. Detection of widespread horizontal pleiotropy in causal relationships inferred from Mendelian randomization between complex traits and diseases. *Nat Genet* 2018; **50**: 693-698 [PMID: 29686387 DOI: 10.1038/s41588-018-0099-7]

26 **Wirtz S**, Neufert C, Weigmann B, Neurath MF. Chemically induced mouse models of intestinal inflammation. *Nat Protoc* 2007; **2**: 541-546 [PMID: 17406617 DOI: 10.1038/nprot.2007.41]

27 **van Sommeren S**, Janse M, Karjalainen J, Fehrmann R, Franke L, Fu J, Weersma RK. Extraintestinal manifestations and complications in inflammatory bowel disease: from shared genetics to shared biological pathways. *Inflamm Bowel Dis* 2014; **20**: 987-994 [PMID: 24739630 DOI: 10.1097/MIB.0000000000000032]

28 **El-Mahdy NA**, Saleh DA, Amer MS, Abu-Risha SE. Role of allopurinol and febuxostat in the amelioration of dextran-induced colitis in rats. *Eur J Pharm Sci* 2020; **141**: 105116 [PMID: 31654756 DOI: 10.1016/j.ejps.2019.105116]

29 **Wu J**, Wei Z, Cheng P, Qian C, Xu F, Yang Y, Wang A, Chen W, Sun Z, Lu Y. Rhein modulates host purine metabolism in intestine through gut microbiota and ameliorates experimental colitis. *Theranostics* 2020; **10**: 10665-10679 [PMID: 32929373 DOI: 10.7150/thno.43528]

30 **Major TJ**, Topless RK, Dalbeth N, Merriman TR. Evaluation of the diet wide contribution to serum urate levels: meta-analysis of population based cohorts. *BMJ* 2018; **363**: k3951 [PMID: 30305269 DOI: 10.1136/bmj.k3951]

31 **Halmos EP**, Gibson PR. Dietary management of IBD--insights and advice. *Nat Rev Gastroenterol Hepatol* 2015; **12**: 133-146 [PMID: 25645969 DOI: 10.1038/nrgastro.2015.11]

World Journal of Clinical Cases

Submit a Manuscript: https://www.f6publishing.com

World J Clin Cases 2024 February 16; 12(5): 903-912

DOI: 10.12998/wjcc.v12.i5.903

ISSN 2307-8960 (online)

ORIGINAL ARTICLE

Retrospective Cohort Study

Effect of health education based on information-motivation-behavioral skills model on patients with unilateral vestibular dysfunction

Qiong Shi, Ruo-Jun Wu, Jiang Liu

Specialty type: Medicine, research and experimental

Provenance and peer review: Unsolicited article; Externally peer reviewed.

Peer-review model: Single blind

Peer-review report's scientific quality classification

Grade A (Excellent): 0
Grade B (Very good): 0
Grade C (Good): C
Grade D (Fair): 0
Grade E (Poor): 0

P-Reviewer: Karras S, Greece

Received: October 26, 2023
Peer-review started: October 26, 2023
First decision: November 8, 2023
Revised: December 5, 2023
Accepted: January 19, 2024
Article in press: January 19, 2024
Published online: February 16, 2024

Qiong Shi, Jiang Liu, Department of Neurology, Wuahan Fourth Hospital, Wuhan 430000, Hubei Province, China

Ruo-Jun Wu, Department of Critical Care Medicine, Wuhan No. 1 Hospital, Wuhan 430033, Hubei Province, China

Corresponding author: Jiang Liu, Nurse, Department of Neurology, Wuahan Fourth Hospital, No. 473 Hanzheng Street, Wuhan 430000, Hubei Province, China. shiqiong202307@163.com

Abstract

BACKGROUND

Vestibular dysfunction (VH) is a common concomitant symptom of late peripheral vestibular lesions, which can be trauma, poisoning, infection, heredity, and neurodegeneration, but about 50% of the causes are unknown. The study uses the information-motivation-behavioral skills (IMB) model for health education, effectively improve the quality of life, increase their self-confidence, reduce anxiety and depression, and effectively improve the psychological state of patients.

AIM

To explore the effect of health education based on the IMB model on the degree of vertigo, disability, anxiety and depression in patients with unilateral vestibular hypofunction.

METHODS

The clinical data of 80 patients with unilateral vestibular hypofunction from January 2019 to December 2021 were selected as the retrospective research objects, and they were divided into the control group and the observation group with 40 cases in each group according to different nursing methods. Among them, the control group was given routine nursing health education and guidance, and the observation group was given health education and guidance based on the IMB model. The changes in self-efficacy, anxiety and depression, and quality of life of patients with unilateral VH were compared between the two groups.

RESULTS

There was no significant difference in General Self-Efficacy Scale (GSES) scale

scores between the two groups of patients before nursing ($P > 0.05$), which was comparable; after nursing, the GSES scale scores of the two groups were higher than those before nursing. The nursing group was higher than the control group, and the difference was statistically significant ($P < 0.05$). There was no significant difference in the scores of Hospital Anxiety and Depression Scale (HADS) and anxiety and depression subscales between the two groups before nursing ($P > 0.05$). After nursing, the HADS score, anxiety, and depression subscale scores of the two groups of patients were lower than those before nursing, and the nursing group was lower than the control group, and the difference was statistically significant ($P < 0.05$). After nursing, the Dizziness Handicap Inventory (DHI) scale and DHI-P, DHI-E and DHI-F scores in the two groups were decreased, and the scores in the nursing group were lower than those in the control group, and the difference was statistically significant ($P < 0.05$).

CONCLUSION

Health education based on the IMB model can effectively improve patients' quality of life, increase self-efficacy of patients with unilateral vestibular hypofunction, enhance patients' confidence, enable patients to resume normal work and life as soon as possible, reduce patients' anxiety and depression, and effectively improve patients' psychological status.

Key Words: Information-motivation-behavioral skills model; Health education; Vestibular function; Quality of life; Self-efficacy

Core Tip: Vestibular dysfunction (VH) is a common concomitant symptom in the late stage of various external vestibular diseases, and the etiology is unknown in about 50% of cases. In this paper, 80 patients with unilateral VH were selected as retrospective research objects. We found that health education based on information-motivation-behavioral skills model can effectively improve the quality of life of patients, improve the self-efficacy of patients with unilateral VH, enhance their self-confidence, enable them to return to normal work and life as soon as possible, and reduce their anxiety and depression. Effectively improve the psychological state of patients.

Citation: Shi Q, Wu RJ, Liu J. Effect of health education based on information-motivation-behavioral skills model on patients with unilateral vestibular dysfunction. *World J Clin Cases* 2024; 12(5): 903-912
URL: https://www.wjgnet.com/2307-8960/full/v12/i5/903.htm
DOI: https://dx.doi.org/10.12998/wjcc.v12.i5.903

INTRODUCTION

Vestibular dysfunction (VH) is a common concomitant symptom in the late stages of a variety of peripheral vestibular lesions, and although the cause of VH may be traumatic, toxic, infectious, genetic, or neurodegenerative, the etiology is unknown in approximately 50% of cases[1,2]. Postural instability, blurred vision during head movements, dizziness, and imbalance can occur in the decompensated phase after vestibular function injury[3]. In recent years, the incidence of vestibular vertigo has been increasing with the increase of various adverse factors and the aging of the population[4]. Vertigo and dizziness due to vestibular hypofunction can also cause a series of psychological problems, such as depression and anxiety, if not taken care of in a timely manner. Unilateral VH (UVH) is observed and measured by video nystagmography, and vestibular function is assessed using the slow-phase velocity of the vestibular oculomotor reflex with a hemiplegic value greater than or equal to 25% on one side[5]. The information-motivation-behavioral skills (IMB) model can be used both as a model to predict health behaviors and as a framework of care for patients in terms of information, motivation, and behavioral skills to induce behavioral change[6]. Information is an important component in the IMB model, but it is not sufficient by itself to change behavior; information and motivation lead to changes in individual attitudes, but individuals need behavioral skills to put their behaviors into practice[7]. The IMB model posits that information and motivation activate behavioral skills that lead to behavior change and maintenance of change; information and motivation may also have a direct impact on health behaviors, especially when accomplishing specific Behavior does not require complex or new behavioral skills when the IMB model has the advantage of incorporating self-efficacy theory, drawing on rational behavior theory's understanding of motivation, and integrating various factors that influence behavior, which has higher feasibility[8].

Currently, no studies have been seen using the IMB model of health education for the care of patients with VH. Although research on vestibular rehabilitation started earlier in China, there is still a gap between the research on vestibular rehabilitation and foreign countries, and the development of vestibular rehabilitation exercises and the implementation of individualized vestibular rehabilitation are not ideal[9]. Nowadays, with economic development people's requirements for quality of life are increasing, and the benefits that patients can obtain from vestibular rehabilitation should not be ignored. Our study attempts to use the IMB model of health education as a guide, aiming to

improve patients' self-efficacy, reduce symptoms, improve their quality of life, return them to normal life sooner and use their professional knowledge to avoid health misconceptions in their daily life.

MATERIALS AND METHODS

Research object

The clinical data of 80 patients with unilateral VH from January 2019 to December 2021 were selected as the subjects of a retrospective study and divided into a comparison group and an observation group of 40 cases each according to the mode of care. UVH diagnosis[6]: Vestibular oculomotor reflexes were observed and measured by video nystagmography, and vestibular function was assessed using the slow-phase velocity of the vestibular oculomotor reflex with a value of light paralysis of the semicircular canal on one side The value of hemiplegia on one side was greater than or equal to 25%. The data collected in our study were used only for clinical research and data analysis, not for other purposes, and no other personnel had the right to use the study data without the consent of the study subjects, which helped the patients to improve their dizziness symptoms and did not cause any physical or mental harm to them.

Include exclusion criteria

Inclusion criteria: (1) Vestibular function examination (hot and cold test) with results reported as unilateral VH, age ≥ 18 years, with elementary school or above education; (2) patients with self-care ability, able to understand and cooperate with our study, detailed and complete clinical information of patients and their families; and (3) patients in non-acute vertigo period, able to cooperate with hot and cold test examination.

Exclusion criteria: (1) Those with cognitive impairment or mental illness, unable to communicate normally, with otolithic balance test (+); (2) those with other types of vertigo, such as acute vertigo, central vertigo, traumatic vertigo, with serious cardiovascular system diseases, respiratory system diseases or major diseases in other parts of the body and serious systemic diseases; and (3) those with a history of malignant tumors, unable to rehabilitation training, such as cervical spondylosis, bone and joint disease, visual impairment, hemiplegia, pregnancy, *etc.*, and the use of vestibular inhibitory drugs such as flunarizine hydrochloride, vertigo stop, diazepam, *etc.* within 48 h.

Routine nursing health education and guidance

Patients fill out questionnaires and scales in detail at the first visit. Nurses introduce patients to knowledge related to vestibular function, high-risk factors, medication guidance, *etc.*, and carefully answer patients' questions about disease treatment and rehabilitation. Psychological care: anxiety and depression can interact with vertigo and dizziness symptoms, so you should divert your attention appropriately and keep a relaxed state of mind. Treatment in case of vertigo attack: When vertigo occurs, lie down close to the bed or sit on the ground to avoid falling. Inform patients that vestibular rehabilitation exercises can help relieve the symptoms of dizziness and vertigo, and instruct them on general vestibular rehabilitation exercises: (1) Patients take a lying or sitting position to practice repeatedly according to the situation (the speed is first slow and then fast: Look up and down with both eyes; look left and right with both eyes; stare at fingers with both eyes and move from 1 meter to 0.3 meter in front of you; tilt your head forward and then backward; turn your head left and right (the latter two practice with eyes open first and then with eyes closed); (2) patients take a sitting position: shrugging shoulders around; upper body leaning forward and picking up objects from the floor; (3) patients were in the standing position for the first two steps, and then practiced separately: Sitting to standing with eyes open and closed; passing the ball from left to right hand; turning and standing from the seat; and (4) activities: Patients practiced walking across the room with eyes open and closed, respectively; walking back and forth up ramps and steps; any movement that required bending and stretching. Repeat each movement 20 times, 2-3 times a day. The method and precautions. At the biweekly review, the questions raised by the patients were answered and the patients were instructed to review on time.

Health education and guidance based on the IMB model

Information care: Patients were given the "Knowledge manual related to vestibular hypofunction" to explain the knowledge about vestibular hypofunction, high-risk factors, clinical manifestations, *etc.*, and to inform patients of the importance of vestibular rehabilitation exercises for symptom relief, *etc.*, so as to eliminate patients' potential anxiety due to lack of disease knowledge; when the care was repeated, the patients' mastery of the previous care was first assessed, and the weak points were supplemented. Commonly used drugs for vestibular hypofunction mainly include drugs to improve microcirculation, symptomatic supportive therapy, glucocorticoids, *etc.*; inform patients of the name, dosage, usage, and adverse effects of commonly used drugs. Inform patients of the risks of the disease to their own safety, make a good assessment of the safety of their home environment, ensure adequate rest and sleep, and avoid overexertion. Normal daily activities can be performed, avoid strenuous exercise, and to reduce the risk of falls, elderly patients need to be accompanied by family members when going out. Patients are invited to add WeChat or contact phone numbers to answer questions related to rehabilitation treatment, send weekly information about diseases related to vestibular hypofunction, rehabilitation exercise videos, *etc.*, and instruct patients to review on time.

Behavioral care: Provide patients with a good environment for medical care, receive only one patient at a time, fully protect patients' privacy, actively communicate with patients, understand the impact of the disease on their work and life, listen to patients' concerns during the disease treatment process, encourage patients to express their inner thoughts and health needs, and answer patients' questions one by one. We also use this as a basis to assess the patient's perception of

the disease so that we can give appropriate guidance to the patient's specific situation in educational nursing care and provide strong support to the patient. Patients were introduced to cases of successful treatment of dizziness and vertigo to enhance their confidence, encouraged to state the reasons that led to their lack of confidence in treatment and affected their health behaviors, enhanced their determination to actively cooperate with treatment through comfort, encouragement and praise, and set goals for rehabilitation exercises together with patients to motivate them to join rehabilitation exercises on their own initiative. Ask patients about the difficulties they encounter in the rehabilitation process and answer them during the biweekly review. Understand the support status of the patient's family and friends; provide guidance to the patient's family along with health guidance, instruct the family on ways to help the patient improve his anxiety and depression, and encourage and supervise the patient's daily rehabilitation exercises at home.

Vestibular rehabilitation exercises instruction: Patients raise their arms, put their fingers in front of their eyes and keep them still, look at their fingers levelly and turn their heads from side to side. The patient raises the arm, places the finger in front of the eyes and keeps it still, looks at the finger with the eyes level, then closes the eyes while trying to fix the eyes on the position where the finger rests, then turns the head from side to side, then opens the eyes to see if the eyes are looking at the finger, starting with the head in the center position. The patient keeps gazing at the fixed target in front while moving the head up and down and repeating the previous movements. Each movement is practiced for 1-2 min, 2-3 times a day. Patients stand with eyes open, gradually reduce the distance between the feet, and practice standing with eyes closed after being able to maintain stability. Patients open their eyes and stand on their toes next to their heels and walk with their feet back and forth, and practice walking with eyes closed after being able to maintain balance, and instruct patients to intersperse head movements (*e.g.*, head twisting, turning, *etc.*) while walking. Each posture for 15-30 s, 2-3 times a day. The patient's upper body is upright and sits on the edge of the bed with legs naturally hanging down; quickly lie on the bed to the right side, turn the face 45° to the opposite side in front and above, keep the position of legs unchanged, sit up for 30 s after waiting for the vertigo to disappear, if the patient does not feel vertigo, sit up for 30 s after resting, quickly lie on the bed to the left side, turn the face 45° to the opposite side in front and above, sit up after 30 s, alternate sides. Repeat each movement 10-20 times, 2-3 times a day.

Observation ation indicator

The Self-Efficacy Scale (SES) consists of 10 items, each with 4 options and a score range of 1 to 4. The total score of the scale is the sum of the items divided by 10, and the higher the score, the higher the patient's self-efficacy. The consistency coefficient was 0.87, the retest reliability was 0.83, and the half reliability was 0.82, which had good reliability and validity. The Dizziness Handicap Inventory (DHI) is a 25-item, 3-dimensional scale that assesses the functional, emotional and physical impairment and quality of life of patients with vertigo, with 3 answers for each item: "yes (4 points), sometimes (2 points), no (0 points)"; the total score ranges from 0 to 100. The higher the score, the higher the impact of vertigo on the patient. The Hospital Anxiety and Depression Scale (HADS) is used to screen patients attending general medical clinics for anxiety and depression. It has the advantage of being simple, quick and easy to use, and consists of two subscales that rate depression and anxiety, each with 7 entries, 4 answers per entry, and a score of 0 to 3. The scores of the two subscales of anxiety and depression are divided as follows: 0-7 for asymptomatic; 8-10 for suspicious symptoms; and 11-21 for definitely present symptoms.

Statistical analysis

All data from our study were checked using Excel double entry, and SPSS 23.0 was used for statistical analysis, setting the test level $\alpha = 0.05$ and considering $P < 0.05$ as a statistically significant difference. Statistical descriptions of measurement data obeyed normal distribution were described by mean ± SD, and those not obeying normal distribution were described by median (interquartile spacing), and count data were described by frequency and composition ratio. General patient data were analyzed: Categorical data were analyzed by chi-square test, continuity-corrected chi-square test, and Fisher's exact probability method; measurement data were analyzed by *t*-test. Obedience to normal distribution, paired samples *t*-test was used for within-group comparisons and two independent samples *t*-test for between-group comparisons; disobedience to normal distribution, nonparametric test-Wilcoxon signed-rank test was used for within-group comparisons and rank sum test was used for between-group comparisons for analysis.

RESULTS

Comparison of baseline information

The mean age, gender, and education of the patients in the observation group were not significantly different from those in the weight comparison group, and none of the comparative differences were statistically significant ($P > 0.05$) (Table 1).

Comparison of self-efficacy

The difference between the General SES (GSES) scores of the two groups of patients before care was not statistically significant ($P > 0.05$) and was comparable; the GSES scale scores of the two groups of patients after care were higher than those before care, and the difference between the GSES scale scores of the two groups of patients after care was higher than that of the control group ($P < 0.05$) (Figure 1).

Anxiety and depression comparison

There was no significant difference in the scores of HADS and anxiety and depression subscales between the two groups

Table 1 Comparison of baseline information between the two groups of patients

Group	Average age (yr)	Gender (male/female)	Body weight (kg)	Education level		
				Junior high school	High school	University and above
Comparison group (40)	60.90 ± 1.71	24/26	66.35 ± 2.10	12	12	16
Observation group (40)	61.10 ± 1.62	23/27	64.10 ± 1.10	13	10	17
t value	0.377	0.731	2.107	0.252		
P value	0.051	0.067	0.079	0.882		

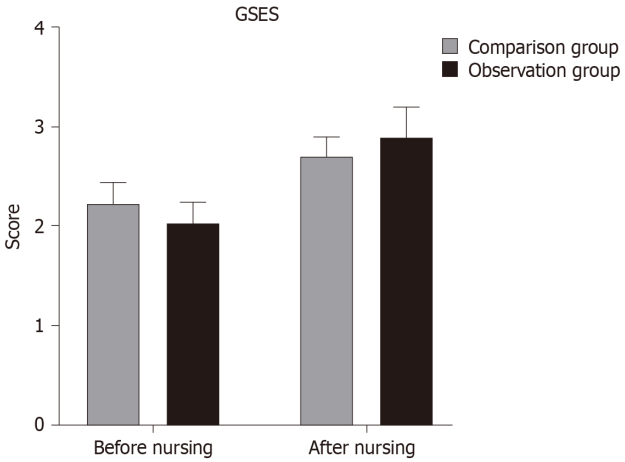

DOI: 10.12998/wjcc.v12.i5.903

Figure 1 Self-efficacy comparison (all self-efficacy data in our study were checked by Excel double entry, SPSS 23.0 was used for statistical analysis, and the mean ± SD was used for description. Using *t* test, it was found that there was no significant difference in the General Self-Efficacy Scale (GSES) score between the two groups of patients before nursing ($P > 0.05$), with comparability; the GSES scale scores of the two groups of patients after nursing were higher than those before nursing, and the comparison of the GSES scale scores of the two groups after nursing showed that the nursing group was higher than the control group, and the difference was statistically significant ($P < 0.05$). GSES: General Self-Efficacy Scale.

before nursing ($P > 0.05$). After nursing, the HADS score, anxiety (HADS-A), and depression (HADS-D) subscale scores of the two groups of patients were lower than those before nursing, and the nursing group was lower than the control group, and the difference was statistically significant ($P < 0.05$) (Figure 2).

Quality of life comparison

Before nursing, there was no significant difference in the total DHI scale score and DHI-P, DHI-E and DHI-F dimension scores between the two groups ($P > 0.05$). After nursing, the DHI scale and DHI-P, DHI-E and DHI-F scores in the two groups were all decreased, and the scores in the nursing group were lower than those in the control group, and the difference was statistically significant ($P < 0.05$) (Figure 3).

DISCUSSION

Initially, care for vertigo in China was mainly directed at the etiology of the disease, but different etiologies often leave similar dysfunctions, which continue to have an impact on the quality of life of patients[10]. In recent years, research on the care of VH has gradually increased, and studies by scholars have confirmed that vestibular rehabilitation exercises can reduce clinical symptoms such as vertigo and improve the quality of life of patients[11]. Some scholars used the medical-nursing cooperation model to care for patients with VH, and the results showed that this model can effectively promote the functional recovery of patients[12]. The effect of health guidance based on the WeChat platform on the rehabilitation management of patients with vestibular function was investigated[13]. The rehabilitation management based on the WeChat platform enhanced the supervision of patients' rehabilitation training and promoted the improvement of patients' vertigo symptoms[14].

In our study, the GSES scale scores of patients in both groups were higher after care than before care, and the GSES scale scores of patients in both groups were higher in the care group than in the control group after care, with statistically significant differences. It indicates that both intervention methods have a certain effect on improving patients' self-efficacy. The reasons for this were analyzed as, on the one hand, the patients did not know much about vestibular hypofunction before the consultation and knew little about the management of vertigo and dizziness episodes, and the

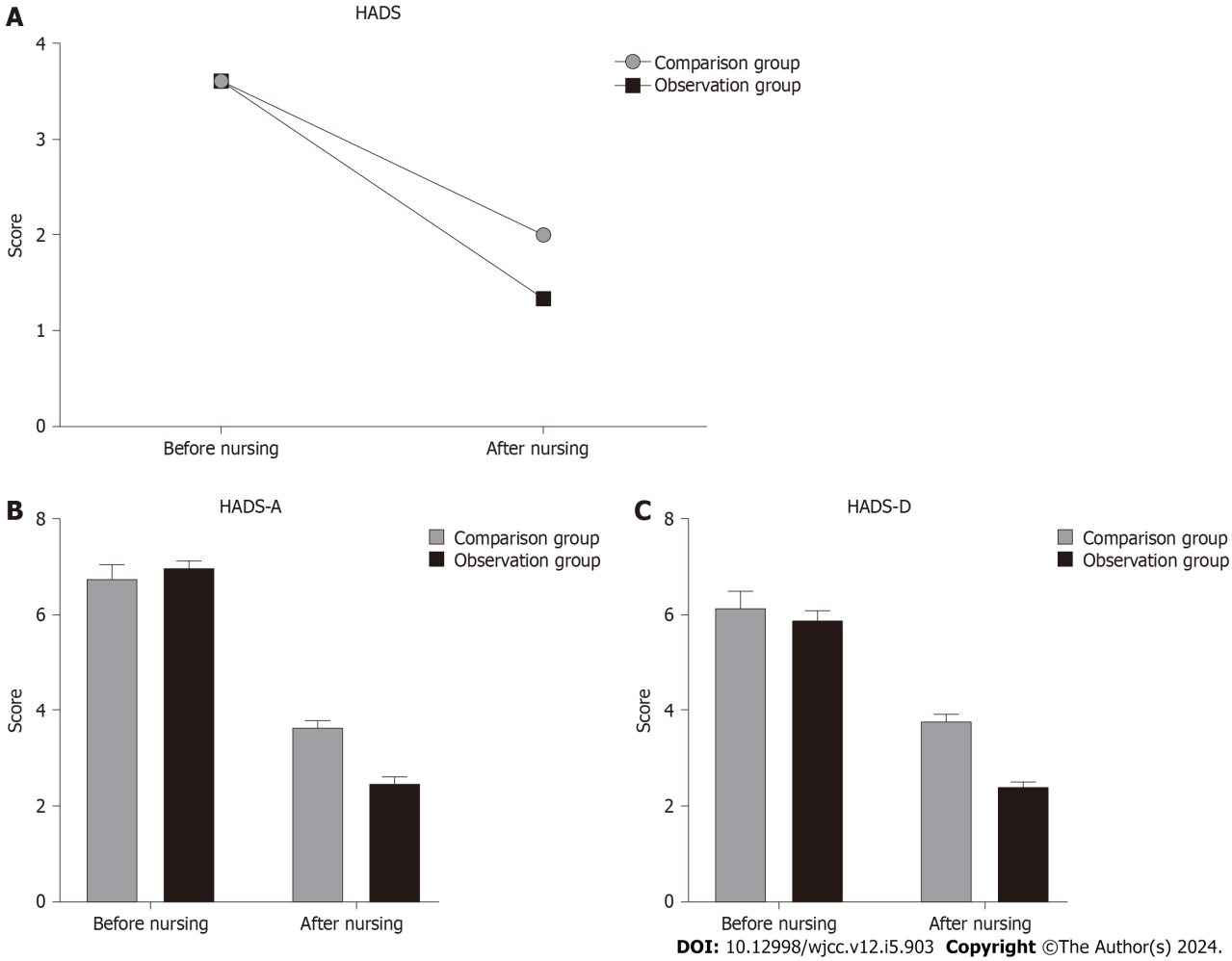

DOI: 10.12998/wjcc.v12.i5.903

Figure 2 Anxiety and depression comparison. A: Hospital Anxiety and Depression Scale (HADS) scores in the comparison group and observation group; B: Hospital Anxiety and Depression Scale-anxiety (HADS-A) scores in the comparison group and observation group; C: Hospital Anxiety and Depression Scale-depression (HADS-D) scores in the comparison group and observation group. All anxiety and depression data in our study were checked by Excel double entry, SPSS 23.0 was used for statistical analysis, and the mean ± SD was used for description. The *t* test found that the scores of the HADS scale and anxiety and depression subscale scores of the two groups of patients before nursing were compared, the difference was not statistically significant ($P > 0.05$). After nursing, the HADS score, HADS-A and HADS-D subscale scores of the two groups of patients were lower than those before nursing, and the nursing group was lower than the control group, and the difference was statistically significant ($P < 0.05$).

repeated vertigo and dizziness episodes affected the patients' work and life[15]. After the consultation patients received more information about the disease, learned the appropriate skills to relieve vertigo and dizziness, and improved their self-confidence to cope with the disease[16]. On the other hand, IMB mode health education was provided to patients through disease knowledge, communication through WeChat, video explanation of rehabilitation exercises, knowledge booklet distribution, case sharing, and motivational interventions[7]. It enables patients to receive more professional and comprehensive information and participate in the rehabilitation training of the disease, so that they have a more positive attitude and more confidence to cope with the current disease condition[17]. No domestic studies on the intervention of IMB model health education for patients with vestibular hypofunction have been retrieved.

The HADS-A and HADS-D subscale scores of patients in both groups after our study care were lower than before care, and both care groups were lower than the control group, and the differences were statistically significant. The classical treatment of VH relies on vestibular rehabilitation and symptomatic medication, of which vestibular rehabilitation is an exercise-based dizziness treatment that is mainly used to reduce vestibular symptoms[18]. Studies by scholars have shown that nurse-led vestibular rehabilitation exercises improve patients' vestibular discomfort symptoms earlier and enhance their balance confidence[19]. The patients' DHI scale scores decreased significantly, similar to the results of our study[20]. Conventional health education is mostly delivered verbally; in our study, IMB model-based health education was used to train patients on rehabilitation exercises and explain the exercise steps to them in detail[21]. Not only is the appropriate exercise method selected according to the individual patient, but it is also adjusted according to the patient's rehabilitation progress at the time of review[16]. Patients were also intervened through personal motivation and social motivation aspects to enhance their self-efficacy, strengthened their understanding of the importance of vestibular rehabilitation, and given appropriate guidance by understanding the reasons that prevented them from performing rehabilitation training[22]. The patients and their families were made to actively participate in vertigo treatment and rehabilitation exercises, and the patients had more motivation and confidence to adhere to the exercises[23]. With the

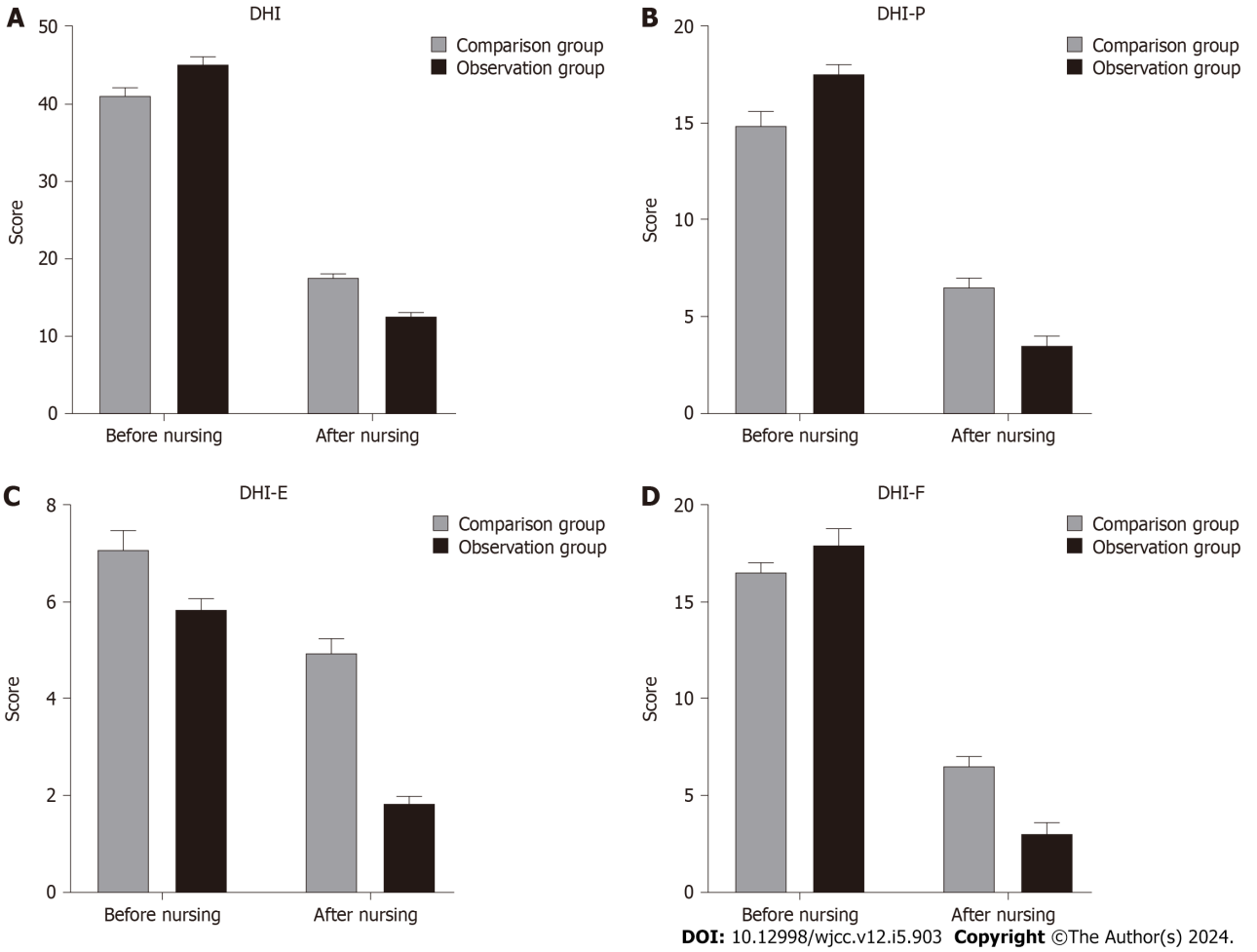

DOI: 10.12998/wjcc.v12.i5.903

Figure 3 Quality of life comparison. A: Dizziness Handicap Inventory (DHI) scores in the comparison group and observation group; B: DHI-P scores in the comparison group and observation group; C: DHI-E scores in the comparison group and observation group; D: DHI-F scores in the comparison group and observation group. All quality of life data in our study were checked by Excel double entry, SPSS23.0 was used for statistical analysis, and the mean ± SD was used for description. Using t test, it was found that the total score of DHI scale, DHI-P, DHI-E of the two groups of patients before nursing Compared with DHI-F dimension score, the difference was not statistically significant ($P > 0.05$). After nursing, the DHI scale and DHI-P, DHI-E and DHI-F scores in the two groups were decreased, and the scores in the nursing group were lower than those in the control group, and the difference was statistically significant ($P < 0.05$).

relief of vertigo and dizziness symptoms and functional recovery, the patients' DHI scale scores decreased in all dimensions and their quality of life improved[24]. Meanwhile, in addition to vestibular rehabilitation exercises, IMB model health education also intervened in some of the patients' high-risk factors, corrected their bad habits, and reduced the triggering factors of vertigo and dizziness, so that the patients' quality of life was improved[25].

The DHI scale and DHI-P, DHI-E and DHI-F scores were reduced in both groups after care in our study, and the scores in the care group were lower than those in the control group, with statistically significant differences. The reason for this analysis is that patients with vertigo often face dizziness attacks and somatic discomfort with unpredictable occurrence times, which seriously affect the ability to work and social activities, and cause mood changes that lead to physical and mental health disorders[26]. Vertigo treatment and vestibular rehabilitation exercises promoted vestibular function compensation and relieved patients' symptoms of vertigo and dizziness, therefore, patients' anxiety and depression were significantly improved[27]. Moreover, our study intervened with patients through three aspects: information, motivation, and behavioral skills, patients deepened their understanding of the disease, acquired skills to relieve symptoms, and through repeated communication and encouragement, patients received more attention and support, had more opportunities to express their concerns and worries, and their anxiety and depression were further relieved[28].

Our study has some innovation and some limitations. The patients included in our study were outpatients attending the clinic without hospital admission, the level of vertigo disability was mostly mild and moderate, and there were fewer severe patients; a stratified study should be conducted and inpatients should be included to make the data more comprehensive. Our study was limited by the time factor, the intervention time was only six weeks, and the follow-up and evaluation of long-term intervention effects were lacking. Our study only explored the effect of health education and guidance based on the IMB model on the rehabilitation of patients with unilateral vestibular hypofunction, and failed to comprehensively assess the reliability of care for patients with unilateral vestibular hypofunction, as well as failed to thoroughly study and follow up the rehabilitation of patients with unilateral vestibular hypofunction after care for a long period of time.

CONCLUSION

In conclusion, health education based on the IMB model can effectively improve patients' quality of life, increase self-efficacy of patients with unilateral hypovestibular function, enhance patients' confidence, enable patients to resume normal work and life as soon as possible, reduce patients' anxiety and depression, and effectively improve patients' psychological status.

ARTICLE HIGHLIGHTS

Research background

Vestibular dysfunction (VH) can have a significant impact on a person's quality of life, as it can result in dizziness, imbalance, nausea, and fatigue. In addition, vestibular hypofunction can lead to a decrease in activity levels and an increase in anxiety and depression symptoms. As such, it is important for healthcare professionals to recognize the signs and symptoms of vestibular hypofunction and to provide appropriate treatment and support to patients who are experiencing these symptoms.

Research motivation

VH is a common concomitant of advanced peri-court disease and may be due to trauma, poisoning, infection, genetic and neurodegenerative changes, but the cause is unknown in about 50%. In recent years, with the increase of various unfavorable factors and the aging of the population, the incidence of vestibular vertigo has been increasing. The advantage of information-motivation-behavioral skills (IMB) model is that it integrates self-efficacy theory, draws on the understanding of motivation from rational behavior theory, integrates various factors that affect behavior, and has higher feasibility. Therefore, there is an urgent need to study the effects of health education based on the IMB model on the degree of vertigo, disability, anxiety and depression in patients with unilateral VH.

Research objectives

In order to explore the effect of health education based on the IMB model on vertigo, disability, anxiety, and depression in patients with unilateral VH, a study was conducted.

Research methods

Patients with lateral VH from January 2019 to December 2021 were selected as the retrospective study objects and divided into control group (n = 40) and observation group (n = 40) according to nursing methods. The control group received usual care and health education guidance, and the observation group received health education and guidance based on the IMB model. Changes in self-efficacy, anxiety and depression were compared between the two groups.

Research results

Before nursing, there was no significant difference in General Self-Efficacy Scale, Hospital Anxiety and Depression Scale, anxiety and depression; they were higher/lower than those before nursing and lower than the control group, the difference was statistically significant. After nursing, the Dizziness Handicap Inventory (DHI) and DHI-P, DHI-E and DHI-F scores decreased in both groups; the nursing group was lower than the control group, and the difference was statistically significant.

Research conclusions

IMB model-based health education can effectively improve patients 'quality of life, improve the self-efficacy of patients with unilateral vestibular function, enhance their self-confidence, restore their normal work and life as soon as possible, reduce patients' anxiety and depression, and effectively improve the psychological state of patients.

Research perspectives

The treatment of VH remains challenging, and future research should depend on the type and severity of symptoms experienced by patients, which may involve vestibular rehabilitation therapy, medication, or surgical intervention.

FOOTNOTES

Co-first authors: Qiong Shi and Ruo-Jun Wu.

Author contributions: Shi Q and Wu RJ designed the research; Liu J, Shi Q and Wu RJ contributed new reagents/analytic tools; Liu J, Shi Q and Wu RJ analyzed the data; Shi Q and Wu RJ wrote the paper. All authors were involved in the critical review of the results and have contributed to, read, and approved the final manuscript. Shi Q and Wu RJ contributed equally to this work as co-first authors equally to this work. The reasons for naming Shi Q and Wu RJ as co-first authors are threefold. First, the research was a collaborative effort, and co-first authorship accurately reflects the distribution of responsibilities and burdens. This ensures effective communication and post-submission management, enhancing the paper's quality and reliability. Second, the team encompassed diverse expertise and skills, and co-first authorship reflects this diversity. This promotes a comprehensive and in-depth examination, enriching readers'

understanding. Third, Shi Q and Wu RJ contributed equally throughout the research process. Their co-first authorship acknowledges and respects this equal contribution, recognizing the teamwork spirit. In summary, naming Shi Q and Wu RJ as co-first authors accurately reflects the team's collaborative spirit, equal contributions, and diversity.

Institutional review board statement: The study was reviewed and approved for publication by our Institutional Reviewer.

Informed consent statement: All study participants or their legal guardian provided informed written consent about personal and medical data collection prior to study enrolment.

Conflict-of-interest statement: The authors declared no conflict of interest existing in this paper.

Data sharing statement: Data generated from this investigation are available upon reasonable quest from the corresponding author.

STROBE statement: The authors have read the STROBE Statement—checklist of items, and the manuscript was prepared and revised according to the STROBE Statement—checklist of items.

Country/Territory of origin: China

ORCID number: Jiang Liu 0009-0003-1633-1752.

S-Editor: Qu XL
L-Editor: A
P-Editor: Zheng XM

REFERENCES

1 **Kim SH**, Lee SY, Kim JS, Koo JW. Parameters of Off-Vertical Axis Rotation in Unilateral and Bilateral Vestibulopathy and Their Correlation with Vestibular Evoked Myogenic Potentials. *J Clin Med* 2021; **10** [PMID: 33668577 DOI: 10.3390/jcm10040756]
2 **Kitazawa M**, Morita Y, Yagi C, Takahashi K, Ohshima S, Yamagishi T, Izumi S, Koizuka I, Horii A. Test Batteries and the Diagnostic Algorithm for Chronic Vestibular Syndromes. *Front Neurol* 2021; **12**: 768718 [PMID: 34867755 DOI: 10.3389/fneur.2021.768718]
3 **Abu-Halima M**, Meese E, Saleh MA, Keller A, Abdul-Khaliq H, Raedle-Hurst T. MicroRNA-29b/c-3p Indicate Advanced Liver Fibrosis/Cirrhosis in Univentricular Heart Patients With and Without Fontan Palliation. *Front Cardiovasc Med* 2020; **7**: 619083 [PMID: 33490119 DOI: 10.3389/fcvm.2020.619083]
4 **Chen PY**, Jheng YC, Huang SE, Po-Hung Li L, Wei SH, Schubert MC, Kao CL. Gaze shift dynamic visual acuity: A functional test of gaze stability that distinguishes unilateral vestibular hypofunction. *J Vestib Res* 2021; **31**: 23-32 [PMID: 33325420 DOI: 10.3233/VES-201506]
5 **Micarelli A**, Viziano A, Granito I, Micarelli RX, Felicioni A, Alessandrini M. Changes in body composition in unilateral vestibular hypofunction: relationships between bioelectrical impedance analysis and neuro-otological parameters. *Eur Arch Otorhinolaryngol* 2021; **278**: 2603-2611 [PMID: 33392761 DOI: 10.1007/s00405-020-06561-z]
6 **Idorn L**, Olsen M, Jensen AS, Juul K, Reimers JI, Sørensen K, Johnsen SP, Søndergaard L. Univentricular hearts in Denmark 1977 to 2009: incidence and survival. *Int J Cardiol* 2013; **167**: 1311-1316 [PMID: 22521378 DOI: 10.1016/j.ijcard.2012.03.182]
7 **Hall CD**, Herdman SJ, Whitney SL, Anson ER, Carender WJ, Hoppes CW, Cass SP, Christy JB, Cohen HS, Fife TD, Furman JM, Shepard NT, Clendaniel RA, Dishman JD, Goebel JA, Meldrum D, Ryan C, Wallace RL, Woodward NJ. Vestibular Rehabilitation for Peripheral Vestibular Hypofunction: An Updated Clinical Practice Guideline From the Academy of Neurologic Physical Therapy of the American Physical Therapy Association. *J Neurol Phys Ther* 2022; **46**: 118-177 [PMID: 34864777 DOI: 10.1097/NPT.0000000000000382]
8 **Hillier S**, McDonnell M. Is vestibular rehabilitation effective in improving dizziness and function after unilateral peripheral vestibular hypofunction? An abridged version of a Cochrane Review. *Eur J Phys Rehabil Med* 2016; **52**: 541-556 [PMID: 27406654]
9 **Dunlap PM**, Holmberg JM, Whitney SL. Vestibular rehabilitation: advances in peripheral and central vestibular disorders. *Curr Opin Neurol* 2019; **32**: 137-144 [PMID: 30461465 DOI: 10.1097/WCO.0000000000000632]
10 **Erikssen G**, Aboulhosn J, Lin J, Liestøl K, Estensen ME, Gjesdal O, Skulstad H, Døhlen G, Lindberg HL. Survival in patients with univentricular hearts: the impact of right versus left ventricular morphology. *Open Heart* 2018; **5**: e000902 [PMID: 30364544 DOI: 10.1136/openhrt-2018-000902]
11 **Paul SS**, Dibble LE, Walther RG, Shelton C, Gurgel RK, Lester ME. Reduced Purposeful Head Movements During Community Ambulation Following Unilateral Vestibular Loss. *Neurorehabil Neural Repair* 2018; **32**: 309-316 [PMID: 29676210 DOI: 10.1177/1545968318770271]
12 **Sasaki T**, Asou T, Takeda Y, Onakatomi Y, Tominaga T, Yamamoto Y. Extracorporeal life support after cardiac surgery in children: outcomes from a single institution. *Artif Organs* 2014; **38**: 34-40 [PMID: 24117701 DOI: 10.1111/aor.12191]
13 **Hautala J**, Gissler M, Ritvanen A, Vahlberg T, Ojala T. Monthly variation in univentricular heart and transposition of the great arteries - 10-year national population-based cohort study. *Eur J Obstet Gynecol Reprod Biol* 2021; **258**: 418-423 [PMID: 33567397 DOI: 10.1016/j.ejogrb.2021.01.040]
14 **Micarelli A**, Viziano A, Micarelli B, Di Fulvio G, Alessandrini M. Usefulness of postural sway spectral analysis in the diagnostic route and clinical integration of cervicogenic and vestibular sources of dizziness: A cross-sectional preliminary study. *J Vestib Res* 2021; **31**: 353-364 [PMID: 33843709 DOI: 10.3233/VES-190729]
15 **Alessandrini M**, Viziano A, Pistillo R, Granito I, Basso L, Preziosi N, Micarelli A. Changes in daily energy expenditure and movement

behavior in unilateral vestibular hypofunction: Relationships with neuro-otological parameters. *J Clin Neurosci* 2021; **91**: 200-208 [PMID: 34373028 DOI: 10.1016/j.jocn.2021.07.012]

16 **Micarelli A**, Viziano A, Pistillo R, Granito I, Micarelli B, Alessandrini M. Sleep Performance and Chronotype Behavior in Unilateral Vestibular Hypofunction. *Laryngoscope* 2021; **131**: 2341-2347 [PMID: 34191310 DOI: 10.1002/lary.29719]

17 **Meldrum D**, Jahn K. Gaze stabilisation exercises in vestibular rehabilitation: review of the evidence and recent clinical advances. *J Neurol* 2019; **266**: 11-18 [PMID: 31385017 DOI: 10.1007/s00415-019-09459-x]

18 **Meldrum D**, Burrows L, Cakrt O, Kerkeni H, Lopez C, Tjernstrom F, Vereeck L, Zur O, Jahn K. Vestibular rehabilitation in Europe: a survey of clinical and research practice. *J Neurol* 2020; **267**: 24-35 [PMID: 33048219 DOI: 10.1007/s00415-020-10228-4]

19 **Pérez-Fernández N**, Alvarez-Gomez L, Manrique-Huarte R. Bilateral Vestibular Hypofunction in the Time of the Video Head Impulse Test. *Audiol Neurootol* 2020; **25**: 72-78 [PMID: 31825921 DOI: 10.1159/000504286]

20 **Sestak A**, Maslovara S, Zubcic Z, Vceva A. Influence of vestibular rehabilitation on the recovery of all vestibular receptor organs in patients with unilateral vestibular hypofunction. *NeuroRehabilitation* 2020; **47**: 227-235 [PMID: 32741787 DOI: 10.3233/NRE-203113]

21 **Likhachev SA**, Maryenko IP. [Statokinetic characteristics of vestibular dysfunction in patients with vascular compression of the cochleo-vestibular nerve]. *Zh Nevrol Psikhiatr Im S S Korsakova* 2015; **115**: 35-39 [PMID: 26356513 DOI: 10.17116/jnevro20151157135-39]

22 **Castellucci A**, Malara P, Brandolini C, Del Vecchio V, Giordano D, Ghidini A, Ferri GG, Pirodda A. Isolated horizontal canal hypofunction differentiating a canalith jam from an acute peripheral vestibular loss. *Am J Otolaryngol* 2019; **40**: 319-322 [PMID: 30665622 DOI: 10.1016/j.amjoto.2018.12.005]

23 **Barreto RG**, Yacovino DA, Cherchi M, Nader SN, Teixeira LJ, Silva DAD, Verdecchia DH. The Role of the Smartphone in the Diagnosis of Vestibular Hypofunction: A Clinical Strategy for Teleconsultation during the COVID-19 Pandemic and Beyond. *Int Arch Otorhinolaryngol* 2021; **25**: e602-e609 [PMID: 34777592 DOI: 10.1055/s-0041-1736340]

24 **Ramos BF**, Cal R, Carmona S, Weber KP, Zuma E Maia F. Corrective Saccades in Unilateral and Bilateral Vestibular Hypofunction During Slow Rotation Expressed by Visually Enhanced VOR and VOR Suppression: Role of the Cerebellum. *Cerebellum* 2021; **20**: 673-677 [PMID: 31396823 DOI: 10.1007/s12311-019-01066-w]

25 **Balami AD**, Said SM, Zulkefli NAM, Norsa'adah B, Audu B. Improving malaria preventive practices and pregnancy outcomes through a health education intervention: A randomized controlled trial. *Malar J* 2021; **20**: 55 [PMID: 33478529 DOI: 10.1186/s12936-021-03586-5]

26 **Porta Etessam J**, González N, García-Azorín D, Silva L. Bilateral vestibular hypofunction occurring between migraine attacks: toward an integrative hypothesis. *Neurologia (Engl Ed)* 2020; **35**: 448-449 [PMID: 29784472 DOI: 10.1016/j.nrl.2018.03.010]

27 **Stewart CE**, Bauer DS, Altschuler RA, King WM. Transient peripheral vestibular hypofunction measured with vestibular short-latency evoked potentials following noise exposure in rats. *J Neurophysiol* 2021; **126**: 1547-1554 [PMID: 34550030 DOI: 10.1152/jn.00131.2021]

28 **Chow MR**, Ayiotis AI, Schoo DP, Gimmon Y, Lane KE, Morris BJ, Rahman MA, Valentin NS, Boutros PJ, Bowditch SP, Ward BK, Sun DQ, Treviño Guajardo C, Schubert MC, Carey JP, Della Santina CC. Posture, Gait, Quality of Life, and Hearing with a Vestibular Implant. *N Engl J Med* 2021; **384**: 521-532 [PMID: 33567192 DOI: 10.1056/NEJMoa2020457]

World Journal of Clinical Cases

Submit a Manuscript: https://www.f6publishing.com

World J Clin Cases 2024 February 16; 12(5): 913-921

DOI: 10.12998/wjcc.v12.i5.913

ISSN 2307-8960 (online)

ORIGINAL ARTICLE

Retrospective Study

Removal of intrahepatic bile duct stone could reduce the risk of cholangiocarcinoma: A single-center retrospective study in South Korea

Tae In Kim, Sung Yong Han, Jonghyun Lee, Dong Uk Kim

Specialty type: Medicine, research and experimental

Provenance and peer review: Invited article; Externally peer reviewed.

Peer-review model: Single blind

Peer-review report's scientific quality classification

Grade A (Excellent): A
Grade B (Very good): 0
Grade C (Good): 0
Grade D (Fair): D
Grade E (Poor): 0

P-Reviewer: Rizzo A, Italy

Received: October 18, 2023
Peer-review started: October 18, 2023
First decision: November 22, 2023
Revised: December 6, 2023
Accepted: January 15, 2024
Article in press: January 15, 2024
Published online: February 16, 2024

Tae In Kim, Sung Yong Han, Jonghyun Lee, Dong Uk Kim, Division of Gastroenterology, Biomedical Research Institute, Pusan National University Hospital, Busan 49241, South Korea

Sung Yong Han, Dong Uk Kim, Department of Internal Medicine, Pusan National University, College of Medicine, Yangsan 50612, South Korea

Corresponding author: Dong Uk Kim, MD, PhD, Adjunct Associate Professor, Division of Gastroenterology, Biomedical Research Institute, Pusan National University Hospital, 179 Gudeok-ro, Seo-gu, Busan 49241, South Korea. amlm3@hanmail.net

Abstract

BACKGROUND

Intrahepatic duct (IHD) stones are among the most important risk factors for cholangiocarcinoma (CCC). Approximately 10% of patients with IHD stones develop CCC; however, there are limited studies regarding the effect of IHD stone removal on CCC development.

AIM

To investigate the association between IHD stone removal and CCC development.

METHODS

We retrospectively analyzed 397 patients with IHD stones at a tertiary referral center between January 2011 and December 2020.

RESULTS

CCC occurred in 36 of the 397 enrolled patients. In univariate analysis, chronic hepatitis B infection (11.1% *vs* 3.0%, $P = 0.03$), carbohydrate antigen 19-9 (CA19-9, 176.00 *vs* 11.96 II/mL, $P = 0.010$), stone located in left or both lobes (86.1% *vs* 70.1%, $P = 0.042$), focal atrophy (52.8% *vs* 26.9%, $P = 0.001$), duct stricture (47.2% *vs* 24.9%, $P = 0.004$), and removal status of IHD stone (33.3% *vs* 63.2%, $P < 0.001$) were significantly different between IHD stone patients with and without CCC. In the multivariate analysis, CA19-9 > upper normal limit, carcinoembryonic antigen > upper normal limit, stones located in the left or both lobes, focal atrophy, and complete removal of IHD stones without recurrence were independent factors influencing CCC development. However, the type of removal method was not associated with CCC risk.

CONCLUSION
Complete removal of IHD stones without recurrence could reduce CCC risk.

Key Words: Intrahepatic bile duct stone; Cholangiocarcinoma; Percutaneous transhepatic cholangioscopy; Endoscopic retrograde cholangiopancreatography; Carbohydrate antigen 19-9

Core Tip: It is well known that intrahepatic duct (IHD) stones are the most important risk factors for cholangiocarcinoma (CCC), but there are limited studies regarding the effect of IHD stone removal on CCC development. It has been reported that remnant stones after percutaneous transhepatic cholangioscopy could be a risk factor for CCC, but the effect of recurrence after complete removal of stones on CCC is unclear. Based on this, we investigated the association of IHD stone removal and CCC development.

Citation: Kim TI, Han SY, Lee J, Kim DU. Removal of intrahepatic bile duct stone could reduce the risk of cholangiocarcinoma: A single-center retrospective study in South Korea. *World J Clin Cases* 2024; 12(5): 913-921
URL: https://www.wjgnet.com/2307-8960/full/v12/i5/913.htm
DOI: https://dx.doi.org/10.12998/wjcc.v12.i5.913

INTRODUCTION

Cholangiocarcinoma (CCC) has a poor prognosis, and its incidence is increasing worldwide, especially in East Asia[1]. Surgical resection is the optimal method for curing cancer, but only about 10%-40% of patients that are diagnosed are considered suitable for operation at the time of diagnosis[2]. Research on the use of immune checkpoint inhibitors to treat local advanced or metastatic CCC is rapidly progressing[2]. A recent study found that adding durvalumab to gemcitabine and cisplatin, the standard first-line treatment for advanced CCC, can extend patients' overall survival[3]. However, the 5-year survival rate for advanced CCC that is not amenable to surgery has not exceeded 5% until now. Therefore, one of the main approaches to increasing CCC survival rate of is to identify and eliminate its risk factors.

While the most common risk factor in Western countries is primary biliary cirrhosis, parasitic infections, intrahepatic duct (IHD) stones, and viral hepatitis are more common causes of CCC in Eastern countries[4]. IHD stones cause repetitive inflammation of the liver parenchyma and structural changes, and 10% of these result in CCC[5]. Therefore, it is important to consistently manage IHD stones. Hence, most patients undergo operative or endoscopic removal of stones. While operative treatment is known to be more effective in managing IHD stones, the endoscopic method can be an option in cases of bilateral IHD stones without structural change, while considering severe comorbidity.

Depending on the method, the removal rate in surgical treatment is 95%-100%, with a recurrence rate of 5.7%-13.9%. The non-surgical treatments such as percutaneous transhepatic cholangioscopy (PTCS) and endoscopic retrograde cholangiopancreatography (ERCP) have a removal rate of approximately 80% and a recurrence rate of 35%-63.2%[6,7]. It has been reported that remnant stones after non-surgical treatment could be a risk factor for CCC[8]; however, research on the risk of CCC development after IHD stone removal is still lacking. Therefore, this study aimed to investigate the relationship between IHD stone removal and the risk of CCC development.

MATERIALS AND METHODS

Patients

From January 2011 to December 2020, we retrospectively analyzed the medical records of patients diagnosed with IHD stones who underwent imaging tests such as computed tomography (CT) or magnetic resonance (MR) and had a follow-up record of more than 6 mo. We excluded patients who had a possibility of malignancy on diagnosis of IHD stones. We reviewed age, sex, past medical history, medication, laboratory findings, imaging tests, and pathologic results. A total of 397 patients with IHD stones were enrolled and 36 were diagnosed with CCC. This study was performed in accordance with the ethical principles of the Declaration of Helsinki (2013) and was approved by the institutional review board of Pusan National University Hospital (IRB No. 2103-010-101).

Medical record review

We checked for remnants and recurrence after IHD stone removal. A remnant stone was defined as a stone confirmed by CT or MR within 6 mo after IHD stone removal, while a recurrent stone was confirmed more than 6 mo after treatment. We then investigated the occurrence rate of CCC in accordance with the presence of remnant stones from pathological data.

We analyzed sex, age, height, body weight, and body mass index (BMI) and the presence of liver cirrhosis, viral hepatitis, diabetes mellitus, and hypertension for past medical history. As serologic markers, carbohydrate antigen 19-9 (CA19-9) and carcinoembryonic antigen (CEA) were analyzed for their minimal value in consecutive tests during the follow-up period. For medication history, aspirin, ursodeoxycholic acid (UDCA), and statin use for 6 mo or more were considered. In imaging tests, we analyzed the location, size, number of stones, and the presence of stricture of the bile duct or atrophy of the liver parenchyma and distinguished stones larger than the duct by comparing the size of the stone with the duct diameter. Regardless of treatment, we defined recurrent cholangitis as taking antibiotics in outpatient or hospital administration two times or more (Figure 1).

Statistical analysis

We used SPSS statistical software (version 26.0, IBM, Armonk, NY) for statistical analysis. Qualitative data, including differences between the two groups, were summarized and expressed as frequencies and percentile using the χ^2 test. For continuous variables, we analyzed the difference between the two groups and expressed it as the median with or without standard deviation using an independent two-sample *t*-test. The effect of independent variables on response variable was analyzed using the multivariate logistic regression, and the statistically significant variables were included in the univariate logistic regression with 0.05 alpha level.

RESULTS

Patient data

The data of the 397 patients enrolled in this study are summarized in Table 1. CCC occurred in 36 patients. The two groups' mean follow-up period was approximately 7 years (96.3 *vs* 83.9 mo). In the two groups, 33.3% and 39.6% were male, and the median age at the diagnosis of IHD stone was 60.75-years-old and 61.31-years-old, respectively. There was no significant difference in BMI and underlying viral hepatitis between the two groups. The number of patients with diabetes mellitus and hypertension was similar between the group (13.9% and 14.7%, 13.9% and 18.4%, respectively). In serologic tests, the minimum value of CA19-9 showed statistically significant differences [CA19-9 (176.00 *vs* 11.96, P = 0.010)] and the number of patients who had results exceeding the reference showed significant differences in CA19-9 (19.4% *vs* 1.9%, P < 0.001) and CEA (13.9% *vs* 1.9%, P = 0.002). On imaging, there was no statistical difference in the occurrence of multiple stones or stones bigger than the duct diameter. IHD stones on the left or both sides of the liver showed a higher rate of accompanying CCC than stones only on the right side (86.1% *vs* 70.1%, P = 0.042). Furthermore, the coexistence of atrophy of the liver parenchyma (52.8% *vs* 26.9%, P = 0.001) and bile duct stricture (47.2% *vs* 24.9%, P = 0.004) showed a statistically significant difference in the rate of CCC.

Although the number of patients who underwent IHD stone removal was lower in those with CCC (33.3% *vs* 63.2%, P < 0.001), there was no statistical difference in the method of stone removal, recurrence rate (5.6% *vs* 8.0%) or the incomplete stone removal rate (5.6% *vs* 9.4%). Medication history also showed no difference in the use of aspirin (0% *vs* 3.9%), UDCA (77.8% *vs* 73.4%), metformin (8.3% *vs* 5.3%), or statins (5.6% *vs* 6.4%). There was no difference in the occurrence of recurrent cholangitis (55.6% *vs* 51.2%) (Table 1).

Risk analysis of CCC in IHD patients

We calculated the odds ratio (OR) of each factor and conducted multivariate regression analysis of seven factors that showed statistical importance (Table 2): the number of patients who exceeded the reference for CA19-9 (P < 0.001) and CEA (P = 0.001), IHD stone on the left side (P = 0.049), atrophy of the liver parenchyma (P = 0.002), bile duct stricture (P = 0.005), complete removal without recurrence (P = 0.009), and non-surgical removal method (P = 0.004) (Table 2). Of these, the frequency of bile duct stricture and removal method of non-surgery showed a P value of 0.061 and 0.141, respectively, indicating that they were not significant risk factors for CCC. We verified the ORs of CA19-9 (P < 0.001), CEA (0.005), left-sided and both IHD stone (0.013). In the case of complete removal without recurrence, the OR of CCC showed a statistically significant decrease to 0.21 (P < 0.001) (Table 2).

Results analysis according to the removal method

Table 1 also shows the CCC occurrence rate according to the state of IHD stones. Of 157 patients who did not undergo IHD stone removal, 24 were diagnosed with CCC, resulting in an occurrence rate of 15.3%. Conversely, 12 of the 240 patients who underwent IHD stone removal treatment were diagnosed with CCC, with an occurrence rate of 5.0%. Among the 173 patients with complete removal of IHD stone without recurrence, eight were diagnosed with CCC, showing an occurrence rate of 4.6% and a statistically significant difference (P = 0.007). Complete removal with recurrent (6.4%) and incomplete removal with remnant (5.6%) stone groups showed a tendency toward decreased CCC risk (OR = 0.57-0.67) in univariate analysis, however, the difference was not statistically significant (Table 2).

Regardless of removal methods, surgical (ERCP and PTCS) or non-surgical (hepatectomy), all patients who underwent IHD stone removal showed a decreased risk of CCC, and there was no difference between the two groups in CCC development (P = 0.676) (Table 3). However, the rates of remnant or recurrent stones and recurrent cholangitis were higher in non-surgically treated patients (Table 3).

Table 1 Baseline characteristics between intrahepatic duct stone patient with or without cholangiocarcinoma

Variable	IHD stone with CCC, *n* = 36	IHD stone without CCC, *n* = 361	*P* value
Male sex	12 (33.3)	143 (39.6)	0.461[3]
Age	60.75 ± 10.20	61.31 ± 10.58	0.687[2]
BMI	23.27 ± 3.23	22.93 ± 3.27	0.551[1]
Hepatitis			
None	31 (86.1)	342 (94.7)	0.049[4]
HBV	4 (11.1)	11 (3.0)	
HCV	1 (2.8)	8 (2.2)	
DM	5 (13.9)	53 (14.7)	0.893[3]
HT	5 (13.9)	66 (18.4)	0.503[3]
CA19-9, minimum	176.00 ± 463.47	11.96 ± 15.65	0.010[2]
CA19-9 > UNL	7 (19.4)	7 (1.9)	< 0.001[4]
CEA, minimum	8.23 ± 29.45	1.96 ± 1.32	0.332[2]
CEA > UNL	5 (13.9)	7 (1.9)	0.002[4]
Location			
Lt & both	31 (86.1)	253 (70.1)	0.042[3]
Rt	5 (13.9)	108 (29.9)	
Multiple stone	30 (83.3)	254 (70.4)	0.100[3]
Stone size > duct diameter	19 (52.8)	173 (47.9)	0.578[3]
Focal atrophy	19 (52.8)	97 (26.9)	0.001[3]
Duct stricture	17 (47.2)	90 (24.9)	0.004[3]
IHD stone removal	12 (33.3)	228 (63.2)	< 0.001[3]
Complete removal & no recurrence	8 (22.2)	165 (45.7)	0.007[3]
Complete removal & recurrence	2 (5.6)	29 (8.0)	10.000[4]
Incomplete removal	2 (5.6)	34 (9.4)	0.759[4]
Removal method			
Non-surgery, PTCS, ERCP	6 (50.0)	128 (56.1)	0.676[3]
Surgery	6 (50.0)	100 (43.9)	
Medication			
Aspirin	0 (0.0)	14 (3.9)	0.626[4]
UDCA	28 (77.8)	265 (73.4)	0.570[3]
Metformin	3 (8.3)	19 (5.3)	0.4374
Statin	2 (5.6)	23 (6.4)	1.000[4]
Recurrent cholangitis	20 (55.6)	185 (51.2)	0.622[3]
F/U period, mean ± SD	96.33 ± 59.06	83.93 ± 60.38	0.164[2]

[1]*P* values were derived from independent *t*-test.
[2]*P* values were derived from Mann-Whitney *U* test.
[3]*P* values were derived by χ^2 test.
[4]*P* values were derived from Fisher's exact test. Shapiro-Wilk test was employed for test of normality assumption. Values are either frequency with percentage in parentheses or mean ± standard deviation (SD) or median (interquartile range). BMI: Body mass index; CA19-9: Carbohydrate antigen 19-9; CCC: Cholangiocarcinoma; CEA: Carcinoembryonic antigen; DM: Diabetes mellitus; ERCP: Endoscopic retrograde cholangiopancreatography; F/U: Follow up; HBV: Hepatitis B virus; HCV: Hepatitis C virus; IHD: Intrahepatic duct; HT: Hypertension; PTCS: Percutaneous transhepatic cholangioscopy; UDCA: Ursodeoxycholic acid; UNL: Upper normal limit.

Table 2 Risk factor analysis for cholangiocarcinoma

Variable	Univariate analysis			Multivariate analysis		
	OR	95%CI	*P* value	OR	95%CI	*P* value[1]
Male sex	0.76	0.37-1.57	0.463			
Age	0.99	0.96-1.03	0.761			
BMI	1.03	0.93-1.15	0.550			
Hepatitis						
None	Reference					
HBV	4.01	1.21-13.35	0.023			
HCV	1.38	0.17-11.39	0.765			
DM	0.93	0.35-2.51	0.893			
HT	0.72	0.27-1.91	0.505			
CA19-9, minimum	1.01	1.00-1.02	0.013			
CA19-9 > UNL	12.21	4.01-37.19	0.000	15.85	3.79-66.31	0.000
CEA, minimum	1.28	1.03-1.59	0.026			
CEA > UNL	8.16	2.44-27.21	0.001	8.12	1.87-35.35	0.005
Location, Lt and both	2.65	1.00-6.99	0.049	4.37	1.37-13.94	0.013
Multiple stone	2.11	0.85-5.21	0.107			
Stone size > duct diameter	1.21	0.61-2.41	0.579			
Focal atrophy	3.04	1.52-6.09	0.002	2.59	1.13-5.94	0.025
Duct stricture	2.69	1.34-5.41	0.005	2.24	0.96-5.23	0.061
IHD stone removal						
Complete removal and no recurrence	0.34	0.15-0.76	0.009	0.21	0.09-0.50	0.000
Complete removal and recurrence	0.67	0.15-2.95	0.600			
Incomplete removal	0.57	0.13-2.46	0.447			
Removal method						
None	Reference					
Non-surgery, PTCS, ERCP	0.26	0.10-0.66	0.004	0.33	0.07-1.45	0.141
Surgery	0.33	0.13-0.84	0.021	0.37	0.08-1.70	0.200
Medication						
Aspirin	0.00	0.00-0.00	0.999			
UDCA	1.27	0.56-2.88	0.570			
Metformin	1.64	0.46-5.82	0.447			
Statin	0.86	0.20-3.83	0.848			

[1]Effect of independent variables on response variable was analyzed using multivariate logistic regression, and the statistically significant variables were included in the univariate logistic regression with 0.05 alpha level. BMI: Body mass index; CA19-9: Carbohydrate antigen 19-9; CEA: Carcinoembryonic antigen; CI: Confidence interval; DM: Diabetes mellitus; ERCP: Endoscopic retrograde cholangiopancreatography; HBV: Hepatitis B virus; HCV: Hepatitis C virus; HT: Hypertension; IHD: Intrahepatic duct; OR: Odds ratio; PTCS: Percutaneous transhepatic cholangioscopy; UNL: Upper normal limit; UDCA: Ursodeoxycholic acid.

DISCUSSION

In the current study, we found that the CCC occurrence rate was lower in patients who underwent IHD stone removal than in those who did not. The CCC occurrence rate (9%) was similar to that of another study (1.3%-13%)[5,9]. In multivariate analysis, the factors affecting CCC were increased CA19-9 (OR = 15.85, $P < 0.001$) and CEA (OR = 8.12, P =

Table 3 Comparison of results according to stone removal method, *n* = 240

Removal method	Surgery, *n* = 106	Non-surgery, *n* = 134	*P* value
Cholangiocarcinoma	6 (5.7)	6 (4.5)	0.676
Remnant stone	9 (8.5)	27 (20.1)	0.012
Recurrent stone	12 (11.3)	52 (38.8)	< 0.001
Recurrent cholangitis	37 (34.9)	96 (71.6)	< 0.001

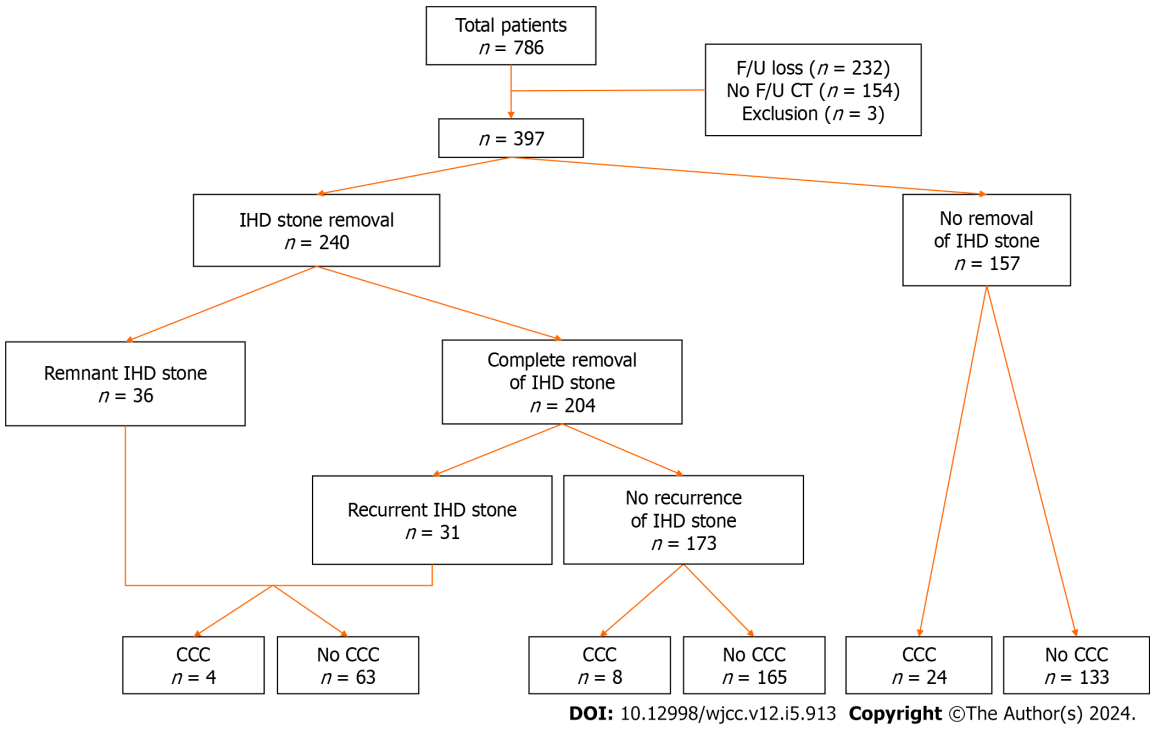

DOI: 10.12998/wjcc.v12.i5.913

Figure 1 Long-term results in 397 patients undergoing intrahepatic duct stone removal. CCC: Cholangiocarcinoma; CT: Computed tomography; F/U: Follow up; IHD: Intrahepatic duct.

0.005) above the reference value, left-sided or bilateral IHD stones (OR = 4.37, *P* = 0.013), and atrophy of the liver parenchyma (OR = 2.59, *P* = 0.025). Complete removal of IHD stones without recurrence was identified as a factor decreasing CCC risk to 79% (OR = 0.21, *P* = 0.001). Although not in CCC development, there was a difference in the rate of remnant and recurrence between the surgically and non-surgically treated groups, including the rate of recurrent cholangitis. These results could suggest that surgical treatment can be better for younger patients or those with higher risk of CCC like *Clonorchis sinensis* or viral hepatitis infection and primary sclerosing cholangitis, *etc.*

The stone removal rate was 91.5% and 79.9% in surgically treated groups and the others, respectively. This was similar to another study. In the case of recurrence rate, there was no significant difference with other studies (5.7%-13.9%, 35%-63.2%) compared to 11.5% in operation and 45.5% in the PTCS group[6,7]. Although the number of patients who underwent ERCP was too small to directly compare with other groups, the removal rate was high, and the recurrence rate was low in this study because it was applied to patients with relatively small stones in the hilum.

It is well known that structural changes are risk factors for CCC, including atrophy of the parenchyma and bile duct stricture. Therefore, hepatectomy, including resection, could lower the risk of CCC. In multivariate analysis, atrophy of the liver parenchyma was identified as a risk factor; however, focal bile duct stricture did not affect CCC. This may be due to the relief of congestion by balloon dilatation during PTCS, which could influence cancer development. In this study, we expect that PTCS can be preferentially applied to patients with IHD stones since PTCS does not increase CCC risk if there are no structural changes, such as atrophy or stricture.

The risk factors for CCC were elevated tumor markers, atrophy of the liver parenchyma, and left-sided IHD stones. In one cohort study in Japan, it was reported that bile duct stricture and age above 65 years were risk factors for CCC[9], and in Korea, there was a study that remnant stone increased the risk[10]. These factors were all related to chronic inflammation, which was reported as a major factor of CCC. This was thought to be related to the increased risk in the remnant stone group from another study and the group with remnant or recurrent stone in this study[11]. In our study, remnant or recurrent stone showed a tendency of decreased CCC risk, though it did not reach statistical significance. This result emphasized the importance of reducing stones to relieve the obstruction and the complete removal and long-term surveillance after treatment. Additionally, there is a possibility that the effect of remnant or recurrent stones on the risk of

CCC could not be fully evaluated because of the short follow-up period. In one study about IHD stones in Korea, the average period of occurrence of CCC was approximately 10 years; therefore, the 7-year follow-up period in this study could be too short to verify the effect of remnant stones on CCC[9,10,12].

Recently, there have been reports that drugs such as aspirin, metformin, and statins reduce cancer risk[13-15]. Some studies suggested that aspirin may help prevent cancer, and there are ongoing studies to address how metabolic factors like diabetes, hypertension, and obesity affect malignancy[16]. In a study of 2395 CCC patients and 4769 controls in 2016, Choi *et al*[17] reported that aspirin reduced the risk of bile duct cancer to 65%-71%, specifically 65% in intrahepatic CCC. However, they simultaneously reported that patients with bile duct disease had a 12.1-fold increase in CCC risk; thus, we expect that the higher risk of CCC could offset aspirin use in patients with IHD stones. Although there were a small number of aspirin users in this study, none were diagnosed with CCC. Tseng[18] reported that the risk of CCC was lower in metformin users than in non-users by approximately 50%-60%. However, in this study, metformin users had a higher proportion of CCC without statistical significance. Liu *et al*[19] revealed that statins could reduce the risk of CCC by approximately 12% in a big-data study of 3118 CCC patients and 15519 controls. These studies about drugs decreasing cancer risk were big data research generally conducted on a large number of people, so our small study on approximately 400 patients could not prove drug efficacy. In the future, large-scale studies should be conducted to investigate the effects of drugs or metabolic factors on CCC occurrence. In the long term, we need to actively implement education and campaigns targeting the general population to identify and address these risk factors.

Our study had some limitations. First, this was a single-center study with a small number of patients, approximately 400. Because IHD stones are more common among East Asian countries than in the Western world[20], there might be some limitation to generalize the conclusion of a retrospective study conducted at a single center study in South Korea. Second, some patients' medications could not be precisely investigated due to dropout. Third, this was a retrospective study, so it requires attention for interpretation because of defective data. This study has no information about *Clonorchis sinensis* infection as an important risk factor for CCC. Finally, this study's relatively short average follow-up period of 7 years could have affected the risk evaluation for CCC.

CONCLUSION

In conclusion, patients who underwent removal of IHD stones showed a decreased risk of CCC regardless of the methods, especially in the absence of remnant stone after treatment. Therefore, it is important to remove IHD stones as much as possible. Medications such as statins, metformin, and aspirin[13-15] are not expected to affect CCC occurrence. Further studies are warranted to verify these results.

ARTICLE HIGHLIGHTS

Research background

Cholangiocarcinoma (CCC) is a type of gastrointestinal malignancy that has a poor prognosis and is difficult to treat. It has a low possibility of operative resection for cure at the time of diagnosis, so research for systemic chemotherapy is underway, including the use of immune check point inhibitors. In East Asia, the incidence of CCC is increasing, but there are few methods for early diagnosis. Therefore, it is very important to recognize and estimate CCC risk factors.

Research motivation

In East Asia, intrahepatic duct (IHD) stones have been recognized as a risk factor for developing CCC. They block the normal outflow of bile, resulting in repetitive inflammation of liver parenchyma. Chronic inflammation of biliary tract and liver parenchyma are known to contribute to malignant change, so it is important to relieve the obstruction. There have been several studies about IHD stones and CCC, but most of them had a small number of subjects and few studies identified the correlation between removal of IHD stones and CCC development.

Research objectives

We wanted to perform a large cohort study about the effect of IHD stone removal on CCC development, including the optimal method for removal. We also analyzed the effect of medication for metabolic disease like diabetes mellitus, dyslipidemia, and hypertension.

Research methods

We retrospectively analyzed patients who were diagnosed with IHD stone with imaging tests and underwent removal in Pusan National University Hospital from January 2011 to December 2020. Based on medical records, we investigated the occurrence of CCC and factors affecting CCC development.

Research results

CCC occurred in 36 of the 397 enrolled patients. In multivariate analysis, carbohydrate antigen 19-9 > upper normal limit, carcinoembryonic antigen > upper normal limit, stones located in the left or both lobes, focal atrophy, and complete removal of IHD stones without recurrence were independent factors influencing CCC development. However, the type of

removal method or medication for metabolic disease did not seem to affect CCC development.

Research conclusions

Regardless of methods, the complete removal of IHD stones without recurrence could reduce CCC development. Therefore, it is important to choose the optimal method for removal depending on the patient and follow up. Repetitive tests or procedures may be necessary.

Research perspectives

In the future, optimal method for removal of IHD stone regarding patient's age, sex, social or economic factors and underlying disease should be studied. In addition, systemic treatment for CCC including cytotoxic or immune-targeted chemotherapy specific to CCC should be developed.

FOOTNOTES

Author contributions: Kim TI, Han SY, Lee J, and Kim DU contributed to the design, writing and data analysis of the manuscript.

Supported by a grant from the National R&D Program for Cancer Control, Ministry of Health and Welfare, Republic of Korea, No. HA20C0009.

Institutional review board statement: The study was reviewed and approved by the Biomedical Research Institute, Pusan National University Hospital, Institutional Review Board (Approval No. 2103-010-101).

Informed consent statement: We have no signed informed consent because this is a retrospective study and we analyzed medical records of patients in our center. We obtained a consent exemption for our research.

Conflict-of-interest statement: Dr. Kim reports grants from the National R&D Program for Cancer Control, Ministry of Health and Welfare, Republic of Korea, during the conduct of the study.

Data sharing statement: No additional data are available.

Country/Territory of origin: South Korea

ORCID number: Tae In Kim 0000-0001-6068-561X; Sung Yong Han 0000-0002-0256-9781; Jonghyun Lee 0000-0002-9752-5860; Dong Uk Kim 0000-0002-7208-7753.

S-Editor: Wang JJ
L-Editor: Filipodia
P-Editor: Zhao S

REFERENCES

1 **Banales JM**, Marin JJG, Lamarca A, Rodrigues PM, Khan SA, Roberts LR, Cardinale V, Carpino G, Andersen JB, Braconi C, Calvisi DF, Perugorria MJ, Fabris L, Boulter L, Macias RIR, Gaudio E, Alvaro D, Gradilone SA, Strazzabosco M, Marzioni M, Coulouarn C, Fouassier L, Raggi C, Invernizzi P, Mertens JC, Moncsek A, Rizvi S, Heimbach J, Koerkamp BG, Bruix J, Forner A, Bridgewater J, Valle JW, Gores GJ. Cholangiocarcinoma 2020: the next horizon in mechanisms and management. *Nat Rev Gastroenterol Hepatol* 2020; **17**: 557-588 [PMID: 32606456 DOI: 10.1038/s41575-020-0310-z]

2 **Rizzo A**, Brandi G. Neoadjuvant therapy for cholangiocarcinoma: A comprehensive literature review. *Cancer Treat Res Commun* 2021; **27**: 100354 [PMID: 33756174 DOI: 10.1016/j.ctarc.2021.100354]

3 **Oh DY**, He AR, Qin S, Chen LT, Okusaka T, Vogel A, Kim JW, Suksombooncharoen T, Lee MA, Kitano M, Burris H, Bouattour M, Tanasanvimon S, McNamara MG, Zaucha R, Avallone A, Tan B, Cundom J, Lee C, Takahashi H, Ikeda M, Chen JS, Wang J, Makowsky M, Rokutanda N, He P, Kurland JF, Cohen G, Valle JW. Durvalumab plus Gemcitabine and Cisplatin in Advanced Biliary Tract Cancer. *NEJM Evid* 2022; **1** [DOI: 10.1056/EVIDoa2200015]

4 **Tyson GL**, El-Serag HB. Risk factors for cholangiocarcinoma. *Hepatology* 2011; **54**: 173-184 [PMID: 21488076 DOI: 10.1002/hep.24351]

5 **Kim HJ**, Kim JS, Joo MK, Lee BJ, Kim JH, Yeon JE, Park JJ, Byun KS, Bak YT. Hepatolithiasis and intrahepatic cholangiocarcinoma: A review. *World J Gastroenterol* 2015; **21**: 13418-13431 [PMID: 26730152 DOI: 10.3748/wjg.v21.i48.13418]

6 **Cha SW**. [Management of Intrahepatic Duct Stone]. *Korean J Gastroenterol* 2018; **71**: 247-252 [PMID: 29791982 DOI: 10.4166/kjg.2018.71.5.247]

7 **Park JS**, Han HS, Hwang DW, Yoon YS, Cho JY, Koh YS, Kwon CH, Kim KS, Kim SB, Kim YH, Kim HC, Chu CW, Lee DS, Kim HJ, Park SJ, Han SS, Song TJ, Ahn YJ, Yoo YK, Yu HC, Yoon DS, Lee MK, Lee HK, Min SK, Jeong CY, Hong SC, Choi IS, Hur KY. Current status

of laparoscopic liver resection in Korea. *J Korean Med Sci* 2012; **27**: 767-771 [PMID: 22787372 DOI: 10.3346/jkms.2012.27.7.767]

8 **Huang MH**, Chen CH, Yang JC, Yang CC, Yeh YH, Chou DA, Mo LR, Yueh SK, Nien CK. Long-term outcome of percutaneous transhepatic cholangioscopic lithotomy for hepatolithiasis. *Am J Gastroenterol* 2003; **98**: 2655-2662 [PMID: 14687812 DOI: 10.1111/j.1572-0241.2003.08770.x]

9 **Suzuki Y**, Mori T, Yokoyama M, Nakazato T, Abe N, Nakanuma Y, Tsubouchi H, Sugiyama M. Hepatolithiasis: analysis of Japanese nationwide surveys over a period of 40 years. *J Hepatobiliary Pancreat Sci* 2014; **21**: 617-622 [PMID: 24824191 DOI: 10.1002/jhbp.116]

10 **Cheon YK**, Cho YD, Moon JH, Lee JS, Shim CS. Evaluation of long-term results and recurrent factors after operative and nonoperative treatment for hepatolithiasis. *Surgery* 2009; **146**: 843-853 [PMID: 19744434 DOI: 10.1016/j.surg.2009.04.009]

11 **Roy S**, Glaser S, Chakraborty S. Inflammation and Progression of Cholangiocarcinoma: Role of Angiogenic and Lymphangiogenic Mechanisms. *Front Med (Lausanne)* 2019; **6**: 293 [PMID: 31921870 DOI: 10.3389/fmed.2019.00293]

12 **Chang JS**, Tsai CR, Chen LT. Medical risk factors associated with cholangiocarcinoma in Taiwan: a population-based case-control study. *PLoS One* 2013; **8**: e69981 [PMID: 23894567 DOI: 10.1371/journal.pone.0069981]

13 **Brower V**. Of cancer and cholesterol: studies elucidate anticancer mechanisms of statins. *J Natl Cancer Inst* 2003; **95**: 844-846 [PMID: 12813163 DOI: 10.1093/jnci/95.12.844]

14 **Patrignani P**, Patrono C. Aspirin and Cancer. *J Am Coll Cardiol* 2016; **68**: 967-976 [PMID: 27561771 DOI: 10.1016/j.jacc.2016.05.083]

15 **Saraei P**, Asadi I, Kakar MA, Moradi-Kor N. The beneficial effects of metformin on cancer prevention and therapy: a comprehensive review of recent advances. *Cancer Manag Res* 2019; **11**: 3295-3313 [PMID: 31114366 DOI: 10.2147/CMAR.S200059]

16 **Rose PW**, Watson EK, Jenkins LS. Aspirin for prevention of cancer and cardiovascular disease. *Br J Gen Pract* 2011; **61**: 412-415 [PMID: 21801534 DOI: 10.3399/bjgp11X578133]

17 **Choi J**, Ghoz HM, Peeraphatdit T, Baichoo E, Addissie BD, Harmsen WS, Therneau TM, Olson JE, Chaiteerakij R, Roberts LR. Aspirin use and the risk of cholangiocarcinoma. *Hepatology* 2016; **64**: 785-796 [PMID: 26940227 DOI: 10.1002/hep.28529]

18 **Tseng CH**. Metformin and Biliary Tract Cancer in Patients With Type 2 Diabetes. *Front Oncol* 2020; **10**: 587666 [PMID: 33194743 DOI: 10.3389/fonc.2020.587666]

19 **Liu Z**, Alsaggaf R, McGlynn KA, Anderson LA, Tsai HT, Zhu B, Zhu Y, Mbulaiteye SM, Gadalla SM, Koshiol J. Statin use and reduced risk of biliary tract cancers in the UK Clinical Practice Research Datalink. *Gut* 2019; **68**: 1458-1464 [PMID: 30448774 DOI: 10.1136/gutjnl-2018-317504]

20 **Pausawasdi A**, Watanapa P. Hepatolithiasis: epidemiology and classification. *Hepatogastroenterology* 1997; **44**: 314-316 [PMID: 9164496 DOI: 10.3138/9781442672789-053]

World Journal of Clinical Cases

Submit a Manuscript: https://www.f6publishing.com

World J Clin Cases 2024 February 16; 12(5): 922-930

DOI: 10.12998/wjcc.v12.i5.922

ISSN 2307-8960 (online)

ORIGINAL ARTICLE

Retrospective Study

Effect of nursing on postoperative respiratory function and mental health of lung cancer patients

Xiang Yang, Dan Yin, Shi-Qing Chen

Specialty type: Nursing

Provenance and peer review: Unsolicited article; Externally peer reviewed.

Peer-review model: Single blind

Peer-review report's scientific quality classification

Grade A (Excellent): 0
Grade B (Very good): 0
Grade C (Good): C
Grade D (Fair): 0
Grade E (Poor): 0

P-Reviewer: Chemaly RF, United States

Received: November 22, 2023
Peer-review started: November 22, 2023
First decision: December 8, 2023
Revised: December 12, 2023
Accepted: December 29, 2023
Article in press: December 29, 2023
Published online: February 16, 2024

Xiang Yang, Department of Rehabilitation, The First People's Hospital of Jiangxia District, Wuhan (Union Jiangnan Hospital Huazhong University of Science and Technology), Wuhan 430200, Hubei Province, China

Dan Yin, Department of Intensive Care, The First People's Hospital of Jiangxia District, Wuhan (Union Jiangnan Hospital Huazhong University of Science and Technology), Wuhan 430200, Hubei Province, China

Shi-Qing Chen, Department of Neurology, The First People's Hospital of Jiangxia District, Wuhan (Union Jiangnan Hospital Huazhong University of Science and Technology), Wuhan 430200, Hubei Province, China

Corresponding author: Shi-Qing Chen, MNurs, Nurse, Department of Neurology, The First People's Hospital of Jiangxia District, Wuhan (Union Jiangnan Hospital Huazhong University of Science and Technology), No. 1 Cultural Avenue, Jiangxia District, Wuhan 430200, Hubei Province, China. 623305925@qq.com

Abstract

BACKGROUND

Both pulmonary rehabilitation training and psychological care have been shown to have a positive effect on the postoperative recovery of patients with lung cancer. However, few studies have combined the two to explore their combined effect. Therefore, this study aimed to investigate the effects of pulmonary rehabilitation training combined with psychological care on postoperative respiratory function and mental health in lung cancer patients.

AIM

To investigate effect of nursing on postoperative respiratory function and mental health of lung cancer patients.

METHODS

122 cases of lung cancer patients who underwent surgical treatment in our hospital and were treated in our department from January 2022 to April 2023 were selected and randomly divided into the control group and observation group. The control group performed the routine care intervention. The observation group was given pulmonary rehabilitation training and psychological care based on conventional nursing interventions. Forced expiratory volume, forced vital capacity. Maximum ventilatory volume (MVV) in one second was measured,

and the patient's 6-min walking distance and dyspnoea index scale were used to assess the patient's respiratory condition. The Connor-Davidson resilience scale (CD-RISC), self-rating anxiety scale (SAS), and self-rating depression scale (SDS) were used to evaluate the mental health of the patients.

RESULTS

There was no difference between the two groups regarding age, gender, education level, surgical procedure, type of pathology, and treatment ($P > 0.05$). After treatment, MVV, 6-min walking distance, toughness, strength, optimism, and total CD-RISC scores were significantly higher in the observation group ($P < 0.05$), dyspnoea scores, SAS, and SDS scores were substantially lower in the control group compared to the observation group ($P < 0.05$).

CONCLUSION

Pulmonary rehabilitation training combined with psychological care for patients after lung cancer resection could improve lung function, enhance daily activities, effectively relieve negative emotions such as anxiety and depression, and reduce complications.

Key Words: Pulmonary rehabilitation training; Psychological care; Lung cancer; Postoperative care; Respiratory function

Core Tip: Lung cancer is the malignant tumor with the highest case fatality rate worldwide. Explore the effects of pulmonary rehabilitation training combined with psychological care on postoperative respiratory function and psychological health of lung cancer patients. Pulmonary rehabilitation training combined with psychological nursing for patients after lung cancer resection can improve lung function, improve daily activities, effectively relieve anxiety, depression, and other negative emotions, and reduce the occurrence of complications.

Citation: Yang X, Yin D, Chen SQ. Effect of nursing on postoperative respiratory function and mental health of lung cancer patients. *World J Clin Cases* 2024; 12(5): 922-930
URL: https://www.wjgnet.com/2307-8960/full/v12/i5/922.htm
DOI: https://dx.doi.org/10.12998/wjcc.v12.i5.922

INTRODUCTION

Lung cancer is a malignant tumor originating mainly from lung organs, bronchial mucosa, or glands, and is the most common primary cancer of the lungs[1,2]. The cause of lung cancer was not yet clear, but the main causative factors were smoking, diet, heredity, occupational exposure, *etc*[3]. The main symptoms were cough, sputum, and blood, fever, and dyspnoea. To date, lung cancer is still the malignant tumor with the highest mortality rate worldwide, and its incidence rate is also at a high level[4-5]. Currently, lung cancer is mainly treated with comprehensive therapy based on surgical resection and postoperative radiotherapy[6], and new treatments such as traditional Chinese medicine and targeted therapy have also developed rapidly in recent years[7]. Still, the 5-year survival rate of patients has not been significantly improved. Neoadjuvant chemotherapy was often an adjuvant therapy after surgical resection of lung cancer[8], which could reduce disease recurrence and distant metastasis and improve patients' prognosis[9]. However, chemotherapy could damage patients' healthy lung tissues[10]. In addition, as part of the lung tissues had been removed by surgery, the lungs might be squeezed, and the chest muscles might be damaged during the operation, which might easily lead to decreased respiratory and lung functions, dyspnoea, atelectasis, or even respiratory failure after the operation, and ultimately lead to death.

Some studies have been conducted to use this method in nursing interventions for lung cancer chemotherapy patients. Still, most of them mainly observe the patients' quality of life, and fewer of them study its improvement of lung function [11,12]. Pulmonary rehabilitation training could improve patients' lung function through interventions such as respiratory function training and exercise instruction[13-15]. Some studies have shown that by communicating with patients, improving their cognition, and grasping their psychological changes, negative emotions such as anxiety and depression could be effectively alleviated[16,17]. In this study, we implemented pulmonary rehabilitation training combined with psychological care for postoperative lung cancer patients and evaluated respiratory function and psychological health before and after training.

MATERIALS AND METHODS

General information

One hundred and twenty-two patients with lung cancer who underwent surgical treatment in our hospital from January

2022 to April 2023 and were treated in our department were selected. The inclusion criteria were: Age ≥ 18 and < 65 years old, patients with postoperative pathological confirmation of lung cancer, no history of neurological, muscular, or joint diseases and other malignant tumors affecting movement, clear consciousness, everyday thinking, ability to hear, read, and write in Chinese, and patients signing an informed consent form.

Exclusion criteria: patients with preoperative complications such as lung infection and respiratory failure and those with cardiac, cerebrovascular, or other severe complications after surgery. Patients with combined serious organic lesions or insufficiency of other organs such as heart, brain, and kidney. Patients with an exercise participation rate of less than 80% were excluded.

Methods

Postoperative rehabilitation nursing: The control group includes health education, environmental care, observation of patients' condition changes, complications prevention, and treatment of adverse reactions during chemotherapy. After the patients are admitted to the hospital, let the patients know about the knowledge about the disease and increase the patient's understanding of their disease. Answer patients' concerns and prevent patients from infection appropriately. Give patients appropriate dietary care and instruct them to have a reasonable diet and balanced nutrition[18].

Based on the control group, the observation group was given pulmonary rehabilitation training (rehabilitation mode and intensity suitable for the patients themselves) and psychological care.

Pulmonary rehabilitation: Lung rehabilitation training is every four weeks as a rehabilitation cycle, with three consecutive cycles[14,19,20]. (1) Breathing training, including abdominal and lip-contraction breathing training. Abdominal respiratory training: the patient takes a suitable position, keeps quiet, and relaxes the whole body, inhales slowly through the nasal cavity to the maximum lung capacity, holds the breath, exhales slowly through the mouth, and then rests for 3-5 min, repeat the above training, 30-60 min per day. Contracted lip respiratory training: The patient takes a suitable position, keeps quiet and relaxes the whole body, inhales slowly through the nasal cavity to the maximum lung capacity, and then exhales slowly through the mouth; the ratio of Inhalation: exhalation time was 1:2. Inhalation: exhalation time ratio of 1:2, rest 3-5 min after repeating the above training, daily training 30-60 min; (2) Coughing sputum training: the patient's sitting position, abdominal breathing, deep Inhalation, rapid exhalation, feeling phlegm forceful coughing action; if the patient cannot cough up phlegm, the rehabilitation division could use the palm to quickly knock on the back, to promote the discharge of phlegm; and (3) Walking training: the patient first performs stretching activities for 5 min, then walks at a slow speed on the electric flatbed machine, and then gradually accelerates to the speed that the patient could be suitable for themself within 5 min, and then walks at a suitable speed, and the time for each walking training was 20-40 min, according to the patient's self-tolerance, and the training was done three times a day; or you could also choose to perform the walking training on the flat road, and the requirement was that the patient strolls for 5 min, and then gradually accelerates the speed of the walking. The patient could also walk on the level road, first stroll for 5 min, then gradually accelerate, and maintain the faster walking speed for 20-40 min under a tolerable situation.

Psychological care: The observation group implemented positive psychological intervention based on the control group. Positive psychological intervention methods[12,21-23]: (1) Establishment of psychological foundation. After the patients were admitted to the hospital, specialized medical staff assisted them in understanding the hospital environment, answered the questions raised by the patients, assessed their psychological conditions, helped eliminate their inner sense of strangeness, and made the patients feel warm; (2) Cognitive improvement. Professional healthcare workers explain cancer-related knowledge to patients, such as the causes, incidence, clinical manifestations, and treatment of cancer, *etc.*, to guide patients to understand cancer correctly, and at the same time, adopt the form of cancer health lectures and interviews to help patients and their families to understand the basic situation of cancer; (3) Establish social and family support. Medical staff encouraged family members to give emotional support to patients so that they could feel love and warmth, gradually restore self-confidence and self-esteem, and maintain their social roles and functions; (4) Excretion of negative emotions. Healthcare workers record the patient's condition changes in detail, provide targeted psychological counseling, guide the patient to control their negative emotions and encourage them to take the initiative to talk about their distress and vent their unhappiness; and (5) Positive thinking intervention. Through positive thinking breathing training, help patients cultivate emotional feeling and body awareness, learn how to get along with life's problems, learn positive thinking about interpersonal relationships, and instruct patients to practice more.

Testing indexes: Respiratory function: the lung function instrument was used to monitor the respiratory function of the patients; the patients were instructed to take the sitting position, the patients' noses were clamped to ensure that they breathed through their mouths, and they made exhalation and inhalation movements by the instructions, and the indicators of vital capacity (VC), forced expiratory volume in the first second (FEV_1), forceful vital capacity (FVC) and maximal voluntary ventilation (MVV) were monitored before and After treatment of the two groups, and the ratio of FEV_1 /FVC% was calculated. Ratio.

Dyspnoea: The patients' 6-min walking distance was measured before and After treatment, and the dyspnoea index scale was also used to assess the patient's respiratory condition, which had a total score of 0-4, with higher scores indicating more severe dyspnoea[24].

Psychological resilience: The Connor-Davidson resilience scale (CD-RISC) was used to assess the psychological resilience of the two groups of patients before and after treatment[23], which was divided into three dimensions, including resilience, strength, and optimism, with a total of 25 entries, and a 5-level scoring method, with never, rarely, sometimes, often, and consistently scoring 0-4 points, and a total score range of 0-4 points. The total score ranges from 0 to 100, with higher scores indicating higher levels of psychological resilience.

Table 1 Comparison of basic information of patients in two groups

Group	Cases	Sex (male/female)	Age (yr old)	Surgical resection site (Cases)				Pathological type (Cases)		Treatment (Cases)	
				Upper lobe	Middle lobe	Lower lobe	Partial wedge resection	Squamous	Adenocarcinoma	Radiotherapy/chemotherapy	Radiotherapy/chemotherapy+targeted therapies
Control	61	30/31	56.37 ± 9.43	12	11	14	24	13	48	19	42
Observation	61	28/33	57.82 ± 10.27	11	13	14	23	11	50	17	44
t		0.258	2.529	0.852				0.367		0.511	
P value		0.456	0.537	0.683				0.576		0.492	

Anxiety and depression evaluation[25]: Self-rating anxiety scale (SAS) was used to assess the patient's anxiety before and after nursing care. The scale contains five positive questions and 15 negative questions, and the score was the sum of the scores on a scale of 1 to 44, with 50-59 for mild anxiety, 60-69 for moderate anxiety, and ≥ 70 for severe anxiety. The self-rating depression scale (SDS) was used to rate the depression of patients and their families. The scale contains ten items, each of positive and negative questions, using a scale of 1 to 44; the score was the sum of the scores, of which 53-62 points for mild depression, 63-72 points for moderate depression, and ≥ 73 points for severe depression.

Statistical methods

SPSS 22.0 statistical software was used for data processing. Measurement data were expressed as mean ± standard deviation (mean ± SD), and a *t*-test was performed for comparison between groups. The count data were expressed as a rate (%), and the comparison between groups was conducted by χ^2 test. The difference was considered statistically significant at $P > 0.05$.

RESULTS

Basic information

After surgery, the two groups of patients chose the most appropriate treatment methods according to the patient's condition, economic situation, and wishes, including radiotherapy, targeted therapy, and so on. In a comparison of the two groups of patients in terms of age, gender, education level, surgical methods, pathological types, treatment methods, *etc.*, the difference was not significant ($P > 0.05$). It was comparable, as shown in Table 1.

Comparison of respiratory function between the two groups of patients

Before treatment, the VC, FEV_1/FVC, and MVV levels of patients in the two groups were compared, and the differences were not statistically significant ($P > 0.05$). After treatment, the levels of VC, FEV_1/FVC, and MVV of patients in the control group and the observation group were increased compared with those Before treatment, and the MVV of the observation group was increased compared with that of the control group, and the differences were statistically

significant ($P < 0.05$), as shown in Table 2.

Comparison of the degree of dyspnoea between the two groups of patients

Before treatment, the 6-min walking distance and dyspnoea scale score of the two groups of patients were compared, and the differences were not statistically significant ($P > 0.05$). After treatment, the 6-min walking distance of patients in both groups increased, and the increase of patients in the observation group was more significant than that of the control group. The dyspnoea scores of patients in both groups decreased, and the patients in the observation group were lower than those in the control group. The differences were statistically significant ($P < 0.05$), as shown in Table 3.

Comparison of CD-RISC between the two groups before and after treatment

Before treatment, the comparison of toughness, strength, optimism, and total CD-RISC scores between the two groups was not statistically significant ($P > 0.05$). After treatment, the toughness, stability, and full CD-RISC scores of those in the control group and the toughness, strength, optimism, and total CD-RISC scores of the observation group improved significantly compared with the before-treatment period. The observation group's toughness, stability, optimism, and total CD-RISC scores were enhanced considerably compared to the control group. The differences were statistically significant ($P < 0.05$), as shown in Table 4.

Comparison of patient's anxiety and depression scores

Before treatment, the SAS and SDS scores of patients in the two groups were compared, and the differences were not statistically significant ($P > 0.05$). After treatment, the SAS and SDS scores of the patients in the control group and the observation group were significantly lower than those before treatment, and the SAS and SDS scores of the observation group were significantly lower than those of the control group, and the differences were statistically significant ($P < 0.05$), as shown in Table 5.

DISCUSSION

Globally, the incidence rate and mortality rate of lung cancer had been at a high level and were constantly rising, followed by radiotherapy and chemotherapy, *etc*[26]. However, it would cause damage to the patient's body, destroying internal organs and bronchial tubes, *etc.*, increasing inflammatory reaction of the body, affecting postoperative compliance, aggravating psychological and physiological pain, and leading to a decline in the quality of life[6,9].

After lung cancer resection, patients' lung volume and lung capacity were reduced, which was easy to cause hypoxemia. The body overflows with inflammatory factors, reducing lung surface-active substances and decreasing lung compliance. The lumen narrowed, which led to a decrease in the function of gas exchange and lung ventilation[27]. Pulmonary rehabilitation exercise improved the contraction function of abdominal muscles and diaphragm through abdominal breathing to increase the airway pressure and achieve the effect of correcting hypoxia[14,15]. Positive pressure at the end of respiration was generated through lip-contracted breathing, which reduces the functional residual air volume in the alveoli and helps the reexpansion of atrophied lung tissues. Effective cough and sputum expectoration training could reduce the deposition of secretions, keep the airway open, and reduce lung infection and pulmonary atelectasis[28]. Postoperative activities, such as out-of-bed and limb exercise, could promote lung expansion and blood circulation, which improves ventilation function and the body's adaptive ability[29]. The result of this study showed that After treatment, levels of VC, FEV1/FVC, and MVV in the control group patients and the observation group increased compared with those before the intervention, and MVV in the observation group increased compared with those in the control group, which indicated that pulmonary rehabilitation exercises combined with psychological care could effectively improve the lung function of patients. After treatment, the 6-min walking distance of both groups increased, and the increase in patients in the observation group was more significant than that of the control group. The dyspnoea score of both groups was reduced. The patients in the observation group were lower than those in the control group, which indicated that getting out of bed as early as possible could avoid the dyspnoea problem caused by prolonged lying in bed and resting.

Psychological care could help patients understand lung cancer and resection-related knowledge[21], introduce successful cases of surgery, and let family members participate in psychological counseling to make patients clear that taking the initiative to accept treatment was the key to recovery[30], establish self-confidence in treatment, and thus actively cooperate with postoperative rehabilitation training[31]. Psychological resilience refers to an individual's ability to handle and cope with adversity, which allows individuals to protect themselves[32]. Good psychological resilience enables patients to handle adversity optimistically when encountering hardship or bad luck. The improvement of psychological resilience determines the improvement of the psychological quality of cancer patients to cope with adverse events, and they were able to face their cancer condition calmly and rationally, and their bad moods could be improved. In this study, After treatment, the resilience, strength, and CD-RISC total scores of the control group and the resilience, strength, optimism, and CD-RISC total scores of the observation group improved significantly compared to the before-treatment period, and the resilience, strength, optimism and CD-RISC full scores of the observation group improved significantly compared to the control group. This indicates that psychological care could improve the psychological resilience of cancer patients. Positive psychological intervention taps the patients' inner positive potential through cognitive improvement, positive thought training, negative emotion discharge, instilling positive energy, and other measures to improve their adaptability and coping ability, thus enhancing their resilience, strength, and optimism. Anxiety and depression were common emotions in patients with advanced cancer and were the main reasons affecting the quality of their survival[33].

Table 2 Comparison of respiratory function indexes between the two groups before and after treatment

Group	Cases	Vital capacity (%)		Forceful vital capacity$_1$/forceful vital capacity (%)		Maximal voluntary ventilation (%)	
		Before treatment	After treatment	Before treatment	After treatment	Before treatment	After treatment
Control	61	59.84 ± 6.25	72.47 ± 8.02[a]	64.58 ± 8.34	71.83 ± 7.26[a]	51.62 ± 5.92	57.39 ± 5.02
Observation	61	60.61 ± 5.93	79.95 ± 7.39[a]	64.95 ± 7.39	80.64 ± 8.31[a]	50.97 ± 6.02	66.48 ± 5.43[a]
t		0.827	3.141	0.256	4.362	-1.249	2.345
P value		0.568	0.186	0.682	0.136	0.721	0.042

[a]*P* < 0.05 *vs* before treatment.

Table 3 Comparison of the degree of dyspnoea between the two groups of patients

Group	Cases	6 min walking distance (m)		Dyspnoea scale score	
		Before treatment	After treatment	Before treatment	After treatment
Control	61	320.64 ± 43.28	399.83 ± 34.26[a]	2.84 ± 0.53	2.06 ± 0.37[a]
Observation	61	321.73 ± 38.45	452.65 ± 37.46[a]	2.88 ± 0.35	1.45 ± 0.22[a]
t		11.247	8.305	0.132	-0.083
P value		0.637	0.032	0.593	0.002

[a]*P* < 0.05 *vs* before treatment.

Table 4 Comparison of between the two groups before and after treatment

Group	Cases	Toughness		Strength		Optimism		Total scores	
		Before treatment	After treatment	Before treatment	After treatment	Before treatment	After treatment	Before treatment	After treatment
Control	61	20.46 ± 2.93	25.62 ± 3.11[a]	14.89 ± 1.63	17.76 ± 2.21[a]	8.06 ± 1.02	9.75 ± 1.21	43.41 ± 4.32	53.13 ± 5.98[a]
Observation	61	20.13 ± 3.14	31.59 ± 2.89[a]	15.02 ± 1.75	20.94 ± 2.85[a]	8.12 ± 0.92	13.26 ± 1.93[a]	43.27 ± 5.01	65.79 ± 6.75[a]
t		-0.252	2.561	1.257	1.683	0.731	4.523	-1.953	8.247
P value		0.453	0.012	0.682	0.045	0.472	0.015	0.583	0.007

[a]*P* < 0.05 *vs* before treatment.

Table 5 Comparison of self-rating anxiety scale and self-rating depression scale between the two groups before and after treatment

Group	Cases	SAS scores		SDS scores	
		Before treatment	After treatment	Before treatment	After treatment
Control	61	53.15 ± 6.03	43.25 ± 5.64[a]	52.89 ± 6.24	45.79 ± 5.75[a]
Observation	61	53.68 ± 5.82	32.15 ± 5.02[a]	53.34 ± 5.89	30.46 ± 4.93[a]
t		1.464	-3.285	1.245	-4.845
P value		0.574	0.000	0.634	0.000

[a]*P* < 0.05 *vs* before treatment. SAS: Self-rating anxiety scale; SDS: Self-rating depression scale.

This study showed that after treatment, the SAS and SDS scores of the patients in the control and observation groups were significantly lower than those before the treatment. The SAS and SDS scores of the observation group were significantly lower than those of the control group, indicating that the pulmonary rehabilitation exercise combined with psychological care improved the negative emotions of patients, such as anxiety and depression, and improved the ability of patients to perform activities of daily living.However, this study has some shortcomings, such as a small sample size, a single study subject, and geographical restrictions on the source of cases. Therefore, it is necessary to increase the sample size, include multi-center study subjects, and expand the source range of cases in future studies to confirm the accuracy of this study.

CONCLUSION

In conclusion, the implementation of pulmonary rehabilitation exercise combined with psychological care for patients after lung cancer resection could effectively alleviate negative emotions such as anxiety and depression, improve lung function, enhance daily activity ability, and reduce the occurrence of complications.

ARTICLE HIGHLIGHTS

Research background

Lung cancer is a malignant tumor arising from the pulmonary organs, bronchial mucosa or glands, and it is also the most common primary lung cancer. For many people, lung cancer is a fatal disease, but with the continuous progress of medical technology, the treatment methods and prognosis of lung cancer have also been greatly improved.

Research motivation

We also found that pulmonary rehabilitation training and psychological care have a positive impact on the treatment of lung cancer patients, which is worth further promotion and application.

Research objectives

This paper conducts a comprehensive analysis on the effects of pulmonary rehabilitation training combined with psychological care on postoperative respiratory function and psychological health of lung cancer patients.

Research methods

This study used the design of a randomized controlled trial to divide patients after lung cancer surgery meeting the inclusion criteria into two groups, control and experimental groups. The control group received conventional treatment and nursing care, while the experimental group received pulmonary rehabilitation training combined with psychological nursing care on the basis of the control group.

Research results

By comparing the respiratory function and mental health indicators of the observation group and the control group before and after the intervention, it was found that the respiratory function and mental health status of the patients in the experimental group were significantly improved.

Research conclusions

Pulmonary rehabilitation training combined with psychological nursing for patients after lung cancer resection can improve lung function, improve daily activities, effectively relieve anxiety, depression, and other negative emotions, and reduce the occurrence of complications.

Research perspectives

The importance of rehabilitation care.

FOOTNOTES

Co-first authors: Xiang Yang and Dan Yin.

Author contributions: Yang X and Yin D designed the research; Chen SQ contributed new reagents/analytic tools; Chen SQ, Yang X, and Yin D analyzed the data; Yang X and Yin D wrote the paper; All authors were involved in the critical review of the results and have contributed to, read, and approved the final manuscript. Yang X and Yin D contributed equally to this work as co-first authors equally to this work. The reasons for designating Yang X and Yin D as co-first authors are threefold. First, the research was performed as a collaborative effort, and the designation of co-corresponding authorship accurately reflects the distribution of responsibilities and burdens associated with the time and effort required to complete the study and the resultant paper. This also ensures effective communication and management of post-submission matters, ultimately enhancing the paper's quality and reliability. Second, the

overall research team encompassed authors with a variety of expertise and skills from different fields, and the designation of co-first authors best reflects this diversity. This also promotes the most comprehensive and in-depth examination of the research topic, ultimately enriching readers' understanding by offering various expert perspectives. Third, Yang X and Yin D contributed efforts of equal substance throughout the research process. The choice of these researchers as co-first authors acknowledges and respects this equal contribution, while recognizing the spirit of teamwork and collaboration of this study. In summary, we believe that designating Yang X and Yin D as co-first authors of is fitting for our manuscript as it accurately reflects our team's collaborative spirit, equal contributions, and diversity.

Institutional review board statement: This study protocol was approved by the First People's Hospital of Jiangxia District, and all the families have voluntarily participated in the study and have signed informed consent forms.

Informed consent statement: All study participants or their legal guardian provided informed written consent about personal and medical data collection prior to study enrolment.

Conflict-of-interest statement: All the authors declared no conflict of interest existing in this paper.

Data sharing statement: Data generated from this investigation are available upon reasonable quest from the corresponding author.

Country/Territory of origin: China

ORCID number: Shi-Qing Chen 0009-0003-9861-2266.

S-Editor: Liu JH
L-Editor: A
P-Editor: Yu HG

REFERENCES

1 **Bade BC**, Dela Cruz CS. Lung Cancer 2020: Epidemiology, Etiology, and Prevention. *Clin Chest Med* 2020; **41**: 1-24 [PMID: 32008623 DOI: 10.1016/j.ccm.2019.10.001]
2 **Wu F**, Wang L, Zhou C. Lung cancer in China: current and prospect. *Curr Opin Oncol* 2021; **33**: 40-46 [PMID: 33165004 DOI: 10.1097/CCO.0000000000000703]
3 **Schabath MB**, Cote ML. Cancer Progress and Priorities: Lung Cancer. *Cancer Epidemiol Biomarkers Prev* 2019; **28**: 1563-1579 [PMID: 31575553 DOI: 10.1158/1055-9965.EPI-19-0221]
4 **Malhotra J**, Malvezzi M, Negri E, La Vecchia C, Boffetta P. Risk factors for lung cancer worldwide. *Eur Respir J* 2016; **48**: 889-902 [PMID: 27174888 DOI: 10.1183/13993003.00359-2016]
5 **Schmeck B**, Bertrams W, Lai X, Vera J. Systems Medicine for Lung Diseases: Phenotypes and Precision Medicine in Cancer, Infection, and Allergy. *Methods Mol Biol* 2016; **1386**: 119-133 [PMID: 26677183 DOI: 10.1007/978-1-4939-3283-2_8]
6 **Hoy H**, Lynch T, Beck M. Surgical Treatment of Lung Cancer. *Crit Care Nurs Clin North Am* 2019; **31**: 303-313 [PMID: 31351552 DOI: 10.1016/j.cnc.2019.05.002]
7 **Shen G**, Zheng F, Ren D, Du F, Dong Q, Wang Z, Zhao F, Ahmad R, Zhao J. Anlotinib: a novel multi-targeting tyrosine kinase inhibitor in clinical development. *J Hematol Oncol* 2018; **11**: 120 [PMID: 30231931 DOI: 10.1186/s13045-018-0664-7]
8 **Saw SPL**, Ong BH, Chua KLM, Takano A, Tan DSW. Revisiting neoadjuvant therapy in non-small-cell lung cancer. *Lancet Oncol* 2021; **22**: e501-e516 [PMID: 34735819 DOI: 10.1016/S1470-2045(21)00383-1]
9 **Chaft JE**, Shyr Y, Sepesi B, Forde PM. Preoperative and Postoperative Systemic Therapy for Operable Non-Small-Cell Lung Cancer. *J Clin Oncol* 2022; **40**: 546-555 [PMID: 34985966 DOI: 10.1200/JCO.21.01589]
10 **Leo F**, Pelosi G, Sonzogni A, Chilosi M, Bonomo G, Spaggiari L. Structural lung damage after chemotherapy fact or fiction? *Lung Cancer* 2010; **67**: 306-310 [PMID: 19477548 DOI: 10.1016/j.lungcan.2009.04.013]
11 **Rueda JR**, Solà I, Pascual A, Subirana Casacuberta M. Non-invasive interventions for improving well-being and quality of life in patients with lung cancer. *Cochrane Database Syst Rev* 2011; **2011**: CD004282 [PMID: 21901689 DOI: 10.1002/14651858.CD004282.pub3]
12 **Xiao J**, Chow KM, Choi KC, Ng SNM, Huang C, Ding J, Chan WHC. Effects of family-oriented dignity therapy on dignity, depression and spiritual well-being of patients with lung cancer undergoing chemotherapy: A randomised controlled trial. *Int J Nurs Stud* 2022; **129**: 104217 [PMID: 35339908 DOI: 10.1016/j.ijnurstu.2022.104217]
13 **Spruit MA**. Pulmonary rehabilitation. *Eur Respir Rev* 2014; **23**: 55-63 [PMID: 24591662 DOI: 10.1183/09059180.00008013]
14 **Cornelison SD**, Pascual RM. Pulmonary Rehabilitation in the Management of Chronic Lung Disease. *Med Clin North Am* 2019; **103**: 577-584 [PMID: 30955523 DOI: 10.1016/j.mcna.2018.12.015]
15 **Cameron-Tucker HL**, Wood-Baker R, Owen C, Joseph L, Walters EH. Chronic disease self-management and exercise in COPD as pulmonary rehabilitation: a randomized controlled trial. *Int J Chron Obstruct Pulmon Dis* 2014; **9**: 513-523 [PMID: 24876771 DOI: 10.2147/COPD.S58478]
16 **Ball H**, Moore S, Leary A. A systematic literature review comparing the psychological care needs of patients with mesothelioma and advanced lung cancer. *Eur J Oncol Nurs* 2016; **25**: 62-67 [PMID: 27865254 DOI: 10.1016/j.ejon.2016.09.007]
17 **Aubin M**, Vézina L, Verreault R, Simard S, Desbiens JF, Tremblay L, Dumont S, Fillion L, Dogba MJ, Gagnon P. Effectiveness of an

intervention to improve supportive care for family caregivers of patients with lung cancer: study protocol for a randomized controlled trial. *Trials* 2017; **18**: 304 [PMID: 28676071 DOI: 10.1186/s13063-017-2044-y]

18 **Wang M**, Sun Y, Zhang M, Yu R, Fu J. Effects of high-quality nursing care on quality of life, survival, and recurrence in patients with advanced nonsmall cell lung cancer. *Medicine (Baltimore)* 2022; **101**: e30569 [PMID: 36123938 DOI: 10.1097/MD.0000000000030569]

19 **Chen Z**, Cai R, Liao X, Huang X, Zhao C, Chen M. The efficacy of pulmonary rehabilitation exercise training on complications and mortality after lung cancer resection: a systematic review and meta-analysis. *Transl Cancer Res* 2022; **11**: 1321-1329 [PMID: 35706789 DOI: 10.21037/tcr-22-978]

20 **Zhou T**, Sun C. Effect of physical manipulation pulmonary rehabilitation on lung cancer patients after thoracoscopic lobectomy. *Thorac Cancer* 2022; **13**: 308-315 [PMID: 34882313 DOI: 10.1111/1759-7714.14225]

21 **Tu M**, Wang F, Shen S, Wang H, Feng J. Influences of Psychological Intervention on Negative Emotion, Cancer-Related Fatigue and Level of Hope in Lung Cancer Chemotherapy Patients Based on the PERMA Framework. *Iran J Public Health* 2021; **50**: 728-736 [PMID: 34183922 DOI: 10.18502/ijph.v50i4.5997]

22 **Krebber AH**, van Uden-Kraan CF, Melissant HC, Cuijpers P, van Straten A, Becker-Commissaris A, Leemans CR, Verdonck-de Leeuw IM. A guided self-help intervention targeting psychological distress among head and neck cancer and lung cancer patients: motivation to start, experiences and perceived outcomes. *Support Care Cancer* 2017; **25**: 127-135 [PMID: 27585808 DOI: 10.1007/s00520-016-3393-x]

23 **Sun V**, Kim JY, Raz DJ, Chang W, Erhunmwunsee L, Uranga C, Ireland AM, Reckamp K, Tiep B, Hayter J, Lew M, Ferrell B, McCorkle R. Preparing Cancer Patients and Family Caregivers for Lung Surgery: Development of a Multimedia Self-Management Intervention. *J Cancer Educ* 2018; **33**: 557-563 [PMID: 27542378 DOI: 10.1007/s13187-016-1103-5]

24 **Rutkowska A**, Jastrzebski D, Rutkowski S, Żebrowska A, Stanula A, Szczegielniak J, Ziora D, Casaburi R. Exercise Training in Patients With Non-Small Cell Lung Cancer During In-Hospital Chemotherapy Treatment: A RANDOMIZED CONTROLLED TRIAL. *J Cardiopulm Rehabil Prev* 2019; **39**: 127-133 [PMID: 30801436 DOI: 10.1097/HCR.0000000000000410]

25 **Lei J**, Yang J, Dong L, Xu J, Chen J, Hou X, Bai Z. An exercise prescription for patients with lung cancer improves the quality of life, depression, and anxiety. *Front Public Health* 2022; **10**: 1050471 [PMID: 36466452 DOI: 10.3389/fpubh.2022.1050471]

26 **Provencio M**, Calvo V, Romero A, Spicer JD, Cruz-Bermúdez A. Treatment Sequencing in Resectable Lung Cancer: The Good and the Bad of Adjuvant Versus Neoadjuvant Therapy. *Am Soc Clin Oncol Educ Book* 2022; **42**: 1-18 [PMID: 35561296 DOI: 10.1200/EDBK_358995]

27 **Yin X**, Liao H, Yun H, Lin N, Li S, Xiang Y, Ma X. Artificial intelligence-based prediction of clinical outcome in immunotherapy and targeted therapy of lung cancer. *Semin Cancer Biol* 2022; **86**: 146-159 [PMID: 35963564 DOI: 10.1016/j.semcancer.2022.08.002]

28 **Okura K**, Takahashi Y, Hatakeyama K, Saito K, Kasukawa Y, Imai K, Minamiya Y. Preoperative inspiratory muscle training in a patient with lung cancer and comorbid chronic obstructive pulmonary disease and respiratory sarcopenia: A case report. *Physiother Res Int* 2023; **28**: e1987 [PMID: 36533560 DOI: 10.1002/pri.1987]

29 **Dreyfus JF**, Kassoul A, Michel-Cherqui M, Fischler M, Le Guen M. A French version of Ringsted's questionnaire on pain-related impairment of daily activities after lung surgery: A cohort study. *Anaesth Crit Care Pain Med* 2019; **38**: 615-621 [PMID: 30826390 DOI: 10.1016/j.accpm.2019.02.014]

30 **Avancini A**, Sartori G, Gkountakos A, Casali M, Trestini I, Tregnago D, Bria E, Jones LW, Milella M, Lanza M, Pilotto S. Physical Activity and Exercise in Lung Cancer Care: Will Promises Be Fulfilled? *Oncologist* 2020; **25**: e555-e569 [PMID: 32162811 DOI: 10.1634/theoncologist.2019-0463]

31 **Brown NM**, Lui CW, Robinson PC, Boyle FM. Supportive care needs and preferences of lung cancer patients: a semi-structured qualitative interview study. *Support Care Cancer* 2015; **23**: 1533-1539 [PMID: 25394711 DOI: 10.1007/s00520-014-2508-5]

32 **Temel JS**, Petrillo LA, Greer JA. Patient-Centered Palliative Care for Patients With Advanced Lung Cancer. *J Clin Oncol* 2022; **40**: 626-634 [PMID: 34985932 DOI: 10.1200/JCO.21.01710]

33 **Wang YH**, Li JQ, Shi JF, Que JY, Liu JJ, Lappin JM, Leung J, Ravindran AV, Chen WQ, Qiao YL, Shi J, Lu L, Bao YP. Depression and anxiety in relation to cancer incidence and mortality: a systematic review and meta-analysis of cohort studies. *Mol Psychiatry* 2020; **25**: 1487-1499 [PMID: 31745237 DOI: 10.1038/s41380-019-0595-x]

World Journal of Clinical Cases

Submit a Manuscript: https://www.f6publishing.com

World J Clin Cases 2024 February 16; 12(5): 931-941

DOI: 10.12998/wjcc.v12.i5.931

ISSN 2307-8960 (online)

ORIGINAL ARTICLE

Retrospective Study

Value of glucose transport protein 1 expression in detecting lymph node metastasis in patients with colorectal cancer

Hongsik Kim, Song-Yi Choi, Tae-Young Heo, Kyeong-Rok Kim, Jisun Lee, Min Young Yoo, Taek-Gu Lee, Joung-Ho Han

Specialty type: Gastroenterology and hepatology

Provenance and peer review: Unsolicited article; Externally peer reviewed.

Peer-review model: Single blind

Peer-review report's scientific quality classification

Grade A (Excellent): 0
Grade B (Very good): B
Grade C (Good): C
Grade D (Fair): 0
Grade E (Poor): 0

P-Reviewer: Shah SIA, Pakistan; Yan B, China

Received: November 9, 2023
Peer-review started: November 9, 2023
First decision: December 21, 2023
Revised: January 4, 2024
Accepted: January 22, 2024
Article in press: January 22, 2024
Published online: February 16, 2024

Hongsik Kim, Department of Internal Medicine, Chungbuk National University Hospital, Cheongju 28644, South Korea

Song-Yi Choi, Department of Pathology, Chungnam National University College of Medicine, Daejeon 35015, South Korea

Tae-Young Heo, Kyeong-Rok Kim, Information and Statistics, Chungbuk National University, Cheongju 28644, South Korea

Jisun Lee, Department of Radiology, College of Medicine, Chungbuk National University, Chungbuk National University Hospital, Cheongju-si 28644, South Korea

Min Young Yoo, Department of Nuclear Medicine, School of Medicine, Inha University, Incheon 22332, South Korea

Taek-Gu Lee, Department of Surgery, Chungbuk National University, College of Medicine, Cheongju-si 28644, South Korea

Joung-Ho Han, Department of Internal Medicen, Chungbuk National University, College of medicine, Cheongju-si 28644, South Korea

Corresponding author: Joung-Ho Han, MD, PhD, Professor, Department of Internal Medicen, Chungbuk National University, College of medicine, No. 1 Chungdae-ro, Seowon-gu, Cheongju-si 28644, South Korea. joungho@chungbuk.ac.kr

Abstract

BACKGROUND

There are limited data on the use of glucose transport protein 1 (GLUT-1) expression as a biomarker for predicting lymph node metastasis in patients with colorectal cancer. GLUT-1 and GLUT-3, hexokinase (HK)-II, and hypoxia-induced factor (HIF)-1 expressions may be useful biomarkers for detecting primary tumors and lymph node metastasis when combined with fluorodeoxyglucose (FDG) uptake on positron emission tomography/computed tomography (PET/CT).

AIM

To evaluate GLUT-1, GLUT-3, HK-II, and HIF-1 expressions as biomarkers for detecting primary tumors and lymph node metastasis with 18F-FDG-PET/CT.

METHODS
This retrospective study included 169 patients with colorectal cancer who underwent colectomy and preoperative 18F-FDG-PET/CT at Chungbuk National University Hospital between January 2009 and May 2012. Two tissue cores from the central and peripheral areas of the tumors were obtained and were examined by a dedicated pathologist, and the expressions of GLUT-1, GLUT-3, HK-II, and HIF-1 were determined using immunohistochemical staining. We analyzed the correlations among their expressions, various clinicopathological factors, and the maximum standardized uptake value (SUVmax) of PET/CT.

RESULTS
GLUT-1 was found at the center or periphery of the tumors in 109 (64.5%) of the 169 patients. GLUT-1 positivity was significantly correlated with the SUVmax of the primary tumor and lymph nodes, regardless of the biopsy site (tumor center, $P < 0.001$ and $P = 0.012$; tumor periphery, $P = 0.030$ and $P = 0.010$, respectively). GLUT-1 positivity and negativity were associated with higher and lower sensitivities of PET/CT, respectively, for the detection of lymph node metastasis, regardless of the biopsy site. GLUT3, HK-II, and HIF-1 expressions were not significantly correlated with the SUVmax of the primary tumor and lymph nodes.

CONCLUSION
GLUT-1 expression was significantly correlated with the SUVmax of 18F-FDG-PET/CT for primary tumors and lymph nodes. Clinicians should consider GLUT-1 expression in preoperative endoscopic biopsy in interpreting PET/CT findings.

Key Words: 18F-FDG-PET-CT; Biomarker; Colorectal neoplasms; Glucose transporter type 1; Lymph node

Core Tip: Glucose transport protein 1 (GLUT-1) expression is a significant predictor of lymph node metastasis in patients with colorectal cancer. Positron emission tomography/computed tomography showed a higher sensitivity for detecting lymph node metastasis for GLUT-1-positive tumors, suggesting that GLUT-1 expression can be used to improve the accuracy of preoperative staging and guide treatment planning in patients with colorectal cancer.

Citation: Kim H, Choi SY, Heo TY, Kim KR, Lee J, Yoo MY, Lee TG, Han JH. Value of glucose transport protein 1 expression in detecting lymph node metastasis in patients with colorectal cancer. *World J Clin Cases* 2024; 12(5): 931-941
URL: https://www.wjgnet.com/2307-8960/full/v12/i5/931.htm
DOI: https://dx.doi.org/10.12998/wjcc.v12.i5.931

INTRODUCTION

Colorectal cancer is the third most common malignant tumor globally, with a high incidence in developed countries[1]. Preoperative staging is important for predicting prognosis and determining appropriate treatment modalities. Although various imaging techniques such as computed tomography (CT), magnetic resonance imaging (MRI), and positron emission tomography (PET)/CT are used, the diagnostic accuracy for lymph node metastasis varies from 54% to 80%[2,3]. Several studies have suggested the importance of PET/CT in patients with colorectal cancer; however, the extent of its contribution has not been well-established[4,5]. Its sensitivity for diagnosing the primary site is as high as 95%-100%, while its sensitivity for diagnosing lymph node metastasis remains low (29%-37%), although a high specificity of 83%-96% has been reported[6-9].

18F-fluorodeoxyglucose (18F-FDG)-PET/CT is widely used to detect primary tumors and metastasis, monitor recurrence, and evaluate therapeutic response[10]. It is based on the enhanced glucose metabolism of malignant tumors. Malignant tumors increase glucose utilization *via* increasing the expression of glucose transporter (GLUT) and upregulating intracellular enzymes such as hexokinase (HK) that promote glycolysis and result in the accumulation of FDG[11,12]. Further, malignant tumors grow abnormally and become hypoxic, which induces the expression of hypoxia induced factor-1 (HIF-1). HIF-1 is a transcription factor that promotes the expression of several genes involved in glucose utilization, including glucose transporters and glycolytic enzymes such as GLUT and HK-II[13]. Some studies have evaluated the relationship between the expression of several proteins, including GLUT, HK-II, and HIF-1, and FDG uptake on PET/CT to increase the accuracy of PET/CT in detecting various malignancies[14-16]. However, the correlation between protein expression and FDG uptake in various malignancies remains controversial[11]. While FDG uptake in colorectal cancer has been reported, its correlation with protein expression has not been established[17,18].

Previous studies have shown that low GLUT expression at the tumor center (tissue obtained by surgery) is correlated with a false-negative diagnosis based on PET/CT[19,20]. Therefore, further studies investigating whether PET/CT findings in combination with GLUT expression in preoperative endoscopic biopsy of colorectal cancer can help provide a more accurate assessment of lymph node staging are in demand. Studies assessing GLUT expressions in relation to

biopsy sites (tumor center with the tissue being obtained by surgery *vs* tumor periphery with the sample being obtained by endoscopy) are also needed.

In this study, we used immunohistochemistry (IHC) to determine the correlation between GLUT-1, GLUT-3, HK-II, and HIF-1 expressions in the central and peripheral areas of a primary tumor and investigated their values as biomarkers for detecting primary colorectal cancer and lymph node metastasis in combination with FDG uptake on PET/CT.

MATERIALS AND METHODS

Patients

We retrospectively analyzed 240 patients with colorectal cancer who had undergone colectomy and were diagnosed with adenocarcinoma at Chungbuk National University Hospital between January 2009 and May 2012. The histologic findings were interpreted based on the World Health Organization classification. The colon cancer stage evaluation was based on the American Joint Committee on Cancer 7th Edition Cancer Staging Manual. A total of 71 patients were excluded from this study: 66 patients were not examined with 18F-FDG-PET/CT, and 5 patients were not followed up. None of the patients had received neoadjuvant chemotherapy or radiotherapy.

Two tissue cores from the central and peripheral areas of the tumor were obtained from the 169 included patients for pathological examination, and GLUT-1 expression was evaluated using IHC staining. The samples were examined by a dedicated pathologist (SYC). All clinical, laboratory, and radiological data were collected from the electronic medical records. The Institutional Review Board (IRB No. 2013-03-003) of Chungbuk National University Hospital approved this study, and the requirement for informed consent was waived due to the retrospective nature of the study.

Immunohistochemical staining

All cases were reviewed, and 3 mm-sized tissue microarrays (TMA) were reconstructed. Two cores (tumor center and periphery) were obtained for each case. The core obtained from the center of the tumor close to the mucosa was indicated as "tumor center," and the core obtained from the deep invasive front was designated as "periphery." Sections of 4-μm thickness were cut and placed on SuperfrostPlus microscope slides (Fisher Scientific). IHC staining was performed using the BenchMark XT automated immunohistochemistry stainer (Ventana Medical Systems, Inc., United States) and signal was detected using a Ventana Ultraview DAB Kit (Ventana Medical Systems). Briefly, sections were deparaffinized using the EZ Prep solution. Antigen retrieval was performed using the CC1 standard automated process (pH 8.4 buffer contained Tris/Borate/EDTA). A DAB inhibitor (3% H_2O_2 endogenous peroxidase) was blocked for 4 min at 37 °C temperature. The slides were incubated with primary antibodies specific to GLUT-1 (1:100, Thermo Fisher Scientific, USA), GLUT-3 (1:50, Thermo Fisher Scientific, USA), HK-II (1:100, Cell Signaling Technology, United States), and HIF-1 (1:50, Thermo Fisher Scientific) for 30 min at 37 °C followed by incubation with a secondary antibody (Universal HRP Multimer) for 8 min at 37 °C. The slides were incubated with DAB (chromogen) + H_2O_2 (substrate) for 8 min, followed by counterstaining using hematoxylin and DAPI at 37 °C. Tris buffer (pH 7.6) was used as the washing solution.

GLUT-1, GLUT-3, HK-II, and HIF-1 expressions were considered positive when > 5% of tumor cells demonstrated cytoplasmic or membranous staining. The immunoreactive score was rated as 0 (negative), 1 (weak), 2 (moderate), or 3 (strong) based on the average staining intensity. A score of 2 or higher indicated positivity. HIF-1 expression was considered positive when > 5% of tumor cells demonstrated nuclear staining (Figures 1 and 2).

Statistics

Descriptive statistics were used to summarize the patient and tumor characteristics, and the data are reported as proportions and medians for continuous variables. The categorical data are presented as numbers (%). The continuous variables were compared using the Student's *t*-test, and the categorical variables were compared using the chi-squared or Fisher's exact test. Statistical significance was set at $P < 0.05$. Statistical analyses were performed using IBM SPSS Statistics version 25 (IBM, Armonk, NY, United States).

RESULTS

Relationship between GLUT-1 expression and clinicopathologic parameters

Table 1 presents the relationship between GLUT-1 expression and clinicopathological parameters. Among the 169 patients, 86 (50.9%) and 91 (53.8%) patients showed GLUT-1 positivity in the tumor center and periphery, respectively. GLUT-1 positivity was significantly correlated with the SUVmax of the primary tumor and lymph nodes, regardless of the biopsy site (tumor center, $P < 0.001$ and $P = 0.012$; tumor periphery $P = 0.030$ and $P = 0.010$, respectively).

Lymph node metastasis prediction based on PET/CT findings combined with GLUT-1 expression

We analyzed the predictive values of PET/CT, including sensitivity, specificity, positive predictive value (PPV), and negative predictive value (NPV) for lymph node metastasis (Table 2).

Among the 169 patients, 53 were classified as positive for lymph node metastasis on PET/CT, and 35 were histologically confirmed positive, with a sensitivity of 50.0% and a PPV of 66.0%. A total of 116 patients were classified as negative for lymph node metastasis on PET/CT, and 81 patients were histologically confirmed as negative with a specificity of 81.8% and an NPV of 69.8%.

Table 1 Correlation between glucose transport protein 1 expression and clinicopathological parameters

	GLUT-1 (center)		*P* value	GLUT-1 (periphery)		*P* value
	(-) (*n* = 83)	(+) (*n* = 86)		(-) (*n* = 78)	(+) (*n* = 91)	
Age (yr ± SD)	64.0 ± 11.4	64.7 ± 12.6	0.740	64.0 ± 11.6	64.7 ± 12.4	0.718
Sex						
Male	52	54	0.985	51	55	0.507
Female	31	32		27	36	
Tumor size (mean ± SD)	4.9 ± 1.8	5.2 ± 2.0	0.277	5.1 ± 1.7	5.1 ± 2.1	0.932
T stage						
T1, 2	16	7	0.035	11	12	0.836
T3, 4	67	79		67	79	
N stage						
N0	51	48	0.457	48	51	0.47
N1-2	32	38		30	40	
AJCC stage						
I, II	49	48	0.672	47	50	0.486
III, IV	34	38		31	41	
Lymphatic invasion						
Negative	70	72	0.913	64	78	0.517
Positive	13	14		14	13	
Perineural invasion						
Negative	66	73	0.361	68	71	0.12
Positive	17	13		10	20	
Blood glucose level (mean ± SD)	110.5 ± 36.2	111.6 ± 25.8	0.818	112.4 ± 38.8	109.9 ± 23.2	0.612
SUVmax of primary tumor (mean ± SD)	12.3 ± 5.9	16.1 ± 7.4	<0.001	13.0 ± 6.4	15.3 ± 7.3	0.030
SUVmax of lymph node (mean ± SD)	1.04 ± 2.6	2.15 ± 3.1	0.012	0.99 ± 2.6	2.13 ± 3.0	0.010

GLUT-1: Glucose transport protein 1; SD: Standard deviation; AJCC: American Joint Committee on Cancer; SUV: Standardized uptake value.

We investigated whether GLUT-1 expression in peripheral and central sites of the primary tumor could facilitate a more accurate assessment of lymph node staging based on FDG uptake on PET/CT (Table 2). Patients with GLUT-1 positivity demonstrated higher sensitivity of lymph node metastasis prediction by PET/CT than all patients considered together (overall patients, 50.0%; tumor center, 60.5%; tumor periphery, 65.0%). In contrast, patients with GLUT-1 negativity demonstrated overall lower sensitivity for the prediction of lymph node metastasis by PET/CT than all patients considered together (overall patients, 50.0%; tumor center, 37.5%; tumor periphery, 29.0%).

Relationship between GLUT-3, HK-II, and HIF-1 expressions and clinicopathologic parameters

We investigated the expressions of other proteins associated with glucose metabolism that could be associated with false-negative prediction of lymph node metastasis by PET/CT. Due to the staining of TMA slides, a few tissue cores were lost; therefore, different cases were analyzed using each antibody. The GLUT3, HK-II, and HIF-1 expressions did not significantly correlate with the SUVmax of the primary tumor and lymph nodes, other than for GLUT-3 in the tumor periphery ($P = 0.013$) (Tables 3-5).

DISCUSSION

In this study, we analyzed the role of GLUT-1 expression as a biomarker for lymph node metastasis detected by FDG uptake on PET/CT and assessed whether GLUT-1 expression differed in the peripheral and central areas of the tumor. We discovered that 109/169 patients (64.5%) exhibited GLUT-1 positivity in the center or periphery of the primary tumor. The expression of GLUT-1 was significantly correlated with the SUVmax of the primary tumor and lymph node,

Table 2 Predictive value of fluorodeoxyglucose-positron emission tomography/computed tomography based on glucose transport protein 1 expression

		Pathology	PET/CT diagnosis		Sensitivity	Specificity	PPV (%)	NPV (%)
			PET LN (+)	PET LN (-)	(%)	(%)		
All patients (n = 169)		LN (+)	35	35	50	81.8	66.03	69.82
		LN (-)	18	81				
Tumor center	GLUT-1 negative (n = 83)	LN (+)	12	20	37.5	88.2	66.6	69.2
		LN (-)	6	45				
	GLUT-1 positive (n = 86)	LN (+)	23	15	60.5	75	65.7	70.6
		LN (-)	12	36				
Tumor periphery	GLUT-1 negative (n = 78)	LN (+)	9	21	29	87.5	60	66.6
		LN (-)	6	42				
	GLUT-1 positive (n = 91)	LN (+)	26	14	65	76.5	68.4	73.6
		LN (-)	12	39				

GLUT-1: Glucose transport protein 1; FDG: Fluorodeoxyglucose; PET/CT: Positron emission tomography/computed tomography; LN: Lymph node; PPV: Positive predictive value; NPV: Negative predictive value

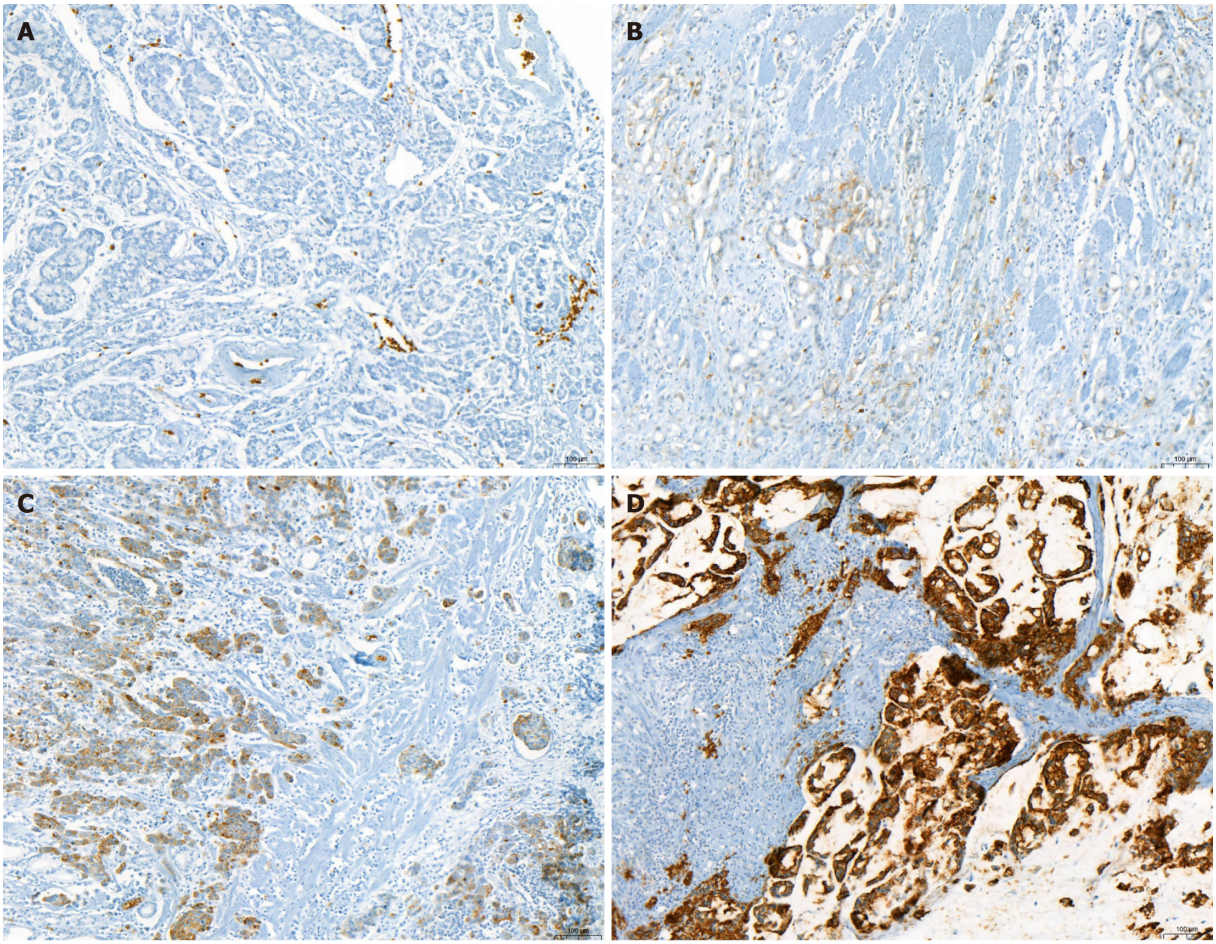

DOI: 10.12998/wjcc.v12.i5.931

Figure 1 Immunohistochemical staining for glucose transport protein 1 in colorectal cancer. Glucose transport protein 1 expression was demonstrated as cytoplasmic or membranous staining. A-D: The score was assessed according to the intensity [0 = negative (A), 1 = weak (B), 2 = moderate (C), 3 = strong (D); × 100]. A score of 2 or higher was considered as positive.

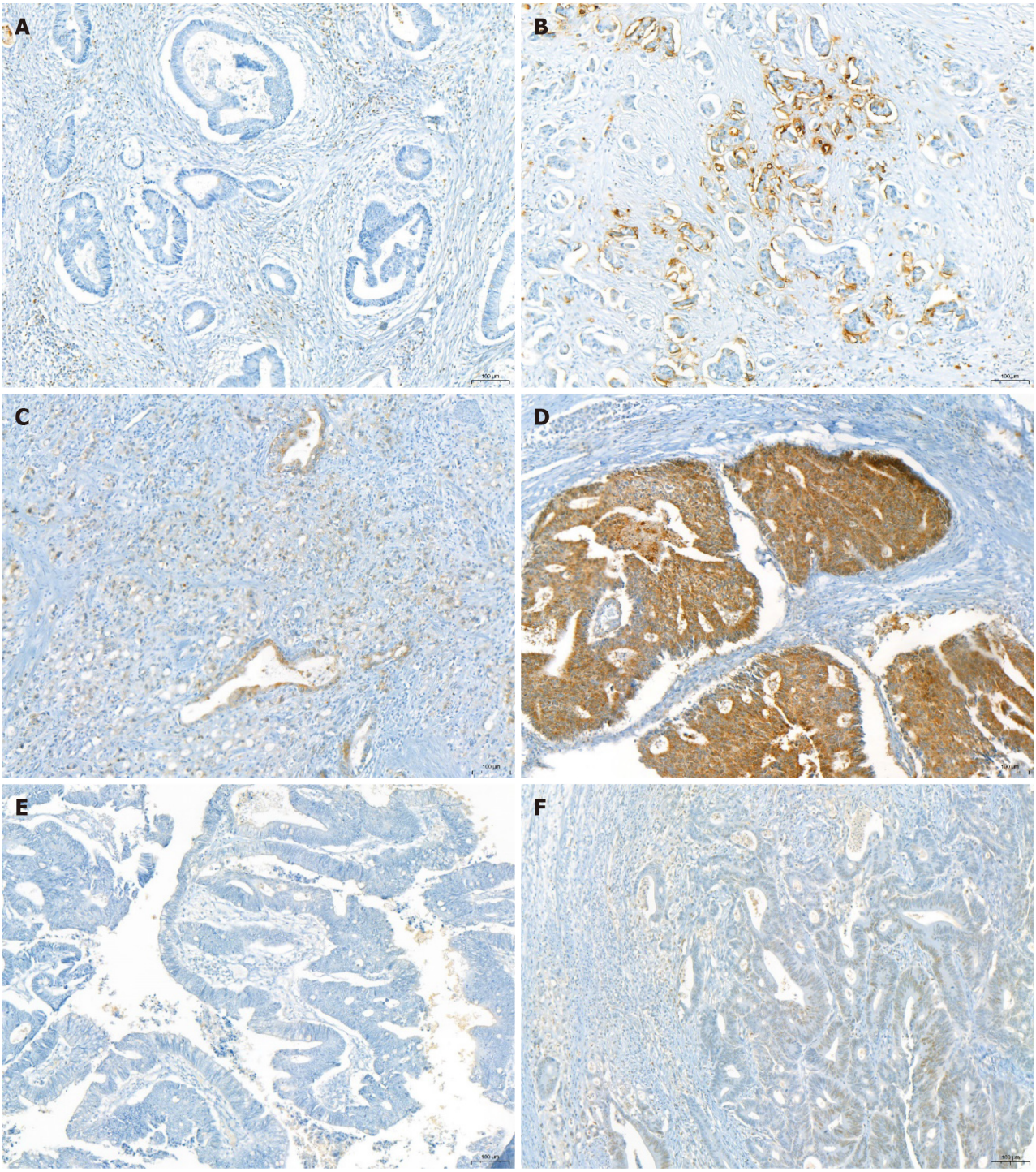

DOI: 10.12998/wjcc.v12.i5.931

Figure 2 Immunohistochemical staining for glucose transport protein 3, hexokinase-II, and hypoxia-inducible factor-1 in colorectal cancer. Glucose transport protein 3 (GLUT-3) and hexokinase-II expressions were demonstrated as cytoplasmic or membranous staining. A: GLUT-3 negative; B: GLUT-3 positive; C: Hexokinase-II negative; D: Hexokinase-II positive; E and F: Hypoxia-inducible factor-1 (HIF-1) expression was demonstrated as nuclear staining (E: HIF-1 negative, F: HIF-1 positive).

regardless of the biopsy site. In addition, patients with GLUT-1 positivity demonstrated overall higher sensitivity for the prediction of lymph node metastasis by PET/CT. These findings suggest that GLUT-1 expression is a useful biomarker for predicting lymph node metastasis when combined with PET/CT. In this study, the tumor periphery was regarded as the edge of the tumor close to the mucosa; this is the part of the tumor that can be reached during preoperative endoscopic biopsy, which suggests that the measurement of GLUT-1 expression in endoscopic tumor biopsy specimens can predict lymph node metastasis. Therefore, we recommend that clinicians evaluate GLUT-1 expression in preoperative endoscopic biopsy specimens and consider interpreting PET/CT results according to GLUT-1 expression. Since lymph node metastasis is underestimated in patients with colorectal cancer with GLUT-1 negativity, clinicians should be cautious when interpreting PET/CT results in preoperative patients, because of the possibility of false negative findings.

Table 3 The correlation between glucose transport protein 3 expression and clinicopathologic parameters

	GLUT-3 (center)		*P* value	GLUT-3 (periphery)		*P* value
	(-) (*n* = 153)	(+) (*n* = 12)		(-) (*n* = 78)	(+) (*n* = 91)	
Age (yr), mean ± SD	64.5 ± 11.8	63.0 ± 14.6	0.729	64.1 ± 11.9	67.8 ± 13.0	0.194
Sex						
Male	98	5	0.135	93	7	0.013
Female	55	7		49	13	
Tumor size (mean ± SD)	5.07 ± 2.0	5.02 ± 2.0	0.931	5.05 ± 2.0	5.20 ± 1.6	0.743
T stage						
T1, 2	20	2	0.663	20	1	0.475
T3, 4	133	10		122	19	
N stage						
N0	93	4	0.074	89	6	0.007
N1-2	60	8		53	14	
AJCC stage						
I, II	91	4	0.127	87	6	0.014
III, IV	62	8		53	14	
Lymphatic invasion						
Negative	128	11	0.693	120	17	1.000
Positive	25	1		22	33	
Perineural invasion						
Negative	127	8	0.234	117	17	1.000
Positive	26	4		25	3	
Blood sugar level (mean ± SD)	111.3 ± 32.0	109.2 ± 26.9	0.803	112.7 ± 33.0	101.8 ± 20.3	0.150
SUV max of primary tumor (mean ± SD)	14.1 ± 7.5	13.5 ± 4.7	0.678	14.3 ± 7.6	12.9 ± 4.8	0.433
SUV max of lymph node (mean ± SD)	1.6 ± 2.8	2.8 ± 4.0	0.328	1.4 ± 2.7	3.8 ± 4.0	0.013

GLUT-3: Glucose transport protein 3; SD: Standard deviation; AJCC: American Joint Committee on Cancer; SUV: Standardized uptake value.

Previous studies have reported a correlation between GLUT-1 expression and SUVmax in various carcinomas; however, discordant findings were reported[21-23]. Meyer *et al*[11] conducted a meta-analysis and reported that GLUT-1 and SUVmax were highly correlated in patients with pancreatic cancer and cervical cancer but not in those with colorectal cancer and endometrial cancer. However, Zhang *et al*[23] and Gu *et al*[24] reported a significant correlation between GLUT-1 expression and SUVmax in patients with colorectal cancer, which is consistent with our results. However, both studies included a small number of patients ($n < 40$), and the correlation between GLUT-1 expression and the SUVmax of the primary tumor remains unclear. In addition, few studies have reported an association between GLUT-1 expression and the prediction of lymph node metastasis by PET/CT in patients with non-small cell lung cancer. Taira *et al*[22] demonstrated that the predictive accuracy of lymph node metastasis by PET/CT differed from that obtained when GLUT-1 expression in patient samples was incorporated in the assessment, which is consistent with our results. However, to date, the exact reasons underlying these controversial results remains unclear. Probably, the complex glucose metabolism of malignant tumors differ between tumor types and might affect the association between GLUT-1 expression and SUVmax. In addition, GLUT-1 expression is not only specific for tumor cells, as GLUT-1 is also expressed on erythrocytes and immune cells. Moreover, a low burden of tumors and some good differentiated tumor types might reduce GLUT-1 expression, which could be the reason for false-negativity on PET/CT[25].

We analyzed the expression of other proteins (including GLUT3, HK-II, and HIF-1) associated with glucose metabolism, which could influence false-negative identification of lymph node metastasis on PET/CT. Our results revealed that GLUT-3, HK-II, and HIF-1 expressions did not significantly correlate with the SUVmax of the primary tumor and lymph nodes. This suggests that the expressions of these proteins are less useful than that of GLUT-1 when determining lymph node staging before surgery. However, further studies are needed to evaluate more biomarkers to increase the effectiveness of PET/CT.

Table 4 The correlation between hexokinase-II expression and clinicopathologic parameters

	Hexokinase-II (center)		*P* value	Hexokinase-II (periphery)		*P* value
	(-) (*n* = 94)	(+) (*n* = 70)		(-) (*n* = 114)	(+) (*n* = 48)	
Age (yr ± SD)	65.1 ± 12.3	63.5 ± 11.6	0.403	64.3 ± 12.3	64.8 ± 11.5	0.806
Sex						
Male	61	41	0.409	73	27	0.352
Female	33	29		41	21	
Tumor size (mean ± SD)	5.1 ± 1.8	5.1 ± 2.2	0.976	5.1 ± 2.0	5.1 ± 1.9	0.977
T stage						
T1, 2	15	7	0.268	16	5	0.531
T3, 4	79	63		98	43	
N stage						
N0	54	42	0.743	68	28	0.876
N1-2	40	28		46	20	
AJCC stage						
I, II	53	41	0.779	67	27	0.766
III, IV	41	29		47	21	
Lymphatic invasion						
Negative	77	61	0.365	97	40	0.778
Positive	17	9		17	8	
Perineural invasion						
Negative	75	60	0.325	95	38	0.528
Positive	19	10		19	10	
Blood glucose level (mean ± SD)	105.2 ± 22.8	116.8 ± 35.1	0.017	110.2 ± 32.0	113.9 ± 31.3	0.493
SUVmax of primary tumor (mean ± SD)	14.0 ± 7.1	14.2 ± 7.7	0.874	14.3 ± 7.2	13.9 ± 7.7	0.786
SUVmax of lymph node (mean ± SD)	1.6 ± 2.8	1.8 ± 3.2	0.712	1.5 ± 2.6	2.0 ± 3.7	0.450

SD: Standard deviation; AJCC: American Joint Committee on Cancer; SUV: Standardized uptake value.

To the best of our knowledge, this is the first study to evaluate the relationship between GLUT-1 expression and the SUVmax of primary tumors and lymph node metastasis in patients with colorectal cancer, as well as its role in detecting lymph node metastasis using 18F-FDG-PET/CT according to biopsy sites. We discovered that GLUT-1 expression was significantly correlated with the SUVmax of primary tumors and facilitated the prediction of lymph node metastasis using 18F-FDG-PET/CT. Moreover, GLUT-1 expression did not differ based on whether it was measured in either central or peripheral primary tumor biopsy sites in patients with colorectal cancer.

Our study has several limitations. First, it was retrospective, and our results should be confirmed in a prospective study. Second, only Asian patients with colorectal cancer were analyzed in this study, limiting the generalizability of our results as molecular profiles and clinical features of Western and Eastern populations differ significantly. Third, IHC cannot differentiate membranous from cytoplasmic GLUT-1 expressions. Cytoplasmic GLUT-1 is known to be inactive. Thus, to determine the clinical effects of GLUT-1, it is necessary to measure the expression of membranous GLUT-1. However, this distinction is presently challenging and limits the application of our findings[21].

CONCLUSION

GLUT-3, HK-II, and HIF-1 expressions were not significantly correlated with the SUVmax of the primary tumor and lymph nodes. GLUT-1 expression, on the other hand, demonstrated a significant correlation and may be a useful biomarker to be used in conjunction with PET/CT to diagnose colorectal cancers. Clinicians should consider GLUT-1 expression during preoperative endoscopic biopsy in interpreting PET/CT findings for the diagnosis of colorectal cancers and lymph node metastases.

Table 5 The correlation between hypoxia-induced factor-1 expression and clinicopathologic parameters

	HIF-1 (center)		*P* value	HIF-1 (periphery)		*P* value
	(-) (*n* = 94)	(+) (*n* = 72)		(-) (*n* = 89)	(+) (*n* = 75)	
Age (yr), mean ± SD	64.0 ± 12.4	65.1 ± 11.5	0.576	63.5 ± 12.6	65.6 ± 11.3	0.246
Sex						
Male	59	45	0.972	58	45	0.495
Female	35	27		31	30	
Tumor size (mean ± SD)	4.7 ± 1.7	5.5 ± 2.2	0.014	4.8 ± 1.7	5.3 ± 2.2	0.082
T stage						
T1, 2	17	6	0.071	16	7	0.112
T3, 4	77	66		73	68	
N stage						
N0	59	38	0.196	57	40	0.164
N1-2	35	34		32	35	
AJCC stage						
I, II	57	38	0.310	55	40	0.274
III, IV	37	34		34	35	
Lymphatic invasion						
Negative	80	60	0.755	76	62	0.634
Positive	14	12		13	13	
Perineural invasion						
Negative	77	59	0.996	73	61	0.909
Positive	17	13		16	14	
Blood glucose level (mean ± SD)	109.91 ± 30.8	112.29 ± 32.6	0.632	108.97 ± 32.2	113.69 ± 31.1	0.342
SUVmax of primary tumor (mean ± SD)	14.0 ± 7.1	14.0 ± 7.6	0.979	14.2 ± 7.0	13.8 ± 7.9	0.754
SUVmax of lymph node (mean ± SD)	1.4 ± 2.9	2.0 ± 2.9	0.229	1.6 ± 2.9	1.8 ± 2.9	0.713

HIF-1: Hypoxia-inducible factor-1; SD: Standard deviation; AJCC: American Joint Committee on Cancer; SUV: Standardized uptake value.

ARTICLE HIGHLIGHTS

Research perspectives

Further studies are needed to evaluate clinical benefit of glucose transport protein 1 (GLUT-1) expression as biomarkers for detecting primary tumors and lymph node metastasis *via* fluorodeoxyglucose (FDG)-positron emission tomography/computed tomography (PET/CT).

Research conclusions

GLUT-1 expression was significantly correlated with the maximum standardized uptake value (SUVmax) of 18F-FDG-PET/CT for primary tumors and lymph nodes. Clinicians should consider GLUT-1 expression in preoperative endoscopic biopsy when interpreting PET/CT findings.

Research results

GLUT-1 positivity was significantly correlated with the SUVmax of the primary tumor and lymph nodes, regardless of biopsy site (tumor center, $P < 0.001$ and $P = 0.012$; tumor periphery, $P = 0.030$ and $P = 0.010$, respectively). GLUT-1 positivity and negativity were associated with higher and lower sensitivities of PET/CT, respectively, for the detection of lymph node metastasis, regardless of biopsy site. GLUT3, HK-II, and HIF-1 expressions were not significantly associated with the SUVmax of the primary tumor and lymph nodes.

Research methods

Two tissue cores from the central and peripheral areas of the tumors were examined and the expressions of GLUT-1,

GLUT-3, HK-II, and HIF-1 were determined *via* immunohistochemical staining. We analyzed the correlations among their expressions, various clinicopathological factors, and the SUVmax of PET/CT.

Research objectives

The research objective was to investigate the role of GLUT-1 expression as a biomarker for lymph node metastasis detected by FDG uptake on PET/CT; in addition, we aimed to assess whether GLUT-1 expression differed in the peripheral and central areas of the tumor.

Research motivation

The research motivation was to evaluate GLUT-1, GLUT-3, HK-II, and HIF-1 expressions as biomarkers for detecting primary tumors and lymph node metastasis with 18F-FDG-PET/CT.

Research background

There are limited data on the use of GLUT-1 and GLUT-3, HK-II, and HIF-1 expressions as biomarkers for predicting lymph node metastasis when combined with FDG uptake on PET/CT in patients with colorectal cancer.

FOOTNOTES

Co-first authors: Hongsik Kim and Song-Yi Choi.

Author contributions: contributed to Kim H, Choi SY, Heo TY, Kim KR, Lee J, Yoo MY, Lee TG, and Han JH conceptualization, data curation, writing—review & editing; Heo TY and Kim KR contributed to formal analysis, software; Han JH contributed to funding acquisition, project administration, supervision; Kim H, Choi SY, Heo TY, Kim KR, and Han JH contributed to investigation, methodology, validation; Kim H and Choi SY contributed to visualization; Kim H, Choi SY, and Han JH contributed to writing - original draft.

Institutional review board statement: The Institutional Review Board (IRB No. 2013-03-003) of Chungbuk National University Hospital approved this study.

Informed consent statement: The requirement for written informed consent was waived due to retrospective design of the study.

Conflict-of-interest statement: The authors have no conflict of interest to declare regarding the publication of this work.

Data sharing statement: IRB of CBNUH did not permit sharing the raw data of patients without consent.

Country/Territory of origin: South Korea

ORCID number: Hongsik Kim 0000-0002-9469-6699; Jisun Lee 0000-0002-6264-7171; Taek-Gu Lee 0000-0002-3765-5655; Joung-Ho Han 0000-0003-4469-9215.

S-Editor: Liu JH
L-Editor: A
P-Editor: Zheng XM

REFERENCES

1 **Sung H**, Ferlay J, Siegel RL, Laversanne M, Soerjomataram I, Jemal A, Bray F. Global Cancer Statistics 2020: GLOBOCAN Estimates of Incidence and Mortality Worldwide for 36 Cancers in 185 Countries. *CA Cancer J Clin* 2021; **71**: 209-249 [PMID: 33538338 DOI: 10.3322/caac.21660]

2 **Al-Sukhni E**, Milot L, Fruitman M, Beyene J, Victor JC, Schmocker S, Brown G, McLeod R, Kennedy E. Diagnostic accuracy of MRI for assessment of T category, lymph node metastases, and circumferential resection margin involvement in patients with rectal cancer: a systematic review and meta-analysis. *Ann Surg Oncol* 2012; **19**: 2212-2223 [PMID: 22271205 DOI: 10.1245/s10434-011-2210-5]

3 **Dighe S**, Purkayastha S, Swift I, Tekkis PP, Darzi A, A'Hern R, Brown G. Diagnostic precision of CT in local staging of colon cancers: a meta-analysis. *Clin Radiol* 2010; **65**: 708-719 [PMID: 20696298 DOI: 10.1016/j.crad.2010.01.024]

4 **Nasseri Y**, Langenfeld SJ. Imaging for Colorectal Cancer. *Surg Clin North Am* 2017; **97**: 503-513 [PMID: 28501243 DOI: 10.1016/j.suc.2017.01.002]

5 **Park IJ**, Kim HC, Yu CS, Ryu MH, Chang HM, Kim JH, Ryu JS, Yeo JS, Kim JC. Efficacy of PET/CT in the accurate evaluation of primary colorectal carcinoma. *Eur J Surg Oncol* 2006; **32**: 941-947 [PMID: 16843635 DOI: 10.1016/j.ejso.2006.05.019]

6 **Abdel-Nabi H**, Doerr RJ, Lamonica DM, Cronin VR, Galantowicz PJ, Carbone GM, Spaulding MB. Staging of primary colorectal carcinomas

with fluorine-18 fluorodeoxyglucose whole-body PET: correlation with histopathologic and CT findings. *Radiology* 1998; **206**: 755-760 [PMID: 9494497 DOI: 10.1148/radiology.206.3.9494497]

7 **Kijima S**, Sasaki T, Nagata K, Utano K, Lefor AT, Sugimoto H. Preoperative evaluation of colorectal cancer using CT colonography, MRI, and PET/CT. *World J Gastroenterol* 2014; **20**: 16964-16975 [PMID: 25493009 DOI: 10.3748/wjg.v20.i45.16964]

8 **Kantorová I**, Lipská L, Bêlohlávek O, Visokai V, Trubaĉ M, Schneiderová M. Routine (18)F-FDG PET preoperative staging of colorectal cancer: comparison with conventional staging and its impact on treatment decision making. *J Nucl Med* 2003; **44**: 1784-1788 [PMID: 14602860]

9 **Mukai M**, Sadahiro S, Yasuda S, Ishida H, Tokunaga N, Tajima T, Makuuchi H. Preoperative evaluation by whole-body 18F-fluorodeoxyglucose positron emission tomography in patients with primary colorectal cancer. *Oncol Rep* 2000; **7**: 85-87 [PMID: 10601597]

10 **Boellaard R**, Delgado-Bolton R, Oyen WJ, Giammarile F, Tatsch K, Eschner W, Verzijlbergen FJ, Barrington SF, Pike LC, Weber WA, Stroobants S, Delbeke D, Donohoe KJ, Holbrook S, Graham MM, Testanera G, Hoekstra OS, Zijlstra J, Visser E, Hoekstra CJ, Pruim J, Willemsen A, Arends B, Kotzerke J, Bockisch A, Beyer T, Chiti A, Krause BJ; European Association of Nuclear Medicine (EANM). FDG PET/CT: EANM procedure guidelines for tumour imaging: version 2.0. *Eur J Nucl Med Mol Imaging* 2015; **42**: 328-354 [PMID: 25452219 DOI: 10.1007/s00259-014-2961-x]

11 **Meyer HJ**, Wienke A, Surov A. Associations between GLUT expression and SUV values derived from FDG-PET in different tumors-A systematic review and meta analysis. *PLoS One* 2019; **14**: e0217781 [PMID: 31206524 DOI: 10.1371/journal.pone.0217781]

12 **van Berkel A**, Rao JU, Kusters B, Demir T, Visser E, Mensenkamp AR, van der Laak JA, Oosterwijk E, Lenders JW, Sweep FC, Wevers RA, Hermus AR, Langenhuijsen JF, Kunst DP, Pacak K, Gotthardt M, Timmers HJ. Correlation between *in vivo* 18F-FDG PET and immunohistochemical markers of glucose uptake and metabolism in pheochromocytoma and paraganglioma. *J Nucl Med* 2014; **55**: 1253-1259 [PMID: 24925884 DOI: 10.2967/jnumed.114.137034]

13 **Busk M**, Horsman MR, Jakobsen S, Bussink J, van der Kogel A, Overgaard J. Cellular uptake of PET tracers of glucose metabolism and hypoxia and their linkage. *Eur J Nucl Med Mol Imaging* 2008; **35**: 2294-2303 [PMID: 18682937 DOI: 10.1007/s00259-008-0888-9]

14 **Yang HJ**, Xu WJ, Guan YH, Zhang HW, Ding WQ, Rong L, Qiu ZB, Zhong L. Expression of Glut-1 and HK-II in Pancreatic Cancer and Their Impact on Prognosis and FDG Accumulation. *Transl Oncol* 2016; **9**: 583-591 [PMID: 27916293 DOI: 10.1016/j.tranon.2016.08.004]

15 **Krzeslak A**, Wojcik-Krowiranda K, Forma E, Jozwiak P, Romanowicz H, Bienkiewicz A, Brys M. Expression of GLUT1 and GLUT3 glucose transporters in endometrial and breast cancers. *Pathol Oncol Res* 2012; **18**: 721-728 [PMID: 22270867 DOI: 10.1007/s12253-012-9500-5]

16 **Krishnamachary B**, Berg-Dixon S, Kelly B, Agani F, Feldser D, Ferreira G, Iyer N, LaRusch J, Pak B, Taghavi P, Semenza GL. Regulation of colon carcinoma cell invasion by hypoxia-inducible factor 1. *Cancer Res* 2003; **63**: 1138-1143 [PMID: 12615733]

17 **Saigusa S**, Toiyama Y, Tanaka K, Okugawa Y, Fujikawa H, Matsushita K, Uchida K, Inoue Y, Kusunoki M. Prognostic significance of glucose transporter-1 (GLUT1) gene expression in rectal cancer after preoperative chemoradiotherapy. *Surg Today* 2012; **42**: 460-469 [PMID: 22072148 DOI: 10.1007/s00595-011-0027-2]

18 **Yang J**, Wen J, Tian T, Lu Z, Wang Y, Wang Z, Wang X, Yang Y. GLUT-1 overexpression as an unfavorable prognostic biomarker in patients with colorectal cancer. *Oncotarget* 2017; **8**: 11788-11796 [PMID: 28052033 DOI: 10.18632/oncotarget.14352]

19 **Carvalho KC**, Cunha IW, Rocha RM, Ayala FR, Cajaíba MM, Begnami MD, Vilela RS, Paiva GR, Andrade RG, Soares FA. GLUT1 expression in malignant tumors and its use as an immunodiagnostic marker. *Clinics (Sao Paulo)* 2011; **66**: 965-972 [PMID: 21808860 DOI: 10.1590/s1807-59322011000600008]

20 **Hong R**, Lim SC. ^{18}F-fluoro-2-deoxyglucose uptake on PET CT and glucose transporter 1 expression in colorectal adenocarcinoma. *World J Gastroenterol* 2012; **18**: 168-174 [PMID: 22253523 DOI: 10.3748/wjg.v18.i2.168]

21 **Choi WH**, Yoo IeR, O JH, Kim TJ, Lee KY, Kim YK. Is the Glut expression related to FDG uptake in PET/CT of non-small cell lung cancer patients? *Technol Health Care* 2015; **23** Suppl 2: S311-S318 [PMID: 26410497 DOI: 10.3233/THC-150967]

22 **Taira N**, Atsumi E, Nakachi S, Takamatsu R, Yohena T, Kawasaki H, Kawabata T, Yoshimi N. Comparison of GLUT-1, SGLT-1, and SGLT-2 expression in false-negative and true-positive lymph nodes during the (18)F-FDG PET/CT mediastinal nodal staging of non-small cell lung cancer. *Lung Cancer* 2018; **123**: 30-35 [PMID: 30089592 DOI: 10.1016/j.lungcan.2018.06.004]

23 **Zhang M**, Yang J, Jiang H, Wang Z. Correlation between glucose metabolism parameters derived from FDG and tumor TNM stages and metastasis-associated proteins in colorectal carcinoma patients. *BMC Cancer* 2021; **21**: 258 [PMID: 33750337 DOI: 10.1186/s12885-021-07944-z]

24 **Gu J**, Yamamoto H, Fukunaga H, Danno K, Takemasa I, Ikeda M, Tatsumi M, Sekimoto M, Hatazawa J, Nishimura T, Monden M. Correlation of GLUT-1 overexpression, tumor size, and depth of invasion with 18F-2-fluoro-2-deoxy-D-glucose uptake by positron emission tomography in colorectal cancer. *Dig Dis Sci* 2006; **51**: 2198-2205 [PMID: 17080242 DOI: 10.1007/s10620-006-9428-2]

25 **Baek HJ**, Chung JH, Park JH, Zo JI, Cheon GJ, Choi CW, Lim SM, Choi SY, Hong JM, Hong JS. FDG-PET in Mediastinal Nodal Staging of Non-small Cell Lung Cancer: Correlation of False Results with Histopathologic Finding. *Cancer Res Treat* 2003; **35**: 232-238 [PMID: 26680941 DOI: 10.4143/crt.2003.35.3.232]

World Journal of Clinical Cases

Submit a Manuscript: https://www.f6publishing.com

World J Clin Cases 2024 February 16; 12(5): 942-950

DOI: 10.12998/wjcc.v12.i5.942

ISSN 2307-8960 (online)

ORIGINAL ARTICLE

Observational Study

Clinical efficacy and mechanism study of mid-frequency anti-snoring device in treating moderate obstructive sleep apnea-hypopnea syndrome

Bao Qian, Zhan-Jun Chen, Yong-Sheng Wang, Xiao-Yan Hu, Xiao-Biao Hu, Yong-Hua Zheng

Specialty type: Respiratory system

Provenance and peer review: Unsolicited article; Externally peer reviewed.

Peer-review model: Single blind

Peer-review report's scientific quality classification

Grade A (Excellent): 0
Grade B (Very good): 0
Grade C (Good): C
Grade D (Fair): 0
Grade E (Poor): 0

P-Reviewer: Nooripour R, Iran

Received: November 2, 2023
Peer-review started: November 2, 2023
First decision: December 5, 2023
Revised: December 14, 2023
Accepted: January 23, 2024
Article in press: January 23, 2024
Published online: February 16, 2024

Bao Qian, Zhan-Jun Chen, Xiao-Yan Hu, Xiao-Biao Hu, Yong-Hua Zheng, Pulmonary Medicine, Shanghai Jinshan Tinglin Hospital, Shanghai 201505, China

Yong-Sheng Wang, Radiology Medicine, Shanghai Jinshan Tinglin Hospital, Shanghai 201505, China

Corresponding author: Yong-Hua Zheng, MD, Deputy Chief Physician, Pulmonary Medicine, Shanghai Jinshan Tinglin Hospital, No. 80 North Siping Road, Jinshan District, Shanghai 201505, China. zhengyonghua0118@hotmail.com

Abstract

BACKGROUND

Obstructive sleep apnea-hypopnea syndrome (OSAHS) is primarily caused by airway obstruction due to narrowing and blockage in the nasal and nasopharyngeal, oropharyngeal, soft palate, and tongue base areas. The mid-frequency anti-snoring device is a new technology based on sublingual nerve stimulation. Its principle is to improve the degree of oropharyngeal airway stenosis in OSAHS patients under mid-frequency wave stimulation. Nevertheless, there is a lack of clinical application and imaging evidence.

AIM

To investigate the clinical efficacy and mechanisms of a mid-frequency anti-snoring device in treating moderate OSAHS.

METHODS

We selected 50 patients diagnosed with moderate OSAHS in our hospital between July 2022 and August 2023. They underwent a 4-wk treatment regimen involving the mid-frequency anti-snoring device during nighttime sleep. Following the treatment, we monitored and assessed the sleep apnea quality of life index and Epworth Sleepiness Scale scores. Additionally, we performed computed tomography scans of the oropharynx in the awake state, during snoring, and while using the mid-frequency anti-snoring device. Cross-sectional area measurements in different states were taken at the narrowest airway point in the soft palate posterior and retrolingual areas.

RESULTS

Compared to pretreatment measurements, patients exhibited a significant reduction in the apnea-hypopnea index, the percentage of time with oxygen saturation below 90%, snoring frequency, and the duration of the most prolonged apnea event. The lowest oxygen saturation showed a notable increase, and both sleep apnea quality of life index and Epworth Sleepiness Scale scores improved. Oropharyngeal computed tomography scans revealed that in OSAHS patients cross-sectional areas of the oropharyngeal airway in the soft palate posterior area and retrolingual area decreased during snoring compared to the awake state. Conversely, during mid-frequency anti-snoring device treatment, these areas increased compared to snoring.

CONCLUSION

The mid-frequency anti-snoring device demonstrates the potential to enhance various sleep parameters in patients with moderate OSAHS, thereby improving their quality of life and reducing daytime sleepiness. These therapeutic effects are attributed to the device's ability to ameliorate the narrowing of the oropharynx in OSAHS patients.

Key Words: Mid-frequency anti-snoring device; Obstructive sleep apnea-hypopnea syndrome; Sleep monitoring; Oropharyngeal computed tomography; Curative effect

Core Tip: We investigated the clinical efficacy and underlying mechanisms of a mid-frequency anti-snoring device in treating 50 moderate obstructive sleep apnea-hypopnea syndrome patients for 4 wk. Our results indicated significant improvements in the apnea-hypopnea index, the percentage of time with oxygen saturation below 90%, and the sleep apnea quality of life index and Epworth Sleepiness Scale scores. Additionally, we found compelling evidence that the mid-frequency anti-snoring device positively influenced the narrowing of the oropharynx in sleep apnea-hypopnea syndrome patients during snoring.

Citation: Qian B, Chen ZJ, Wang YS, Hu XY, Hu XB, Zheng YH. Clinical efficacy and mechanism study of mid-frequency anti-snoring device in treating moderate obstructive sleep apnea-hypopnea syndrome. *World J Clin Cases* 2024; 12(5): 942-950
URL: https://www.wjgnet.com/2307-8960/full/v12/i5/942.htm
DOI: https://dx.doi.org/10.12998/wjcc.v12.i5.942

INTRODUCTION

Obstructive sleep apnea-hypopnea syndrome (OSAHS) is primarily caused by airway obstruction due to narrowing and blockage in the nasal and nasopharyngeal, oropharyngeal, soft palate, and tongue base areas. Its main clinical manifestations include snoring and associated breathing pauses during nighttime sleep. Most patients experience dry mouth upon waking in the morning, and some may also have symptoms such as headaches, daytime sleepiness, fatigue, lack of concentration, *etc*[1].

Transcutaneous electrical stimulation of the genioglossus muscle is a non-invasive treatment method for OSAHS [2]. Recently, a mid-frequency anti-snoring device has been developed that delivers specific pulse-modulated compound waves to provide intermittent electrical stimulation to the genioglossus muscle and its sublingual nerve branches. This leads to a responsive contraction of the genioglossus muscle, an increase in upper airway tension, a reduction in the severity of oropharyngeal upper airway collapse, and the maintenance of an open upper airway, ultimately terminating snoring. This device is beneficial for improving the quality of sleep in OSAHS patients.

This study focused on patients with moderate OSAHS and investigated whether the treatment with a mid-frequency anti-snoring device can improve various sleep parameters in OSAHS patients and enhance their quality of daily life. Additionally, it explores whether the airways in the oropharyngeal region expand under the stimulation of mid-frequency waves. Currently, there is a lack of imaging evidence in this regard. Therefore, this study conducted oropharyngeal computed tomography (CT) scans in OSAHS patients in awake, snoring, and mid-frequency anti-snoring device treatment states to measure the cross-sectional area at the narrowest points in the soft palate posterior and retrolingual areas. This approach aimed to provide imaging-based confirmation of the working mechanism of this technology in treating OSAHS.

MATERIALS AND METHODS

General information

This study was conducted on 50 patients diagnosed with moderate OSAHS in our hospital from July 2022 to August 2023. The primary patient information is shown in Table 1. Upon diagnosis, patients began wearing a mid-frequency anti-snoring device during nighttime sleep. Before treatment, the study's purpose and relevant precautions were explained to the patients. Upon the patients' understanding and agreement, informed consent forms were signed.

Table 1 Baseline characteristics of the study participants

Variable	Data
Male/female	35/15
Age in yr	38.5 ± 6.8
Height in cm	170.3 ± 10.8
Weight in kg	89.7 ± 15.6
BMI in kg/m^2	29.5 ± 3.4
Systolic blood pressure in mmHg	122.3 ± 11.4
Diastolic blood pressure in mmHg	71.6 ± 10.2

Data are mean ± SD or *n*/*N*. BMI: Body mass index.

Inclusion criteria: (1) An apnea-hypopnea index (AHI) ≥ 30 events per hour during 7 h of sleep at night or an AHI ≥ 5 events per hour. The criterion for moderate OSAHS was an AHI index of 15-30 events per hour; (2) Voluntary participation and signed informed consent; (3) Complete clinical data; and (4) Good patient compliance and the ability to fully participate in the entire study.

Exclusion criteria: (1) Patients with mild or severe OSAHS; (2) Patients who have recently experienced acute illness and received related treatments; (3) Patients with severe cardiovascular or cerebrovascular diseases or multiorgan dysfunction; (4) Patients with mental illnesses or cognitive communication disorders; (5) Patients who have participated in other clinical studies in the past 3 months; and (6) Contraindications for the mid-frequency anti-snoring device, including acute purulent inflammation in the submental region, bleeding tendency, malignant tumors, severe heart diseases, severe cardiopulmonary diseases, airway obstruction due to nasal disorders, the presence of implantable devices such as pacemakers, skin allergies, and inability to express self-awareness, such as infants.

Sleep monitoring

Sleep monitoring was conducted using a Sleep-Disordered Breathing Analyzer (SOMNOcheck micro, Weinmann, Germany). The first monitoring was performed before the mid-frequency anti-snoring device treatment to establish the diagnosis and assess severity. Subsequently, the mid-frequency anti-snoring device was used during nighttime sleep for 4 wk. The second sleep monitoring was conducted after the treatment and compared with the data from the first monitoring. Key sleep monitoring parameters included the AHI, lowest pulse oxygen saturation ($LSPO_2$), and snoring percentage (the percentage of time spent snoring during sleep).

Mid-frequency anti-snoring device treatment

Treatment was performed using a mid-frequency anti-snoring device (JLY-Y3 or JLY-Z3, Taizhou Jinliyou Medical Technology Co. Ltd.). The device parameters included a rated voltage of D.C 3.7 V, a power of 0.1 W, a modulation waveform of bidirectional symmetric trapezoidal waves, and a frequency of 20 KHz. The treatment process involved fixing the anti-snoring device to the lower jaw using either the ear-worn (Figure 1A) or patch (Figure 1B) method. After wearing the device, it was powered on by pressing and holding the device's switch for approximately 3 s. The power indicator would blink to confirm a successful startup. Patients would lie flat for sleep, and the anti-snoring device would automatically operate. If snoring or breathing pauses were detected, it would provide mid-frequency electrical pulses for intervention.

Oropharyngeal CT

To better detect upper airway obstruction or narrowing in patients, overnight upper airway CT scans were conducted while they were sleeping. The United Imaging uCT760-64 slice spiral CT scanner and its matching workstation were used. Patients were placed supine, with their eyes closed, and proper positioning was ensured. The scanning range extended from the top of the maxillary sinus to 5 cm below the hyoid bone. The scanning parameters were set at 125 KV, 200 mA, a scanning pitch of 1.5, a slice thickness of 5.0 mm, and an interlayer spacing of 5.0 mm. Reconstructed images included coronal and sagittal multiplanar reformation images and three-dimensional maximum intensity projection images. The narrowest cross-sectional area of the upper airway (soft palate and retrolingual airway) was measured three times using multi-slice spiral CT 3D software. Measurements were taken with a fixed window width and window level. Upper airway CT scans were conducted 1 wk after mid-frequency anti-snoring device treatment. Patients wore the device and laid flat on the CT examination bed. The first upper airway CT scan was performed while the patient was awake. The second scan was performed when the patient started snoring, with the device switched off, and the third scan was completed when snoring ceased with the device switched on.

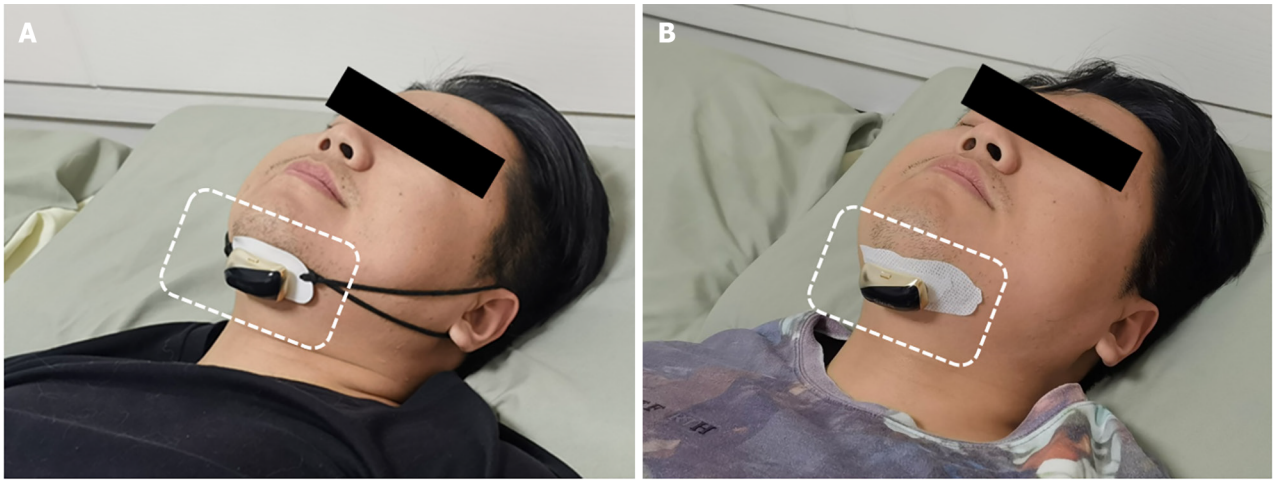

DOI: 10.12998/wjcc.v12.i5.942

Figure 1 Proper method of wearing the mid-frequency anti-snoring device. A: Ear-worn style; B: Patch style.

Ethical permission

The study protocol was approved by the medical ethics committee of Shanghai Jinshan Tinglin Hospital for research ethics. Each patient was informed of the nature of the study and signed an informed consent form.

Statistical analysis

SPSS 22.0 software was used for analysis. Quantitative data were represented as (mean ± SEM). Self-matching paired *t*-tests were employed, with $P < 0.05$ considered statistically significant.

RESULTS

Comparison of sleep monitoring parameters

After 4 wk of treatment with the mid-frequency anti-snoring device, the patient's sleep monitoring parameters, including AHI, snoring percentage, the most prolonged apnea duration(s), and the duration of $SPO_2 < 90\%$, decreased compared to before treatment ($P < 0.05$). $LSPO_2$ increased compared to before treatment ($P < 0.05$). Various indicators of the autonomous arousal index (AAI resp) improved, with AAI resp decreased compared to before treatment ($P < 0.05$). AAI non-resp also decreased compared to before treatment ($P < 0.05$), as did respiratory effort-related arousals ($P < 0.05$), as shown in Table 2.

Comparison of sleep apnea quality of life index and Epworth Sleepiness Scale scores

After 4 wk of treatment with the mid-frequency anti-snoring device, patients showed improvements in sleep apnea quality of life index scale scores, including social activity, emotional state, and symptom scores, all of which increased compared to before treatment. Epworth Sleepiness Scale scores decreased, and these differences were statistically significant ($P < 0.05$), as shown in Table 3.

Analysis of oropharyngeal CT examination results

In this study, we selected the narrowest points of the oropharyngeal airway in the soft palate posterior area and retrolingual area of OSAHS patients as the measurement points. These two areas were relatively stable during CT scanning and less susceptible to external interference. In the awake, snoring, and mid-frequency anti-snoring device treatment states, the cross-sectional areas of the narrowest part of the soft palate airway in OSAHS patients were 80.47 ± 18.56 mm², 22.05 ± 16.47 mm², and 71.61 ± 17.38 mm², respectively.

Compared to the awake state, OSAHS patients had a reduction in the cross-sectional areas of the soft palate posterior area and retrolingual area during snoring ($P < 0.05$), as shown in Table 4 and Figure 2A-C. The cross-sectional areas of the narrowest part of the retrolingual airway in OSAHS patients were 155.36 ± 13.29 mm², 120.45 ± 12.23 mm², and 150.61 ± 12.35 mm² in the awake, snoring, and mid-frequency anti-snoring device treatment states, respectively. Compared to snoring, OSAHS patients experienced an increase in the cross-sectional areas of the soft palate and retrolingual airways during treatment with the mid-frequency anti-snoring device ($P < 0.05$), as shown in Table 4 and Figure 2D-F.

DISCUSSION

With the advancement of medical diagnostic technology and increased awareness of personal health, the incidence of

Table 2 Comparison of sleep monitoring parameters before and after treatment (mean ± SD)

Parameter	Before treatment	After treatment	*t* value	*P* value
AHI, %	24.38 ± 9.16	12.63 ± 8.27	7.47	< 0.05
$LSPO_2$, %	72.62 ± 9.53	84.84 ± 8.71	4.32	< 0.05
SPO_2 < 90%, %	14.65 ± 7.26	10.33 ± 5.32	3.15	< 0.05
Snoring, %	44.54 ± 26.13	15.07 ± 9.25	3.37	< 0.05
Most prolonged apnea duration in s	56.08 ± 20.11	25.58 ± 11.27	4.21	< 0.05
AAI resp as events/h	19.89 ± 11.61	11.74 ± 6.39	5.01	< 0.05
AAI non resp as events/h	15.71 ± 7.18	9.37 ± 4.27	6.11	< 0.05
RERA as events/h	5.91 ± 3.99	2.61 ± 2.65	5.69	< 0.05

Data are mean ± SD. AAI: Autonomous arousal index; AHI: Apnea-hypopnea index; $LSPO_2$: Lowest pulse oxygen saturation; RERA: Respiratory effort-related arousals; SPO_2: Oxygen saturation.

Table 3 Comparison of sleep apnea quality of life index and Epworth Sleepiness Scale before and after treatment (mean ± SD)

Index	Before treatment	After treatment	*t* value	*P* value
Daily life activity rating	3.8 ± 0.9	5.4 ± 1.3	5.67	< 0.05
Social activity rating	3.7 ± 1.0	4.8 ± 0.7	5.92	< 0.05
Emotional state score	4.6 ± 1.1	5.3 ± 1.2	3.15	< 0.05
Symptom score	4.4 ± 1.2	5.2 ± 0.9	3.37	< 0.05
SAQLI scale score	4.2 ± 0.5	4.8 ± 0.4	8.94	< 0.05
ESS scale score	14.8 ± 5.7	10.2 ± 4.3	3.31	< 0.05

ESS: Epworth Sleepiness Scale; SAQLI: Sleep apnea quality of life index.

Table 4 Comparison of soft palate posterior airway area and retrolingual airway area computed tomography scan results in obstructive sleep apnea-hypopnea syndrome patients in different states (mean ± SD)

Position	Awake	Snoring	Anti-snoring
Soft palate posterior airway area	80.47 ± 18.56	22.05 ± 16.47[1]	71.61 ± 17.38[2]
Retrolingual airway area	155.36 ± 13.29	120.45 ± 12.23[3]	150.61 ± 12.35[4]

[1]Compared to the awake state, the airway cross-sectional area decreased during snoring (t = 5.301, P = 0.000).
[2]Compared to the snoring state, the airway cross-sectional area increased (t = 2.806, P = 0.021).
[3]Compared to the awake state, the airway cross-sectional area decreased during snoring (t = 5.021, P = 0.001).
[4]In contrast, when compared to the snoring state, the airway cross-sectional area increased (t = 5.029, P = 0.001).

OSAHS in the population has increased. For example, a recent study found that out of 38000 Russian citizens (aged 30-70 years), 48.9% suffered from an AHI ≥ 5, 18.1% from an AHI ≥ 15, and 4.5% from an AHI ≥ 30[3]. OSAHS significantly impacts people's safety, quality of life, social interactions, and relationships with family members. As such, it requires active intervention and treatment[4]. The pathological mechanism of OSAHS lies in the obstruction and collapse of the upper airway during sleep. The obstruction can occur in the nasopharynx, oropharynx, or hypopharynx, with over 80% of patients experiencing combined oropharyngeal obstruction[5]. Therefore, the core of OSAHS treatment is to relieve narrowing in the oropharyngeal region and keep the airway open.

Currently, OSAHS treatment includes general therapy, medication, devices, surgery, and rehabilitation[6]. Each treatment method has its advantages and limitations, and the treatment choice should be based on the patient's specific condition. Hypoglossal nerve stimulation is one effective method for treating OSAHS, where a nerve stimulator is implanted under the patient's skin in the neck and is connected to a sublingual nerve[7]. It stimulates the sublingual nerve to generate nerve signals synchronized with inhalation, helping the muscles tighten, pulling the tongue forward, expanding the pharynx, and relieving airway narrowing caused by the posterior displacement of the tongue root. However, this method is only effective in the short term, with limited long-term efficacy, and the equipment is expensive,

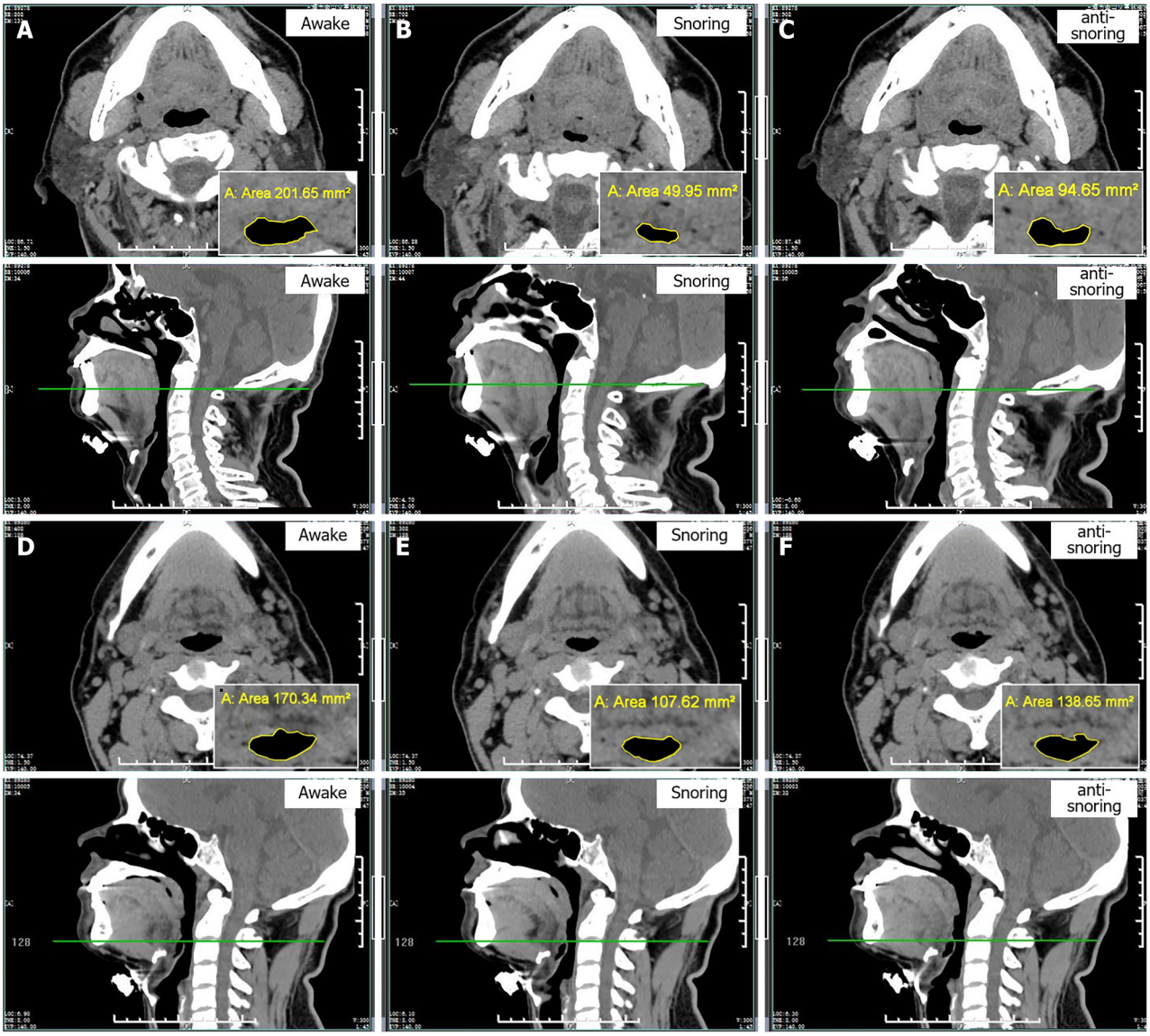

DOI: 10.12998/wjcc.v12.i5.942

Figure 2 Computed tomography scan. A-C: Computed tomography (CT) scan representation and cross-sectional area measurement of the soft palate posterior airway in wakefulness, snoring, and during treatment with the middle-frequency anti-snoring device; D-F: CT scan representation and cross-sectional area measurements of the retrolingual airway area in wakefulness, snoring, and during treatment with the middle-frequency anti-snoring device.

restricting its clinical use[8].

In recent years, the mid-frequency anti-snoring device has been developed based on hypoglossal nerve stimulation, and it is a new technology used to treat OSAHS. It delivers specific frequency pulse-modulated composite waves and provides intermittent electrical stimulation to the genioglossus muscle and its sublingual nerve branches. This stimulates the genioglossus muscle to contract responsively, increases the tension of the upper airway, reduces airway collapse, and maintains airway patency, thus terminating snoring and apnea and improving sleep quality. While this method is theoretically feasible, it lacks clinical practice and research support. Therefore, this study aimed to explore this issue.

In the preliminary experiments of this study, it was found that mild OSAHS patients had low treatment willingness, poor compliance, and could not complete the entire study due to their mild symptoms. Therefore, they were not included in the study. Severe OSAHS patients, on the other hand, had more severe symptoms and showed unclear effects of the mid-frequency anti-snoring device. Clinically, they were mainly treated with non-invasive positive pressure ventilation. Therefore, they were not included either. Nevertheless, moderate OSAHS patients had a strong willingness to be treated, good compliance, and could complete the study. Therefore, they were chosen as the subjects of this study. The results of this study indicated that after 4 wk of treatment with the mid-frequency anti-snoring device, the AHI of moderate OSAHS patients decreased, the time of snoring during nighttime sleep decreased, the duration of the most prolonged apnea decreased, the duration of SPO_2 < 90% decreased, and the $LSPO_2$ increased, confirming a significant improvement in the patients' nighttime sleep quality. The study results also indicated that the sleep apnea quality of life index scores of patients increased after treatment compared to before treatment, including social activity scores, emotional state scores, and symptom scores. The Epworth Sleepiness Scale scores decreased, confirming that this treatment improved the patient's clinical symptoms and quality of life.

The study results also showed that after using the mid-frequency anti-snoring device, the number of AAI resp occurrences decreased, AAI non-resp decreased, and respiratory effort-related arousals decreased. OSAHS patients experience repeated awakenings during sleep, which hurts sleep quality. During the initial treatment phase, this study found that mid-frequency anti-snoring treatment increased patient awakenings, affecting sleep quality. The main reasons were that the initial stimulation intensity was too high, and patients had a low tolerance for stimulation. The study continuously adjusted stimulation intensity based on patients' actual experiences. After a period, patients fully adapted, and the number of awakenings significantly decreased.

This study conducted oropharyngeal CT examinations on OSAHS patients in awake, snoring, and mid-frequency anti-snoring treatment states to confirm that the mid-frequency anti-snoring device worked by expanding the narrow oropharyngeal airway. The narrowest points of the airway in the soft palate posterior area and retrolingual area were chosen as measurement points, and the cross-sectional areas of the airways were measured. The results showed that in the awake state the cross-sectional area of the narrowest part of the soft palate posterior airway was 80.47 ± 18.56 mm^2 and the narrowest part of the retrolingual airway was 155.36 ± 13.29 mm^2. When patients snored during sleep, there was evidence of tongue root or uvula collapse, leading to oropharyngeal airway narrowing or obstruction. The cross-sectional area of the narrowest part of the soft palate posterior airway decreased to 22.05 ± 16.47 mm^2, and the cross-sectional area of the retrolingual airway decreased to 120.45 ± 12.23 mm^2 showing significant reductions. During mid-frequency anti-snoring treatment, the cross-sectional area of the narrowest part of the soft palate posterior airway was 71.61 ± 17.38 mm^2, and the cross-sectional area of the retrolingual airway was 150.61 ± 12.35 mm^2, showing significant improvement compared to the snoring state. The study results confirmed that during treatment with the anti-snoring device, the relaxation of the tongue root and uvula was alleviated, and the degree of oropharyngeal airway narrowing was significantly improved, providing strong evidence from an imaging perspective for the working mechanism of the mid-frequency anti-snoring device.

Several objective issues were encountered throughout this study, resulting in some limitations in the examination results. First, this study employed a natural sleep approach and did not use sedative-hypnotic drugs to induce sleep. The examination process was time-consuming and challenging. In addition, patients were influenced by unfamiliar environments, such as the low temperature and high noise in the CT examination room, making it difficult for OSAHS patients to fall asleep naturally. Consequently, CT examinations were prone to interruptions and were not reflective of the patient's actual home sleep state, potentially affecting the accuracy of the examination results. Second, the number of cases included in this study was relatively small, which may lead to statistical bias. Third, differences in patient height, weight, and disease severity, as well as differences in upper airway anatomy, could impact CT examination results. Fourth, during treatment with the anti-snoring device, high pulse stimulation intensity could cause patient awakenings, affecting the accuracy of CT examinations. Resolving the above issues requires further increasing the number of patients, expanding the sample size, improving the environment in the CT examination room, optimizing the CT examination process, and using sedative-hypnotic drugs to induce sleep if necessary.

CONCLUSION

In conclusion, this study confirmed that the mid-frequency anti-snoring device can expand the oropharyngeal airway in patients with moderate OSAHS, thereby improving their clinical symptoms and sleep quality. Our study provided a new method for the clinical treatment of OSAHS.

ARTICLE HIGHLIGHTS

Research background

The mid-frequency anti-snoring device is a new technology based on sublingual nerve stimulation. Its principle is to improve the degree of oropharyngeal airway stenosis in obstructive sleep apnea-hypopnea syndrome (OSAHS) patients under mid-frequency wave stimulation.

Research motivation

There is a lack of clinical application and imaging evidence for the use of mid-frequency anti-snoring devices in the treatment of moderate OSAHS.

Research objectives

To provide imaging-based confirmation of the working mechanism of mid-frequency anti-snoring devices in treating OSAHS. This study also aimed to observe the clinical efficacy of medium-frequency anti-snoring devices in treating moderate obstructive OSAHS.

Research methods

Fifty patients diagnosed with moderate OSAHS underwent a 4-wk treatment regimen involving the mid-frequency anti-snoring device during nighttime sleep. Following the treatment, we monitored and assessed the sleep apnea quality of life index and Epworth Sleepiness Scale scores. Additionally, we performed computed tomography scans of the

oropharynx in the awake state, during snoring, and while using the mid-frequency anti-snoring device. Cross-sectional area measurements in different states were taken at the narrowest airway point in the soft palate posterior and retrolingual areas.

Research results

Compared to pretreatment measurements, patients exhibited a significant reduction in the apnea-hypopnea index, the percentage of time with oxygen saturation below 90%, snoring frequency, and the duration of the most prolonged apnea event. The lowest oxygen saturation (%) showed a notable increase, and both sleep apnea quality of life index and Epworth Sleepiness Scale scores improved. Oropharyngeal computed tomography scans revealed that in OSAHS patients the cross-sectional areas of the oropharyngeal airway in the soft palate posterior area and retrolingual area decreased during snoring compared to the awake state. Conversely, during mid-frequency anti-snoring device treatment, these areas increased compared to snoring.

Research conclusions

This study confirmed that the mid-frequency anti-snoring device can expand the oropharyngeal airway in patients with moderate OSAHS, thereby improving their clinical symptoms and sleep quality.

Research perspectives

The sample size of this study was limited, and there may be statistical bias. Further efforts are needed to increase the number of patients, expand the sample size, and conduct in-depth research on some scientific issues, such as the therapeutic effect of mid-frequency anti-snoring devices on patients with only snoring, the patient dependency and efficacy of long-term use, the impact on the anatomical structure of the upper airway of the oropharynx, and the impact of long-term use on abnormal lipid metabolism in patients.

FOOTNOTES

Co-first authors: Bao Qian and Zhan-Jun Chen.

Author contributions: Qian B and Chen ZJ contributed equally to this work; Qian B and Chen ZJ performed the study; Wang YS performed the computed tomography scan examination; Hu XY and Hu XB analyzed the data; Zheng YH designed the research and wrote the manuscript; all authors read and approve the final manuscript.

Institutional review board statement: The study was reviewed and approved by the Institutional Review Board of the Shanghai Jinshan Tinglin Hospital (Approval No. 2022-06-01).

Informed consent statement: All study participants, or their legal guardian, provided informed written consent before enrollment.

Conflict-of-interest statement: The authors declare that they have no conflicts of interest.

Data sharing statement: No additional data are available.

STROBE statement: The authors have read the STROBE Statement—checklist of items, and the manuscript was prepared and revised according to the STROBE Statement—checklist of items.

Country/Territory of origin: China

ORCID number: Yong-Hua Zheng 0000-0002-7799-9612.

S-Editor: Chen YL
L-Editor: Filipodia
P-Editor: Yu HG

REFERENCES

1 **Gottlieb DJ**, Punjabi NM. Diagnosis and Management of Obstructive Sleep Apnea: A Review. *JAMA* 2020; **323**: 1389-1400 [PMID: 32286648 DOI: 10.1001/jama.2020.3514]
2 **Olson MD**, Junna MR. Hypoglossal Nerve Stimulation Therapy for the Treatment of Obstructive Sleep Apnea. *Neurotherapeutics* 2021; **18**: 91-99 [PMID: 33559036 DOI: 10.1007/s13311-021-01012-x]
3 **Khokhrina A**, Andreeva E, Degryse JM. The prevalence of sleep-disordered breathing in Northwest Russia: The ARKHsleep study. *Chron*

Respir Dis 2020; **17**: 1479973120928103 [PMID: 32666810 DOI: 10.1177/1479973120928103]

4 **Lee JJ**, Sundar KM. Evaluation and Management of Adults with Obstructive Sleep Apnea Syndrome. *Lung* 2021; **199**: 87-101 [PMID: 33713177 DOI: 10.1007/s00408-021-00426-w]

5 **Lv R**, Liu X, Zhang Y, Dong N, Wang X, He Y, Yue H, Yin Q. Pathophysiological mechanisms and therapeutic approaches in obstructive sleep apnea syndrome. *Signal Transduct Target Ther* 2023; **8**: 218 [PMID: 37230968 DOI: 10.1038/s41392-023-01496-3]

6 **Gambino F**, Zammuto MM, Virzì A, Conti G, Bonsignore MR. Treatment options in obstructive sleep apnea. *Intern Emerg Med* 2022; **17**: 971-978 [PMID: 35460431 DOI: 10.1007/s11739-022-02983-1]

7 **Mashaqi S**, Patel SI, Combs D, Estep L, Helmick S, Machamer J, Parthasarathy S. The Hypoglossal Nerve Stimulation as a Novel Therapy for Treating Obstructive Sleep Apnea-A Literature Review. *Int J Environ Res Public Health* 2021; **18** [PMID: 33572156 DOI: 10.3390/ijerph18041642]

8 **Zhu Z**, Hofauer B, Wirth M, Heiser C. Long-term changes of stimulation intensities in hypoglossal nerve stimulation. *J Clin Sleep Med* 2020; **16**: 1775-1780 [PMID: 32026804 DOI: 10.5664/jcsm.8320]

World Journal of Clinical Cases

Submit a Manuscript: https://www.f6publishing.com

World J Clin Cases 2024 February 16; 12(5): 951-965

DOI: 10.12998/wjcc.v12.i5.951

ISSN 2307-8960 (online)

ORIGINAL ARTICLE

Observational Study

Urinary metabolic profiles during *Helicobacter pylori* eradication in chronic gastritis

Wen-Ting An, Yu-Xia Hao, Hong-Xia Li, Xing-Kang Wu

Specialty type: Gastroenterology and hepatology

Provenance and peer review: Unsolicited article; Externally peer reviewed.

Peer-review model: Single blind

Peer-review report's scientific quality classification

Grade A (Excellent): 0
Grade B (Very good): 0
Grade C (Good): C, C
Grade D (Fair): 0
Grade E (Poor): 0

P-Reviewer: Sato T, Japan

Received: November 3, 2023
Peer-review started: November 3, 2023
First decision: December 6, 2023
Revised: December 14, 2023
Accepted: January 22, 2024
Article in press: January 22, 2024
Published online: February 16, 2024

Wen-Ting An, Department of Pharmacy, Shanxi Provincial People's Hospital, Taiyuan 030012, Shanxi Province, China

Yu-Xia Hao, Department of Gastroenterology, Shanxi Provincial People's Hospital, Taiyuan 030012, Shanxi Province, China

Hong-Xia Li, Department of Oncology, Shanxi Provincial People's Hospital, Taiyuan 030012, Shanxi Province, China

Xing-Kang Wu, Modern Research Center for Traditional Chinese Medicine, Shanxi University, Taiyuan 030006, Shanxi Province, China

Corresponding author: Hong-Xia Li, MMed, Chief Physician, Department of Oncology, Shanxi Provincial People's Hospital, No. 29 Shuangta Road, Taiyuan 030012, Shanxi Province, China. 345lihongxia@163.com

Abstract

BACKGROUND

Helicobacter pylori (*H. pylori*) infection is a major risk factor for chronic gastritis, affecting approximately half of the global population. *H. pylori* eradication is a popular treatment method for *H. pylori*-positive chronic gastritis, but its mechanism remains unclear. Urinary metabolomics has been used to elucidate the mechanisms of gastric disease treatment. However, no clinical study has been conducted on urinary metabolomics of chronic gastritis.

AIM

To elucidate the urinary metabolic profiles during *H. pylori* eradication in patients with chronic gastritis.

METHODS

We applied LC–MS-based metabolomics and network pharmacology to investigate the relationships between urinary metabolites and *H. pylori*-positive chronic gastritis *via* a clinical follow-up study.

RESULTS

Our study revealed the different urinary metabolic profiles of *H. pylori*-positive chronic gastritis before and after *H. pylori* eradication. The metabolites regulated by *H. pylori* eradication therapy include cis-aconitic acid, isocitric acid, citric acid,

L-tyrosine, L-phenylalanine, L-tryptophan, and hippuric acid, which were involved in four metabolic pathways: (1) Phenylalanine metabolism; (2) phenylalanine, tyrosine, and tryptophan biosynthesis; (3) citrate cycle; and (4) glyoxylate and dicarboxylate metabolism. Integrated metabolomics and network pharmacology revealed that MPO, COMT, TPO, TH, EPX, CMA1, DDC, TPH1, and LPO were the key proteins involved in the biological progress of *H. pylori* eradication in chronic gastritis.

CONCLUSION

Our research provides a new perspective for exploring the significance of urinary metabolites in evaluating the treatment and prognosis of *H. pylori*-positive chronic gastritis patients.

Key Words: LC-MS; metabolomics; chronic gastritis; Helicobacter pylori; urinary metabolites

Core Tip: Urinary metabolomics has been used to elucidate the mechanisms of gastric disease treatment, whereas no clinical study is conducted on metabolomics of chronic gastritis. In this manuscript, we carried out LC-MS-based metabolomics to investigate urinary metabolites changes in *Helicobacter pylori* (*H. pylori*)-positive chronic gastritis treatment. Our study revealed the urinary metabolic profiles of *H. pylori*-positive chronic gastritis after *H. pylori* eradication. Integrated metabolomics and network pharmacology revealed the key proteins involved in H. pylori eradication of chronic gastritis. Our research provides a new perspective for exploring the significance of urinary metabolites in evaluating the treatment and prognosis of *H. pylori*-positive chronic gastritis.

Citation: An WT, Hao YX, Li HX, Wu XK. Urinary metabolic profiles during *Helicobacter pylori* eradication in chronic gastritis. *World J Clin Cases* 2024; 12(5): 951-965
URL: https://www.wjgnet.com/2307-8960/full/v12/i5/951.htm
DOI: https://dx.doi.org/10.12998/wjcc.v12.i5.951

INTRODUCTION

Chronic gastritis is a common digestive system disease affecting approximately half of the global population[1]. Chronic gastritis is also the most important risk factor for gastric cancer, the fifth most commonly diagnosed cancer and the fourth leading cause of cancer-related mortality[1,2]. Chronic gastritis can be classified into two major stages, non-atrophic and atrophic, according to the phenotypes of the gastric mucosa[3]. Chronic non-atrophic gastritis will develop into chronic atrophic gastritis if left untreated. A 16-year follow-up study revealed that up to 2% of patients with chronic atrophic gastritis develop gastric cancer annually[4]. Additionally, 24% of gastric cancer patients are first diagnosed with chronic atrophic gastritis[5]. Thus, managing chronic gastritis is an important approach for preventing gastric cancer development.

Helicobacter pylori (*H. pylori*) infection, a major risk factor for chronic gastritis, infects approximately 50% of the global population[6,7]. A portion of infected people will develop various degrees of gastrointestinal disease, such as dyspepsia (5%–10%), chronic gastritis (90%), peptic ulcers (15%–20%), and gastric malignancies (1%)[8]. *H. pylori* has been described as a first-class carcinogen for gastric cancer by the World Health Organization since 1994 and accounts for 16.1% of gastric cancer cases[9,10]. A 26.5-year follow-up report indicated that *H. pylori* eradication might confer long-term protection against gastric cancer in high-risk populations[11]. Therefore, eradication of *H. pylori* is recommended to reduce the occurrence of gastric diseases[8]. Numerous double, triple, and quadruple therapies have been proposed as first-line empiric treatments for *H. pylori* infection[12]. However, the molecular mechanisms underlying these treatment regimens are complicated and remain unclear[13].

Urinary metabolomics has been gradually applied to mine metabolic profiles for diagnosis, prognostic evaluation, and research of treatment mechanisms in gastric diseases. NMR-based urinary metabolomics revealed that urine metabolite levels were changed during oncogenesis in gastric cancer, and 4-hydroxyphenylacetate, alanine, phenylacetylglycine, mannitol, glycolate, and arginine are potential metabolic biomarkers for effectively diagnosing gastric cancer[14,15]. NMR- and UPLC-Q/TOF MS-mediated urinary metabolomics revealed that a traditional Chinese medicine, Huangqi Jianzhong Tang, treated chronic atrophic gastritis by balancing energy consumption, inhibiting inflammation, improving the immune system, and reducing oxidative stress in rats[16]. UPLC-Q-TOF/MS-based urinary metabolomics has also been applied to investigate the therapeutic effect and potential mechanism of berberine on chronic atrophic gastritis[17] and the therapeutic mechanism of palmatine in chronic atrophic gastritis induced by *H. pylori*[18]. However, no clinical study has been conducted on urinary metabolomics in chronic gastritis.

MATERIALS AND METHODS

Clinical characteristics of participants

This study was conducted according to the guidelines of the Declaration of Helsinki and approved by the Ethics Committee of Shanxi Provincial People's Hospital (Grant No. 2022-167). Patients with *H. pylori*-positive chronic gastritis who were hospitalized or outpatients in the Gastroenterology Department of Shanxi Provincial People's Hospital were selected as the research participants. Patients with *H. pylori*-positive chronic gastritis were enrolled. These patients were diagnosed with chronic gastritis by endoscopy and pathological examination. For the diagnostic criteria of *H. pylori* infection, refer to the "Fifth National Consensus Report on the Treatment of *H. pylori* Infection." Those with a positive ^{14}C or ^{13}C urea breath test (UBT) were diagnosed with *H. pylori* infection. Fasting morning urine was collected from patients diagnosed with *H. pylori*-positive chronic gastritis and marked as "HP(+)". Subsequently, the patients were treated with therapeutic strategies of *H. pylori* eradication for 2 wk (Figure 1). *H. pylori* eradication was conducted using conventional quadruple therapy, *i.e.*, a proton pump inhibitor combined with two antibiotics and a colloidal bismuth agent. In this study, the quadruple therapy strategies included omeprazole/amoxicillin/furazolidone/bismuth pectin, ilaprazole/amoxicillin/ furazolidone/bismuth pectin, and pantoprazole/amoxicillin/furazolidone/bismuth pectin (Table 1). The patients were subjected to the ^{14}C or ^{13}C UBT at the end of treatment to evaluate *H. pylori* infection severity. The fasting morning urine of *H. pylori*-negative patients was collected and marked as "HP(−)" (Figure 1), and the fasting morning urine of *H. pylori*-negative healthy individuals was marked as "Health" (Figure 1). The HP(−), HP(+), and Health urine samples were subjected to an LC–MS-based metabolomics analysis.

In this study, approximately 180 patients were diagnosed with *H. pylori*-positive chronic gastritis, and their urine samples were collected at the first diagnosis. However, only 17 patients met the clinical assessment inclusion criteria and were willing to be reexamined for *H. pylori* infection after treatment (Table 1). These patients were treated with quadruple therapy strategies for *H. pylori* eradication. After 2 wk of treatment, 17 patients in our study were *H. pylori*-negative and discontinued treatment.

Sample preparation

The first morning urine was collected from fasting patients and healthy individuals and stored at −80°C. The frozen urine samples were thawed in an ice bath and centrifuged at a low temperature for 10 min (10000 ×*g*, 4°C). The supernatant was transferred to a new 1.5 mL EP tube. The proteins were precipitated by adding methanol-acetonitrile (2:1). Then, the mixtures were subjected to ultrasonic extraction in an ice water bath for 10 min and centrifuged for 20 min (10000 ×*g*, 4°C). The supernatant was filtered through a 0.22 μm organic phase pinhole filter and transferred to an LC sample vial. Samples were stored at 4°C until the LC–MS analysis. In addition, 10 μL of urine from each group was taken, mixed, and prepared as QC samples according to the sample preparation method.

UHPLC-Q-TOF/MS liquid phase conditions

The mobile phases were A (0.1% formic acid water) and B (0.1% formic acid acetonitrile). Elution was conducted according to the following gradient: 0–2 min, 2% B; 2–3 min, 2%–35% B; 3–17 min, 35%–70% B; 17–18 min, 70% B; 18–29 min, 70%–98% B; 29–31 min, 98% B; 31–33 min, 98%–2% B; and 33–35 min, 2% B. A Waters ACQUITYUPLC HSS T3 (2.1 × 100 mm, 1.7 μm) chromatographic column with a 5 μL injection volume, 0.2 mL/min flow rate, and 40°C temperature was then used for the liquid chromatographic analysis.

UHPLC-Q-TOF/MS mass spectrometry conditions

The mass spectrometry profiles of the urine metabolome were obtained on a UPLC (ExionLC AD) coupled with a Triple TOF 5600+ mass spectrometer (AB Sciex). The mass spectrometry conditions were set as follows: Electronspray ionization (ESI); mode: positive and negative ion scanning; mass scanning range: 50–1500 Da; atomizing gas pressure (GS1) and auxiliary gas pressure (GS2): 0.55 kPa; atomizing gas temperature: 550°C; spray voltage: +5500 V in positive ion mode and −4500 V in negative ion mode; curtain pressure: 0.3 kPa; and cluster fragmentation voltage: 100 V. Data were collected in information association mode, collision energy was ± 35 eV, and the collision energy rolling interval was (35 ± 15) eV.

Data processing of UHPLC-Q-TOF/MS

The raw data from UHPLC-Q-TOF/MS were imported into One-MAP software, and all metabolite names, peak areas, retention times, and other information were calculated. The results were exported as Excel files, and the total peak area data of each group of metabolites were normalized to obtain the peak-normalized data per metabolite.

Multivariate statistical analysis and differential metabolite screening

The above peak-normalized data were imported into Simca-P 14.1. A principal component analysis (PCA) was used for the exploratory analysis to determine possible clusters and outliers, and partial least square discriminant analysis (PLS–DA) and orthogonal partial least square discriminant analysis (OPLS–DA) were performed to explore different metabolites with metabolic profile changes, combining VIP > 1 and a *t* test ($P < 0.05$) in the S-plot to screen different metabolites.

Identification of metabolites

The identification of metabolites was performed by importing the m/z values of metabolites into the One-map database (http://www.5omics.com/) to obtain the names of metabolites. The chemical structures of the metabolites were

Table 1 Clinical and demographic patient data

Parameters	HP(+) and HP(−)	Health
Case	17	20
Sex		
Male	11	12
Female	7	8
Age (yr)		
31–40	2	2
41–50	8	9
51–60	6	7
> 60	1	2
Average age (yr)	49.35	48.65
Treatment		
Omeprazole/amoxicillin/furazolidone/bismuth pectin	3	-
Ilaprazole/amoxicillin/furazolidone/bismuth pectin	6	-
Pantoprazole/amoxicillin/furazolidone/bismuth pectin	8	-

HP(+): *Helicobacter pylori*-positive; HP(−): *Helicobacter pylori*-negative.

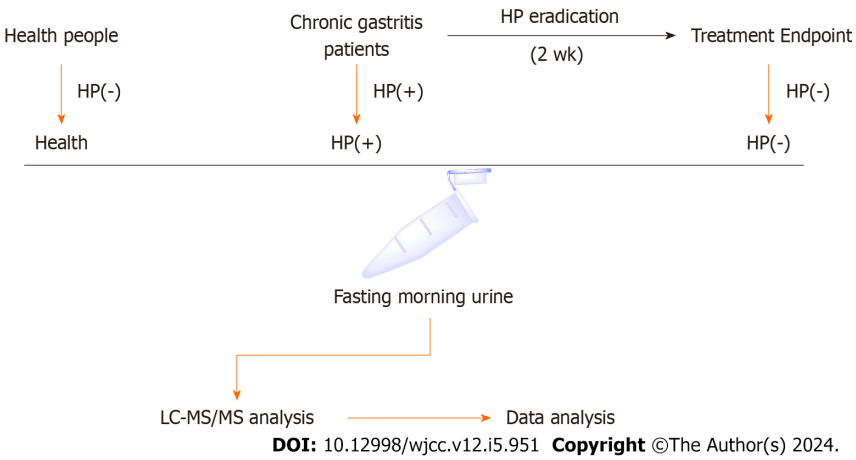

DOI: 10.12998/wjcc.v12.i5.951

Figure 1 Schematic of patient enrollment and sample collection and analysis. Fasting morning urine samples were collected from enrolled patients and subjected to metabolomics using LC–MS/MS analysis. Data were analyzed using One-Map, SIMCA, and MetaboAnalyst. HP(+): *Helicobacter pylori*-positive; HP(−): *Helicobacter pylori*-negative.

confirmed by comparing MS/MS data with the compound information in the One-map database.

Metabolic pathway enrichment analysis and ROC curve analysis

The Pathway Analysis module in MetaboAnalyst 5.0 (https://www.metaboanalyst.ca/) was used to perform metabolic pathway enrichment analyses on differential metabolites, and the pathway with an impact value (impact) greater than or equal to 0.1 was considered to be the main metabolism path.

The area under the receiver operating characteristic (ROC) curve was used to evaluate the quality and the predictive ability of the classification models. Univariate ROC analysis was conducted, and the area under curve (AUC) and *P* values of each ROC curve were used to evaluate the predictability. Then, to improve the discriminatory accuracy, multivariate ROC curves were plotted with false-positive and true-positive rates using a combination of significant metabolites with AUC > 0.5 (*P* value < 0.05).

Integrated metabolomics and network pharmacology

Integrated metabolomics and network pharmacology were applied to reveal the regulatory network of the identified differential metabolites. First, a metabolite-related network construction was performed by importing the identified

differential metabolites into Cytoscape 3.7.2 (Cytoscape Consortium, San Diego, CA, USA) equipped with MetScape. This network was constructed to visualize the interactions among the metabolites, pathways, enzymes, and genes. The key metabolites and proteins were recognized by combining the metabolite-reaction-enzyme-gene network with hub genes and metabolic pathways. Then, the candidate targets of *H. pylori*-positive chronic gastritis were acquired by taking the intersection of targets between chronic gastritis and *H. pylori* infection. The targets of chronic gastritis and *H. pylori* infection were obtained by searching the keywords "chronic gastritis" and "*Helicobacter pylori*" in the Genecards database (https://www.genecards.org/), respectively. Finally, the key proteins involved in regulating the identified differential metabolites were obtained by matching the *H. pylori*-positive chronic gastritis-related targets with the differential metabolite-related targets.

Statistical analysis

GraphPad Prism 8 software was used for generating figures and statistical analyses. Data are presented as the mean ± SD. The normality of data distribution was analyzed with SPSS software. Comparisons between two groups were performed using independent-sample *t* tests; comparisons between multiple groups were performed by one-way ANOVA. $P < 0.05$ was considered to represent significance.

RESULTS

Overall metabolic profiles and the untargeted metabolomics analysis

Metabolic profiling of urine samples was performed in positive and negative ion modes in an unsupervised model without grouping conditions using PCA. The QC samples were clustered, indicating good system stability. The results show that the samples Health, HP(+), and HP(−) cannot be effectively separated (Figure 2A and B). Therefore, PLS–DA was performed to reduce the dimensionality of the complex data obtained from the Health, HP(+), and HP(−) urine samples to distinguish the differences between groups. The results are shown in Figure 2C–F. The Health, HP(+), and HP(−) samples were significantly separated in ESI- and ESI+ modes, indicating that 2 wk of drug treatment alters urinary metabolic disorders in patients with chronic gastritis. In summary, the untargeted metabolomics analysis indicated that the urinary metabolic profiles changed during *H. pylori* eradication.

Metabolic profile of healthy individuals vs H. pylori-positive chronic gastritis patients

The OPLS–DA model was used to further evaluate the changes in metabolic profile in the sixth week after drug treatment. The CV-ANOVA diagnostics, in which the *P* values were 0.0000000894092 (negative ion mode) and 0.00000465157 (positive ion mode), worked well in the OPLS–DA model. The results are shown in Figure 3A and B. The Health and HP(+) groups were clearly separated in the positive and negative ion modes, indicating that the metabolic profiles of the two groups significantly changed. The corresponding S-plot was applied to observe and screen differential variables (Figure 3C and D), of which the values of variable importance in the projection (VIP) were used to evaluate their contribution to the model. The differential metabolites were screened between the Health and HP(+) groups according to S-plots of VIP value (VIP > 1) and a *t* test ($P < 0.05$).

The differential metabolites were imported into the Pathway Analysis module in MetaboAnalyst5.0, and a metabolic pathway analysis was conducted to find the 10 metabolic pathways most related to *H. pylori* eradication: (1) Phenylalanine metabolism; (2) phenylalanine, tyrosine, and tryptophan biosynthesis; (3) citrate cycle; (4) glyoxylate and dicarboxylate metabolism; (5) alanine, aspartate, and glutamate metabolism; (6) ubiquinone and other terpenoid-quinone biosynthesis; (7) arginine and proline; (8) aminoacyl-tRNA biosynthesis; (9) glycine, serine, and threonine metabolism; and (10) pyrimidine metabolism (Figure 3E).

Comparison of metabolic profiles of patients at the treatment endpoint with those before the treatment

In both positive and negative ion modes, the OPLS–DA model was used to evaluate the effects of *H. pylori* eradication on metabolic profiles after 2 wk of treatment. The CV-ANOVA diagnostics, in which the *P* values were 0.000665011 (negative ion mode) and 0.00535801 (positive ion mode), worked well in the OPLS–DA model. The plot of the scores obtained from the urine samples showed a significant separation between the HP(+) and HP(−) groups (Figure 4A and B), indicating that *H. pylori* eradication affected the urinary metabolites. The corresponding S-plot was applied to observe and screen differential variables (Figure 4C and D). The VIP value was used to evaluate their contribution to the model. The differential metabolites between the HP(+) and HP(−) groups were obtained by combining the VIP values (VIP > 1) and *t* test ($P < 0.05$) in the S-plot.

The differential metabolites were imported into MetaboAnalyst 5.0 software for pathway enrichment analysis to find the 10 most relevant metabolic pathways (pathway impact > 0.1) related to *H. pylori* eradication: (1) Phenylalanine metabolism; (2) phenylalanine, tyrosine, and tryptophan biosynthesis ; (3) citrate cycle; (4) glyoxylate and dicarboxylate metabolism; (5) aminoacyl-tRNA biosynthesis; (6) ubiquinone and other terpenoid-quinone biosynthesis; (7) arginine and proline metabolism; (8) purine metabolism; (9) alanine, aspartate, and glutamate metabolism; and (10) glycine, serine, and threonine metabolism (Figure 4E).

Discovery of differential metabolites in urine

A joint pathway analysis was performed on the differential metabolites between the HP(+) and HP(−) groups and the Health and HP(−) groups using the Joint-pathway Analysis module in MetaboAnalyst to screen the key metabolic

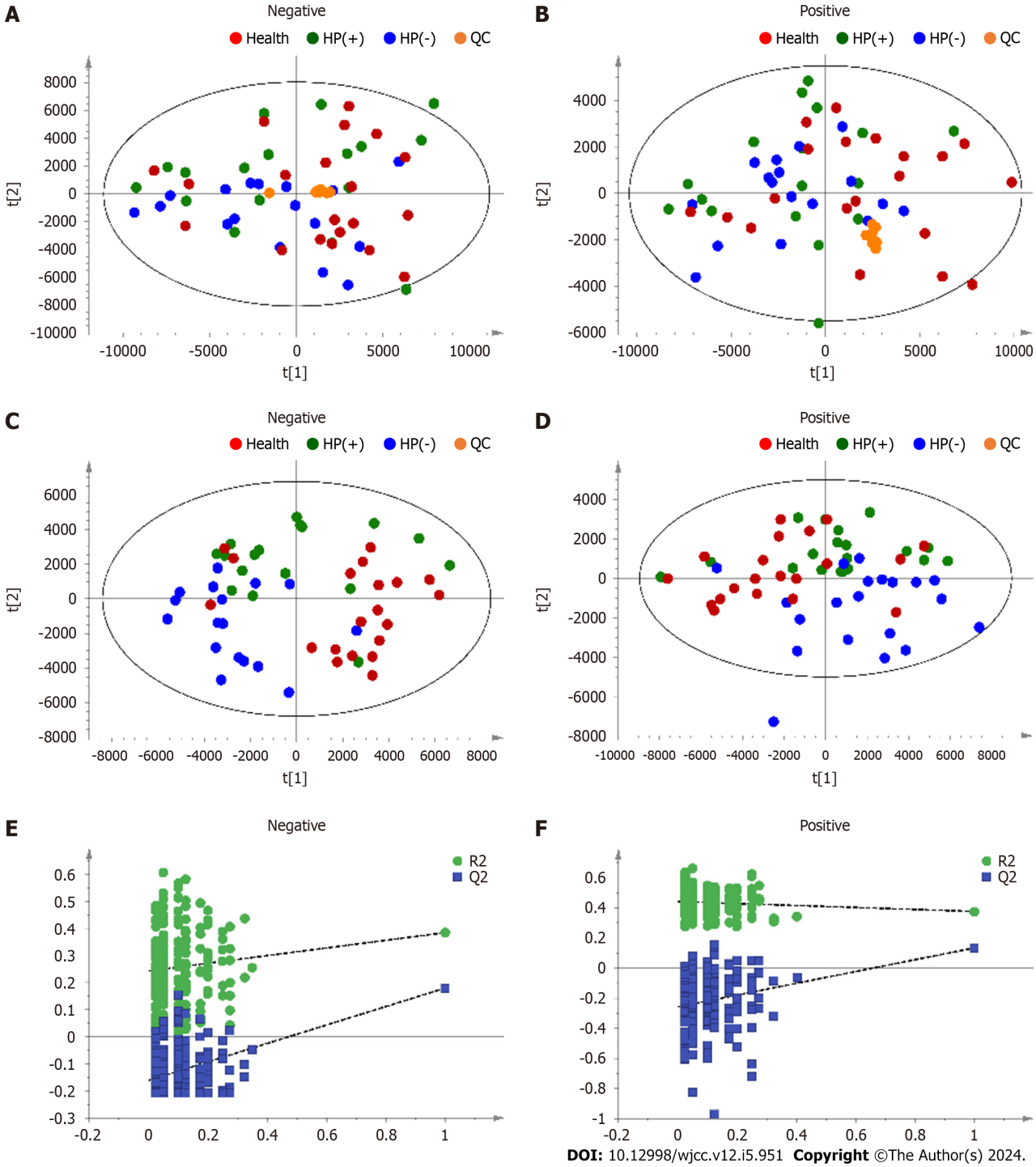

DOI: 10.12998/wjcc.v12.i5.951

Figure 2 Principal component analysis and partial least square discriminant analysis score scatter plots from urine analysis data. A, B: Principal component analysis (PCA) model score scatter plots; C, D: Partial least square discriminant analysis (PLS–DA) model score scatter plots; and (E and F) PLS-DA validation plot; A, C, E: Negative electronspray ionization (ESI) mode; B, D, F: Positive ESI mode. HP(+): *Helicobacter pylori*-positive; HP(−): *Helicobacter pylori*-negative.

pathways. The top four metabolic pathways co-regulated in Health *vs* HP(+) and HP(+) *vs* HP(−) are as follows: (1) Phenylalanine metabolism; (2) phenylalanine, tyrosine, and tryptophan biosynthesis; (3) citrate cycle; and (4) glyoxylate and dicarboxylate. Seven differential metabolites related to these four metabolic pathways were found, and the results are shown in Figure 5A. Cis-aconitic acid, isocitric acid, and citric acid were involved in the citrate cycle, glyoxylate, and dicarboxylate metabolism; L-tyrosine, L-phenylalanine, and L-tryptophan were involved in phenylalanine, L-tyrosine, and L-tryptophan biosynthesis; and hippuric acid, L-tyrosine, and L-phenylalanine were involved in phenylalanine metabolism.

Next, the levels of these differential metabolites were investigated by assessing the peak intensity of ions (Figure 5A). Compared with the Health group, in the HP(+) group, the levels of cis-aconitic acid, isocitric acid, citric acid, L-tyrosine, and L-phenylalanine were decreased, while L-tyrosine and hippuric acid levels were increased. The levels of these seven

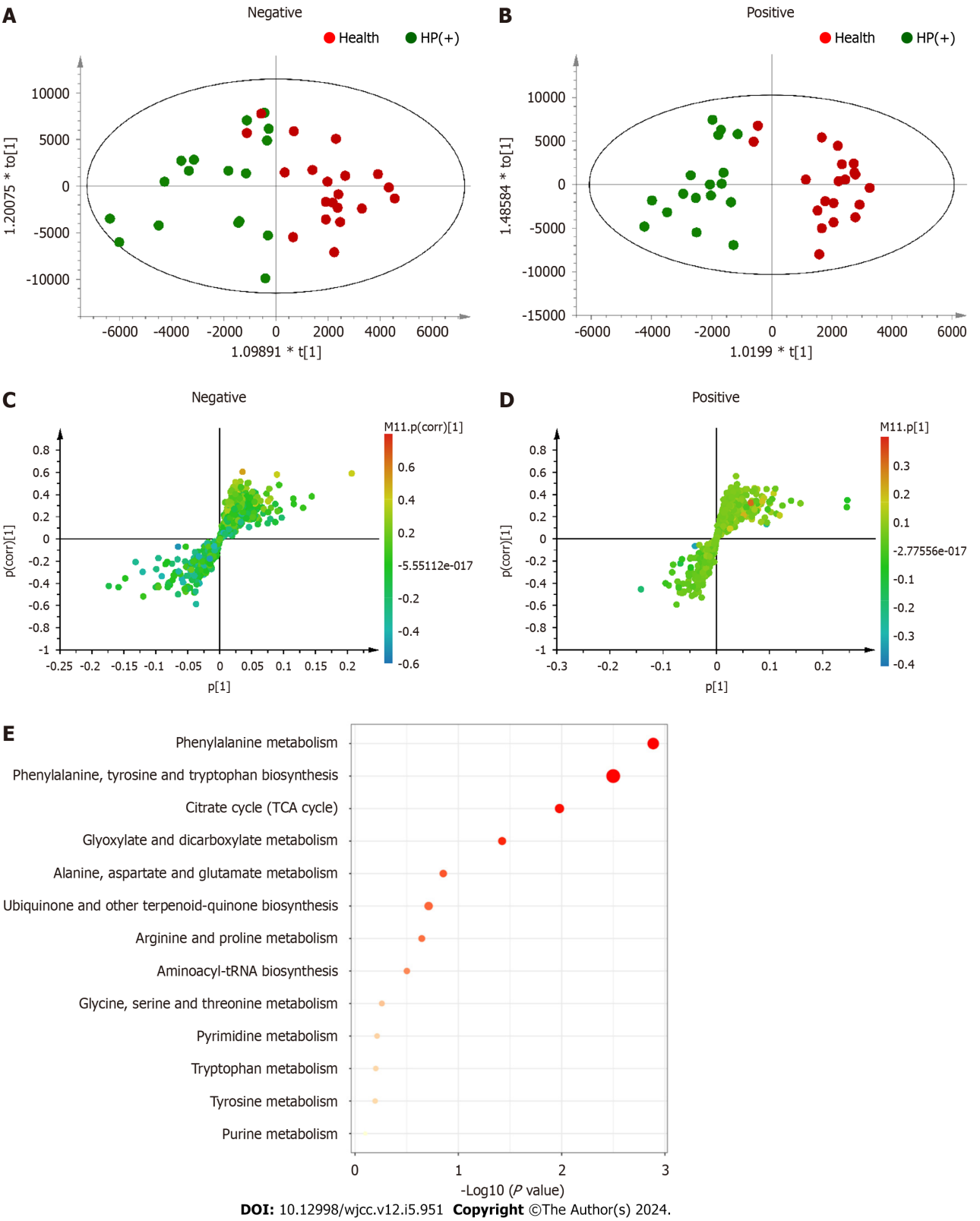

DOI: 10.12998/wjcc.v12.i5.951

Figure 3 Orthogonal partial least square discriminant analysis and pathway enrichment analysis of the health and *Helicobacter pylori*-positive samples. A, B: Orthogonal partial least square (OPLS) score plots; C, D: S-plots; A, C: Negative electronspray ionization (ESI) mode; B, D: Positive ESI mode. Model parameters of the negative ESI mode: R2X = 0.537, R2Y = 0.935, and Q2 = −0.33. Model parameters of the positive ESI mode: R2X = 0.467, R2Y = 0.955, and Q2 = −0.0553; E: Pathway enrichment analysis of differential metabolites between *Helicobacter pylori*-negative and health samples. Differential metabolites were obtained from OPLS–discriminant analysis and subjected to Kyoto encyclopedia of genes and genomes analysis using MetaboAnalyst software. *Helicobacter pylori*-positive; HP(−): *Helicobacter pylori*-negative.

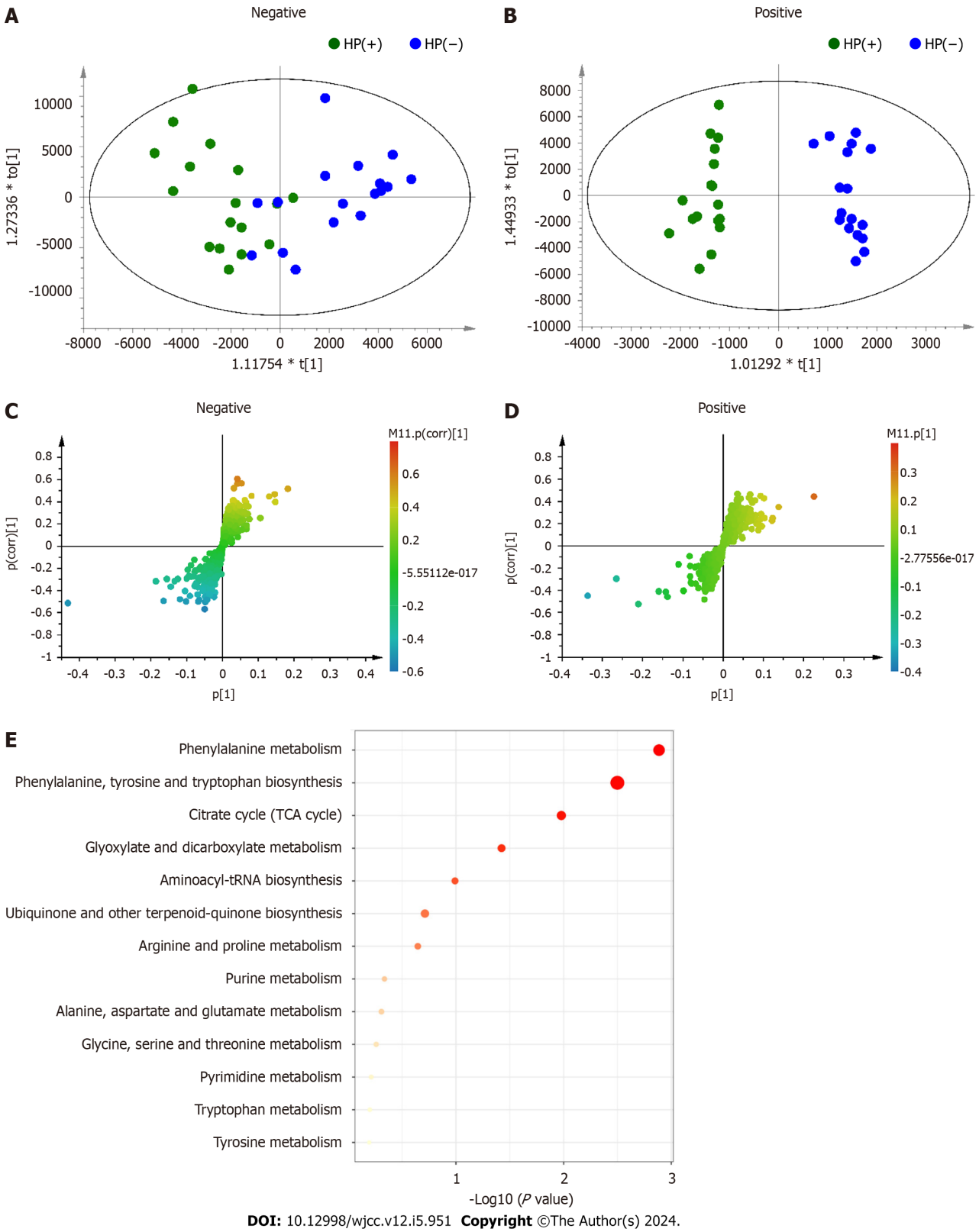

DOI: 10.12998/wjcc.v12.i5.951

Figure 4 Orthogonal partial least square discriminant analysis and pathway enrichment analysis between the *Helicobacter pylori*-positive and -negative samples. A, B: Orthogonal partial least square (OPLS) score plots; C, D: S-plots; A, C: Negative electronspray ionization (ESI) mode; B, D: Positive ESI mode. Model parameters of the negative ESI mode: R2X = 0.472, R2Y = 0.944, and Q2 = 0.119; model parameters of the positive ESI mode: R2X = 0.424, R2Y = 0.985, and Q2 = −0.109; E: Pathway enrichment analysis of differential metabolites between the *Helicobacter pylori*-negative and -positive samples. Differential metabolites were obtained from the OPLS–discriminant analysis and subjected to Kyoto encyclopedia of genes and genomes analysis using MetaboAnalyst. *Helicobacter pylori*-positive; HP(−): *Helicobacter pylori*-negative.

metabolites returned to normal after *H. pylori* eradication.

Evaluation of the predictive effectiveness of significant metabolites

We performed a univariate ROC curve analysis using the prominent seven metabolites to confirm the discriminative accuracy of individual metabolites between groups. The X-axis is the false-positive rate; the closer the X-axis value is to zero, the higher the accuracy is. The Y-axis is the true-positive rate; the larger the Y-axis value is, the higher the accuracy is. The result shows that the false-positive and true-positive rates in the Health *vs* HP(+) groups were higher than those in the HP(+) *vs* HP(−) groups, indicating that these urinary metabolites could reveal the treatment and prognosis progression of chronic gastritis with *H. pylori* infection (Figure 5B).

The criteria for assessing the accuracy of the signature based on AUC were summarized into a single metric, the ROC curve. According to the Swets criterion, AUC < 0.5 indicates that the test has no diagnostic value; AUC 0.5–0.7 indicates that the diagnostic test has low accuracy; AUC 0.7–0.9 indicates that the diagnostic test has good accuracy; and AUC > 0.9 indicates that the diagnostic test has high accuracy. In HP(+) *vs* HP(−) groups, the AUC values of hippuric acid, isocitric acid, L-tryptophan, L-phenylalanine, citric acid, L-tyrosine, and cis-aconitic acid were 0.856, 0.723, 0.723, 0.579, 0.583, 0.502, and 0.54, respectively (Figure 5B). In the Health *vs* HP(+) groups, the AUC values of these metabolites were 0.912, 0.754, 0.648, 0.782, 0.549, 0.585, and 0.438 (Figure 5B). Thus, hippuric acid, isocitric acid, L-tryptophan, and L-phenylalanine were the most related to the treatment effect and prognosis of chronic gastritis patients with *H. pylori* infection.

Exploring the mechanisms of metabolite changes during H. pylori eradication

We constructed an interaction network based on metabolomics and network pharmacology to further explore the relationships between metabolite changes and *H. pylori* eradication in chronic gastritis patients. First, differential metabolites were imported into the MetScape plugin in Cytoscape to collect the metabolite-reaction-enzyme-gene networks. By analyzing the identified metabolites in MetScape analysis, we gathered 60 targets of the significant differential metabolites and found four key metabolism pathways, namely the TCA cycle, tryptophan metabolism, biopterin metabolism, and tyrosine metabolism (Figure 6). Then, we performed network pharmacology to explore the key proteins involved in the regulatory mechanism of the identified differential metabolites in *H. pylori*-positive chronic gastritis. We collected 1313 targets in *H. pylori*-positive chronic gastritis from the Genecards database. After matching the *H. pylori*-positive chronic gastritis-related targets with the significant metabolite-related targets, nine targets were identified as potential key proteins involved in the biological progress of *H. pylori* eradication in chronic gastritis. These nine targets were MPO, COMT, TPO, TH, EPX, CMA1, DDC, TPH1, and LPO, which may play essential roles in the therapeutic effect in *H. pylori*-chronic gastritis.

DISCUSSION

Here, to the best of our knowledge, urinary metabolomics of patients with *H. pylori*-positive chronic gastritis was investigated for the first time. A therapeutic follow-up was conducted to collect urine from patients during *H. pylori* eradication and evaluate the changes in urinary metabolic profiles between *H. pylori*-positive and -negative patients. Urinary metabolic profiles were altered during *H. pylori* eradication. The metabolic pathways involved in *H. pylori* eradication in *H. pylori*-positive chronic gastritis patients included: (1) Phenylalanine metabolism; (2) phenylalanine, tyrosine, and tryptophan biosynthesis; (3) citrate cycle; and (4) glyoxylate and dicarboxylate. The decrease in hippuric acid and the increase in isocitric acid, L-tryptophan, and L-phenylalanine were mostly related to the treatment and prognosis of *H. pylori*-positive chronic gastritis patients. Our results provide a new perspective for evaluating the prognosis of *H. pylori*-positive chronic gastritis patients: the analysis of urinary metabolites.

The citrate cycle was found to be a vital urinary metabolic pathway related to the prognosis of *H. pylori*-positive chronic gastritis patients. After *H. pylori* eradication, the levels of three citrate cycle intermediates, namely cis-aconitic acid, isocitric acid, and citric acid, were elevated in the urine of cured patients with *H. pylori*-positive chronic gastritis. These results were partly consistent with those from *H. pylori*-infected experimental animals reported in the literature. UPLC-Q-TOF/MS-based urinary metabolomics revealed that the citrate cycle was involved in the pathogenesis, development, and prognosis of *H. pylori*-positive chronic gastritis in a rat model[18]. *H. pylori* infection reduced the levels of oxalosuccinate in rat urine, and the cure of chronic gastritis elevated the levels of oxalosuccinate[18]. ^{1}H NMR-based urinary metabolomics showed that *H. pylori* infection disturbs the citrate cycle by elevating the levels of cis-aconitate in *H. pylori*-infected gerbil chronic gastritis models[19]. Indeed, many studies have shown that *H. pylori* infection disrupts the citrate cycle in the stomach. GC/MS-based metabolomics revealed that *H. pylori* infection disturbs the citrate cycle of gastric epithelial cells by elevating the levels of citric acid and isocitric acid[20]. GC-TOF-MS-based metabolomics revealed that *H. pylori* infection disturbs the citrate cycle of the gastric mucosa by elevating the levels of citric, malic, and fumaric acid[21]. Overall, the urinary metabolomics results obtained from patients and animals with *H. pylori*-positive chronic gastritis indicate that urinary metabolites in the citrate cycle are involved in the pathogenesis, development, and treatment of *H. pylori*-positive chronic gastritis. However, the mechanisms underlying the disruption of the citrate cycle by *H. pylori* in patients with chronic gastritis required further exploration.

In this study, hippuric acid was the most differentially expressed urinary metabolite related to the prognosis of *H. pylori*-positive chronic gastritis patients, with AUC values of 0.856 [HP(+) *vs* HP(−)] and 0.912 [(Health *vs* HP(+)]. *H. pylori* eradication decreased the levels of hippuric acid in the urine. These results are consistent with those observed in previously reported chronic gastritis model animals. ^{1}H NMR- and UPLC-Q/TOF MS-based urinary metabolomics

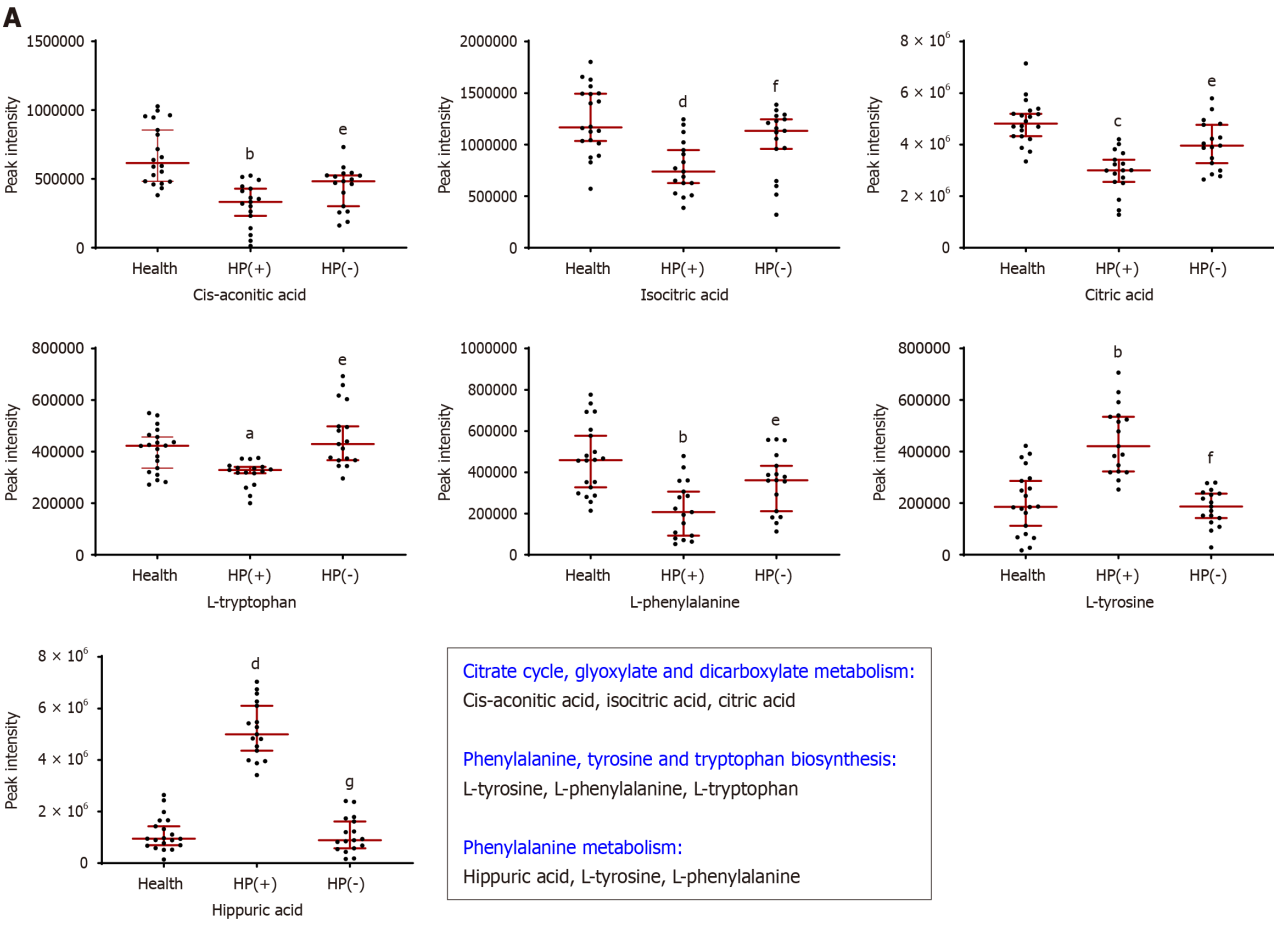
A
Peak intensity
Health
HP(+)
HP(-)
Cis-aconitic acid
Isocitric acid
Citric acid
L-tryptophan
L-phenylalanine
L-tyrosine
Hippuric acid
Citrate cycle, glyoxylate and dicarboxylate metabolism:
Cis-aconitic acid, isocitric acid, citric acid
Phenylalanine, tyrosine and tryptophan biosynthesis:
L-tyrosine, L-phenylalanine, L-tryptophan
Phenylalanine metabolism:
Hippuric acid, L-tyrosine, L-phenylalanine

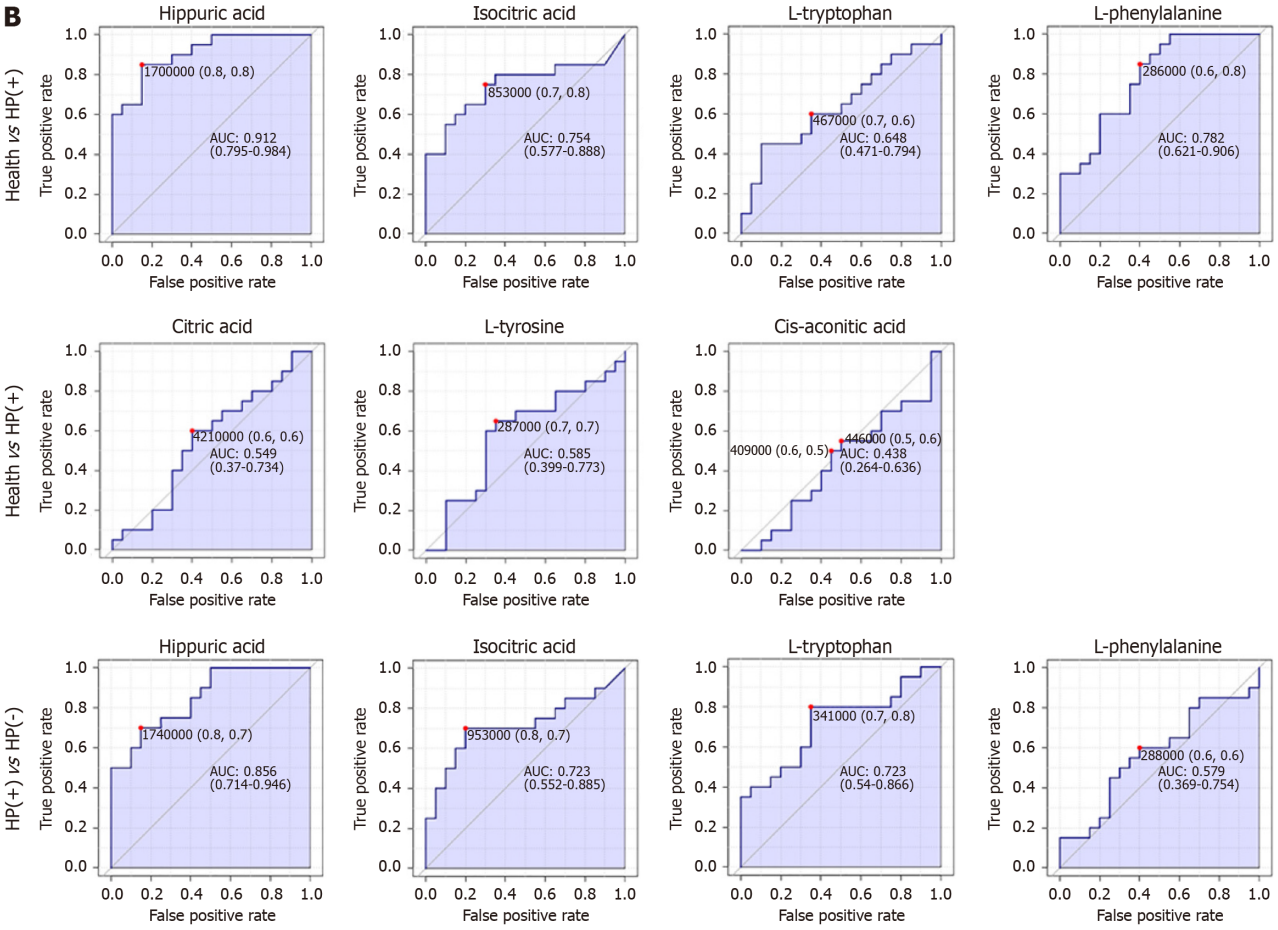
B
Health vs HP(+)
HP(+) vs HP(-)
True positive rate
False positive rate
Hippuric acid
1700000 (0.8, 0.8)
AUC: 0.912
(0.795-0.984)
Isocitric acid
853000 (0.7, 0.8)
AUC: 0.754
(0.577-0.888)
L-tryptophan
467000 (0.7, 0.6)
AUC: 0.648
(0.471-0.794)
L-phenylalanine
286000 (0.6, 0.8)
AUC: 0.782
(0.621-0.906)
Citric acid
4210000 (0.6, 0.6)
AUC: 0.549
(0.37-0.734)
L-tyrosine
287000 (0.7, 0.7)
AUC: 0.585
(0.399-0.773)
Cis-aconitic acid
409000 (0.6, 0.5)
446000 (0.5, 0.6)
AUC: 0.438
(0.264-0.636)
1740000 (0.8, 0.7)
AUC: 0.856
(0.714-0.946)
953000 (0.8, 0.7)
AUC: 0.723
(0.552-0.885)
341000 (0.7, 0.8)
AUC: 0.723
(0.54-0.866)
288000 (0.6, 0.6)
AUC: 0.579
(0.369-0.754)

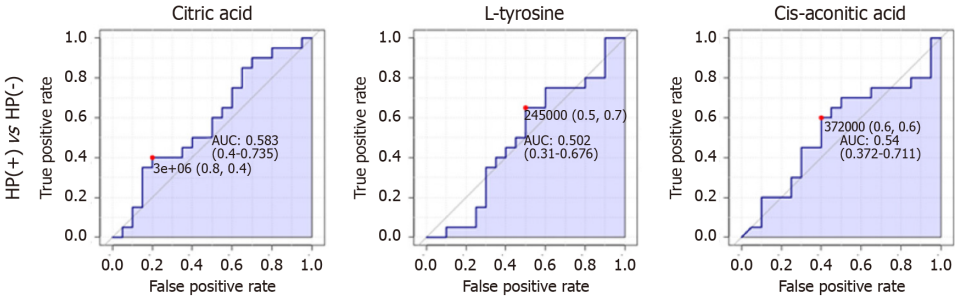

DOI: 10.12998/wjcc.v12.i5.951

Figure 5 Metabolites involved in *Helicobacter pylori* elimination. A: Peak intensity of the significant urinary metabolites associated with chronic gastritis management during *Helicobacter pylori* (*H. pylori*) elimination. Data presented as the mean ± SD (n = 20). $P < 0.05$ was considered to represent significance. Health group *vs H. pylori*-positive [HP(+)] group: $^{a}P < 0.05$, $^{b}P < 0.01$, $^{c}P < 0.001$, and $^{d}P < 0.0001$; HP(+) group *vs H. pylori*-negative group: $^{e}P < 0.05$, $^{f}P < 0.01$, and $^{g}P < 0.0001$; B: Receiver operating characteristic curve analysis of seven identified biomarkers. *Helicobacter pylori*-positive; HP(−): *Helicobacter pylori*-negative.

revealed that hippuric acid increased in the urine of sodium deoxycholate/ammonia-induced chronic atrophic gastritis rats and decreased in the urine of rats cured by a celebrated traditional Chinese medicine, Huangqi Jianzhong Tang[16,22]. In addition, in another analysis of ^{1}H NMR-based metabolomics, compared with control rats and rats cured by electroacupuncture stimulation, hippuric acid concentrations were increased in the urine of chronic atrophic gastritis rats [23]. Overall, our results and the previous literature indicate that the levels of hippuric acid are increased in the urine of patients with chronic gastritis, providing a potential urinary biomarker for evaluating the pathogenesis, development, and prognosis of chronic gastritis. However, the relationships between hippuric acid and chronic gastritis need to be further investigated.

Currently, the standard diagnostic method for the detection of chronic gastritis is gastroscopy, which is relatively invasive and is associated with poor patient compliance[24-27]. In addition, the UBT has been used for almost 30 years to test for *H. pylori* infection in the diagnosis of chronic gastritis; however, this approach also has drawbacks[28,29]. ^{14}C UBT is not suitable for children and pregnant women as it emits higher radiation levels than ^{13}C UBT[7]. H2 receptor antagonists, antibiotics, and bleeding impair the sensitivity of UBT[7,25]. No single method can be considered the gold standard for diagnosing chronic gastritis. Thus, investigations into potential and novel biomarkers of *H. pylori*-positive chronic gastritis have clinical significance for the diagnosis of chronic gastritis. As urine is a completely non-invasive and inexpensive sample, urine biomarkers are promising for clinical application in gastric diseases. One case-control study revealed a novel urinary protein biomarker panel for the early diagnosis of gastric cancer[30]. A follow-up study of gastric cancer patients after curative surgery demonstrated that urinary metabolic profiles are an effective early screening tool for gastric cancer[14]. Urinary 5-hydroxyindoleacetic acid levels are significantly higher in gastric cancer patients than in chronic gastritis patients or normal individuals[31]. Indeed, rapid urine tests that apply antibodies to detect *H. pylori*-specific IgG are convenient for screening for *H. pylori* infection[32-34]. Nevertheless, no urinary biomarkers have been used for the clinical diagnosis of *H. pylori*-positive chronic gastritis. This is a groundbreaking original clinical of the urinary biomarkers of *H. pylori*-positive chronic gastritis. According to our findings and previous literature, the levels of hippuric acid and metabolites in the citrate cycle in the urine are promising biomarkers for the better diagnosis and management of *H. pylori*-positive chronic gastritis. However, some issues still require attention, such as the false-positive results of non-targeted metabolomics. Therefore, future experiments should aim to confirm the roles of hippuric acid and metabolites of the citrate cycle as pivotal urinary biomarkers of *H. pylori*-positive chronic gastritis.

Integrated metabolomics and network pharmacology revealed that MPO, COMT, TPO, TH, EPX, CMA1, DDC, TPH1, and LPO were the key proteins involved in the biological progress of *H. pylori* eradication in chronic gastritis. Many researchers have reported that MPO protein levels are reduced during *H. pylori* eradication. In *H. pylori*-infected gerbils, MPO activity of stomach tissues decreased approximately tenfold[35]. In C57BL/6 mouse, *H. pylori* infection induced substantially higher MPO activity in the submucosa and the lamina propria of the stomach[36]. In one clinical study, MPO serum levels were significantly higher in *H. pylori*-positive chronic gastritis patients than in *H. pylori*-negative controls[37]. However, little research has been conducted on the relationship between proteins other than MPO and *H. pylori* eradication or infection in chronic gastritis. To the best of our knowledge, we are the first to demonstrate that COMT, TPO, TH, EPX, CMA1, DDC, TPH1, and LPO may be related to the therapeutic effect of *H. pylori* eradication in chronic gastritis patients.

In summary, this is the first clinical research that dissected the relationships between urinary metabolites and the therapy of *H. pylori*-positive chronic gastritis. Although this is a groundbreaking original clinical study of *H. pylori*-positive chronic gastritis, it is limited in that the results still require confirmation in further studies, such as targeted metabolomics, larger patient sample size, and animal experimental studies. Through further study, we expect to develop hippuric acid and metabolites of the citrate cycle as faster urinary biomarkers for evaluating the pathogenesis, development, and prognosis of *H. pylori*-positive chronic gastritis.

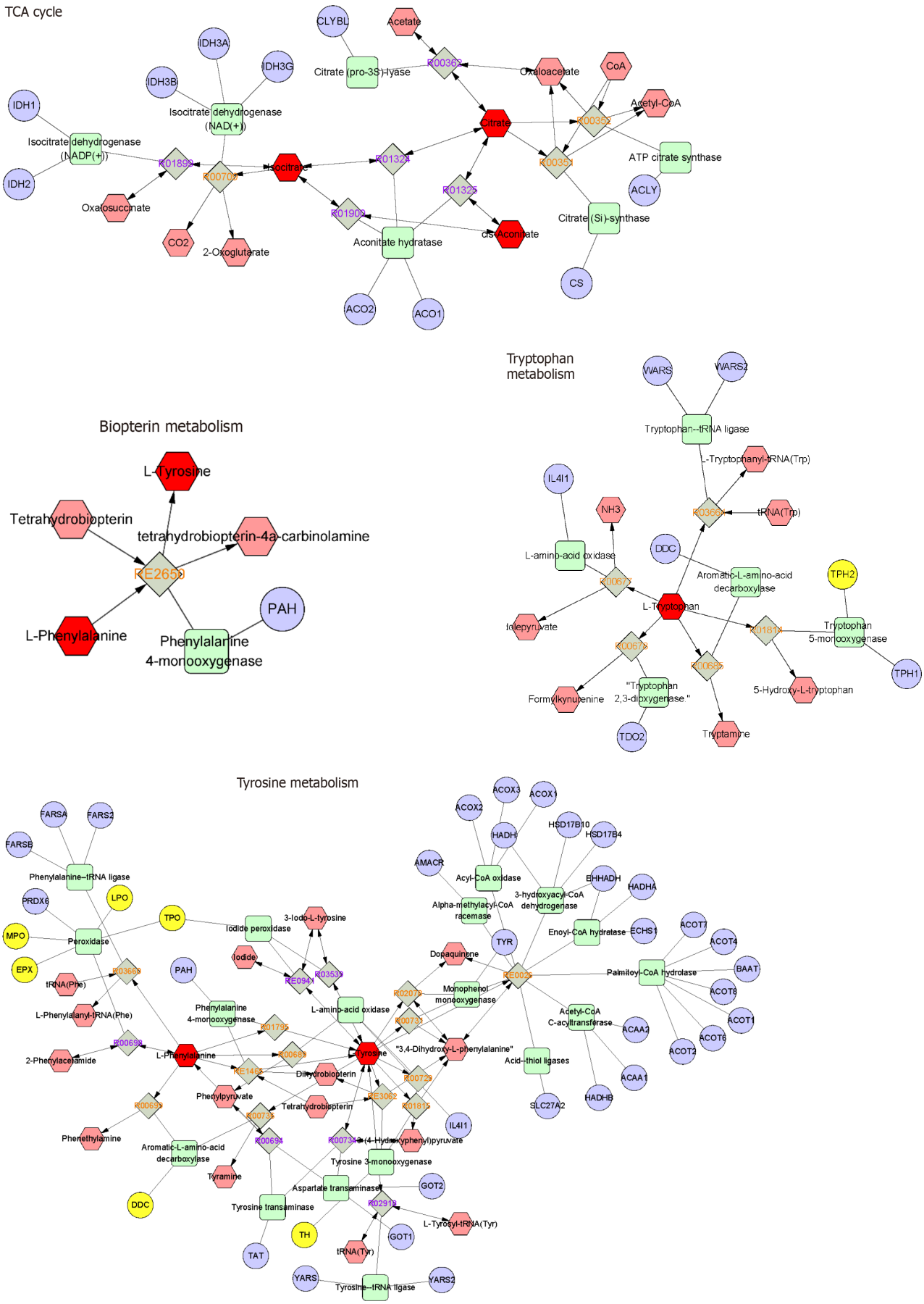

DOI: 10.12998/wjcc.v12.i5.951

Figure 6 The metabolite-reaction-enzyme-gene networks of the key metabolites and targets. The hexagons, diamonds, rounded rectangles, and

circles represent the metabolites, reactions, metabolic enzymes, and regulatory genes of metabolic enzymes, respectively. The differential metabolites and differential metabolite-related metabolites are shown as dark and bright red hexagons, respectively. The yellow circles represent the potential proteins involved in the regulation of the identified differential metabolites in *Helicobacter pylori*-positive chronic gastritis.

CONCLUSION

LC–MS-based metabolomics revealed that the major metabolites regulated by *H. pylori* eradication therapy include cis-aconitic acid, isocitric acid, citric acid, L-tyrosine, L-phenylalanine, L-tryptophan, and hippuric acid, which were involved in four metabolic pathways: (1) Phenylalanine metabolism; (2) phenylalanine, tyrosine, and tryptophan biosynthesis; (3) citrate cycle; and (4) glyoxylate and dicarboxylate metabolism. MPO, COMT, TPO, TH, EPX, CMA1, DDC, TPH1, and LPO were the key proteins involved in the biological process of *H. pylori* eradication in chronic gastritis. Hence, our research provides a new perspective for exploring the clinical significance of urinary metabolites in chronic gastritis.

ARTICLE HIGHLIGHTS

Research background

Helicobacter pylori (*H. pylori*) infection is a major risk factor of chronic gastritis, which perhaps influence approximately one-half of global population. *H. pylori* eradication is a popular treatment method for *H. pylori*-positive chronic gastritis, but its mechanism is far from clear.

Research motivation

Urinary metabolomics is gradually applied to mine the treatment mechanism of gastric diseases. However, there is no clinical study on urinary metabolomics of chronic gastritis.

Research objectives

This article aimed to investigate metabolic profiles of urine obtained during *H. pylori* eradication from patients with chronic gastritis.

Research methods

In this article, we applied LC-MS-based metabolomics and network pharmacology to investigate the relationships between urinary metabolites and *H. pylori*-positive chronic gastritis *via* a clinical follow-up study.

Research results

Our study revealed the different urinary metabolic profiles of *H. pylori*-positive chronic gastritis before and after *H. pylori* eradication. The metabolites regulated by *H. pylori* eradication include: cis-aconitic acid, isocitric acid, citric acid, L-tyrosine, L-phenylalanine, L-tryptophan and hippuric acid, which were involved in four metabolic pathways: (1) Phenylalanine metabolism; (2) phenylalanine, tyrosine and tryptophan biosynthesis; (3) citrate cycle; and (4) glyoxylate and dicarboxylate metabolism. Integrated metabolomics and network pharmacology revealed that MPO, COMT, TPO, TH, EPX, CMA1, DDC, TPH1 and LPO were the key proteins involved in the involved the biological progress of *H. pylori* eradication in chronic gastritis.

Research conclusions

Our research provides a new perspective for exploring the clinical significance of urinary metabolites in chronic gastritis.

Research perspectives

Although this is a groundbreaking original clinical study of *H. pylori*-positive chronic gastritis, it is limited in that the results still require confirmation in further studies, such as targeted metabolomics, larger patient sample size, and animal experimental studies.

FOOTNOTES

Co-first authors: Wen-Ting An and Yu-Xia Hao.

Co-corresponding authors: Hong-Xia Li and Xing-Kang Wu.

Author contributions: An WT contributed to conceptualization, investigation, methodology, project administration, resources, data curation, writing and formal analysis; Hao YX contributed to investigation, methodology, data curation and formal analysis; Wu XK contributed to supervision, writing, review and editing; Li HX contributed to conceptualization, methodology, supervision, funding acquisition, review and editing; all authors read and approved the final manuscript.

Supported by Shanxi Provincial Health Commission, No. 2019022.

Institutional review board statement: This study was approved by the Ethics Committee of Shanxi Provincial People's Hospital (No. 2022-167).

Informed consent statement: All the patients voluntarily participated in the study and signed informed consent forms.

Conflict-of-interest statement: All the authors report no relevant conflicts of interest for this article.

Data sharing statement: All data and materials are available from the corresponding author.

STROBE statement: The authors have read the STROBE Statement—checklist of items, and the manuscript was prepared and revised according to the STROBE Statement—checklist of items.

Country/Territory of origin: China

ORCID number: Yu-Xia Hao 0000-0002-6844-6071; Hong-Xia Li 0009-0006-7856-4270; Xing-Kang Wu 0000-0001-6480-7952.

S-Editor: Wang JL
L-Editor: A
P-Editor: Zheng XM

REFERENCES

1 **Sipponen P**, Maaroos HI. Chronic gastritis. *Scand J Gastroenterol* 2015; **50**: 657-667 [PMID: 25901896 DOI: 10.3109/00365521.2015.1019918]
2 **Sung H**, Ferlay J, Siegel RL, Laversanne M, Soerjomataram I, Jemal A, Bray F. Global Cancer Statistics 2020: GLOBOCAN Estimates of Incidence and Mortality Worldwide for 36 Cancers in 185 Countries. *CA Cancer J Clin* 2021; **71**: 209-249 [PMID: 33538338 DOI: 10.3322/caac.21660]
3 **Rugge M**, Genta RM. Staging and grading of chronic gastritis. *Hum Pathol* 2005; **36**: 228-233 [PMID: 15791566 DOI: 10.1016/j.humpath.2004.12.008]
4 **Lahner E**, Esposito G, Pilozzi E, Purchiaroni F, Corleto VD, Di Giulio E, Annibale B. Occurrence of gastric cancer and carcinoids in atrophic gastritis during prospective long-term follow up. *Scand J Gastroenterol* 2015; **50**: 856-865 [PMID: 25645880 DOI: 10.3109/00365521.2015.1010570]
5 **de Vries AC**, van Grieken NC, Looman CW, Casparie MK, de Vries E, Meijer GA, Kuipers EJ. Gastric cancer risk in patients with premalignant gastric lesions: a nationwide cohort study in the Netherlands. *Gastroenterology* 2008; **134**: 945-952 [PMID: 18395075 DOI: 10.1053/j.gastro.2008.01.071]
6 **Maluf S**, Salgado JV, Cysne DN, Camelo DMF, Nascimento JR, Maluf BVT, Silva LDM, Belfort MRC, Silva LA, Guerra RNM, Salgado Filho N, Nascimento FRF. Increased Glycated Hemoglobin Levels in Patients With Helicobacter pylori Infection Are Associated With the Grading of Chronic Gastritis. *Front Immunol* 2020; **11**: 2121 [PMID: 33013895 DOI: 10.3389/fimmu.2020.02121]
7 **Yang H**, Hu B. Diagnosis of Helicobacter pylori Infection and Recent Advances. *Diagnostics (Basel)* 2021; **11** [PMID: 34441240 DOI: 10.3390/diagnostics11081305]
8 **Ding SZ**, Du YQ, Lu H, Wang WH, Cheng H, Chen SY, Chen MH, Chen WC, Chen Y, Fang JY, Gao HJ, Guo MZ, Han Y, Hou XH, Hu FL, Jiang B, Jiang HX, Lan CH, Li JN, Li Y, Li YQ, Liu J, Li YM, Lyu B, Lu YY, Miao YL, Nie YZ, Qian JM, Sheng JQ, Tang CW, Wang F, Wang HH, Wang JB, Wang JT, Wang JP, Wang XH, Wu KC, Xia XZ, Xie WF, Xie Y, Xu JM, Yang CQ, Yang GB, Yuan Y, Zeng ZR, Zhang BY, Zhang GY, Zhang GX, Zhang JZ, Zhang ZY, Zheng PY, Zhu Y, Zuo XL, Zhou LY, Lyu NH, Yang YS, Li ZS; National Clinical Research Center for Digestive Diseases (Shanghai), Gastrointestinal Early Cancer Prevention & Treatment Alliance of China (GECA), Helicobacter pylori Study Group of Chinese Society of Gastroenterology, and Chinese Alliance for Helicobacter pylori Study. Chinese Consensus Report on Family-Based Helicobacter pylori Infection Control and Management (2021 Edition). *Gut* 2022; **71**: 238-253 [PMID: 34836916 DOI: 10.1136/gutjnl-2021-325630]
9 **Navashenaq JG**, Shabgah AG, Banach M, Jamialahmadi T, Penson PE, Johnston TP, Sahebkar A. The interaction of Helicobacter pylori with cancer immunomodulatory stromal cells: New insight into gastric cancer pathogenesis. *Semin Cancer Biol* 2022; **86**: 951-959 [PMID: 34600095 DOI: 10.1016/j.semcancer.2021.09.014]
10 **Zhang W**, Cui N, Ye J, Yang B, Sun Y, Kuang H. Curcumin's prevention of inflammation-driven early gastric cancer and its molecular mechanism. *Chin Herb Med* 2022; **14**: 244-253 [PMID: 36117672 DOI: 10.1016/j.chmed.2021.11.003]
11 **Yan L**, Chen Y, Chen F, Tao T, Hu Z, Wang J, You J, Wong BCY, Chen J, Ye W. Effect of Helicobacter pylori Eradication on Gastric Cancer Prevention: Updated Report From a Randomized Controlled Trial With 26.5 Years of Follow-up. *Gastroenterology* 2022; **163**: 154-162.e3 [PMID: 35364066 DOI: 10.1053/j.gastro.2022.03.039]
12 **Rokkas T**, Gisbert JP, Malfertheiner P, Niv Y, Gasbarrini A, Leja M, Megraud F, O'Morain C, Graham DY. Comparative Effectiveness of Multiple Different First-Line Treatment Regimens for Helicobacter pylori Infection: A Network Meta-analysis. *Gastroenterology* 2021; **161**: 495-507.e4 [PMID: 33839101 DOI: 10.1053/j.gastro.2021.04.012]

13 **Li H**, Wang R, Sun H. Systems Approaches for Unveiling the Mechanism of Action of Bismuth Drugs: New Medicinal Applications beyond Helicobacter Pylori Infection. *Acc Chem Res* 2019; **52**: 216-227 [PMID: 30596427 DOI: 10.1021/acs.accounts.8b00439]

14 **Jung J**, Jung Y, Bang EJ, Cho SI, Jang YJ, Kwak JM, Ryu DH, Park S, Hwang GS. Noninvasive diagnosis and evaluation of curative surgery for gastric cancer by using NMR-based metabolomic profiling. *Ann Surg Oncol* 2014; **21** Suppl 4: S736-S742 [PMID: 25092158 DOI: 10.1245/s10434-014-3886-0]

15 **Kwon HN**, Lee H, Park JW, Kim YH, Park S, Kim JJ. Screening for Early Gastric Cancer Using a Noninvasive Urine Metabolomics Approach. *Cancers (Basel)* 2020; **12** [PMID: 33050308 DOI: 10.3390/cancers12102904]

16 **Liu Y**, Jin Z, Qin X, Zheng Q. Urinary metabolomics research for Huangqi Jianzhong Tang against chronic atrophic gastritis rats based on (1) H NMR and UPLC-Q/TOF MS. *J Pharm Pharmacol* 2020; **72**: 748-760 [PMID: 32128823 DOI: 10.1111/jphp.13242]

17 **Tong Y**, Zhao X, Wang R, Li R, Zou W, Zhao Y. Therapeutic effect of berberine on chronic atrophic gastritis based on plasma and urine metabolisms. *Eur J Pharmacol* 2021; **908**: 174335 [PMID: 34265298 DOI: 10.1016/j.ejphar.2021.174335]

18 **Chen X**, Zhang J, Wang R, Liu H, Bao C, Wu S, Wen J, Yang T, Wei Y, Ren S, Tong Y, Zhao Y. UPLC-Q-TOF/MS-Based Serum and Urine Metabonomics Study on the Ameliorative Effects of Palmatine on Helicobacter pylori-Induced Chronic Atrophic Gastritis. *Front Pharmacol* 2020; **11**: 586954 [PMID: 33041831 DOI: 10.3389/fphar.2020.586954]

19 **Gao XX**, Ge HM, Zheng WF, Tan RX. NMR-based metabonomics for detection of Helicobacter pylori infection in gerbils: which is more descriptive. *Helicobacter* 2008; **13**: 103-111 [PMID: 18321300 DOI: 10.1111/j.1523-5378.2008.00590.x]

20 **Matsunaga S**, Nishiumi S, Tagawa R, Yoshida M. Alterations in metabolic pathways in gastric epithelial cells infected with Helicobacter pylori. *Microb Pathog* 2018; **124**: 122-129 [PMID: 30138760 DOI: 10.1016/j.micpath.2018.08.033]

21 **Son SY**, Lee CH, Lee SY. Different Metabolites of the Gastric Mucosa between Patients with Current Helicobacter pylori Infection, Past Infection, and No Infection History. *Biomedicines* 2022; **10** [PMID: 35327358 DOI: 10.3390/biomedicines10030556]

22 **Liu Y**, Xu W, Wang G, Qin X. Material basis research for Huangqi Jianzhong Tang against chronic atrophic gastritis rats through integration of urinary metabonomics and SystemsDock. *J Ethnopharmacol* 2018; **223**: 1-9 [PMID: 29777900 DOI: 10.1016/j.jep.2018.05.015]

23 **Xu J**, Zheng X, Cheng KK, Chang X, Shen G, Liu M, Wang Y, Shen J, Zhang Y, He Q, Dong J, Yang Z. NMR-based metabolomics Reveals Alterations of Electro-acupuncture Stimulations on Chronic Atrophic Gastritis Rats. *Sci Rep* 2017; **7**: 45580 [PMID: 28358020 DOI: 10.1038/srep45580]

24 **Rahman I**, Afzal NA, Patel P. The role of magnetic assisted capsule endoscopy (MACE) to aid visualisation in the upper GI tract. *Comput Biol Med* 2015; **65**: 359-363 [PMID: 25934086 DOI: 10.1016/j.compbiomed.2015.03.014]

25 **Wang YK**, Kuo FC, Liu CJ, Wu MC, Shih HY, Wang SS, Wu JY, Kuo CH, Huang YK, Wu DC. Diagnosis of Helicobacter pylori infection: Current options and developments. *World J Gastroenterol* 2015; **21**: 11221-11235 [PMID: 26523098 DOI: 10.3748/wjg.v21.i40.11221]

26 **Domșa AT**, Gheban D, Lazăr C, Pop B, Borzan CM. Particular Morphological Features in the Diagnosis of Pediatric Helicobacter pylori Gastritis: A Morphometry-Based Study. *J Clin Med* 2020; **9** [PMID: 33198263 DOI: 10.3390/jcm9113639]

27 **Uematsu J**, Sugimoto M, Hamada M, Iwata E, Niikura R, Nagata N, Fukuzawa M, Itoi T, Kawai T. Efficacy of a Third-Generation High-Vision Ultrathin Endoscope for Evaluating Gastric Atrophy and Intestinal Metaplasia in Helicobacter pylori-Eradicated Patients. *J Clin Med* 2022; **11** [PMID: 35456291 DOI: 10.3390/jcm11082198]

28 **Alzoubi H**, Al-Mnayyis A, Al Rfoa I, Aqel A, Abu-Lubad M, Hamdan O, Jaber K. The Use of (13)C-Urea Breath Test for Non-Invasive Diagnosis of Helicobacter pylori Infection in Comparison to Endoscopy and Stool Antigen Test. *Diagnostics (Basel)* 2020; **10** [PMID: 32635179 DOI: 10.3390/diagnostics10070448]

29 **Cardos AI**, Maghiar A, Zaha DC, Pop O, Fritea L, Miere Groza F, Cavalu S. Evolution of Diagnostic Methods for Helicobacter pylori Infections: From Traditional Tests to High Technology, Advanced Sensitivity and Discrimination Tools. *Diagnostics (Basel)* 2022; **12** [PMID: 35204598 DOI: 10.3390/diagnostics12020508]

30 **Shimura T**, Dayde D, Wang H, Okuda Y, Iwasaki H, Ebi M, Kitagawa M, Yamada T, Hanash SM, Taguchi A, Kataoka H. Novel urinary protein biomarker panel for early diagnosis of gastric cancer. *Br J Cancer* 2020; **123**: 1656-1664 [PMID: 32934343 DOI: 10.1038/s41416-020-01063-5]

31 **Mokhtari M**, Rezaei A, Ghasemi A. Determination of urinary 5-hydroxyindoleacetic acid as a metabolomics in gastric cancer. *J Gastrointest Cancer* 2015; **46**: 138-142 [PMID: 25761643 DOI: 10.1007/s12029-015-9700-9]

32 **Mabe K**, Kikuchi S, Okuda M, Takamasa M, Kato M, Asaka M. Diagnostic accuracy of urine Helicobacter pylori antibody test in junior and senior high school students in Japan. *Helicobacter* 2017; **22** [PMID: 27400382 DOI: 10.1111/hel.12329]

33 **Aumpan N**, Vilaichone RK, Chotivitayatarakorn P, Pornthisarn B, Cholprasertsuk S, Bhanthumkomol P, Kanokwanvimol A, Siramolpiwat S, Mahachai V. High Efficacy of Rapid Urine Test for Diagnosis of Helicobacter pylori Infection in Thai People. *Asian Pac J Cancer Prev* 2019; **20**: 1525-1529 [PMID: 31128058 DOI: 10.31557/APJCP.2019.20.5.1525]

34 **Syam AF**, Miftahussurur M, Uwan WB, Simanjuntak D, Uchida T, Yamaoka Y. Validation of Urine Test for Detection of Helicobacter pylori Infection in Indonesian Population. *Biomed Res Int* 2015; **2015**: 152823 [PMID: 26824034 DOI: 10.1155/2015/152823]

35 **Chang CC**, Chen SH, Lien GS, Lou HY, Hsieh CR, Fang CL, Pan S. Eradication of Helicobacter pylori significantly reduced gastric damage in nonsteroidal anti-inflammatory drug-treated Mongolian gerbils. *World J Gastroenterol* 2005; **11**: 104-108 [PMID: 15609406 DOI: 10.3748/wjg.v11.i1.104]

36 **Shiomi S**, Toriie A, Imamura S, Konishi H, Mitsufuji S, Iwakura Y, Yamaoka Y, Ota H, Yamamoto T, Imanishi J, Kita M. IL-17 is involved in Helicobacter pylori-induced gastric inflammatory responses in a mouse model. *Helicobacter* 2008; **13**: 518-524 [PMID: 19166417 DOI: 10.1111/j.1523-5378.2008.00629.x]

37 **Rautelin HI**, Oksanen AM, Veijola LI, Sipponen PI, Tervahartiala TI, Sorsa TA, Lauhio A. Enhanced systemic matrix metalloproteinase response in Helicobacter pylori gastritis. *Ann Med* 2009; **41**: 208-215 [PMID: 18979291 DOI: 10.1080/07853890802482452]

World Journal of Clinical Cases

Submit a Manuscript: https://www.f6publishing.com

World J Clin Cases 2024 February 16; 12(5): 966-972

DOI: 10.12998/wjcc.v12.i5.966

ISSN 2307-8960 (online)

ORIGINAL ARTICLE

Observational Study

Clinical significance of platelet mononuclear cell aggregates in patients with sepsis and acute respiratory distress syndrome

Chong-Min Huang, Juan-Juan Li, Wei-Ke Wei

Specialty type: Medicine, research and experimental

Provenance and peer review: Unsolicited article; Externally peer reviewed.

Peer-review model: Single blind

Peer-review report's scientific quality classification

Grade A (Excellent): 0
Grade B (Very good): B, B
Grade C (Good): 0
Grade D (Fair): 0
Grade E (Poor): 0

P-Reviewer: Ghimire R, Nepal

Received: November 16, 2023
Peer-review started: November 16, 2023
First decision: December 26, 2023
Revised: December 30, 2023
Accepted: January 24, 2024
Article in press: January 24, 2024
Published online: February 16, 2024

Chong-Min Huang, Department of Intensive Medicine, The Second People's Hospital of Haining City, Haining 314419, Zhejiang Province, China

Juan-Juan Li, Wei-Ke Wei, Department of Integrated Traditional Chinese and Western Medicine, Qingyang Hospital, Hangzhou 310023, Zhejiang Province, China

Corresponding author: Chong-Min Huang, MD, Doctor, Department of Intensive Medicine, The Second People's Hospital of Haining City, No. 85 Guoque Road, Maqiao Street, Haining 314419, Zhejiang Province, China. 15325307291@163.com

Abstract

BACKGROUND

The diagnosis of sepsis combined with acute respiratory distress syndrome (ARDS) has increased owing to the enhanced awareness among medical professionals and the continuous development of modern medical technologies, while early diagnosis of ARDS still lacks specific biomarkers. One of the main pathogenic mechanisms of sepsis-associated ARDS involves the actions of various pathological injuries and inflammatory factors, such as platelet and white blood cells activation, leading to an increase of surface adhesion molecules. These adhesion molecules further form platelet-white blood cell aggregates, including platelet-mononuclear cell aggregates (PMAs). PMAs has been identified as one of the markers of platelet activation, here we hypothesize that PMAs might play a potential biomarker for the early diagnosis of this complication.

AIM

To investigate the expression of PMAs in the serum of patients with sepsis complicated by ARDS and its clinical significance.

METHODS

We selected 72 hospitalized patients diagnosed with sepsis as the study population between March 2019 and March 2022. Among them, 30 patients with sepsis and ARDS formed the study group, while 42 sepsis patients without ARDS comprised the control group. After diagnosis, venous blood samples were immediately collected from all patients. Flow cytometry was employed to analyze the expression of PMAs, platelet neutrophil aggregates (PNAs), and platelet aggregates (PLyAs) in the serum. Additionally, the Acute Physiology and Chronic Health Evaluation (APACHE) II score was calculated for each patient, and receiver operating characteristic curves were generated to assess diagnostic value.

RESULTS
The study found that the levels of PNAs and PLyAs in the serum of the study group were higher than those in the control group, but the difference was not statistically significant ($P > 0.05$). However, the expression of PMAs in the serum of the study group was significantly upregulated ($P < 0.05$) and positively correlated with the APACHE II score ($r = 0.671$, $P < 0.05$). When using PMAs as a diagnostic indicator, the area under the curve value was 0.957, indicating a high diagnostic value ($P < 0.05$). Furthermore, the optimal cutoff value was 8.418%, with a diagnostic sensitivity of 0.819 and specificity of 0.947.

CONCLUSION
In summary, the serum levels of PMAs significantly increase in patients with sepsis and ARDS. Therefore, serum PMAs have the potential to become a new biomarker for clinically diagnosing sepsis complicated by ARDS.

Key Words: Sepsis; Acute respiratory distress syndrome; Platelet leukocyte aggregates; Platelet mononuclear cell aggregates, Biomarker

Core Tip: Our research aimed to investigate the expression of platelet mononuclear cell aggregates (PMAs) in the serum of patients with sepsis complicated by acute respiratory distress syndrome (ARDS) and its clinical significance. The results indicate that the serum levels of PMAs significantly increase in patients with sepsis and ARDS. Therefore, serum PMAs have the potential to become a new biomarker for clinically diagnosing sepsis complicated by ARDS.

Citation: Huang CM, Li JJ, Wei WK. Clinical significance of platelet mononuclear cell aggregates in patients with sepsis and acute respiratory distress syndrome. *World J Clin Cases* 2024; 12(5): 966-972
URL: https://www.wjgnet.com/2307-8960/full/v12/i5/966.htm
DOI: https://dx.doi.org/10.12998/wjcc.v12.i5.966

INTRODUCTION

Sepsis is a common and critical clinical condition, and in recent years, the number of cases diagnosed as sepsis with concomitant acute respiratory distress syndrome (ARDS) has increased, owing to the enhanced awareness among medical professionals and the continuous development of modern medical diagnostic technologies[1]. Due to the high mortality rate associated with sepsis, it has attracted widespread attention in the clinical community. Despite various diagnostic tools available, early diagnosis of ARDS still lacks specific biomarkers. Recent studies have confirmed that one of the main pathogenic mechanisms of sepsis-associated ARDS involves the actions of various pathological injuries and inflammatory factors[2,3].

In this study, platelets and white blood cells in the patient's body are activated, leading to an increase in surface adhesion molecules. These adhesion molecules further form platelet-white blood cell aggregates, including platelet-neutrophil aggregates (PNAs), platelet aggregates (PLyAs), and platelet-mononuclear cell aggregates (PMAs)[4]. Activated platelets bind to monocytes and neutrophils, with the noteworthy observation that the binding of platelets to monocytes precedes that to neutrophils. PMAs are considered one of the markers of platelet activation[5]. The objective of this study is to investigate whether PMAs in the serum of sepsis patients with ARDS can serve as effective biomarkers for the early diagnosis of this complication.

MATERIALS AND METHODS

Study subjects and diagnostic criteria

This study included 72 adult sepsis patients admitted to our hospital between March 2019 and March 2022. The diagnosis was in accordance with the " International Guidelines for Management of Sepsis and Septic Shock: 2016[6]." Following the 2012 Berlin definition[7], patients were categorized into the study group (sepsis with ARDS, $n = 30$) and the control group (sepsis alone, $n = 42$). Exclusion criteria comprised pregnancy with blood system diseases, pure blood system diseases, HIV infection, ongoing chemotherapy, use of immunosuppressive agents or antiplatelet drugs, pulmonary interstitial fibrosis, and acute exacerbation of chronic obstructive pulmonary disease. The study was approved by our hospital's medical ethics committee, and written informed consent was obtained from all patients or their authorized representatives.

Sample collection

Three milliliters of peripheral venous blood were collected from all confirmed sepsis patients immediately upon admission, placed in anticoagulant tubes, and preserved and transported to the Shanghai Lanwei Medical Laboratory for further testing *via* ice pack refrigeration. To ensure accuracy, the entire blood collection process strictly adhered to standardized procedures to prevent platelet activation-induced errors.

Sample testing

Patients underwent blood gas analysis, and the oxygenation index PaO_2/FiO_2 was calculated. Flow cytometry was employed to classify platelet-mononuclear cell aggregates in the peripheral blood of both sepsis patient groups, including PLyAs, PMAs, and PNAs. The site of infection was recorded, and the nature of the pathogenic bacteria was determined through blood culture.

Acute physiology and chronic health evaluation II Score

Within 24 h of admission, all confirmed sepsis patients had their physiological indicators meticulously recorded by the attending physician, who then calculated the Acute Physiology and Chronic Health Evaluation (APACHE) II score, noting the worst values.

Statistical analysis

Statistical analysis was conducted using SPSS 20.0 software. Descriptive data are presented as mean ± SD, and *t*-tests were used for comparisons. Receiver operating characteristic (ROC) curves were generated to determine the optimal cutoff value, sensitivity, and specificity of serum PMAs in diagnosing sepsis with ARDS. The significance level was set at $P < 0.05$.

RESULTS

General data comparison between the two groups

According to the data in Table 1, there were no significant differences ($P > 0.05$) observed in general information, such as age, gender, infection site, pathogen, and oxygenation index PaO_2/FiO_2, between sepsis patients with ARDS and those with sepsis alone.

Comparison of PNAs, PLyAs, and PMAs between the two groups

As shown in Table 2, the serum levels of PNAs and PLyAs in sepsis patients with ARDS were slightly higher than those in the sepsis-alone group; however, these differences were not statistically significant ($P > 0.05$). Nevertheless, the serum levels of PMAs in sepsis patients with ARDS were significantly higher than those in the sepsis-alone group, and this difference was statistically significant ($P < 0.05$).

Comparison of APACHE II scores between the two groups

According to the data in Table 3, the APACHE II scores of sepsis patients with ARDS were significantly higher than those of sepsis patients without ARDS, and this difference was statistically significant ($P < 0.05$).

Correlation analysis between PMAs and APACHE II scores

As illustrated in Figure 1A, the PMAs levels in sepsis patients with ARDS were significantly higher than those in sepsis patients without ARDS. Further linear correlation analysis revealed a positive correlation between PMAs and APACHE II scores in patients ($r = 0.671$, $P < 0.05$).

Diagnostic value of various indicators for ARDS

Using PMAs and APACHE II scores as test variables and ARDS as the state variable, ROC curves were fitted. When using PMAs as the test variable, the area under the curve (AUC) was 0.957, indicating a significant diagnostic value ($P < 0.05$). The optimal cutoff value for PMAs was 8.418%, with a diagnostic sensitivity of 0.819 and specificity of 0.947. When using APACHE II scores as the test variable, the AUC was 0.940, indicating a significant diagnostic value ($P < 0.05$). The optimal cutoff value for APACHE II scores was 17.115, with a diagnostic sensitivity of 0.837 and specificity of 0.844. Refer to Tables 4 and 5, and Figure 1B for detailed results.

DISCUSSION

Sepsis, as a common complication of severe infections, trauma, acute abdomen, and major surgeries in clinical practice, spans multiple disciplines such as internal medicine, surgery, and gynecology. It leads to multi-organ dysfunction, poor prognosis, and a high mortality rate[8]. The lungs are particularly susceptible to the effects of sepsis, causing pathological damage that is closely related to patient prognosis. Sepsis-induced multi-organ pathology includes the aggregation of white blood cells and platelets at the site of infection, disseminated intravascular coagulation, endothelial damage, resulting in the loss of surfactant on the alveolar surface, and activation of oxidative stress responses. These mechanisms

Table 1 Comparison of general data between the two groups of patients (mean ± SD), *n* (%)

	Study group (*n* = 30)	Control group (*n* = 42)	χ^2/t	*P* value
Male/female	16/14	25/17	0.475	0.523
Age	51.6 ± 11.4	48.6 ± 14.7	1.234	0.224
Infection			1.587	0.904
Urinary tract infection	4 (13.3)	5 (11.9)		
Hematogenous infection	3 (10)	4 (9.5)		
Abdominal infection	6 (20)	8 (19.1)		
Pulmonary infection	15 (50)	22 (52.4)		
Others	2 (6.7)	3 (7.1)		
Microbiology			2.88	0.518
Fungus	3 (10)	5 (11.9)		
G-	12 (40)	17 (40.5)		
G+	5 (16.7)	8 (19)		
Mixed infection	6 (20)	7 (16.7)		
Unknown cause	4 (13.3)	5 (11.9)		
PaO_2/FiO_2	141.85 ± 29.44	145.35 ± 30.28	11.27	0.912

Table 2 Comparison of platelet neutrophil aggregates, platelet aggregates, and platelet-mononuclear cell aggregates between the two groups (mean ± SD)

Groups	*n*	PNAs (%)	PLyAs (%)	PMAs (%)
Study group	30	14.15 ± 8.93	15.42 ± 6.97	27.18 ± 6.14[1]
Control group	42	13.87 ± 9.24	14.78 ± 3.24	17.29 ± 2.05

[1]Compared to the Control groups, the serum levels of platelet-mononuclear cell aggregates increased in sepsis patients with acute respiratory distress syndrome ($P < 0.05$).

APACHE II: Acute Physiology and Chronic Health Evaluation II Scores; PMAs: Platelet-mononuclear cell aggregates; PNAs: platelet neutrophil aggregates; PLyAs: Platelet aggregates.

Table 3 Comparison of Acute Physiology and Chronic Health Evaluation II Scores between the two groups (mean ± SD)

Groups	*n*	APACHE II
Study group	30	35.17 ± 5.44[1]
Control group	42	23.39 ± 4.24

[1]Compared to the Control groups, the Acute Physiology and Chronic Health Evaluation II scores increased in sepsis patients with acute respiratory distress syndrome ($P < 0.05$).

APACHE II: Acute Physiology and Chronic Health Evaluation II Scores.

collectively contribute to the development of severe lung injury[9]. Due to the activation of inflammatory reactions and coagulation mechanisms in sepsis patients, they are prone to developing ARDS, with pathological manifestations in the lungs characterized by increased permeability of the alveolar-capillary barrier, pulmonary tissue edema, and severe hypoxemia. After the onset of typical injury symptoms, some sepsis patients may rapidly deteriorate within a short period, progressing to ARDS, thus affecting their prognosis[10]. Venous blood samples are the most readily available and suitable for laboratory testing. Among various specimens, patient serum is primarily used as a biological specimen for accurately and rapidly assessing the severity of sepsis.

In sepsis, damage to endothelial cells leads to activating inflammatory cells and platelets. Activated inflammatory cells release a large number of inflammatory and cellular factors through a cascade reaction, promoting endothelial cell apoptosis and monocyte release of chemokines. Platelets and white blood cells interact in the microcirculation of damaged tissues, forming platelet-white blood cell aggregates. This process further accelerates the release of inflam-

Table 4 Area under the curve for various parameters

Parameter	AUC	SE	*P* value	95%CI	
				Upper limit	Lower limit
PMAs	0.957	0.022	< 0.05	0.914	0.974
APACHE II	0.93	0.021	< 0.05	0.872	0.981

APACHE II: Acute Physiology and Chronic Health Evaluation II Scores; PMAs: Platelet-mononuclear cell aggregates; AUC: Area under the curve.

Table 5 Diagnostic values for various parameters

Parameter	Cutoff value	Sensitivity	Specificity	Positive predictive value	Negative predictive value
PMAs	8.418	0.819	0.947	0.956	0.819
APACHE II	17.115	0.837	0.844	0.829	0.877

APACHE II: Acute Physiology and Chronic Health Evaluation II Scores; PMAs: Platelet-mononuclear cell aggregates.

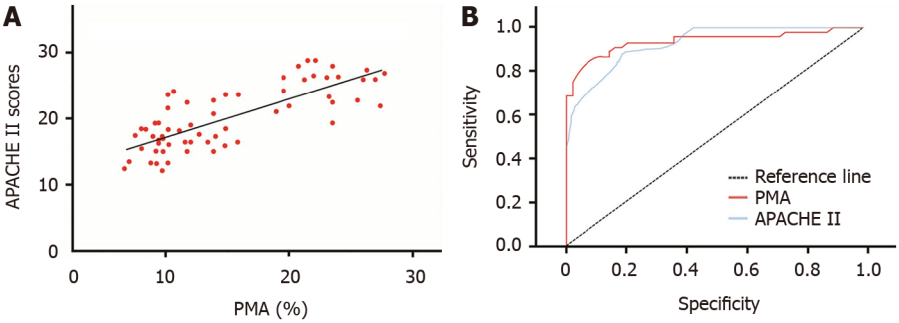

DOI: 10.12998/wjcc.v12.i5.966

Figure 1 Platelet-mononuclear cell aggregates and Acute Physiology and Chronic Health Evaluation II scores. A: Linear correlation between platelet-mononuclear cell aggregates and Acute Physiology and Chronic Health Evaluation (APACHE) II scores; B: Diagnostic Value of platelet-mononuclear cell aggregates and APACHE II Scores for acute respiratory distress syndrome. APACHE II: Acute Physiology and Chronic Health Evaluation II Scores; PMA: Platelet-mononuclear cell aggregate.

matory factors such as interleukin and tumor necrosis factor-alpha[11]. The worsening of the inflammatory response leads to endothelial cell swelling, necrosis and shedding, further worsening the patient's condition. Therefore, platelet-white blood cell aggregates in the serum play a crucial intermediary role between platelet activation and inflammatory response.

The results of this study indicate that the serum levels of PMAs in sepsis patients with ARDS were significantly higher than those in sepsis patients without ARDS ($P < 0.05$), confirming the utility of PMAs as a beneficial indicator for diagnosing sepsis with ARDS. The APACHE II scoring system is commonly used to assess the severity and prognosis of critically ill patients[12], have confirmed the application of the APACHE II score in predicting mortality in sepsis patients. The current study demonstrates that the APACHE II scores of sepsis patients with ARDS were significantly higher than those of sepsis patients without ARDS and were positively correlated with serum PMAs levels ($P < 0.05$). This further confirms the clinical importance of serum PMAs in the early diagnosis of sepsis with ARDS.

Study limitation

One limitation of this study is the relatively small sample size, with a total of 72 hospitalized patients included in the analysis. The limited sample size may affect the generalizability of the findings to a broader population. Additionally, the study focused on patients from a single hospital, which may introduce institutional biases and limit the external validity of the results. Including a more diverse and larger sample from multiple medical centers could enhance the robustness and applicability of the study findings. Furthermore, the retrospective nature of the study poses inherent limitations. The reliance on historical data collected from medical records may lead to incomplete or missing information. The retrospective design also prevents the researchers from controlling the data collection process, potentially introducing biases in the selection of patients or in the measurement of variables. A prospective study with a carefully designed protocol and standardized data collection procedures would provide stronger evidence and allow for better control of confounding variables. The study primarily focused on the expression of PMAs in the serum as a potential biomarker for

sepsis complicated by ARDS. While the findings suggest a significant association, the study does not explore the underlying mechanisms or causality between elevated PMAs levels and the development of ARDS in sepsis patients. Further mechanistic studies are needed to elucidate the pathways through which PMAs may contribute to the pathogenesis of ARDS in sepsis. Finally, the study does not address the specificity of PMAs as a biomarker, and its utility in distinguishing sepsis with ARDS from other conditions that may present with similar clinical manifestations. Future research should explore the specificity and sensitivity of PMAs in differentiating various respiratory and systemic disorders to better understand its diagnostic value in a broader clinical context.

CONCLUSION

In conclusion, the elevation of serum PMAs levels is closely associated with the release of inflammatory factors. Although the exact mechanism of PMAs still requires further research, current studies suggest that its changes have important clinical significance in early diagnosing sepsis with ARDS. Therefore, PMAs may serve as one of the biomarkers for early diagnosing sepsis with ARDS.

ARTICLE HIGHLIGHTS

Research background

The diagnosis of sepsis combined with acute respiratory distress syndrome (ARDS) has increased owing to the enhanced awareness among medical professionals and the continuous development of modern medical technologies, while early diagnosis of ARDS still lacks specific biomarkers. One of the main pathogenic mechanisms of sepsis-associated ARDS involves the actions of various pathological injuries and inflammatory factors, such as platelet and white blood cells activation, leading to an increase of surface adhesion molecules. These adhesion molecules further form platelet-white blood cell aggregates, including platelet-mononuclear cell aggregates (PMAs). PMAs has been identified as one of the markers of platelet activation, here we hypothesize that PMAs might play a potential biomarker for the early diagnosis of this complication.

Research motivation

To investigate whether PMAs could be a potential biomarker for the early diagnosis of sepsis combined with ARDS.

Research objectives

To investigate the clinical significance of PMAs in patients with sepsis complicated by ARDS.

Research methods

72 patients diagnosed with sepsis were enrolled in the study between March 2019 and March 2022. Among them, 30 patients with sepsis and ARDS formed the study group, while 42 sepsis patients without ARDS comprised the control group. After diagnosis, venous blood samples were immediately collected from all patients. Flow cytometry was employed to analyze the expression of PMAs, platelet neutrophil aggregates (PNAs), and Platelet Aggregates (PLyAs) in the serum. Additionally, the Acute Physiology and Chronic Health Evaluation (APACHE) II score was calculated for each patient, and Receiver operating characteristic curves were generated to assess diagnostic value.

Research results

The levels of PNAs and PLyAs in the serum of the study group were higher than those in the control group, but the difference was not statistically significant ($P > 0.05$). However, the expression of PMAs in the serum of the study group was significantly upregulated ($P < 0.05$) and positively correlated with the APACHE II score (r=0.671, $P < 0.05$). When using PMAs as a diagnostic indicator, the area under the curve value was 0.957, indicating a high diagnostic value ($P < 0.05$). Furthermore, the optimal cutoff value was 8.418%, with a diagnostic sensitivity of 0.819 and specificity of 0.947.

Research conclusions

The serum levels of PMAs significantly increase in patients with sepsis and ARDS, which might have the potential to become a new biomarker for clinically diagnosing sepsis complicated by ARDS.

Research perspectives

Our study provides a new method for the early diagnosis of sepsis combined with ARDS, which is the detection of serum PMAs. More samples should be enrolled to confirm this method in the future study.

FOOTNOTES

Author contributions: Huang CM performed the study; Li JJ analyzed the data; Wei WK designed the research and wrote the manuscript;

All authors have read and approve the final manuscript.

Institutional review board statement: The study was reviewed and approved by the Institutional Review Board of the Second People's Hospital of Haining City.

Informed consent statement: All study participants, or their legal guardian, provided informed written consent prior to study enrollment.

Conflict-of-interest statement: All the authors report no relevant conflicts of interest for this article.

Data sharing statement: No additional data are available.

STROBE statement: The authors have read the STROBE Statement—checklist of items, and the manuscript was prepared and revised according to the STROBE Statement—checklist of items.

Country/Territory of origin: China

ORCID number: Chong-Min Huang 0009-0001-7015-3577.

S-Editor: Li L
L-Editor: A
P-Editor: Li L

REFERENCES

1 **Hu Q**, Hao C, Tang S. From sepsis to acute respiratory distress syndrome (ARDS): emerging preventive strategies based on molecular and genetic researches. *Biosci Rep* 2020; **40** [PMID: 32319516 DOI: 10.1042/BSR20200830]
2 **Li X**, Jamal M, Guo P, Jin Z, Zheng F, Song X, Zhan J, Wu H. Irisin alleviates pulmonary epithelial barrier dysfunction in sepsis-induced acute lung injury *via* activation of AMPK/SIRT1 pathways. *Biomed Pharmacother* 2019; **118**: 109363 [PMID: 31545277 DOI: 10.1016/j.biopha.2019.109363]
3 **Chen Y**, Qiu C, Cai W. Identification of key immune genes for sepsis-induced ARDS based on bioinformatics analysis. *Bioengineered* 2022; **13**: 697-708 [PMID: 34898369 DOI: 10.1080/21655979.2021.2012621]
4 **Le Joncour A**, Biard L, Vautier M, Bugaut H, Mekinian A, Maalouf G, Vieira M, Marcelin AG, Rosenzwajg M, Klatzmann D, Corvol JC, Paccoud O, Carillion A, Salem JE, Cacoub P, Boulaftali Y, Saadoun D. Neutrophil-Platelet and Monocyte-Platelet Aggregates in COVID-19 Patients. *Thromb Haemost* 2020; **120**: 1733-1735 [PMID: 33124027 DOI: 10.1055/s-0040-1718732]
5 **Hottz ED**, Azevedo-Quintanilha IG, Palhinha L, Teixeira L, Barreto EA, Pão CRR, Righy C, Franco S, Souza TML, Kurtz P, Bozza FA, Bozza PT. Platelet activation and platelet-monocyte aggregate formation trigger tissue factor expression in patients with severe COVID-19. *Blood* 2020; **136**: 1330-1341 [PMID: 32678428 DOI: 10.1182/blood.2020007252]
6 **Rhodes A**, Evans LE, Alhazzani W, Levy MM, Antonelli M, Ferrer R, Kumar A, Sevransky JE, Sprung CL, Nunnally ME, Rochwerg B, Rubenfeld GD, Angus DC, Annane D, Beale RJ, Bellinghan GJ, Bernard GR, Chiche JD, Coopersmith C, De Backer DP, French CJ, Fujishima S, Gerlach H, Hidalgo JL, Hollenberg SM, Jones AE, Karnad DR, Kleinpell RM, Koh Y, Lisboa TC, Machado FR, Marini JJ, Marshall JC, Mazuski JE, McIntyre LA, McLean AS, Mehta S, Moreno RP, Myburgh J, Navalesi P, Nishida O, Osborn TM, Perner A, Plunkett CM, Ranieri M, Schorr CA, Seckel MA, Seymour CW, Shieh L, Shukri KA, Simpson SQ, Singer M, Thompson BT, Townsend SR, Van der Poll T, Vincent JL, Wiersinga WJ, Zimmerman JL, Dellinger RP. Surviving Sepsis Campaign: International Guidelines for Management of Sepsis and Septic Shock: 2016. *Intensive Care Med* 2017; **43**: 304-377 [PMID: 28101605 DOI: 10.1007/s00134-017-4683-6]
7 **ARDS Definition Task Force**, Ranieri VM, Rubenfeld GD, Thompson BT, Ferguson ND, Caldwell E, Fan E, Camporota L, Slutsky AS. Acute respiratory distress syndrome: the Berlin Definition. *JAMA* 2012; **307**: 2526-2533 [PMID: 22797452 DOI: 10.1001/jama.2012.5669]
8 **Chiu C**, Legrand M. Epidemiology of sepsis and septic shock. *Curr Opin Anaesthesiol* 2021; **34**: 71-76 [PMID: 33492864 DOI: 10.1097/ACO.0000000000000958]
9 **Huang M**, Cai S, Su J. The Pathogenesis of Sepsis and Potential Therapeutic Targets. *Int J Mol Sci* 2019; **20** [PMID: 31671729 DOI: 10.3390/ijms20215376]
10 **Li W**, Li D, Chen Y, Abudou H, Wang H, Cai J, Wang Y, Liu Z, Liu Y, Fan H. Classic Signaling Pathways in Alveolar Injury and Repair Involved in Sepsis-Induced ALI/ARDS: New Research Progress and Prospect. *Dis Markers* 2022; **2022**: 6362344 [PMID: 35726235 DOI: 10.1155/2022/6362344]
11 **Liu D**, Huang SY, Sun JH, Zhang HC, Cai QL, Gao C, Li L, Cao J, Xu F, Zhou Y, Guan CX, Jin SW, Deng J, Fang XM, Jiang JX, Zeng L. Sepsis-induced immunosuppression: mechanisms, diagnosis and current treatment options. *Mil Med Res* 2022; **9**: 56 [PMID: 36209190 DOI: 10.1186/s40779-022-00422-y]
12 **Akinosoglou K**, Kapsokosta G, Mouktaroudi M, Rovina N, Kaldis V, Stefos A, Kontogiorgi M, Giamarellos-Bourboulis E, Gogos C; Hellenic Sepsis Study Group. Diabetes on sepsis outcomes in non-ICU patients: A cohort study and review of the literature. *J Diabetes Complications* 2021; **35**: 107765 [PMID: 33187869 DOI: 10.1016/j.jdiacomp.2020.107765]

World Journal of Clinical Cases

Submit a Manuscript: https://www.f6publishing.com

World J Clin Cases 2024 February 16; 12(5): 973-979

DOI: 10.12998/wjcc.v12.i5.973

ISSN 2307-8960 (online)

CASE REPORT

Left ventricular thrombosis caused cerebral embolism during venoarterial extracorporeal membrane oxygenation support: A case report

Yao-Bang Bai, Feng Zhao, Zhen-Hua Wu, Guo-Ning Shi, Nan Jiang

Specialty type: Medicine, research and experimental

Provenance and peer review: Unsolicited article; Externally peer reviewed.

Peer-review model: Single blind

Peer-review report's scientific quality classification

Grade A (Excellent): 0
Grade B (Very good): B
Grade C (Good): C
Grade D (Fair): 0
Grade E (Poor): 0

P-Reviewer: Arboix A, Spain

Received: October 27, 2023
Peer-review started: October 27, 2023
First decision: December 7, 2023
Revised: December 13, 2023
Accepted: January 18, 2024
Article in press: January 18, 2024
Published online: February 16, 2024

Yao-Bang Bai, Zhen-Hua Wu, Guo-Ning Shi, Intensive Care Unit, Department of Cardiac Surgery, Tianjin Chest Hospital, Tianjin 300222, China

Feng Zhao, Nan Jiang, Department of Cardiac Surgery, Tianjin Chest Hospital, Tianjin 300222, China

Corresponding author: Zhen-Hua Wu, MD, Chief Doctor, Intensive Care Unit, Department of Cardiac Surgery, Tianjin Chest Hospital, No. 261 Taierzhuang South Road, Jinnan District, Tianjin, Tianjin 300222, China. wzh8306@sina.cn

Abstract

BACKGROUND

Venoarterial (VA) extracorporeal membrane oxygenation (ECMO), an effective short-term circulatory support method for refractory cardiogenic shock, is widely applied. However, retrospective analyses have shown that VA-ECMO-assisted cases were associated with a relatively high mortality rate of approximately 60%. Embolization in important organs caused by complications of left ventricular thrombosis (LVT) during VA-ECMO is also an important reason. Although the incidence of LVT during VA-ECMO is not high, the consequences of embolization are disastrous.

CASE SUMMARY

A 37-year-old female patient was admitted to hospital because of fever for 4 d and palpitations for 3 d. After excluding the diagnosis of coronary heart disease, we established a diagnosis of "clinically explosive myocarditis". The patient still had unstable hemodynamics after drug treatment supported by VA-ECMO, with heparin for anticoagulation. On day 4 of ECMO support, a left ventricular thrombus attached to the papillary muscle root of the mitral valve was found by transthoracic echocardiography. Left ventricular decompression was performed and ECMO was successfully removed, but the patient eventually died of multiple cerebral embolism.

CONCLUSION

LVT with high mobility during VA-ECMO may cause embolism in important organs. Therefore, a "wait and see" strategy should be avoided.

Key Words: Venoarterial extracorporeal membrane oxygenation; Left ventricular thrombosis; Cerebral embolism; Magnetic Resonance Imaging; Therapy; Case report

Core Tip: Embolism in vital organs (brain, mesenteric artery, *etc.*) caused by detachment of a left ventricular thrombosis (LVT) can lead to catastrophic consequences. We report a case of explosive myocarditis in which a LVT was attached to the papillary muscle root of the mitral valve, which resulted in massive cerebral emboli. Although a "wait and see" strategy can be adopted considering the autolytic rate of LVT and the fatal complications associated with thrombolysis and surgical thrombectomy, more aggressive treatment methods should be adopted for left ventricular thrombi with high mobility, such as transcatheter left ventricular thrombolysis or surgical thrombectomy.

Citation: Bai YB, Zhao F, Wu ZH, Shi GN, Jiang N. Left ventricular thrombosis caused cerebral embolism during venoarterial extracorporeal membrane oxygenation support: A case report. *World J Clin Cases* 2024; 12(5): 973-979
URL: https://www.wjgnet.com/2307-8960/full/v12/i5/973.htm
DOI: https://dx.doi.org/10.12998/wjcc.v12.i5.973

INTRODUCTION

Venoarterial (VA) extracorporeal membrane oxygenation (ECMO) has been widely performed in short-term circulation support for refractory cardiogenic shock, due to its low cost and mature catheterization and management compared with other mechanical circulation assist devices[1]. In the past decades, the number of VA-ECMO applications both in China and abroad has markedly increased[2,3]. However, the clinical results of VA-ECMO application are disappointing, with the overall mortality rate in patients with refractory cardiogenic shock supported by VA-ECMO reported to be 60%[4]. Although the underlying diseases leading to cardiogenic shock are serious and are the main cause of failure, some complications during the application of VA-ECMO (*e.g.*, fetal hemorrhage, thromboembolism of vital organs, severe hemolysis, infection, *etc.*) can also lead to failure. Embolism of vital organs has become one of the most frightening complications during VA-ECMO support. Thrombosis may occur in the circuit, oxygenator, pump and ventricle, with the incidence reported to range from 3% to 12%. Despite the low incidence of LVT, brain embolism caused by detachment of the thrombus can lead to catastrophic consequences[5]. It is reported that the mortality of cardioembolic stroke is higher compared with other ischemic stroke subtypes[6,7].

We report a case of explosive myocarditis in which a left ventricular thrombus attached to the papillary muscle root of the mitral valve resulted in massive cerebral emboli during VA-ECMO support.

CASE PRESENTATION

Chief complaints

The 37-year-old female patient was admitted to hospital mainly due to fever for 4 d and palpitations for 3 d.

History of present illness

The patient developed a fever 4 d before admission and continued to have intermittent fever after symptomatic treatment. Three days before admission, the patient had palpitations accompanied by chest tightness and fatigue and was admitted to the emergency department of our hospital.

History of past illness

The patient had a history of hyperthyroidism and was treated with iodine-131, and was currently treated with oral levothyroxine tablets for hypothyroidism.

Personal and family history

The patient denied any family history of cardiac disease.

Physical examination

On physical examination, vital signs were as follows: Body temperature, 37.1°C; blood pressure, 90/71 mmHg; heart rate, 95 bpm and respiratory rate, 14 breaths/min. Cardiac auscultation revealed arrhythmia, decreased heart sound, and no heart murmur heard in auscultation areas.

Laboratory examinations

Myocardium zymogram showed the following: Creatine kinase 466 U/L, creatine kinase isoenzyme 41 U/L, Troponin T 2.66 μg/L and N-terminal pro B-type natriuretic peptide 6599 pg/mL. Thyroid function tests demonstrated free triiodothyronine 2.13 pmol/L, free tetraiodothyronine 15.91 pmol/L and thyroid stimulating hormone 3.88 μIU/mL.

No abnormalities were found in routine blood and urine analyses.

Imaging examinations

Cardiac ultrasound in the emergency room revealed the following: Left atrium (LA) 32 mm, left ventricle (LV) 47 mm, right atrium 38 mm, right ventricle 16 mm, pulmonary arterial pressure 30 mmHg, LV ejection fraction (LVEF) 62%, and the contraction and diastolic function of the left heart were normal.

Re-examination with bedside ultrasound showed: LA 33 mm, LV 46 mm, LVEF 35-39%, left ventricular wall thickening, extensive myocardial motility reduction, and reduced left heart function.

FINAL DIAGNOSIS

Combined with the patient's medical history and laboratory examinations, the final diagnosis was explosive myocarditis and arrhythmia.

TREATMENT

After admission, the patient was given myocardial nutrition, volume supplementation, dopamine cardiac strengthening, and norepinephrine vasopressor therapy. The patient's condition progressed rapidly, and 13 h after admission, she developed a third-degree atrioventricular (AV) block with a ventricular rate of approximately 60 bpm, blood pressure of 75/52 mmHg, and distal dampness. Rehydration fluids and high-dose vasoactive drugs continued to maintain circulation (vasoactive drug score: 30), and blood gas analysis showed metabolic acidosis combined with respiratory alkalosis. Blood lactic acid level was 2.5 mmol/L. With the assistance of an emergency endotracheal intubation ventilator, percutaneous ECMO implantation was performed at the bedside, using VA-mode, and a flow rate of 3.5 L/min. Heparin anticoagulation was administered during ECMO to maintain activated coagulation time 180-200 s; chest X-ray and echocardiography were monitored daily. Following implantation of ECMO, the patient had a heart rhythm of third-degree AV block, with a ventricular rate of about 50, occasional ventricular tachycardia and ventricular fibrillation. The cardiologist was contacted for temporary pacemaker support. Echocardiography results after 4 d of ECMO support showed a moderate intensity echoic mass of 2.4 cm 1.5 cm thought to be a left ventricular thrombus attached to the papillary muscle root of the mitral valve with a flow rate of 0.5 m/s (Figure 1); chest X-ray showed increased pulmonary edema. At this time, the patient was considered to have developed a hemodynamic change specific to peripheral VA-ECMO support of left ventricular dilation. Accordingly, the following therapeutic strategies were applied: the auxiliary flow was reduced to 3 L/min, maintaining the negative balance of the inflow and outflow, epinephrine was added to strengthen the heart, positive end-expiratory pressure was increased to improve right ventricular drainage, and Intra-Aortic Balloon Pump support was given to promote aortic valve opening. The patient's cardiac function gradually improved, and the pulmonary edema gradually subsided. On the 7th day of ECMO support, bedside ultrasound showed: LA 32 mm, LV 55 mm, LVEF 30%, the thrombus sound shadow in the heart was not obvious (Figure 2), and there was no abnormality in the patient's neurological examination at this time.

OUTCOME AND FOLLOW-UP

On the 9th day of ECMO support, the autonomic rhythm had recovered, cardiac function continued to improve, pulmonary edema was further reduced, and no abnormalities were found in the neurological examination; thus, ECMO support was removed. The patient then gradually recovered. Twelve days after admission, the patient suddenly lost consciousness, and computed tomography showed multiple cerebral emboli (Figure 3). The patient's family members gave up further treatment and the patient was discharged from hospital.

DISCUSSION

There are limited data on LVT in patients requiring VA-ECMO. One report showed a series of patients (n = 11) who developed LVT due to ischemic cardiomyopathy with cardiogenic shock, which accounted for 3.1% of the center's total VA-ECMO experience[8]. LVT is a serious complication of VA-ECMO. Embolization of vital organs such as the brain, kidneys, and mesentery caused by thrombectomy can have fatal consequences, leading to the failure of ECMO support[9, 10]. The pathophysiology of LVT formation during VA-ECMO support is complex and is the result of multiple factors. Severely impaired cardiac function, left ventricular dilation induced by VA-ECMO, and left ventricular blood stasis are the dominant factors associated with thrombosis. The hypercoagulable state of patients and the inadequacy of current

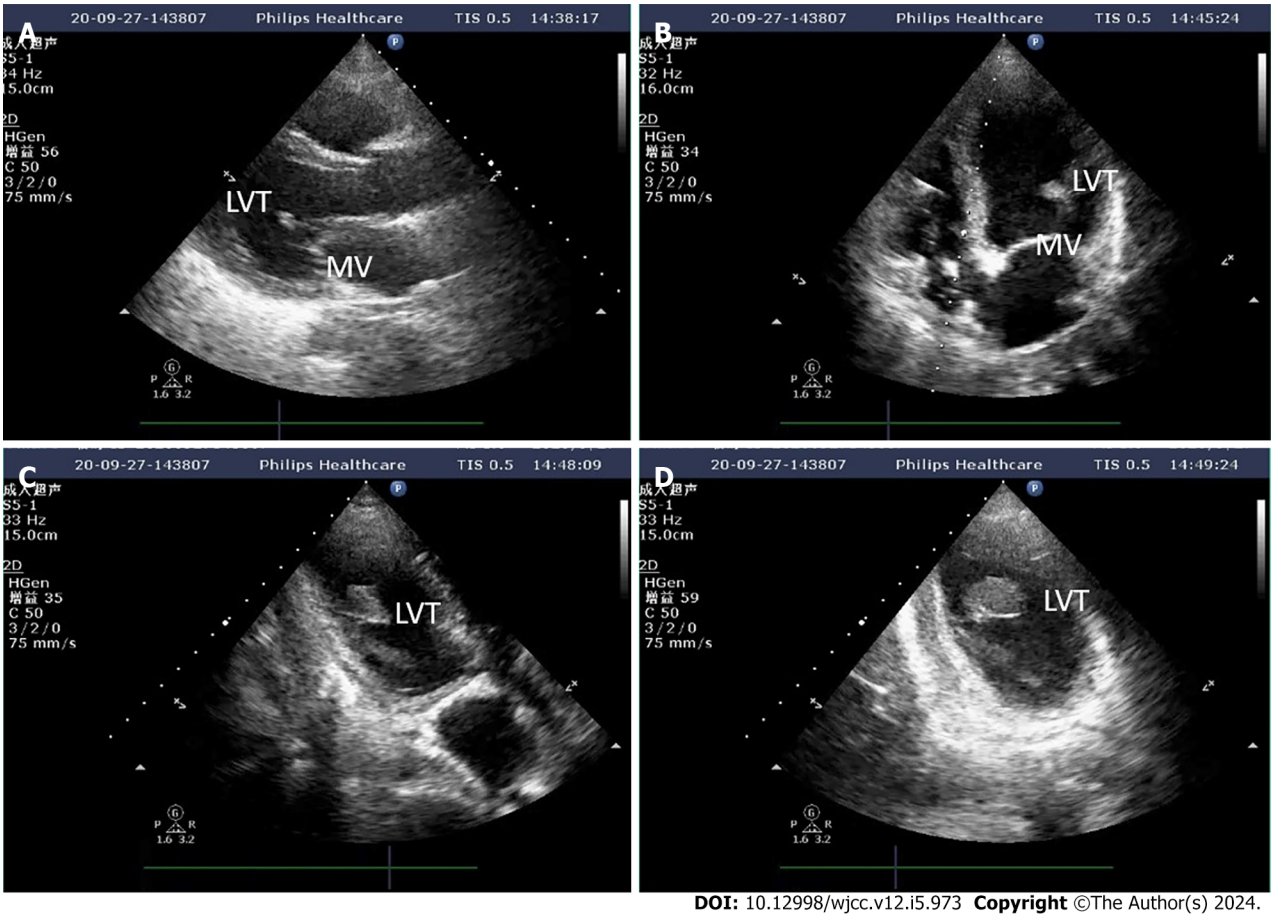

DOI: 10.12998/wjcc.v12.i5.973

Figure 1 Left ventricular thrombosis indicated by transthoracic ultrasonography. A: The long axis of the left ventricle (LV) beside the sternum indicates suspected thrombosis attached to the mitral valve; B: Apical four-chamber heart suggests suspicious attachment of thrombus to the mitral valve; C: The long axis of the LV at the apex of the heart clearly shows thrombus attached to the papillary muscle root; D: Irregular sections also confirm thrombus attachment to the papillary muscle root.

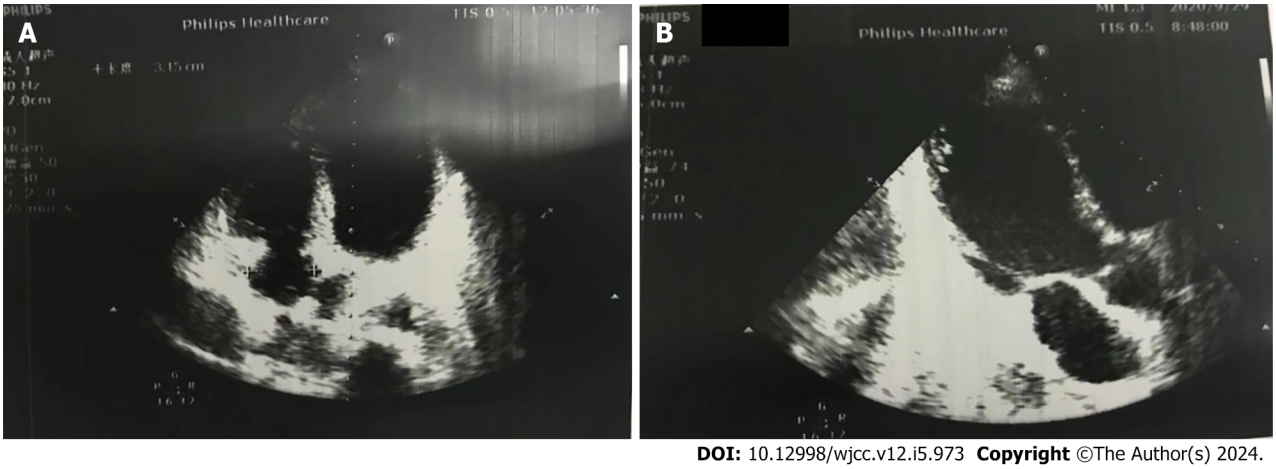

DOI: 10.12998/wjcc.v12.i5.973

Figure 2 The thrombus sound shadow in the heart was not obvious on the apical four-chamber heart section and the long axis of the left ventricle section. A: Apical four-chamber heart suggests no thrombus; B: The thrombus was not detected on the long axis of the left ventricle section.

anticoagulation therapy also play an important role in thrombosis.

Although transthoracic echocardiography (TTE) has been widely used in the diagnosis of LVT, it is greatly affected by the patient's acoustic window (small intercostal space, large body size, chest deformities, or lung disease) and position [11]. In this case, the initial ultrasound images suggested that the thrombus was attached to the mitral valve, but after repeated multi-sectional examinations, the thrombus was eventually found to be attached to the root of the papillary muscle. A possible reason for this is that transthoracic ultrasound is a two-dimensional image and the patient was in the

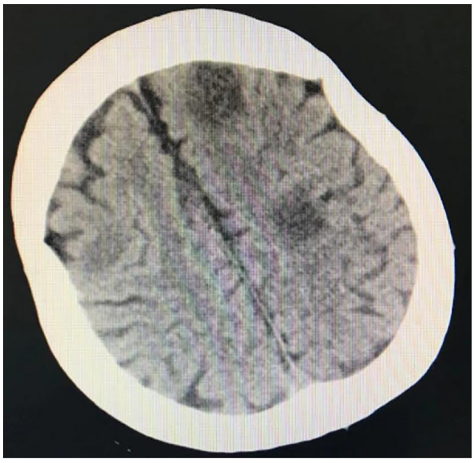

DOI: 10.12998/wjcc.v12.i5.973

Figure 3 Computed tomography revealed multiple low-density lesions in both hemispheres of the brain, which were cerebral emboli.

supine position, so judgement of the overall morphology of the thrombus was poor.

Currently, there are no guidelines or expert consensus recommendations for ECMO support for LVT treatment in patients[12,13]. Some therapeutic options reported include improving anticoagulant strength, surgical thrombectomy and thrombolytic therapy. Heparin: According to most reports[14,15], anticoagulation with heparin can reduce the incidence of LVT, but has no effect on thrombolysis. Surgery: Surgical resection of the LVT is an option when undergoing other open-heart surgeries or transitioning from peripheral VA-ECMO intubation to central intubation[16]. However, the risk-benefit ratio should also be considered, as most patients with LVT have a severely reduced LVEF, which has higher perioperative complications and mortality if patients undergo thrombectomy. Therefore, in the absence of other indications for emergency surgery, surgical thrombectomy should be carefully considered, as the risks for patients far outweigh the benefits[17]. Thrombolysis: Multiple studies have shown that fibrinolytic solvents can dissolve LVT, but the risk of this treatment is high (thrombosis can lead to embolism[18,19]). In one study, four patients with LVT were given intravenous fibrinolytic drugs, and after 8 to 12 h, the size of the thrombus was significantly reduced, and the thrombus disappeared completely in 2 of these patients; but the mobility of the thrombus also increased significantly. The remaining 2 patients in the study developed a severe systemic thromboembolic event. Simultaneous administration of thrombolytics increases the risk of bleeding[15].

In addition to thrombosis, bleeding at the puncture site or surgical site is also a common cause of death in VA-ECMO patients, and thrombolysis for VA-ECMO patients is a challenge[20]. Sangalli *et al*[21] reported a new approach for LVT, in which the patients' LVT was completely dissolved 24 h after a catheterized injection of tenecteplase into the LV, and only moderate bleeding occurred. However, although a case report can provide us with new ideas for the treatment of LVT during VA-ECMO support, the therapeutic effect and related complications need to be studied in large-scale clinical trials.

It is reported that approximately 20%-40% of LVTs resolve spontaneously without anticoagulation with restoration of cardiac function[22,23]. Velangi *et al*[24] showed that the morphology, size and mobility of LVT can change, and there was no obvious correlation between the morphological characteristics and the occurrence of thromboembolism. Lemaître *et al*[17] believed that a "wait-and-see" strategy seems to be a safe and reasonable management plan for LVT in patients with heart failure. Therefore, we selected active conservative treatment measures: (1) To improve the strength of anticoagulation; and (2) to promote the development of aortic valves and improve blood stasis by giving positive inotropic drugs and reducing support flow. At the same time, we adopted a "wait-and-see" strategy and insisted on daily TTE monitoring.

In this case, the patient still had thromboembolism even though ultrasound suggested thrombolysis. This may be due to poor sensitivity of conventional ultrasound to LVT, and the thrombus was not found during routine examination. Therefore, such patients should be examined by magnetic resonance imaging (MRI) after ECMO removal[25] to exclude the existence of thrombosis, and regular anticoagulation should be given according to relevant guidelines if thrombosis is found during the examination[26].

This study had the following limitations: First, an MRI examination was not performed after the removal of ECMO support to confirm the complete disappearance of the LVT. Second, no laboratory tests for hematologic diseases was conducted to rule out stroke, as Arboix *et al*[27] reported that hematological disorders are an easily overlooked cause of acute stroke.

Future research should focus on the overall prognosis and treatment of patients with LVT during ECMO support, and develop relevant treatment guidelines or expert consensus to improve the outcome of ECMO support.

CONCLUSION

The occurrence of LVT during VA-ECMO is the result of multiple factors and has a high mortality rate. Management of LVT is a major challenge for clinicians. Although a "wait and see" strategy can be adopted considering the autolytic rate of LVT and the fatal complications associated with thrombolysis and surgical thrombectomy, more aggressive treatment methods for left ventricular thrombi with high mobility should be attempted, such as transcatheter left ventricular thrombolysis or surgical thrombectomy. In clinical practice, we should pay attention to the patient monitoring and management during operation, and actively prevent and treat left ventricular blood stasis. Continuous improvement of devices to improve biocompatibility and reduce the activation of coagulation and inflammatory reactions is required. Only when each element of ECMO is optimized can the prognosis of patients ultimately be improved.

FOOTNOTES

Author contributions: Zhao F, Shi GN and Jiang N contributed to acquisition, analysis and interpretation of the data; all authors participated in drafting the manuscript; Jiang N and Zhao F critically revised the manuscript; all authors read and approved the final version of the manuscript. Bai YN and Zhao F give substantial contributions to the conception or the design of the manuscript.

Supported by Tianjin Health Science and Technology Project, No. ZC20147.

Informed consent statement: Informed written consent was obtained from the patient for publication of this report and any accompanying images.

Conflict-of-interest statement: The authors declare that they have no conflict of interest to disclose.

CARE Checklist (2016) statement: The authors have read the CARE Checklist (2016), and the manuscript was prepared and revised according to the CARE Checklist (2016).

Country/Territory of origin: China

ORCID number: Yao-Bang Bai 0009-0009-4107-8000; Zhen-Hua Wu 0009-0007-9695-6080.

S-Editor: Lin C
L-Editor: A
P-Editor: Yu HG

REFERENCES

1 **Rao P**, Khalpey Z, Smith R, Burkhoff D, Kociol RD. Venoarterial Extracorporeal Membrane Oxygenation for Cardiogenic Shock and Cardiac Arrest. *Circ Heart Fail* 2018; **11**: e004905 [PMID: 30354364 DOI: 10.1161/CIRCHEARTFAILURE.118.004905]
2 **Whitman GJ**. Extracorporeal membrane oxygenation for the treatment of postcardiotomy shock. *J Thorac Cardiovasc Surg* 2017; **153**: 95-101 [PMID: 27666787 DOI: 10.1016/j.jtcvs.2016.08.024]
3 **Chinese Society of Extracorporeal Circulation**. White book of Chinese cardiovascular surgery and extracorporeal circulation in 2019. *Zhongguo Tiwai Xunhuan Zazhi* 2020; **18**: 193-196
4 **Becher PM**, Schrage B, Sinning CR, Schmack B, Fluschnik N, Schwarzl M, Waldeyer C, Lindner D, Seiffert M, Neumann JT, Bernhardt AM, Zeymer U, Thiele H, Reichenspurner H, Blankenberg S, Twerenbold R, Westermann D. Venoarterial Extracorporeal Membrane Oxygenation for Cardiopulmonary Support. *Circulation* 2018; **138**: 2298-2300 [PMID: 30571518 DOI: 10.1161/CIRCULATIONAHA.118.036691]
5 **Williams B**, Bernstein W. Review of Venoarterial Extracorporeal Membrane Oxygenation and Development of Intracardiac Thrombosis in Adult Cardiothoracic Patients. *J Extra Corpor Technol* 2016; **48**: 162-167 [PMID: 27994255 DOI: 10.1051/ject/201648162]
6 **Kamel H**, Healey JS. Cardioembolic Stroke. *Circ Res* 2017; **120**: 514-526 [PMID: 28154101 DOI: 10.1161/CIRCRESAHA.116.308407]
7 **Arboix A**, Alió J. Cardioembolic stroke: clinical features, specific cardiac disorders and prognosis. *Curr Cardiol Rev* 2010; **6**: 150-161 [PMID: 21804774 DOI: 10.2174/157340310791658730]
8 **Weber C**, Deppe AC, Sabashnikov A, Slottosch I, Kuhn E, Eghbalzadeh K, Scherner M, Choi YH, Madershahian N, Wahlers T. Left ventricular thrombus formation in patients undergoing femoral veno-arterial extracorporeal membrane oxygenation. *Perfusion* 2018; **33**: 283-288 [PMID: 29172999 DOI: 10.1177/0267659117745369]
9 **Huerter M**, Govostis D, Ellenby M, Smith-Singares E. Acute Bowel Ischemia Associated with Left Ventricular Thrombus and Arteriovenous Extracorporeal Membrane Oxygenation. *J Extra Corpor Technol* 2018; **50**: 58-60 [PMID: 29559756 DOI: 10.1051/ject/201850058]
10 **Takei Y**, Ejima Y, Toyama H, Takei K, Ota T, Yamauchi M. A case of a giant cell myocarditis that developed massive left ventricular thrombus during percutaneous cardiopulmonary support. *JA Clin Rep* 2016; **2**: 41 [PMID: 29492436 DOI: 10.1186/s40981-016-0067-0]
11 **Weinsaft JW**, Kim HW, Shah DJ, Klem I, Crowley AL, Brosnan R, James OG, Patel MR, Heitner J, Parker M, Velazquez EJ, Steenbergen C,

Judd RM, Kim RJ. Detection of left ventricular thrombus by delayed-enhancement cardiovascular magnetic resonance prevalence and markers in patients with systolic dysfunction. *J Am Coll Cardiol* 2008; **52**: 148-157 [PMID: 18598895 DOI: 10.1016/j.jacc.2008.03.041]

12 **Habash F**, Vallurupalli S. Challenges in management of left ventricular thrombus. *Ther Adv Cardiovasc Dis* 2017; **11**: 203-213 [PMID: 28589748 DOI: 10.1177/1753944717711139]

13 **Cruz Rodriguez JB**, Okajima K, Greenberg BH. Management of left ventricular thrombus: a narrative review. *Ann Transl Med* 2021; **9**: 520 [PMID: 33850917 DOI: 10.21037/atm-20-7839]

14 **Kontny F**, Dale J, Abildgaard U, Pedersen TR. Randomized trial of low molecular weight heparin (dalteparin) in prevention of left ventricular thrombus formation and arterial embolism after acute anterior myocardial infarction: the Fragmin in Acute Myocardial Infarction (FRAMI) Study. *J Am Coll Cardiol* 1997; **30**: 962-969 [PMID: 9316525 DOI: 10.1016/s0735-1097(97)00258-1]

15 **Delewi R**, Zijlstra F, Piek JJ. Left ventricular thrombus formation after acute myocardial infarction. *Heart* 2012; **98**: 1743-1749 [PMID: 23151669 DOI: 10.1136/heartjnl-2012-301962]

16 **Bolcal C**, Kadan M, Kubat E, Erol G, Doğancı S. Surgical treatment of a left ventricular apical thrombus *via* robotic surgery. *J Card Surg* 2019; **34**: 216-218 [PMID: 30785219 DOI: 10.1111/jocs.14000]

17 **Lemaître AI**, Picard F, Maurin V, Faure M, Dos Santos P, Girerd N. Clinical profile and midterm prognosis of left ventricular thrombus in heart failure. *ESC Heart Fail* 2021; **8**: 1333-1341 [PMID: 33629818 DOI: 10.1002/ehf2.13211]

18 **Garcia A**, Gander JW, Gross ER, Reichstein A, Sheth SS, Stolar CJ, Middlesworth W. The use of recombinant tissue-type plasminogen activator in a newborn with an intracardiac thrombus developed during extracorporeal membrane oxygenation. *J Pediatr Surg* 2011; **46**: 2021-2024 [PMID: 22008344 DOI: 10.1016/j.jpedsurg.2011.06.039]

19 **McCarthy CP**, Murphy S, Venkateswaran RV, Singh A, Chang LL, Joice MG, Rivero JM, Vaduganathan M, Januzzi JL Jr, Bhatt DL. Left Ventricular Thrombus: Contemporary Etiologies, Treatment Strategies, and Outcomes. *J Am Coll Cardiol* 2019; **73**: 2007-2009 [PMID: 30846340 DOI: 10.1016/j.jacc.2019.01.031]

20 **Murphy DA**, Hockings LE, Andrews RK, Aubron C, Gardiner EE, Pellegrino VA, Davis AK. Extracorporeal membrane oxygenation-hemostatic complications. *Transfus Med Rev* 2015; **29**: 90-101 [PMID: 25595476 DOI: 10.1016/j.tmrv.2014.12.001]

21 **Sangalli F**, Greco G, Galbiati L, Formica F, Calcinati S, Avalli L. Regional thrombolysis with tenecteplase during extracorporeal membrane oxygenation: a new approach for left ventricular thrombosis. *J Card Surg* 2015; **30**: 541-543 [PMID: 25940057 DOI: 10.1111/jocs.12556]

22 **Spirito P**, Bellotti P, Chiarella F, Domenicucci S, Sementa A, Vecchio C. Prognostic significance and natural history of left ventricular thrombi in patients with acute anterior myocardial infarction: a two-dimensional echocardiographic study. *Circulation* 1985; **72**: 774-780 [PMID: 4028378 DOI: 10.1161/01.cir.72.4.774]

23 **Stratton JR**, Nemanich JW, Johannessen KA, Resnick AD. Fate of left ventricular thrombi in patients with remote myocardial infarction or idiopathic cardiomyopathy. *Circulation* 1988; **78**: 1388-1393 [PMID: 3191593 DOI: 10.1161/01.cir.78.6.1388]

24 **Velangi PS**, Choo C, Chen KA, Kazmirczak F, Nijjar PS, Farzaneh-Far A, Okasha O, Akçakaya M, Weinsaft JW, Shenoy C. Long-Term Embolic Outcomes After Detection of Left Ventricular Thrombus by Late Gadolinium Enhancement Cardiovascular Magnetic Resonance Imaging: A Matched Cohort Study. *Circ Cardiovasc Imaging* 2019; **12**: e009723 [PMID: 31707810 DOI: 10.1161/CIRCIMAGING.119.009723]

25 **Delewi R**, Nijveldt R, Hirsch A, Marcu CB, Robbers L, Hassell ME, de Bruin RH, Vleugels J, van der Laan AM, Bouma BJ, Tio RA, Tijssen JG, van Rossum AC, Zijlstra F, Piek JJ. Left ventricular thrombus formation after acute myocardial infarction as assessed by cardiovascular magnetic resonance imaging. *Eur J Radiol* 2012; **81**: 3900-3904 [PMID: 22995173 DOI: 10.1016/j.ejrad.2012.06.029]

26 **O'Gara PT**, Kushner FG, Ascheim DD, Casey DE Jr, Chung MK, de Lemos JA, Ettinger SM, Fang JC, Fesmire FM, Franklin BA, Granger CB, Krumholz HM, Linderbaum JA, Morrow DA, Newby LK, Ornato JP, Ou N, Radford MJ, Tamis-Holland JE, Tommaso CL, Tracy CM, Woo YJ, Zhao DX, Anderson JL, Jacobs AK, Halperin JL, Albert NM, Brindis RG, Creager MA, DeMets D, Guyton RA, Hochman JS, Kovacs RJ, Ohman EM, Stevenson WG, Yancy CW; American College of Cardiology Foundation/American Heart Association Task Force on Practice Guidelines. 2013 ACCF/AHA guideline for the management of ST-elevation myocardial infarction: a report of the American College of Cardiology Foundation/American Heart Association Task Force on Practice Guidelines. *Circulation* 2013; **127**: e362-e425 [PMID: 23247304 DOI: 10.1161/CIR.0b013e3182742cf6]

27 **Arboix A**, Jiménez C, Massons J, Parra O, Besses C. Hematological disorders: a commonly unrecognized cause of acute stroke. *Expert Rev Hematol* 2016; **9**: 891-901 [PMID: 27367035 DOI: 10.1080/17474086.2016.1208555]

World Journal of Clinical Cases

Submit a Manuscript: https://www.f6publishing.com

World J Clin Cases 2024 February 16; 12(5): 980-987

DOI: 10.12998/wjcc.v12.i5.980

ISSN 2307-8960 (online)

CASE REPORT

Abnormal uterine bleeding successfully treated *via* ultrasound-guided microwave ablation of uterine myoma lesions: Three case reports

Toshiyuki Kakinuma, Kaoru Kakinuma, Rora Okamoto, Kaoru Yanagida, Michitaka Ohwada, Nobuhiro Takeshima

Specialty type: Obstetrics and gynecology

Provenance and peer review: Unsolicited article; Externally peer reviewed.

Peer-review model: Single blind

Peer-review report's scientific quality classification

Grade A (Excellent): 0
Grade B (Very good): B
Grade C (Good): 0
Grade D (Fair): 0
Grade E (Poor): 0

P-Reviewer: Junior JMA, Brazil

Received: September 7, 2023
Peer-review started: September 7, 2023
First decision: December 18, 2023
Revised: December 27, 2023
Accepted: January 18, 2024
Article in press: January 18, 2024
Published online: February 16, 2024

Toshiyuki Kakinuma, Kaoru Kakinuma, Rora Okamoto, Kaoru Yanagida, Michitaka Ohwada, Nobuhiro Takeshima, Department of Obstetrics and Gynecology, International University of Health and Welfare Hospital, Tochigi 329-2763, Japan

Corresponding author: Toshiyuki Kakinuma, MD, PhD, Doctor, Professor, Department of Obstetrics and Gynecology, International University of Health and Welfare Hospital, 537-3, Iguchi, Nasushiobara, Tochigi 329-2763, Japan. tokakinuma@gmail.com

Abstract

BACKGROUND

Microwave endometrial ablation (MEA) is a minimally invasive treatment method for heavy menstrual bleeding. However, additional treatment is often required after recurrence of uterine myomas treated with MEA. Additionally, because this treatment ablates the endometrium, it is not indicated for patients planning to become pregnant. To overcome these issues, we devised a method for ultrasound-guided microwave ablation of uterine myoma feeder vessels. We report three patients successfully treated for heavy menstrual bleeding, secondary to uterine myoma, using our novel method.

CASE SUMMARY

All patients had a favorable postoperative course, were discharged within 4 h, and experienced no complications. Further, no postoperative recurrence of heavy menstrual bleeding was noted. Our method also reduced the myoma's maximum diameter.

CONCLUSION

This method does not ablate the endometrium, suggesting its potential application in patients planning to become pregnant.

Key Words: Uterine myoma; Microwave; Heavy menstrual bleeding; Dysmenorrhea; Fertility preservation; Case report

Core Tip: Ultrasound-guided microwave ablation of the uterine myoma does not ablate the uterine lining, suggesting the possibility of becoming a new treatment for heavy menstrual bleeding due to uterine fibroids for those who wish to conceive in the future.

Citation: Kakinuma T, Kakinuma K, Okamoto R, Yanagida K, Ohwada M, Takeshima N. Abnormal uterine bleeding successfully treated *via* ultrasound-guided microwave ablation of uterine myoma lesions: Three case reports. *World J Clin Cases* 2024; 12(5): 980-987
URL: https://www.wjgnet.com/2307-8960/full/v12/i5/980.htm
DOI: https://dx.doi.org/10.12998/wjcc.v12.i5.980

INTRODUCTION

Uterine myomas [International Federation of Gynecology and Obstetrics (FIGO) classification system Type 0–7] are benign gynecological tumors commonly encountered in daily clinical practice; they cause abnormal uterine bleeding, especially heavy menstrual bleeding, menstrual pain, and other symptoms that impair the quality of life of women by interfering with their activities of daily living. In recent years, as conservative treatments for uterine myomas, uterine artery embolization (UAE) and magnetic resonance imaging (MRI)-guided focused ultrasound surgery (MRgFUS) have been used and have demonstrated clinical efficacy. However, these treatment strategies cannot always achieve favorable outcomes and reduced complications as those achieved *via* surgical treatment, such as *via* hysterectomy[1,2]. Microwave endometrial ablation (MEA) is a method of protein coagulation using tissue dielectric heating produced by microwave irradiation to destroy the endometrium, including its basal layer, thereby reducing its function. As a result, it aims to reduce the amount of menstrual blood or induce amenorrhea. MEA is a minimally invasive treatment method that can be chosen to avoid heavy menstrual bleeding caused by systemic diseases, therapeutic drugs, and uterine myoma or adenomyosis uteri[3-5].

Our institution introduced this treatment method on January 2016 and has reported its efficacy[3]. Although MEA is expected to be effective in treating heavy menstrual bleeding caused by uterine myomas, numerous cases have been reported where supplementary treatment was required to manage postoperative recurrences of heavy menstrual bleeding [6,7]. In addition, because this treatment method ablates the endometrium, it is not indicated for patients planning for childbirth. Therefore, ultrasound-guided microwave ablation of feeding vessels of the uterine myomas was devised to overcome these issues.

We report the case of three patients who were successfully treated with ultrasound-guided microwave ablation of the vessels feeding the uterine myomas as a new novel treatment modality for heavy menstrual bleeding caused by uterine myomas.

This study was approved by the Ethics Committee of the International University of Health and Welfare Hospital (approval number: 20-B-399, approval date: May 7, 2020).

Ablation technique: The procedure for the ablation technique of transvaginal ultrasound-guided microwave ablation of uterine myoma lesions was initiated in the lithotomy position under intravenous anesthesia. This treatment was performed under transvaginal ultrasound guidance using the Microtaze AFM-712 and a CB-type CMD-16CBL-10/350 needle-shaped deep coagulation electrode (diameter, 1.6 mm) (both are products of Alfresa Pharma Corporation, Osaka, Japan). The schema for this procedure is shown in Figure 1A. Transvaginal ultrasound tomography using the color Doppler method was performed to identify the feeding vessels to the uterine myomas (Figure 1B). The feeding vessels were directly ablated with microwaves at 2.45 GHz using the needle-shaped deep coagulation electrode (Figure 1C). Each ablation was performed under the following conditions: five sets of Microtaze output of 30 W and an ablation duration of 10 s. All feeding vessels of the uterine myomas that could be identified were ablated. A visual analog scale (VAS) with a maximum score of 10 was used to grade menstrual blood loss and dysmenorrhea.

CASE PRESENTATION

Chief complaints

Cases 1-3: Heavy menstrual bleeding, dysmenorrhea.

History of present illness

Case 1: The patient had been experiencing heavy menstrual bleeding for 5 years; however, she had never consulted a gynecologist. At the age of 41 years, she was diagnosed with chronic myelogenous leukemia, and treatment with dasatinib (tyrosine kinase inhibitor) was initiated. A decrease in platelets (17000/μL) and a worsening of heavy menstrual bleeding had been observed since the start of treatment. Massive genital bleeding was observed during the menstrual period, following which she visited our department.

Case 2: The patient had been experiencing heavy menstrual bleeding for 5 years, and it had been managed conservatively

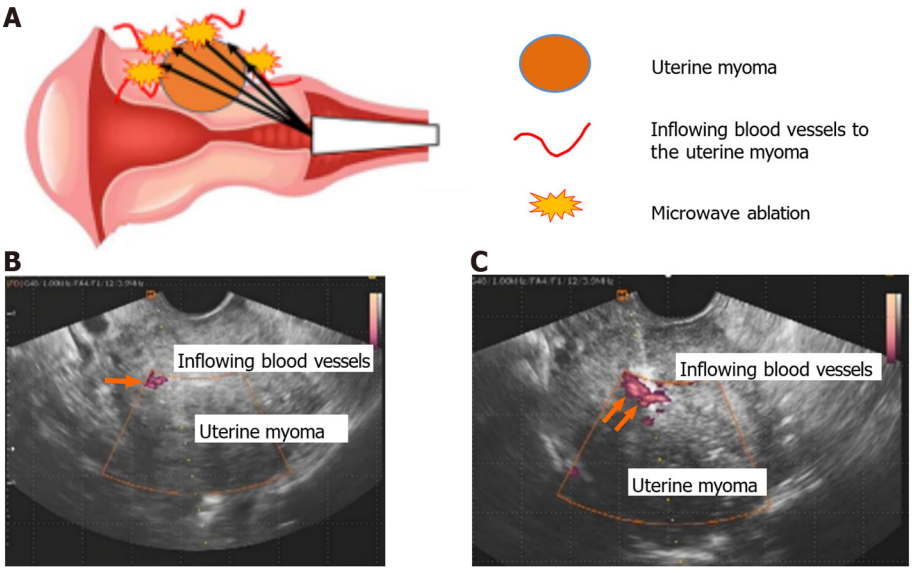

DOI: 10.12998/wjcc.v12.i5.980

Figure 1 Transvaginal ultrasound tomography. A: The schema for this procedure. Transvaginal ultrasound tomography was used to identify the feeding vessels of the uterine myomas *via* the color Doppler method. Using a needle-shaped deep coagulation electrode, the feeding vessels were directly ablated with microwaves at 2.45 GHz; B: Intraoperative transvaginal ultrasound tomography. Transvaginal ultrasound tomography using the color Doppler method was performed to identify the feeding vessels to the uterine myomas (arrow); C: A transvaginal ultrasound-guided microwave ablation of the feeding vessels to the uterine myomas using a needle-shaped deep coagulation electrode is depicted as a hyperechoic area (arrows).

via hormone therapy [the levonorgestrel-releasing intrauterine system (LNG-IUS)] for 2 years. However, as a result of symptom exacerbation, she was referred to our department for treatment.

Case 3: The patient had been experiencing heavy menstrual bleeding for 5 years and had been managed conservatively with hormone therapy (LNG-IUS) for one year. However, she was referred to our department for treatment owing to symptom exacerbation.

History of past illness

Case 1: Past medical history: Chronic myelogenous leukemia (age, 41 years).

Pregnancy and delivery history

Case 1: Pregnancy and delivery history: One pregnancy and one delivery (cesarean section at the age of 30 years).

Cases 2 and 3: Pregnancy and delivery history: Two pregnancies and two deliveries.

Cervical and endometrial cytology

Cases 1-3: Cervical and endometrial cytology: Negative for intraepithelial lesion or malignancy.

Cervical and endometrial cytology: Negative.

Imaging examinations

Case 1: Transvaginal ultrasound tomography findings: A mass of 65 mm in size was found in the anterior wall of the uterus (FIGO classification system Type 4). Pelvic MRI findings: T2-weighted sagittal image showed a mass of 65 mm in the maximum diameter in the anterior wall of the uterus with low signal intensity (Figure 2A).

Case 2: Transvaginal ultrasound tomography findings: A mass of 35 mm in the maximum diameter was found in the anterior wall of the uterus (FIGO classification system Type 4). There were no notable findings in the bilateral uterine appendages. Pelvic MRI findings: T2-weighted sagittal image showed a mass of 35 mm in the maximum diameter in the anterior wall of the uterus with low signal intensity (Figure 2B).

Case 3: Transvaginal ultrasound tomography findings: Masses of 22 mm and 15 mm in the maximum diameter were found in the anterior wall of the uterus (FIGO classification system Type 4 and 5). There were no notable findings in the bilateral uterine appendages. Pelvic MRI findings: T2-weighted sagittal image showed masses of 22 mm and 15 mm in the maximum diameter in the anterior wall of the uterus with low signal intensity (Figure 2C).

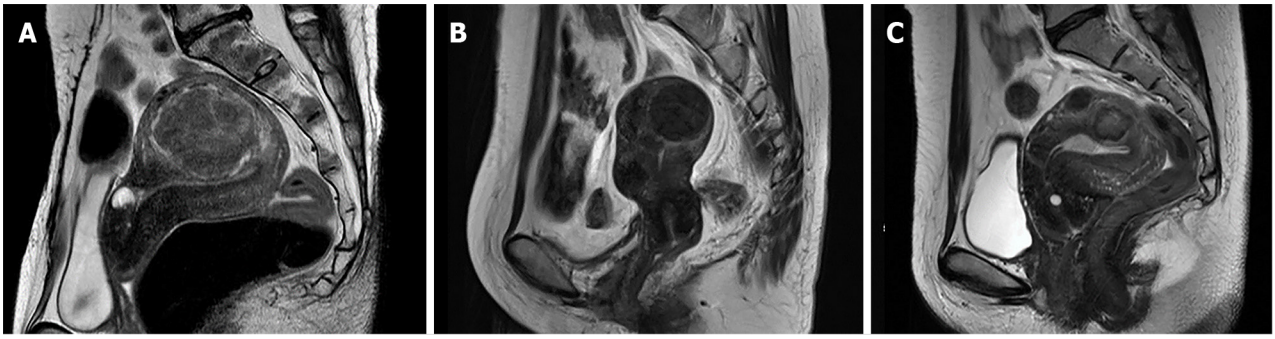

DOI: 10.12998/wjcc.v12.i5.980

Figure 2 Magnetic resonance imaging examination of the pelvis of before the procedure. Magnetic resonance imaging examination of the pelvis of before the procedure. A: Case 1; Sagittal T2-weighted image showed a 65 mm solid mass; B: Case 2; Sagittal T2-weighted image showed a 35 mm solid mass; C: Case 3; Sagittal T2-weighted image showed a 22 mm and 15 mm solid mass.

FINAL DIAGNOSIS

Case 1

Based on the above findings, organic, drug-induced heavy menstrual bleeding was diagnosed (FIGO AUB system 2 AUB-Lo;-I).

Case 2

Based on the above findings, a diagnosis of heavy menstrual bleeding caused by uterine myoma was established (FIGO AUB system 2, AUB-Lo).

Case 3

Based on the above findings, a diagnosis of heavy menstrual bleeding caused by uterine myomas was established (FIGO AUB system 2, AUB-Lo).

TREATMENT

Case 1

Treatment course: Dasatinib administration was stopped, and red blood cell and platelet transfusions were performed. Transvaginal ultrasound-guided microwave ablation of the uterine myoma was planned to control heavy menstrual bleeding after obtaining adequate informed consent.

In the present case, five feeding vessels were identified in the vicinity of the uterine myoma, and this area was ablated. The procedure time was 45 minutes, and the amount of blood loss was minimal. The patient's course was favorable, and she was discharged 4 h after the procedure and followed up on an outpatient basis.

Case 2

Treatment course: Transvaginal ultrasound-guided microwave ablation of the uterine myoma was planned for the purpose of controlling heavy menstrual bleeding after obtaining adequate informed consent. Four feeding vessels were identified in the vicinity of the uterine myoma, and this area was ablated with microwaves at 2.45 GHz. The procedure time was 40 min, and the amount of blood loss was minimal. The patient's course was favorable, and she was discharged 4 h after the procedure and followed up on an outpatient basis.

Case 3

Treatment course: Transvaginal ultrasound-guided microwave ablation of the uterine myomas was planned for the purpose of controlling after obtaining adequate informed consent. Six feeding vessels were identified in the vicinity of the uterine myomas, and this area was ablated with microwaves at 2.45 GHz. The procedure time was 53 min, and the amount of blood loss was minimal. The patient's course was favorable, and she was discharged 4 h after the procedure and followed up on an outpatient basis.

OUTCOME AND FOLLOW-UP

Case 1

Postoperative course: Menstruation resumed 1 month after treatment, and VAS showed that clinical symptoms improved

markedly (heavy menstrual bleeding from 10 preoperatively to 1 postoperatively and menstrual pain from 10 preoperatively to 2 postoperatively) and the Hb value showed a remarkable increase to 12.3 g/dL. In addition, the maximum diameter of the uterine myoma was reduced from 65 mm preoperatively to 27 mm at 3 months postoperatively (Figure 3A). No complications were observed during the course, and 36 months have passed since the procedure without recurrence of heavy menstrual bleeding. In addition, the patient resumed treatment for chronic myelogenous leukemia immediately after surgery.

Case 2

Postoperative course: Menstruation resumed 1 month after treatment, and the VAS showed that clinical symptoms appeared to improve remarkably (both heavy menstrual bleeding and dysmenorrhea from 10 preoperatively to 1 postoperatively) and the Hb value markedly increased to 13.2 g/dL. In addition, the maximum diameter of the uterine myoma was reduced from 35 mm preoperatively to 20 mm at 3 months postoperatively (Figure 3B). No complications were observed during the course, and 18 months have passed since the procedure without recurrence of heavy menstrual bleeding.

Case 3

Postoperative course: Menstruation resumed 1 month after treatment, and the VAS showed that clinical symptoms improved markedly (both heavy menstrual bleeding and dysmenorrhea from 10 preoperatively to 1 postoperatively) and the Hb value markedly increased to 13.2 g/dL. The maximum diameter of the uterine myomas was reduced from 22 mm and 15 mm preoperatively to 15 mm and 13 mm (Figure 3C). No complications were observed during the course, and 12 months have passed since the procedure without recurrence of heavy menstrual bleeding.

DISCUSSION

MEA is an ablation technique that uses 2.45 GHz microwave irradiation for endometrial ablation, including its basal layer. MEA has been reported to be useful as an alternative therapy to avoid total hysterectomy for heavy menstrual bleeding[3-5]. Although MEA is expected to be effective in treating uterine myomas, a small number of cases have been reported where additional treatment was required because of postoperative recurrence[6,7].

Therefore, we performed a microwave ablation of uterine myoma lesions as a new treatment attempt for heavy menstrual bleeding caused by uterine myomas. This treatment method identifies the feeding vessels to the uterine myoma using the color Doppler method before ablation and selectively ablates the feeding vessels with ultrasound-guided microwave ablation. This facilitates in reducing the procedure time by directly ablating the feeding vessels, even for relatively large myomas. In addition, we believe that microwave ablation of the feeding vessels to the uterine myomas not only improved clinical symptoms such as heavy menstrual bleeding and anemia but also reduced the size of the uterine myomas caused by decreased blood flow to the uterine myomas. Furthermore, we used a needle-shaped deep coagulation electrode to ablate the feeding vessels to the uterine myomas; these electrodes are thin as 1.6 mm in diameter and are considered effective for use in minimally invasive procedures. All patients were discharged within 4 h postoperatively and had no postoperative complications. In addition, menstruation resumed 1 month after the procedure; however, no recurrence of heavy menstrual bleeding or other symptoms was observed, confirming the efficacy and safety of the process.

As a conservative treatment for uterine myomas, UAE is available. This is an interventional radiology procedure for the transcatheter embolization uterine arteries or other vessels. Since Ravina from France reported this procedure in 1995 as a treatment for uterine myomas[8], it has been widely performed worldwide as a minimally invasive alternative treatment compared to total hysterectomy. The effectiveness of this treatment was reportedly comparable to that of surgical treatments such as total hysterectomy and myomectomy in terms of improvement of clinical symptoms such as heavy menstrual bleeding and patient satisfaction[9-12]. However, its complications include postoperative fever (4.0%), pain (2.9%), and endometritis (1.1%)[11-14].

As another conservative treatment method for uterine myomas, MRI-guided focused ultrasound is available; the details of which have been described in previous studies[15]. This is a method of treating myomas noninvasively from outside the body using high-intensity focused ultrasound, which uses high-output ultrasound to convert it into thermal energy within the tissue away from the probe, inducing coagulation necrosis in the targeted area while observing it in real time by combining it with MRI. This treatment has been reported to reduce the volume of uterine myomas and improve clinical symptoms such as heavy menstrual bleeding[16-18]. However, ablation of large myomas requires time, and there are concerns regarding increased uterine myoma size and recurrence of clinical symptoms in obese patients and patients with degenerative uterine myomas caused by the uncertainty of the ablation effect[16-18].

Furthermore, as a conservative treatment method for uterine myomas, ultrasound-guided transcervical microwave myolysis (TCMM) using microwaves, as in the present cases, is available. In addition to conventional MEA, this method uses a modified needle-shaped sounding applicator for MEA to ablate uterine myomas themselves with microwaves. Reportedly, the clinical effects of MEA include improving heavy menstrual bleeding and anemia as well as shrinking uterine myomas[19,20]. However, because the area to be ablated is approximately 6 mm from the surface of the sounding applicator, larger myomas require time for ablation. In addition, the sounding applicator used for ablation has a diameter of 4 mm, which is thick and raises concerns regarding procedure invasiveness. Furthermore, it is unclear which method was more successful, conventional MEA or TCMM, because the therapeutic effect of TCMM alone has not been examined.

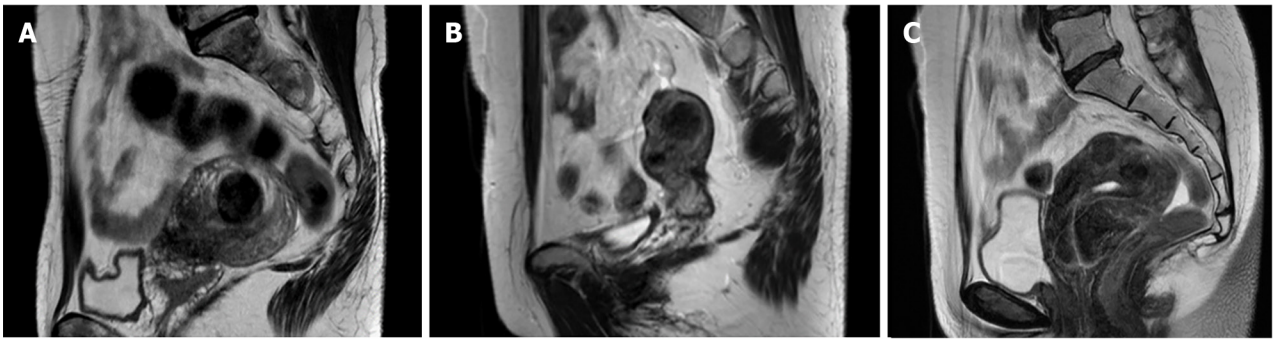

DOI: 10.12998/wjcc.v12.i5.980

Figure 3 Magnetic resonance imaging examination of the pelvis of post the procedure. A: Case 1; The uterine myoma [International Federation of Gynecology and Obstetrics (FIGO) classification system 5] reduced from 65 mm to 27 mm by postoperative month 3; B: Case 2; The uterine myomas (FIGO classification system 5) reduced from 35 mm to 20 mm by postoperative month 3; C: Case 3; The uterine myomas (FIGO classification system 5) reduced from 22 mm and 15 mm to 15 mm and 13 mm by postoperative month 3.s

In contrast, based on the perspective about fertility preservation in conservative treatment of uterine fibroids, UAE may also be selected for those wishing to have children in future. Complications other than those mentioned above include ovarian dysfunction, secondary amenorrhea associated with endometrial atrophy/Lumenal adhesions, and other complications that may affect fertility[9,11,12,21]. Therefore, the indication for UAE in patients who desire to bear a child must be carefully considered. Possible effects on the ovaries after UAE include ovarian failure caused by decreased ovarian blood flow and damage to the fallopian tubes due to infection and resulting infertility. Although there have been multiple reports of pregnancies and deliveries after UAE, there have also been reports of increased miscarriage rates[11,12,22] and placental abnormalities such as placenta accrete[11,12,23] in pregnancies after UAE. Therefore, careful treatment selection for patients who wish to bear a child and strict perinatal management in cases of pregnancy after this treatment should be considered.

Conventional MEA is not indicated for women who desire to bear a child because it is a method to decrease menstrual flow by ablating the endometrium, including its basal layer, thereby inhibiting cyclical endometrial regeneration. In addition, MRgFUS, a conservative treatment for uterine myomas, is not indicated for patients in Japan who desire to bear a child. However, there are several reports of pregnancies after treatment with MRgFUS. These indicate that normal pregnancy outcomes and normal vaginal deliveries are possible[16]. However, given the small number of studies, future, well-powered, and prospective investigations are warranted. TCMM is not indicated for patients who wish to bear a child because it also involves MEA.

The method presented in the current report may minimize the reduction of blood flow to the uterus and ovaries because the microwave directly ablates the feeding vessels to the uterine myomas without ablating the endometrium. If the method we used in the present cases can be expected to improve clinical symptoms, it can potentially become one of the conservative treatment options for uterine myomas wherein fertility preservation is desired. The trend toward late marriage and childbearing has become more pronounced in recent years due to changes in women's lifestyles. Symptomatic uterine myomas in sexually mature women often require not only minimally invasive treatment but also management with consideration for fertility preservation.

In the future, we would like to compile cases of this procedure in patients with uterine myomas associated with heavy menstrual bleeding and verify various aspects of this treatment method, through long-term follow-up, including clinical efficacy and recurrence in heavy menstrual bleeding and other conditions, safety, postoperative changes in hormone dynamics, pregnancy course after pregnancy is established, outcome of delivery, and indication of this procedure.

CONCLUSION

Ultrasound-guided microwave ablation of uterine myomas was as effective and safe as conventional MEA and reduced the maximum diameter of uterine myomas. This technique has the potential to be a novel treatment method for heavy menstrual bleeding caused by uterine myomas.

FOOTNOTES

Author contributions: Kakinuma T contributed to conceptualization, methodology, software, validation, original draft preparation, manuscript review and editing, visualization, supervision, and project administration; all authors contributed to formal analysis, investigation, resources, and data curation; all authors have read and agreed to the published version of the manuscript.

Informed consent statement: Informed written consent was obtained from the patients for publication of this report and any accompanying images.

Conflict-of-interest statement: All the authors declare that they have no competing interests.

CARE Checklist (2016) statement: The authors have read the CARE Checklist (2016), and the manuscript was prepared and revised according to the CARE Checklist (2016).

Country/Territory of origin: Japan

ORCID number: Toshiyuki Kakinuma 0000-0001-7853-4860.

S-Editor: Liu JH
L-Editor: A
P-Editor: Yu HG

REFERENCES

1 **Domenico L Jr**, Siskin GP. Uterine artery embolization and infertility. *Tech Vasc Interv Radiol* 2006; **9**: 7-11 [PMID: 17145479 DOI: 10.1053/j.tvir.2006.08.003]
2 **Wu G**, Li R, He M, Pu Y, Wang J, Chen J, Qi H. A comparison of the pregnancy outcomes between ultrasound-guided high-intensity focused ultrasound ablation and laparoscopic myomectomy for uterine fibroids: a comparative study. *Int J Hyperthermia* 2020; **37**: 617-623 [PMID: 32525708 DOI: 10.1080/02656736.2020.1774081]
3 **Kakinuma T**, Kaneko A, Kakinuma K, Matsuda Y, Yanagida K, Takeshima N, Ohwada M. Effectiveness of treating menorrhagia using microwave endometrial ablation at a frequency of 2.45 GHz. *World J Clin Cases* 2023; **11**: 5653-5659 [PMID: 37727709 DOI: 10.12998/wjcc.v11.i24.5653]
4 **Sharp NC**, Cronin N, Feldberg I, Evans M, Hodgson D, Ellis S. Microwaves for menorrhagia: a new fast technique for endometrial ablation. *Lancet* 1995; **346**: 1003-1004 [PMID: 7475547 DOI: 10.1016/s0140-6736(95)91689-x]
5 **Hodgson DA**, Feldberg IB, Sharp N, Cronin N, Evans M, Hirschowitz L. Microwave endometrial ablation: development, clinical trials and outcomes at three years. *Br J Obstet Gynaecol* 1999; **106**: 684-694 [PMID: 10428525 DOI: 10.1111/j.1471-0528.1999.tb08368.x]
6 **Nakamura K**, Nakayama K, Sanuki K, Minamoto T, Ishibashi T, Sato E, Yamashita H, Ishikawa M, Kyo S. Long-term outcomes of microwave endometrial ablation for treatment of patients with menorrhagia: A retrospective cohort study. *Oncol Lett* 2017; **14**: 7783-7790 [PMID: 29344224 DOI: 10.3892/ol.2017.7208]
7 **Kumar V**, Chodankar R, Gupta JK. Endometrial ablation for heavy menstrual bleeding. *Womens Health (Lond)* 2016; **12**: 45-52 [PMID: 26756668 DOI: 10.2217/whe.15.86]
8 **Ravina JH**, Herbreteau D, Ciraru-Vigneron N, Bouret JM, Houdart E, Aymard A, Merland JJ. Arterial embolisation to treat uterine myomata. *Lancet* 1995; **346**: 671-672 [PMID: 7544859 DOI: 10.1016/s0140-6736(95)92282-2]
9 **Gupta JK**, Sinha A, Lumsden MA, Hickey M. Uterine artery embolization for symptomatic uterine fibroids. *Cochrane Database Syst Rev* 2012; CD005073 [PMID: 22592701 DOI: 10.1002/14651858.CD005073.pub3]
10 **Dariushnia SR**, Nikolic B, Stokes LS, Spies JB; Society of Interventional Radiology Standards of Practice Committee. Quality improvement guidelines for uterine artery embolization for symptomatic leiomyomata. *J Vasc Interv Radiol* 2014; **25**: 1737-1747 [PMID: 25442136 DOI: 10.1016/j.jvir.2014.08.029]
11 **Keung JJ**, Spies JB, Caridi TM. Uterine artery embolization: A review of current concepts. *Best Pract Res Clin Obstet Gynaecol* 2018; **46**: 66-73 [PMID: 29128204 DOI: 10.1016/j.bpobgyn.2017.09.003]
12 **Ludwig PE**, Huff TJ, Shanahan MM, Stavas JM. Pregnancy success and outcomes after uterine fibroid embolization: updated review of published literature. *Br J Radiol* 2020; **93**: 20190551 [PMID: 31573326 DOI: 10.1259/bjr.20190551]
13 **Kitamura Y**, Ascher SM, Cooper C, Allison SJ, Jha RC, Flick PA, Spies JB. Imaging manifestations of complications associated with uterine artery embolization. *Radiographics* 2005; **25** Suppl 1: S119-S132 [PMID: 16227486 DOI: 10.1148/rg.25si055518]
14 **Martin J**, Bhanot K, Athreya S. Complications and reinterventions in uterine artery embolization for symptomatic uterine fibroids: a literature review and meta analysis. *Cardiovasc Intervent Radiol* 2013; **36**: 395-402 [PMID: 23152035 DOI: 10.1007/s00270-012-0505-y]
15 **Fennessy FM**, Tempany CM. MRI-guided focused ultrasound surgery of uterine leiomyomas. *Acad Radiol* 2005; **12**: 1158-1166 [PMID: 16099686 DOI: 10.1016/j.acra.2005.05.018]
16 **Fischer K**, McDannold NJ, Tempany CM, Jolesz FA, Fennessy FM. Potential of minimally invasive procedures in the treatment of uterine fibroids: a focus on magnetic resonance-guided focused ultrasound therapy. *Int J Womens Health* 2015; **7**: 901-912 [PMID: 26622192 DOI: 10.2147/IJWH.S55564]
17 **Kröncke T**, David M. MR-Guided Focused Ultrasound in Fibroid Treatment - Results of the 4th Radiological-Gynecological Expert Meeting. *Rofo* 2019; **191**: 626-629 [PMID: 31137044 DOI: 10.1055/a-0884-3143]
18 **Kong CY**, Meng L, Omer ZB, Swan JS, Srouji S, Gazelle GS, Fennessy FM. MRI-guided focused ultrasound surgery for uterine fibroid treatment: a cost-effectiveness analysis. *AJR Am J Roentgenol* 2014; **203**: 361-371 [PMID: 25055272 DOI: 10.2214/AJR.13.11446]
19 **Tsuda A**, Kanaoka Y. Outpatient transcervical microwave myolysis assisted by transabdominal ultrasonic guidance for menorrhagia caused by submucosal myomas. *Int J Hyperthermia* 2015; **31**: 588-592 [PMID: 26287991 DOI: 10.3109/02656736.2015.1036385]
20 **Kanaoka Y**, Yoshida C, Fukuda T, Kajitani K, Ishiko O. Transcervical microwave myolysis for uterine myomas assisted by transvaginal ultrasonic guidance. *J Obstet Gynaecol Res* 2009; **35**: 145-151 [PMID: 19215562 DOI: 10.1111/j.1447-0756.2008.00872.x]

21 **Khaund A**, Lumsden MA. Impact of fibroids on reproductive function. *Best Pract Res Clin Obstet Gynaecol* 2008; **22**: 749-760 [PMID: 18547868 DOI: 10.1016/j.bpobgyn.2008.01.009]

22 **Homer H**, Saridogan E. Uterine artery embolization for fibroids is associated with an increased risk of miscarriage. *Fertil Steril* 2010; **94**: 324-330 [PMID: 19361799 DOI: 10.1016/j.fertnstert.2009.02.069]

23 **Pron G**, Mocarski E, Bennett J, Vilos G, Common A, Vanderburgh L; Ontario UFE Collaborative Group. Pregnancy after uterine artery embolization for leiomyomata: the Ontario multicenter trial. *Obstet Gynecol* 2005; **105**: 67-76 [PMID: 15625144 DOI: 10.1097/01.AOG.0000149156.07061.1f]

World Journal of Clinical Cases

Submit a Manuscript: https://www.f6publishing.com

World J Clin Cases 2024 February 16; 12(5): 988-994

DOI: 10.12998/wjcc.v12.i5.988

ISSN 2307-8960 (online)

CASE REPORT

Omental fibroma combined with right indirect inguinal hernia masquerades as a scrotal tumor: A case report

Ping Zhou, Chan-Hui Jin, Ying Shi, Guo-Qing Ma, Wen-Hao Wu, Yu Wang, Kun Cai, Wu-Feng Fan, Tian-Bao Wang

Specialty type: Medicine, research and experimental

Provenance and peer review: Unsolicited article; Externally peer reviewed.

Peer-review model: Single blind

Peer-review report's scientific quality classification

Grade A (Excellent): 0
Grade B (Very good): 0
Grade C (Good): C
Grade D (Fair): D
Grade E (Poor): 0

P-Reviewer: Hunasanahalli Giriyappa V, India; Richardson WS, United States

Received: September 22, 2023
Peer-review started: September 22, 2023
First decision: November 13, 2023
Revised: December 11, 2023
Accepted: January 22, 2024
Article in press: January 22, 2024
Published online: February 16, 2024

Ping Zhou, Chan-Hui Jin, Ying Shi, Guo-Qing Ma, Wen-Hao Wu, Yu Wang, Kun Cai, Wu-Feng Fan, Tian-Bao Wang, Department of Gastrointestinal Surgery, South China Hospital of Shenzhen University, Shenzhen 518000, Guangdong Province, China

Corresponding author: Tian-Bao Wang, MD, Chief Physician, Postdoc, Professor, Department of Gastrointestinal Surgery, South China Hospital of Shenzhen University, No. 1 Fuxin Road, Longgang District, Shenzhen 518000, Guangdong Province, China. wangtianbao1@163.com

Abstract

BACKGROUND

The most common causes of scrotal enlargement in patients include primary tumor of the scrotum, inflammation, hydrocele of the tunica vaginalis, and indirect inguinal hernia; scrotal enlargement caused by external tumors of the scrotum is rare. The patient had both a greater omentum tumor and an inguinal hernia, and the tumor protruded into the scrotum through the hernia sac, which is even rarer. Moreover, omental tumors are mostly metastatic, and primary omental fibroma is rare.

CASE SUMMARY

Here, we report a rare case of a 25-year-old young man with scrotal enlargement and pain for 3 months. Preoperative examination and multidisciplinary discussions considered intra-abdominal tumor displacement and inguinal hernia, and intraoperative exploration confirmed that the greater omentum tumor protruded into the scrotum. Therefore, tumor resection and tension-free inguinal hernia repair were performed. The final diagnosis was benign fibroma of the greater omentum accompanied by an indirect inguinal hernia.

CONCLUSION

This unusual presentation of a common inguinal hernia disease illustrates the necessity of performing detailed history taking, physical examination, and imaging before surgery.

Key Words: Hernia; Indirect inguinal hernia; Fibroma; Omental tumor; Scrotal tumor; Greater omentum; Case report

Core Tip: Intrascrotal tumors are common male reproductive system-related tumors and are mostly primary tumors. In this case, the tumor in the scrotum of the patient was not a primary tumor of the scrotum or a metastatic lesion of other tumors. Instead, a primary lesion of the greater omentum fibroma in the abdominal cavity was completely displaced to the scrotum, which is a rare occurrence. We searched the studies included in PubMed since 2011 and found four similar reports of fibromas herniating into the scrotum, originating from the greater omentum, mesentery, and appendix. Analysis showed that the patients' tumor activity was high, and all patients also had an inguinal hernia, which was the basis of the disease. This case reminds us that even the most common diseases may have various unexpected situations, and it is necessary to conduct detailed inquiries and physical examinations on the patient and complete relevant preoperative examinations and tests to avoid misdiagnosis. When the patient's condition is complex, multidisciplinary joint diagnosis and treatment are needed to choose the most suitable treatment method.

Citation: Zhou P, Jin CH, Shi Y, Ma GQ, Wu WH, Wang Y, Cai K, Fan WF, Wang TB. Omental fibroma combined with right indirect inguinal hernia masquerades as a scrotal tumor: A case report. *World J Clin Cases* 2024; 12(5): 988-994
URL: https://www.wjgnet.com/2307-8960/full/v12/i5/988.htm
DOI: https://dx.doi.org/10.12998/wjcc.v12.i5.988

INTRODUCTION

Intrascrotal tumors are common male reproductive system-related tumors and are mostly primary tumors. In this case, the tumor in the scrotum of the patient was not a primary tumor of the scrotum or a metastatic lesion of other tumors. Instead, a primary lesion of the greater omentum fibroma in the abdominal cavity was completely displaced to the scrotum, which is a rare occurrence. We searched the studies included in PubMed since 2011 and found four similar reports of fibromas herniating into the scrotum, originating from the greater omentum, mesentery, and appendix. Analysis showed that the patients' tumor activity was high, and all patients also had an inguinal hernia, which was the basis of the disease. This case reminds us that even the most common diseases may have various unexpected situations, and it is necessary to conduct detailed inquiries and physical examinations on the patient and complete relevant preoperative examinations and tests to avoid misdiagnosis. When the patient's condition is complex, multidisciplinary joint diagnosis and treatment are needed to choose the most suitable treatment method.

CASE PRESENTATION

Chief complaints

A 25-year-old male patient presented to the Department of Urology, South China Hospital of Shenzhen University, because of "right testicular pain for 3 months, aggravated for 1 wk".

History of present illness

The patient developed right testicular pain without obvious cause 3 months prior with intermittent attacks accompanied by gradual enlargement of the scrotum and lower abdominal pain 1 wk prior.

History of past illness

Previously healthy and without any other illnesses.

Personal and family history

No special.

Physical examination

Physical examination revealed that the patient had a mass in the right groin area varying in size with the position of the body, which could be partially returned, and there was a sense of impact in the inner ring opening when coughing. The patient had significant scrotal swelling, and approximately 5 cm of mass could be felt, accompanied by light tenderness.

Laboratory examinations

Carcinoembryonic antigen (CEA) 1.49 ng/mL, alpha-fetoprotein (AFP) 2.90 ng/mL, β- human chorionic gonadotropin (HCG) 0.15 IU/L, lactate dehydrogenase (LDH) 148 u/L ↓.

Imaging examinations

B ultrasound: Right inguinal oblique hernia, hernia sac considered omentum, right scrotal solid mass.

Total abdominal computed tomography (CT) enhancement: Right oblique inguinal hernia, hernia contents may be greater omentum. Right scrotal mass, no obvious enhancement, and superior mesenteric artery branch blood supply? The

possibility of tumors of mesenteric origin was considered (Figure 1).

Pelvic magnetic resonance imaging (MRI) enhancement: Right scrotal mass with slightly short T1T2 signal, low signal in diffusion weighted imaging lesion, mixed apparent dispersion coefficient image with slightly low signal shadow, mild enhancement after enhancement, and clear boundary between the tumor and right testicle.

MULTIDISCIPLINARY EXPERT CONSULTATION

After completing the relevant examinations, after multidisciplinary discussions among doctors in urology, gastrointestinal surgery, and imaging, the patient was considered to have a right inguinal hernia and scrotal tumor before the surgery. Considering the degree of tumor activity and blood supply, the mass was most likely to be a greater omentum tumor, Mesenteric tumors and primary tumors in the scrotum are less likely. The nature of the tumor was unknown, and it was to be surgically removed directly. No preoperative puncture was performed to avoid the risk of tumor spread. We are considering adopting a surgical approach of groin exploration combined with laparoscopic exploration of the abdominal cavity for patients. After determining the source of the tumor, safely and completely remove the tumor.

If laparoscopic exploration considers metastatic cancer originating from within the abdominal cavity, further abdominal surgery may be required under laparoscopy (including resection or biopsy of intra-abdominal lesions, intestinal resection and anastomosis, combined organ resection, *etc.*).

FINAL DIAGNOSIS

Omental fibroma combined with right indirect inguinal hernia.

Postoperative pathological diagnosis: Right greater omentum mass, spindle cell proliferative lesion, considered benign or low-grade mesenchymal tumor, tended to be fibrous or fibroblastic in origin (Figure 2).

Immunohistochemistry: Vimentin +, Ki-67 < 1%. All others are negative: Alpha-smooth muscle actin, Desmin, CD34, s100 proteins (S100), signal transducer and activator of transcription 6, anaplastic lymphoma kinase, mucin 4, epithelial membrane antigen, CD117, discovered on GIST-1, and β-catenin (Guangzhou Kingmed Center for Clinical Laboratory).

Genetic testing

A *CTNNB1* gene mutation was detected (Ruijin Hospital, Shanghai Jiao Tong University School of Medicine).

Pathological consultation

Combined with the results of the original unit's immunohistochemistry and our unit's genetic test, it was judged to be consistent with fibromatosis (Ruijin Hospital, Shanghai Jiao Tong University School of Medicine).

TREATMENT

Intraoperative exploration: Through the right groin incision exploration, the tumor was confirmed to be of greater omentum origin, hard, completely enveloped, and approximately 6 cm × 5 cm in size. In addition, several nodules the size of rice grains were observed in the protruding omentum, and no abnormalities were observed in the right spermatic cord or testicular exploration. No obvious abnormality was found in any organ of the abdominal cavity by laparoscopy combined with exploration.

The greater omentum mass and part of the omentum nodule were resected and sent for rapid frozen section examination (Figure 3).

Intraoperative rapid frozen section examination revealed that the greater omentum mass was a benign spindle cell tumor, and the omentum nodule was considered a benign lesion.

Then, right inguinal oblique hernia tension-free repair was performed, and the operation was complete.

The patient was discharged the following afternoon.

OUTCOME AND FOLLOW-UP

The patient recovered well after the operation, and the stitches were removed in the outpatient department after discharge.

B ultrasound was reviewed 4 months after surgery, and total abdominal CT was reviewed 7 months after surgery. There was no recurrence of inguinal hernia, no recurrence of tumor, and no bad performance was found in the abdominal cavity, inguinal region or scrotum.

At a follow-up visit 7 months after the surgery, the patient felt fine, with no protrusion of the right inguinal hernia, no swelling of the scrotum, and no pain or discomfort.

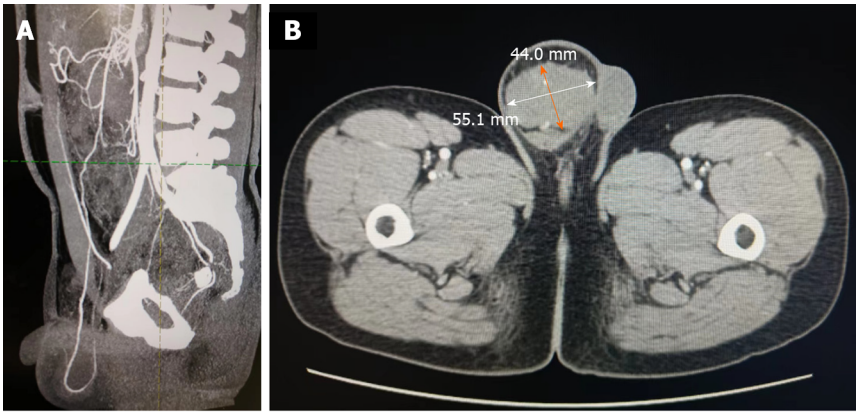

DOI: 10.12998/wjcc.v12.i5.988

Figure 1 Computed tomography findings. A: The blood supply of scrotal masses is from the omentum or mesenteric vessels in the abdominal cavity; B: The scrotal mass's diameter is 44.0 mm × 55.1 mm.

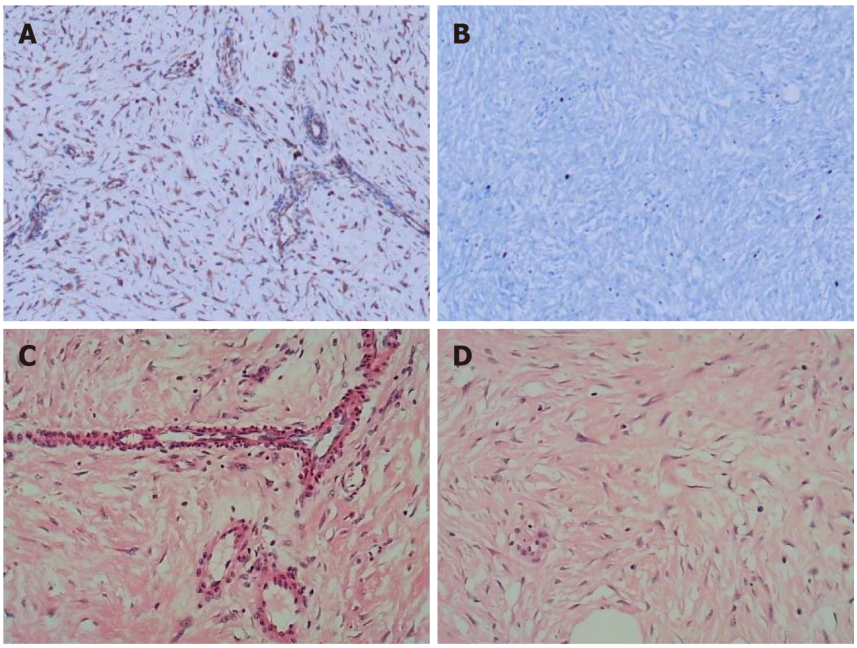

DOI: 10.12998/wjcc.v12.i5.988

Figure 2 Pathological sections were stained. A and B: Image shows immunohistochemical staining; C and D: Image shows hematoxylin and eosin staining.

DISCUSSION

Review

We conducted a systematic search of the PubMed database with the following key words: Inguinal hernia, scrotum, and fibroma. A total of 4 cases of intraabdominal fibroma protruding into the scrotum, with inguinal hernia as the manifestation, have been reported since 2011 (Table 1).

The age of the patients ranged from 18 to 51 years. The medical history ranged from 1 to 4 months, and the tumor diameter ranged from 2.5 to 19 cm. Tumor sources included the greater omentum, mesentery, and appendix, all of which are considered benign lesions.

Omental fibroma

Of all omental tumors, metastatic malignant tumors are the most common, and they mainly occur in the stomach, colon, pancreas, and ovary[1]. Primary peritoneal tumors are rare and can be benign or malignant, accounting for approximately 50% each[2]. Malignant tumors commonly include leiomyosarcoma and hemangiopericytoma. Benign tumors commonly include lipomas, leiomyomas, fibromas, and neurofibromas, with omental fibromas accounting for approximately 2%[3-5]. Cases where tumors fall into the scrotum and manifest as inguinal hernias are even rarer[6-9].

Table 1 A total of 4 cases of intraabdominal fibroma protruding into the scrotum, with inguinal hernia as the manifestation, have been reported since 2011

Ref.	Article	Left/right	Patient age (yr)	Diameter of tumor	Medical history	Tumor location
Alsaif[6], 2011	Mesenteric fibromatosis presenting as an irreducible inguinal hernia	Left	18	19 cm × 9 cm × 7 cm	3 months	Omental fibroma
Khoo and Jacob [9], 2017	An omental fibroma resembling a testicular tumour but presented as an irreducible inguinal hernia	Right	51	7.0 cm × 6.2 cm	4 months	Omental fibroma
Oyelowo *et al* [8], 2020	Appendiceal fibroma in an Amyand's hernia mimicking a supernumerary testis: A case report	Right	28	3 cm × 3 cm × 2 cm	Not reported	Appendiceal fibroma
Liu *et al*[7], 2021	Omental mass combined with indirect inguinal hernia leads to a scrotal mass: A case report	Left	30	2.5 cm	1 month	Omental angiofibroma

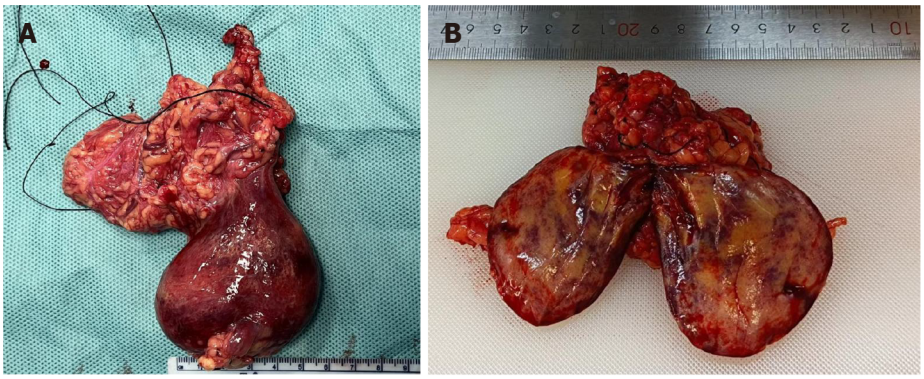

DOI: 10.12998/wjcc.v12.i5.988

Figure 3 Resected scrotal mass: Originating from the greater omentum. A: The mass envelope was complete, and the boundary between the mass and testis was clear; B: Cross-sectional view of the tumor: Slightly hard, gray-yellow, solid mass.

Surgical resection is the main treatment method, in which local resection of benign omental tumors is effective and rarely relapses. Tumor markers, B-ultrasound, and CT examination are helpful for preoperative diagnosis and localization.

Scrotal tumor

Scrotal tumors include primary tumors of the scrotum, metastatic tumors, and tumors that herniate into the abdominal cavity[10]. Primary tumors of the scrotum mainly include testicular tumors and testicular adnexal tumors[11].

The incidence rate of testicular tumors is approximately 1/100000, accounting for 1%-2% of male tumors. More than 90% of testicular tumors are malignant tumors, including germ cell tumors, sex cord/stromal tumors, and secondary tumors, among which germ cell tumors account for more than 90%. Testicular adnexal tumors refer to tumors originating from the epididymis, spermatic cord, white membrane, seminal vesicle, and supporting tissues, which are rarely seen clinically[12,13].

Before surgery, B-ultrasound, CT, MRI, and other examinations are recommended[14,15]. Additionally, complete laboratory tests, such as those for HCG, CEA, AFP, and LDH, are recommended.

Inguinal hernia mistaken for tumor

The common locations of a hernia sac are the omentum and small intestine, while others include the cecum, appendix, sigmoid colon, bladder, uterine appendages, abdominal tumors, and so on[16]. If the hernia content cannot be returned to the abdominal cavity, the possibility of incarceration, adhesion, and tumor invasion should be considered[17]. However, it should be noted that the appendix, fecal mass, incarceration, edematous intestinal canal, and even extraperitoneal fat are easily misdiagnosed as tumors[18].

CONCLUSION

Surgeons need to be aware that scrotal masses caused by inguinal hernia can be associated with tumors. In this case report, a patient with a greater omentum tumor complicated with indirect inguinal hernia had a clinical manifestation of a scrotal mass.

The purpose of the surgery was to remove the tumor while repairing the inguinal hernia. During the operation, the hernia sac and its contents were carefully explored, and the tumor was removed. It was then sent for rapid frozen section examination to determine whether the surgical resection scope needed to be expanded and whether a patch should be placed during the operation[19,20]. The type of pathology after surgery determines whether the patient needs further treatment after surgery. Finally, the follow-up work of surgical patients after discharge is also a factor that cannot be ignored.

This case report provides information to help doctors choose an optimal treatment plan, reducing medical risks and ultimately benefiting patients. These are issues that doctors need to consider.

FOOTNOTES

Author contributions: Zhou P reviewed the literature and drafted the manuscript; Jin CH and Wang Y performed the surgery; Ma GQ and Wu WH validated the images and case data; Cai K and Fan WF examined and photographed the pathological findings; Shi Y conducted the follow-up; Wang TB conceptualized and organized the study; All authors have read and approved the final manuscript.

Informed consent statement: We have informed the patient and obtained his consent for the use of his case as an academic research case report. We promise not to use it for commercial purposes and to protect the patient's privacy.

Conflict-of-interest statement: All the authors report no relevant conflicts of interest for this article.

CARE Checklist (2016) statement: The authors have read CARE Checklist (2016), and the manuscript was prepared and revised according to CARE Checklist (2016).

Country/Territory of origin: China

ORCID number: Ping Zhou 0009-0000-6372-8937; Chan-Hui Jin 0000-0002-2844-1081; Ying Shi 0009-0006-4197-2529; Guo-Qing Ma 0009-0002-9121-7194; Wen-Hao Wu 0000-0002-6350-3874; Yu Wang 0000-0001-5467-6901; Kun Cai 0000-0002-0070-5954; Wu-Feng Fan 0000-0001-9591-0901; Tian-Bao Wang 0009-0002-2343-5587.

S-Editor: Li L
L-Editor: A
P-Editor: Li L

REFERENCES

1 **Guo YC**, Yao LY, Tian ZS, Shi B, Liu Y, Wang YY. Malignant solitary fibrous tumor of the greater omentum: A case report and review of literature. *World J Clin Cases* 2021; **9**: 445-456 [PMID: 33521114 DOI: 10.12998/wjcc.v9.i2.445]
2 **Zong L**, Chen P, Wang GY, Zhu QS. Giant solitary fibrous tumor arising from greater omentum. *World J Gastroenterol* 2012; **18**: 6515-6520 [PMID: 23197901 DOI: 10.3748/wjg.v18.i44.6515]
3 **Ingle A**, Reddy S, Reddy VK. Omental Solitary Fibrous Tumor: A Rare Tumor at Rare Site. *J Lab Physicians* 2021; **13**: 283-285 [PMID: 34602796 DOI: 10.1055/s-0041-1731942]
4 **Garbin O**, Hummel M, Diana M, Wattiez A. Solitary fibrous tumor of the great omentum. *J Minim Invasive Gynecol* 2011; **18**: 694-695 [PMID: 22024257 DOI: 10.1016/j.jmig.2011.01.013]
5 **Rodriguez Tarrega E**, Hidalgo Mora JJ, Paya Amate V, Vega Oomen O. Solitary fibrous tumor of the greater omentum mimicking an ovarian tumor in a young woman. *Gynecol Oncol Rep* 2016; **17**: 16-19 [PMID: 27354994 DOI: 10.1016/j.gore.2016.04.004]
6 **Alsaif FA**. Mesenteric fibromatosis presenting as an irreducible inguinal hernia. *Saudi J Gastroenterol* 2011; **17**: 357-359 [PMID: 21912065 DOI: 10.4103/1319-3767.84498]
7 **Liu JY**, Li SQ, Yao SJ, Liu Q. Omental mass combined with indirect inguinal hernia leads to a scrotal mass: A case report. *World J Clin Cases* 2021; **9**: 7850-7856 [PMID: 34621837 DOI: 10.12998/wjcc.v9.i26.7850]
8 **Oyelowo N**, Halima AO, Muhammed D, Ibrahim AA, Peter O, Muhammed A. Appendiceal fibroma in an Amyand's hernia mimicking a supernumerary testis: a case report. *Trop Doct* 2020; **50**: 380-383 [PMID: 32646292 DOI: 10.1177/0049475520937109]
9 **Khoo PJ**, Jacob S. An omental fibroma resembling a testicular tumour but presented as an irreducible inguinal hernia. *J Surg Case Rep* 2017; **2017**: rjx161 [PMID: 28852466 DOI: 10.1093/jscr/rjx161]
10 **Swofford BP**, Dragovich T. Sigmoid Adenocarcinoma with Regional Scrotal Metastasis. *Case Rep Oncol* 2017; **10**: 416-419 [PMID: 28626399 DOI: 10.1159/000474936]
11 **Ghoreifi A**, Djaladat H. Management of Primary Testicular Tumor. *Urol Clin North Am* 2019; **46**: 333-339 [PMID: 31277728 DOI: 10.1016/j.ucl.2019.04.006]
12 **Gigantino V**, La Mantia E, Franco R, Cecere S, Rossetti S, Di Napoli M, Pisano C, Berretta M, Galzerano A, Botti G, Pignata S, Facchini G. Testicular and testicular adnexa tumors in the elderly. *Anticancer Drugs* 2013; **24**: 228-236 [PMID: 23059385 DOI:

10.1097/CAD.0b013e32835a3598]

13 **Philips S**, Nagar A, Dighe M, Vikram R, Sunnapwar A, Prasad S. Benign non-cystic scrotal tumors and pseudotumors. *Acta Radiol* 2012; **53**: 102-111 [PMID: 22025740 DOI: 10.1258/ar.2011.110185]

14 **Tallen G**, Hernáiz Driever P, Degenhardt P, Henze G, Riebel T. High reliability of scrotal ultrasonography in the management of childhood primary testicular neoplasms. *Klin Padiatr* 2011; **223**: 131-137 [PMID: 21462100 DOI: 10.1055/s-0031-1271813]

15 **Lee S**, Oh YT, Jung DC. [Imaging of Scrotal Tumors]. *Taehan Yongsang Uihakhoe Chi* 2021; **82**: 1053-1065 [PMID: 36238386 DOI: 10.3348/jksr.2021.0110]

16 **HerniaSurge Group**. International guidelines for groin hernia management. *Hernia* 2018; **22**: 1-165 [PMID: 29330835 DOI: 10.1007/s10029-017-1668-x]

17 **Gnaś J**, Bulsa M, Czaja-Bulsa G. An irreducible left scrotal hernia containing a sigmoid colon tumor (adenocarcinoma) - Case report. *Int J Surg Case Rep* 2014; **5**: 491-493 [PMID: 24988210 DOI: 10.1016/j.ijscr.2014.04.013]

18 **Sezgin C**, Duzgun F, Mutevelizade G, Gumuser G, Sayit E. Inguinoscrotal Bladder Hernia Mimicking Testicle Tumor. *Clin Med Insights Case Rep* 2023; **16**: 11795476231151329 [PMID: 36874374 DOI: 10.1177/11795476231151329]

19 **Pahwa HS**, Kumar A, Agarwal P, Agarwal AA. Current trends in laparoscopic groin hernia repair: A review. *World J Clin Cases* 2015; **3**: 789-792 [PMID: 26380826 DOI: 10.12998/wjcc.v3.i9.789]

20 **Liang MK**, Holihan JL, Itani K, Alawadi ZM, Gonzalez JR, Askenasy EP, Ballecer C, Chong HS, Goldblatt MI, Greenberg JA, Harvin JA, Keith JN, Martindale RG, Orenstein S, Richmond B, Roth JS, Szotek P, Towfigh S, Tsuda S, Vaziri K, Berger DH. Ventral Hernia Management: Expert Consensus Guided by Systematic Review. *Ann Surg* 2017; **265**: 80-89 [PMID: 28009730 DOI: 10.1097/SLA.0000000000001701]

World Journal of Clinical Cases

Submit a Manuscript: https://www.f6publishing.com

World J Clin Cases 2024 February 16; 12(5): 995-1003

DOI: 10.12998/wjcc.v12.i5.995

ISSN 2307-8960 (online)

CASE REPORT

Imaging, pathology, and diagnosis of solitary fibrous tumor of the pancreas: A case report and review of literature

Wen-Wen Wang, Shu-Ping Zhou, Xiang Wu, Luo-Luo Wang, Yi Ruan, Jun Lu, Hai-Li Li, Xu-Ling Ni, Li-Li Qiu, Xin-Hua Zhou

Specialty type: Medicine, research and experimental

Provenance and peer review: Unsolicited article; Externally peer reviewed.

Peer-review model: Single blind

Peer-review report's scientific quality classification

Grade A (Excellent): 0
Grade B (Very good): B
Grade C (Good): 0
Grade D (Fair): 0
Grade E (Poor): 0

P-Reviewer: Triantopoulou C, Greece

Received: October 13, 2023
Peer-review started: October 13, 2023
First decision: November 28, 2023
Revised: December 1, 2023
Accepted: January 18, 2024
Article in press: January 18, 2024
Published online: February 16, 2024

Wen-Wen Wang, Xiang Wu, Luo-Luo Wang, Yi Ruan, Li-Li Qiu, Xin-Hua Zhou, Department of Hepatobiliary and Pancreatic Surgery, The Affiliated Li Huili Hospital, Ningbo University School of Medicine, Ningbo 315000, Zhejiang Province, China

Shu-Ping Zhou, Ningbo College of Health Sciences, Ningbo College of Health Sciences, Ningbo 315000, Zhejiang Province, China

Xiang Wu, Health Science Center, Ningbo University, Ningbo 315000, Zhejiang Province, China

Jun Lu, Department of Hepatobiliary and Pancreatic Surgery, The Affiliated Hangzhou First People's Hospital, Zhejiang University School of Medicine, Hangzhou, 310006, Zhejiang Province, China

Hai-Li Li, Xu-Ling Ni, Department of Diagnosis, Ningbo Diagnostic Pathology Center, Ningbo 315000, Zhejiang Province, China

Corresponding author: Xin-Hua Zhou, Doctor, PhD, Chief Doctor, Doctor, Department of Hepatobiliary and Pancreatic Surgery, The Affiliated Li Huili Hospital, Ningbo University School of Medicine, No. 1111 Jiangnan Road, Yinzhou District, Ningbo 315000, Zhejiang Province, China. zhouxinhua1002@163.com

Abstract

BACKGROUND

A solitary fibrous tumor (SFT) is often located in the pleura, while SFT of the pancreas is extremely rare. Here, we report a case of SFT of the pancreas and discuss imaging, histopathology, and immunohistochemistry for accurate diagnosis and treatment.

CASE SUMMARY

A 54-year-old man presented to our hospital with pancreatic occupancy for over a month. There were no previous complaints of discomfort. His blood pressure was normal. Blood glucose, tumor markers, and enhanced computed tomography (CT) suggested a malignant tumor. Because the CT appearance of pancreatic cancer varies, we could not confirm the diagnosis; therefore, we performed endoscopic ultrasound-guided fine-needle biopsy (EUS-FNB). Pathology and immunohistochemistry were consistent with SFT of the pancreas. The posto-perative pathology and immunohistochemistry were consistent with the puncture

results. The patient presented for a follow-up examination one month after discharge with no adverse effects.

CONCLUSION
Other diseases must be excluded in patients with a pancreatic mass that cannot be diagnosed. CT and pathological histology have diagnostic value for pancreatic tumors. Endoscopic puncture biopsy under ultrasound can help diagnose pancreatic masses that cannot be diagnosed preoperatively. Surgery is an effective treatment for SFT of the pancreas; however, long-term follow-up is strongly recommended because of the possibility of malignant transformation of the tumor.

Key Words: Pancreas; Neoplasm fibrous tumor; Endoscopic ultrasound-guided fine-needle biopsy; Treatment; Case report

Core Tip: We need to be more vigilant for indeterminate pancreatic masses, and then computed tomography and histopathology can play a very important role in clinical diagnosis. Surgery is an effective treatment for solitary fibrous tumor of the pancreas; however, long-term follow-up is strongly recommended because of the possibility of malignant transformation of the tumor.

Citation: Wang WW, Zhou SP, Wu X, Wang LL, Ruan Y, Lu J, Li HL, Ni XL, Qiu LL, Zhou XH. Imaging, pathology, and diagnosis of solitary fibrous tumor of the pancreas: A case report and review of literature. *World J Clin Cases* 2024; 12(5): 995-1003
URL: https://www.wjgnet.com/2307-8960/full/v12/i5/995.htm
DOI: https://dx.doi.org/10.12998/wjcc.v12.i5.995

INTRODUCTION

A solitary fibrous tumor (SFT) is histologically characterized as a mesenchymal tumor, probably fibroblastic in origin, located primarily in the pleura; however, it can be found in any other extrapleural region[1-3]. Extrapleural areas include the liver, peritoneum, kidney, and salivary glands[4-7]. SFT of the pancreas is rare, with only about 30 cases reported to date[1-3,6-35]. SFT of the pancreas is usually asymptomatic, and most are detected by physical examination, computed tomography (CT), or ultrasound as pancreatic masses[6,30,32]. The final diagnosis depends on histopathology and immunohistochemistry[7,31].

Here, we report a case of SFT of the pancreas and present the radiological and pathological differential diagnosis.

CASE PRESENTATION

Chief complaints

A 54-year-old man was admitted to our hospital with a pancreatic space-occupying mass of one month's duration, identified on a physical exam.

History of present illness

A 54-year-old man had been one month before a medical CT finding of pancreas space-occupying lesions, with no adverse reactions, patients for further treatment at our hospital.

History of past illness

The patient had no other significant medical history. History of hypertension, diabetes, coronary heart disease, and other chronic disease was denied.

Personal and family history

The patient had no significant personal or family history.

Physical examination

The patient had no discomfort after the physical examination.

Laboratory examinations

There was no abnormal carcinoembryonic antigen [< 0.5 ng/mL (normal 0-5 ng/mL)], carbohydrate antigen 199 3.9 U/mL (average 0-7 U/mL), alpha-fetoprotein 2.4 ng/mL (normal 0-8.8 ng/mL), carbohydrate antigen 125 12.5 (average 0-30.2 U/mL). Fasting glucose was 5. 19 mmol/L (normal 3.89-6. 11 mmol/L).

Imaging examinations

A review of an abdominal enhanced CT showed a tumor of about 3 cm × 2 cm in the tail of the pancreatic body, showing uneven enhancement after enhancement, consistent with a malignant tumor (Figure 1).

FINAL DIAGNOSIS

A SFT of the pancreas.

TREATMENT

CT revealed a mass with mixed density and inadequate blood supply; these findings were inconsistent with a pancreatic tumor; therefore, we considered a pseudopapillary tumor and a non-functional pancreatic neuroendocrine tumor. We performed an ultrasound endoscopic tissue biopsy. The pathology and immunohistochemistry suggested SFT of the pancreas. After excluding contraindications to surgery and obtaining informed written consent, we performed a laparoscopic distal pancreatectomy with splenectomy. No significant adhesions were seen in the peripancreatic tissue. The pancreatic body was approximately 3 cm × 2 cm (Figure 2). Intraoperative frozen sections showed negative margins. Intraoperative blood loss was 100 mL and no blood transfusion was required.

The patient had no postoperative pancreatic fistula, abdominal infection, or bleeding. Ten days after surgery, he was discharged from the hospital after removing the drainage tube. One month after surgery, the patient returned to the hospital for examination. He did not complain of discomfort. The complete blood count, liver enzymes and renal function were normal.

Histopathological and immunohistochemical results of the postoperative specimen suggested an SFT of the pancreas of 3.0 cm × 2.5 cm × 1.0 cm, negative margins, no tumor involvement in the surrounding lymph nodes, and no tumor involvement in the spleen. Markers were as follows: Signal transducer and activator of transcription 6 (STAT6) (+), cluster of differentiation (CD) 34 (+), B cell CLL/lymphoma-2 (Bc1-2) (+), vimentin (+), CD99 (+), CD117 (-), Ki-67 (+40%), discovered on GIST-1 (+), transducin-like enhancer protein 1 (+), S- 100 (-), cytokeratin pan (pan) (-), somatostatin receptor 2 (-) (Figure 3).

OUTCOME AND FOLLOW-UP

No specific treatment was given after the patient was discharged from the hospital, and he had no complaints for three months after the procedure. He returned for regular follow-up. No abnormalities were found on complete blood counts, blood glucose, tumor markers, or CT.

DISCUSSION

SFT is a mesenchymal tumor comprising less than 2% of soft tissue tumors[36]. About 65% of SFTs originate from the pleura[3]; however, they can also be found in extrapleural areas[6], with only 34 cases reported to date, including the present case (Tables 1 and 2). SFT of the pancreas is extremely rare. We searched PubMed and Google Scholar for pancreatic tumors and SFT and found 34 cases. Of these, 14 (41. 1%) were male, and 20 (58.9%) were female. The mean age was 54. 17 ± 15.4, and the median age was 54; 17 patients had lesions in the pancreatic tumor head [three (17.6%) male and 13 (76.4%) female]. Seventeen had tumors in the tail of the pancreatic body [ten (58.8%) male and seven (41.2%) female]. The mean tumor diameter was 5.2 cm ± 3.8 cm. Of the 34 patients, 12 presented with pain (12/34), 12 were discovered on physical examination (12/34), four presented with jaundice (4/34), one presented with an abdominal mass (1/34), and five were detected by other means (5/34) (Table 1).

Most SFTs of the pancreas are detected by physical examination; clinical signs and symptoms include abdominal pain and jaundice. Because these are not typical symptoms, it is challenging to differentiate SFT from other pancreatic diseases. Histopathology and immunohistochemistry are the gold standards for diagnosis. We recommend ultrasound endoscopic aspiration biopsy for space-occupying pancreatic lesions that cannot be diagnosed on imaging.

Our preoperative diagnosis relied on ultrasound endoscopic puncture biopsy in the present case. The preoperative and postoperative pathological histological examination and immunohistochemistry were consistent with SFT of the pancreas with no tumor involvement in the peripheral lymph nodes, no tumor involvement in the incised margin of the pancreas, and no tumor involvement in the spleen.

The immunohistochemical differential diagnosis of SFT of the pancreas should include spindle cell tumors such as gastrointestinal stromal tumor (GIST), smooth muscle sarcoma, nerve sheath tumor, fibrous mucinous sarcoma, perivascular epithelioid cell tumor, and vascular tumors[3,16,20,37]. The immunomarkers of SFT of the pancreas include STAT6, CD34, bc1-2, vimentin, and CD99[34]. These features help to distinguish SFT from other mesenchymal tumors[34, 37]. SFT expresses CD34 and vimentin in 80%-90% of cases and CD99 and bcl-2 in 70%. SFTs are usually negative for c-kit (CD117), smooth muscle actin, junctional protein, S-100 protein, and cytokeratin (markers for GIST, smooth muscle

Table 1 Characteristics of pancreatic solitary fibrous tumors

No	Ref.	Age	Sex	Pancreatic site	Symptoms	Size (cm)	Pancreatic surgery
1	Lüttges *et al*[1]	50	F	Body	Incidental	55	DP
2	Chatti *et al*[8]	41	M	Body	Abdominal pain	13	DP
3	Gardini *et al*[9]	62	F	Head	Abdominal pain	3	PD
4	Miyamoto *et al*[10]	41	F	Head	Abdominal pain	18 × 15	Enucleation
5	Kwon *et al*[11]	54	M	Body	Incidental	76 × 6	MS
6	Srinivasan *et al*[12]	78	F	Body	Back pain, weight loss	5	DP
7	Chetty *et al*[13]	67	F	Head	Incidental	26	PD
8	Ishiwatari *et al*[14]	58	F	Head	Incidental	3	PD
9	Sugawara *et al*[15]	55	F	Head	Incidental	6 × 4	PD
10	Santos *et al*[16]	40	M	Body	Incidental	3	Enucleation
11	Tasdemir *et al*[17]	24	F	Body	Epigastric pain	11	Enucleation
12	van der *et al*[18]	67	F	Head	Abdominal pain	28 × 16	Enucleation
13	Chen *et al*[19]	49	F	Head	Abdominal pain	13	PD
14	Hwang *et al*[20]	53	F	Head	Incidental	52 × 45 × 40	PHR
15	Baxter *et al*[21]	58	F	Head	Abdominal pain	35 × 3	LPD
16	Estrella *et al*[22]	52	F	Head	Jaundice	15 × 10 × 10	LPD
17	Han *et al*[23]	77	F	Head	Jaundice	15 × 14	Biopsy
18	Murakami *et al*[24]	82	M	Body	Hypokalemia hypertension, edema	6	DP
19	Spasevska *et al*[3]	47	M	Head	jaundice	35 × 2 × 18	LPD
20	Paramythiotis *et al*[7]	55	M	Body	Abdominal pain	31 × 28	DP
21	D'Amico FE *et al*[25]	52	M	Body	Incidental	12	DP
22	Oana *et al*[26]	73	M	Head	Abdominal discomfort	65 × 55	Enucleation
23	Sheng *et al*[27]	1	M	Head	Jaundice	20	DP
24	Geng *et al*[28]	48	M	Body	Hypoglycemia	65 × 5	DP
25	Qian *et al*[29]	46	M	Body	Hypoglycemia	70 × 61	DP
26	Rogers *et al*[30]	37	F	Head	Abdominal pain	23	PD
27	Taguchi *et al*[31]	60	M	Head	Palpable mass	9 × 7 × 7	PD
28	Jariwalla *et al*[32]	64	F	Body	Abdominal pain	19	DP
29	Marotti *et al*[33]	75	F	Body	Incidental	13	Enucleation
30	Addeo *et al*[6]	59	M	Body	Incidental	4	DP
31	Rodriguez *et al*[2]	48	F	Body	Abdominal pain	13 × 10 × 95	TP
32	Jones *et al*[34]	61	F	Body	NA	27	DP
33	Liu *et al*[35]	54	F	Head	Incidental	31 × 23	LDPPHRt
34	Present case	54	M	Body	Incidental	3 × 2	DP

LDPPHRt: Laparoscopic duodenum-preserving pancreatic head resection; Ms: median segmentectomy; PHR: Pancreatic head resection; TP: Total pancreatectomy; PD: Pancreaticoduodenectomy; DP: Distal pancreatectomy.

sarcoma, nerve sheath tumor, and fibrous mucinous sarcoma, respectively) are negative[3]. NAB2-STAT6 fusion is a driver mutation in SFT, where transcriptional repressors of the cytokinesis pathway are converted into transcriptional activators[31,38,39]. STAT6 has a sensitivity of 98% and a specificity of 85% for SFT and is therefore considered the most characteristic SFT marker[40,41]. In our case, the tumor was positive for STAT6, while CD34, bc1-2, vimentin, and CD99 were positive.

Table 2 Histological features and outcomes of pancreatic solitary fibrous tumors

No	Ref.	Immunohistochemistry	Outcome	Follow-up
1	Lüttges *et al*[1]	CD34, CD99, Bcl-2, vimentin	Alive	20 months
2	Chatti *et al*[8]	CD34, CD99, Bcl-2, vimentin	Death	3 d
3	Gardini *et al*[9]	CD34, CD99, Bcl-2, vimentin, SMA	Alive	16 months
4	Miyamoto *et al*[10]	CD34, Bcl-2	Alive	7 months
5	Kwon *et al*[11]	CD34, CD99, vimentin	NA	NA
6	Srinivasan *et al*[12]	CD34, Bcl-2	Alive	7 months
7	Chetty *et al*[13]	CD34, CD99, Bcl-2	42 mo	6 v
8	Ishiwatari *et al*[14]	CD34, Bcl-2	Alive	42 months
9	Sugawara *et al*[15]	CD34	NA	NA
10	Santos *et al*[16]	CD34, betacatenin	NA	NA
11	Tasdemir *et al*[17]	CD34, Bcl-2, beta-catenin, vimentin, Ki67 < 2%	Alive	3 months
12	van der *et al*[18]	CD34, CD99, Bcl-2	NA	NA
13	Chen *et al*[19]	CD34, Bcl-2, vimentin, CD68, muscle-specific actin	Alive	30 months
14	Hwang *et al*[20]	CD34, Bcl-2, muscle-specific actin, CD10, ER, PR	Alive	30 months
15	Baxter *et al*[21]	CD34, Bcl-2	NA	NA
16	Estrella *et al*[22]	CD34, Bcl-2, keratin (rare), p16, p53	Alive	40 months
17	Han *et al*[23]	CD34, CD99	No progression	10 months
18	Murakami *et al*[24]	STAT6, CD34, Bcl-2, ACTH, POMC, NSE	Death	4 months
19	Spasevska *et al*[3]	CD34, vimentin, CD99, Bcl-2, nuclear betacatenin	Death	1 wk
20	Paramythiotis *et al*[7]	CD34, CD99, Bcl-2 vimentin, S-100	Alive	40 months
21	D'Amico FE *et al*[25]	STAT6, CD34	Alive	24 months
22	Oana *et al*[26]	CD34, Bcl-2	Alive	36 months
23	Sheng *et al*[27]	CD34, vimentin, SMA, Ki67 < 3%	Alive	12 months
24	Geng *et al*[28]	STAT6, CD34, Bcl-2, CD31, PHH-3, D2-40, Ki67 > 10%	Alive	6 months
25	Qian *et al*[29]	STAT6, CD34, Bcl-2, Ki67 10%	Alive	10 months
26	Rogers *et al*[30]	STAT6, CD34, Bcl-2, CD99	Alive	4 months
27	Taguchi *et al*[31]	STAT6, CD34, Bcl-2, vimentin, cytokeratin AE1/AE3	Alive	12 months
28	Jariwalla *et al*[32]	STAT6, CD34	NA	NA
29	Marotti *et al*[33]	STAT6, CD34	Alive	6 months
30	Addeo *et al*[6]	STAT6, CD34, Bcl-2, Ki67 7%	NA	NA
31	Rodriguez *et al*[2]	STAT6	Alive	12 months
32	Jones *et al*[34]	STAT6, CD34	Alive	1 months
33	Liu *et al*[35]	CD34, STAT6, CD99	Alive	6 months
34	Present case	TAT6, CD34, Bc1-2, Vimentin, CD99, Ki67 40%	Alive	3 months

STAT6: Signal transducer and activator of transcription 6; ER: Estrogen receptor; PR: Progesterone receptor; SMA: Smooth muscle actin; NA: Not applicable.

In this case, CT showed no enhancement in the arterial phase and heterogeneous enhancement in the venous area. We believe that it should be distinguished from neuroendocrine tumors, which show enhanced CT from the arterial phase to the portal venous phase[13,37], which makes it difficult for us to distinguish the disease, so many scholars before us also misdiagnosed it before surgery[1,10,11,13,26]. At the same time, we believe that it should also be differentiated from pancreatic cancer and solid pseudopapillary tumors of the pancreas. The imaging features of this tumor have been described in detail in our previous work on pancreatic tumors[42].

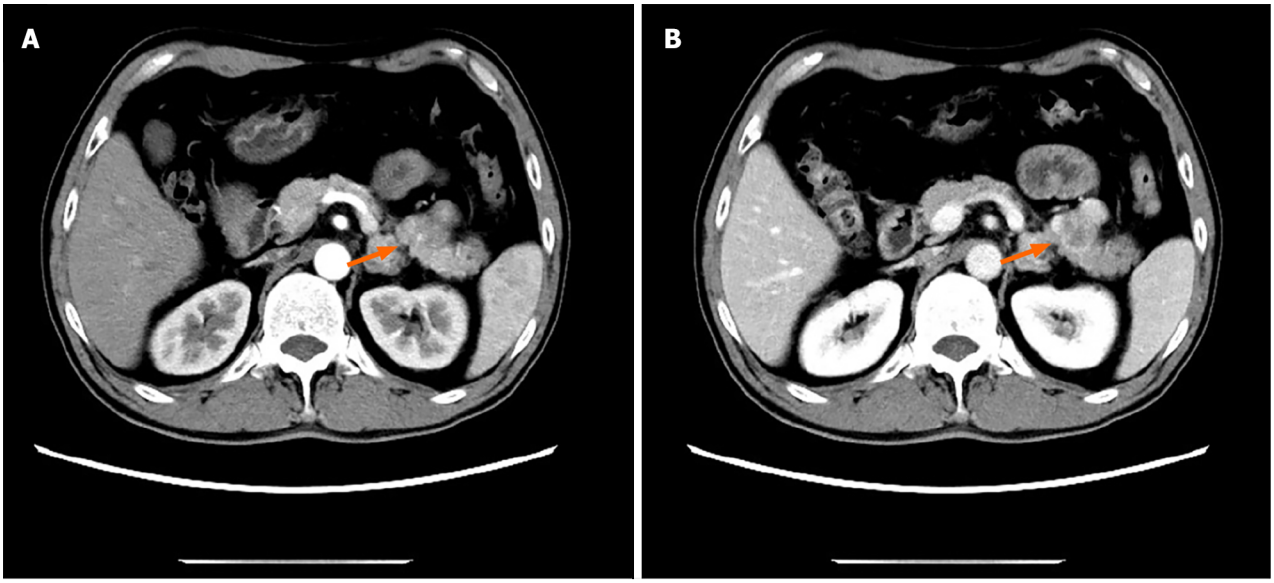

DOI: 10.12998/wjcc.v12.i5.995

Figure 1 Abdominal computed tomography scan showing a 5.52 cm × 2.82 cm × 2 cm mass in the pancreas (orange arrows). A: No enhancement in the arterial region. B: Heterogeneous enhancement in the venous area.

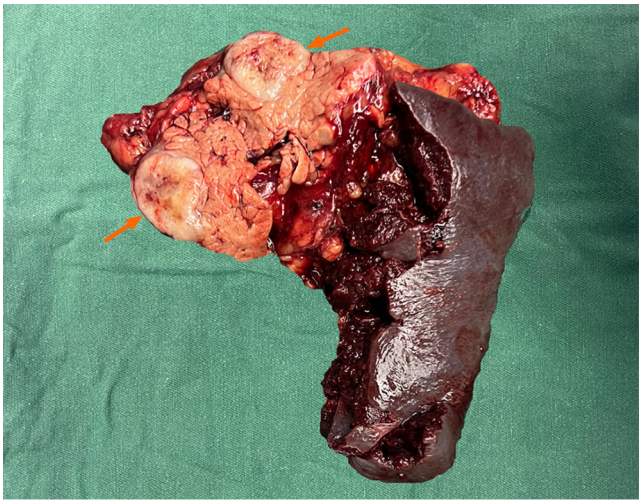

DOI: 10.12998/wjcc.v12.i5.995

Figure 2 Postoperative surgical specimen: Pancreatic tail and spleen (tumor cut open chart) (orange arrows).

Most SFTs are benign[43], and malignant SFTs account for 10%-15%[30,39,44,45]. The histopathological features of malignant SFT: (1) Hypercellularity; (2) more than four mitotic figures per ten high-power fields; (3) nuclear pleomorphism; (4) hemorrhage and necrosis; (5) tumor diameter ≥10 cm; and (6) positive margins[15,21,46]. Ki-67 can also differentiate benign from malignant tumors, with a cutoff value of 0%-5% (indeterminate in 5%-10%) for benign tumors and > 10% for malignant SFTs[40,47]. In our case, our patient had a Ki-67 proliferation index of 40%; therefore, the tumor was possibly malignant. Because SFT of the pancreas is rare, there are no uniform treatment criteria; nevertheless, complete resection is the treatment of choice for intra-abdominal SFTs[1,7,10-12,15], and post-surgical follow-up is critical because SFTs have a high recurrence rate. Due to the increasing number of reported cases of SFT, we believe there will be a complete system of treatment.

CONCLUSION

Because of the non-specific clinical symptoms and radiological features of SFT of the pancreas, the diagnosis is challenging with preoperative radiological and laboratory examinations alone. A definitive diagnosis relies on histopathology and immunohistochemistry. In cases where the tumor is found in the pancreas, and the diagnosis cannot be confirmed, it is recommended to obtain histopathology with ultrasound aspiration. As this presentation is rarely

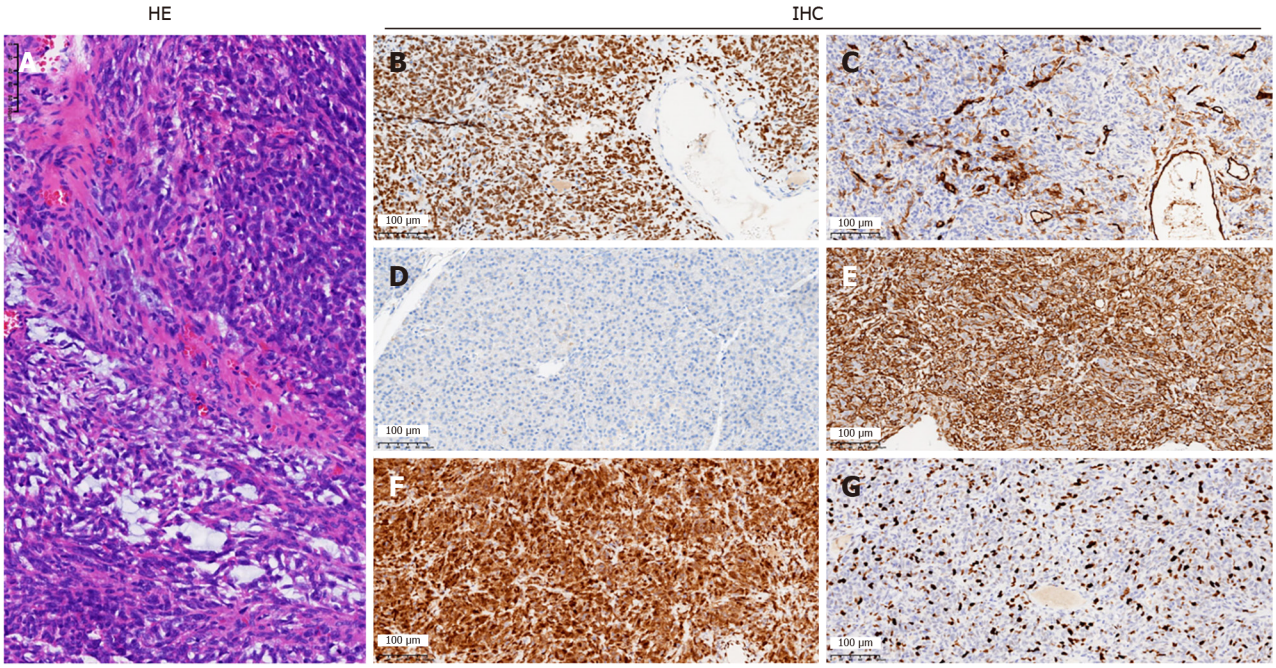

DOI: 10.12998/wjcc.v12.i5.995

Figure 3 Representative results of hematoxylin and eosin and immunohistochemical staining of surgical specimens of solitary fibrous tumor of the pancreas. A: Hematoxylin and Eosin staining (hematoxylin and Shuhong); B: Immunohistochemistry (original magnifcation of × 400) signal transducer and activator of transcription 6; C: CD34; D: CD99; E: Vimentin; F: Vimentin; G: Ki-67.

reported, there is a lack of uniform treatment criteria, and surgery is effective. However, the tumor may lead to potential recurrence or metastasis; therefore, long-term follow-up is recommended.

ACKNOWLEDGEMENTS

We thank the patient's family members for providing detailed treatment information and Dr. Kevin Li for revising the language.

FOOTNOTES

Co-first authors: Wen-Wen Wang and Xiang Wu.

Co-corresponding authors: Xin-Hua Zhou and Li-Li Qiu.

Author contributions: Wang WW, Zhou SP and Wu X, investigation, data curation, writing-original draft; Wang LL investigation, provide image pictures; Ruan Y investigation, funding acquisition, medical history collection; Lu J investigation, supervision; Li HL pathology to provide; Ni XL pathology to provide; Qiu LL and Zhou XH resources, writing-review and editing, supervision, project administration funding acquisition; all authors read and approved the final manuscript. The author contributions of Wang WW and Wu X as co-first authors, Qiu LL and Zhou XH as corresponding authors are as follows: Wang WW and Wu X are co-first authors because they made equal contributions to the research and were involved in all stages of the study, from design to data collection and analysis. They both contributed significantly to the writing of the manuscript and are responsible for the accuracy and validity of the results reported. Qiu LL and Zhou XH are corresponding authors because they supervised the research project, provided guidance and expertise throughout the study, and ensured the quality and reliability of the data presented. As senior researchers, they are responsible for the overall content and implications of the study and act as points of contact for further information or queries.

Informed consent statement: Informed written consent was obtained from the patient for publication of this report and any accompanying images.

Conflict-of-interest statement: The authors declare that they have no conflict of interest.

CARE Checklist (2016) statement: The authors have read the CARE Checklist (2016), and the manuscript was prepared and revised according to the CARE Checklist (2016).

Country/Territory of origin: China

ORCID number: Xiang Wu 0000-0002-2134-1184; Jun Lu 0000-0001-6225-1225; Xin-Hua Zhou 0000-0001-6707-9655.

S-Editor: Qu XL
L-Editor: A
P-Editor: Yu HG

REFERENCES

1 **Lüttges J**, Mentzel T, Hübner G, Klöppel G. Solitary fibrous tumour of the pancreas: a new member of the small group of mesenchymal pancreatic tumours. *Virchows Arch* 1999; **435**: 37-42 [PMID: 10431844 DOI: 10.1007/s004280050392]
2 **Rodríguez AH**, Martino MD, Mazeyra MV, Martín-Pérez E. Solitary fibrous tumor of the pancreas. *Autops Case Rep* 2021; **11**: e2021245 [PMID: 34307213 DOI: 10.4322/acr.2021.245]
3 **Spasevska L**, Janevska V, Janevski V, Noveska B, Zhivadinovik J. Solitary Fibrous Tumor of the Pancreas: A Case Report and Review of the Literature. *Pril (Makedon Akad Nauk Umet Odd Med Nauki)* 2016; **37**: 115-120 [PMID: 27883325 DOI: 10.1515/prilozi-2016-0024]
4 **Xie GY**, Zhu HB, Jin Y, Li BZ, Yu YQ, Li JT. Solitary fibrous tumor of the liver: A case report and review of the literature. *World J Clin Cases* 2022; **10**: 7097-7104 [PMID: 36051139 DOI: 10.12998/wjcc.v10.i20.7097]
5 **Afzal A**, Maldonado-Vital M, Khan S, Farooque U, Luo W. Solitary Fibrous Tumor of Pancreas With Unusual Features: A Case Report. *Cureus* 2020; **12**: e10833 [PMID: 33173639 DOI: 10.7759/cureus.10833]
6 **Addeo P**, Averous G, Bachellier P. Solitary Fibrous Tumor of the Pancreas. *J Gastrointest Surg* 2021; **25**: 569-570 [PMID: 32583321 DOI: 10.1007/s11605-020-04698-0]
7 **Paramythiotis D**, Kofina K, Bangeas P, Tsiompanou F, Karayannopoulou G, Basdanis G. Solitary fibrous tumor of the pancreas: Case report and review of the literature. *World J Gastrointest Surg* 2016; **8**: 461-466 [PMID: 27358679 DOI: 10.4240/wjgs.v8.i6.461]
8 **Chatti K**, Nouira K, Ben Reguigua M, Bedioui H, Oueslati S, Laabidi B, Alaya M, Ben Abdallah N. [Solitary fibrous tumor of the pancreas. A case report]. *Gastroenterol Clin Biol* 2006; **30**: 317-319 [PMID: 16565671 DOI: 10.1016/s0399-8320(06)73174-8]
9 **Gardini A**, Dubini A, Saragoni L, Padovani F, Garcea D. [Benign solitary fibrous tumor of the pancreas: a rare location of extra-pleural fibrous tumor. Single case report and review of the literature]. *Pathologica* 2007; **99**: 15-18 [PMID: 17566307]
10 **Miyamoto H**, Molena DA, Schoeniger LO, Haodong Xu. Solitary fibrous tumor of the pancreas: a case report. *Int J Surg Pathol* 2007; **15**: 311-314 [PMID: 17652547 DOI: 10.1177/1066896907302419]
11 **Kwon HJ**, Byun JH, Kang J, Park SH, Lee MG. Solitary fibrous tumor of the pancreas: imaging findings. *Korean J Radiol* 2008; **9** Suppl: S48-S51 [PMID: 18607126 DOI: 10.3348/kjr.2008.9.s.s48]
12 **Srinivasan VD**, Wayne JD, Rao MS, Zynger DL. Solitary fibrous tumor of the pancreas: case report with cytologic and surgical pathology correlation and review of the literature. *JOP* 2008; **9**: 526-530 [PMID: 18648147]
13 **Chetty R**, Jain R, Serra S. Solitary fibrous tumor of the pancreas. *Ann Diagn Pathol* 2009; **13**: 339-343 [PMID: 19751911 DOI: 10.1016/j.anndiagpath.2009.02.006]
14 **Ishiwatari H**, Hayashi T, Yoshida M, Kuroiwa G, Sato Y, Kobune M, Takimoto R, Kimura Y, Hasegawa T, Hirata K, Kato J. [A case of solitary fibrous tumor of the pancreas]. *Nihon Shokakibyo Gakkai Zasshi* 2009; **106**: 1078-1085 [PMID: 19578317]
15 **Sugawara Y**, Sakai S, Aono S, Takahashi T, Inoue T, Ohta K, Tanada M, Teramoto N. Solitary fibrous tumor of the pancreas. *Jpn J Radiol* 2010; **28**: 479-482 [PMID: 20661701 DOI: 10.1007/s11604-010-0453-x]
16 **Santos LA**, Santos VM, Oliveira OC, De Marco M. Solitary fibrous tumour of the pancreas: a case report. *An Sist Sanit Navar* 2012; **35**: 133-136 [PMID: 22552135 DOI: 10.4321/s1137-66272012000100013]
17 **Tasdemir A**, Soyuer I, Yurci A, Karahanli I, Akyildiz H. A huge solitary fibrous tumor localized in the pancreas: a young women. *JOP* 2012; **13**: 304-307 [PMID: 22572138]
18 **van der Vorst JR**, Vahrmeijer AL, Hutteman M, Bosse T, Smit VT, van de Velde CJ, Frangioni JV, Bonsing BA. Near-infrared fluorescence imaging of a solitary fibrous tumor of the pancreas using methylene blue. *World J Gastrointest Surg* 2012; **4**: 180-184 [PMID: 22905287 DOI: 10.4240/wjgs.v4.i7.180]
19 **Chen JW**, Lü T, Liu HB, Tong SX, Ai ZL, Suo T, Ji Y. A solitary fibrous tumor in the pancreas. *Chin Med J (Engl)* 2013; **126**: 1388-1389 [PMID: 23557579]
20 **Hwang JD**, Kim JW, Chang JC. Imaging Findings of a Solitary Fibrous Tumor in Pancreas: A Case Report. *J Korean Soc Radiol* 2014; **70** [DOI: 10.3348/jksr.2014.70.1.53]
21 **Baxter AR**, Newman E, Hajdu CH. Solitary fibrous tumor of the pancreas. *J Surg Case Rep* 2015; **2015** [PMID: 26628714 DOI: 10.1093/jscr/rjv144]
22 **Estrella JS**, Wang H, Bhosale PR, Evans HL, Abraham SC. Malignant Solitary Fibrous Tumor of the Pancreas. *Pancreas* 2015; **44**: 988-994 [PMID: 26166470 DOI: 10.1097/MPA.0000000000000350]
23 **Han SH**, Baek YH, Han SY, Lee SW, Jeong JS, Cho JH, Kwon HJ. Solitary Fibrous Tumor of the Pancreas: A Case Report and Review of the Literature. *Korean J Med* 2015; **88** [DOI: 10.3904/kjm.2015.88.3.293]
24 **Murakami K**, Nakamura Y, Felizola SJ, Morimoto R, Satoh F, Takanami K, Katakami H, Hirota S, Takeda Y, Meguro-Horike M, Horike S, Unno M, Sasano H. Pancreatic solitary fibrous tumor causing ectopic adrenocorticotropic hormone syndrome. *Mol Cell Endocrinol* 2016; **436**: 268-273 [PMID: 27585487 DOI: 10.1016/j.mce.2016.08.044]
25 **D'Amico FE**, Ruffolo C, Romano M, DI Domenico M, Sbaraglia M, Dei Tos AP, Garofalo T, Giordano A, Bassi I, Massani M. Rare Neoplasm Mimicking Neuoroendocrine Pancreatic Tumor: A Case Report of Solitary Fibrous Tumor with Review of the Literature. *Anticancer Res* 2017; **37**: 3093-3097 [PMID: 28551649 DOI: 10.21873/anticanres.11665]

26 **Oana S**, Matsuda N, Sibata S, Ishida K, Sugai T, Matsumoto T. A case of a "wandering" mobile solitary fibrous tumor occurring in the pancreas. *Clin J Gastroenterol* 2017; **10**: 535-540 [PMID: 28956313 DOI: 10.1007/s12328-017-0774-8]

27 **Sheng Q**, Xu W, Liu J, Shen B, Deng X, Wu Y, Wu W, Yu S, Wang X, Lv Z. Pancreatic solitary fibrous tumor in a toddler managed by pancreaticoduodenectomy: a case report and review of the literature. *Onco Targets Ther* 2017; **10**: 1853-1858 [PMID: 28392706 DOI: 10.2147/OTT.S133650]

28 **Geng H**, Ye Y, Jin Y, Li BZ, Yu YQ, Feng YY, Li JT. Malignant solitary fibrous tumor of the pancreas with systemic metastasis: A case report and review of the literature. *World J Clin Cases* 2020; **8**: 343-352 [PMID: 32047784 DOI: 10.12998/wjcc.v8.i2.343]

29 **Qian X**, Zhou D, Gao B, Wang W. Metastatic solitary fibrous tumor of the pancreas in a patient with Doege-Potter syndrome. *Hepatobiliary Surg Nutr* 2020; **9**: 112-115 [PMID: 32140495 DOI: 10.21037/hbsn.2019.12.01]

30 **Rogers C**, Samore W, Pitman MB, Chebib I. Solitary fibrous tumor involving the pancreas: report of the cytologic features and first report of a primary pancreatic solitary fibrous tumor diagnosed by fine-needle aspiration biopsy. *J Am Soc Cytopathol* 2020; **9**: 272-277 [PMID: 32423685 DOI: 10.1016/j.jasc.2020.02.001]

31 **Taguchi Y**, Hara T, Tamura H, Ogiku M, Watahiki M, Takagi T, Harada T, Miyazaki S, Hayashi T, Kanai T, Mori H, Ozawa T, Nishiwaki Y. Malignant solitary fibrous tumor of the pancreas: a case report. *Surg Case Rep* 2020; **6**: 287 [PMID: 33188464 DOI: 10.1186/s40792-020-01067-6]

32 **Jariwalla NR**, Park N, El Hage Chehade N, Truong A, Choi AY, Samarasena J. Solitary Fibrous Tumor of the Pancreas: Really? 2021; 116: S686 [DOI: 10.14309/01.ajg.0000779548.39251.46]

33 **Marotti JD**, Liu X, Jamot S, Gardner TB, Gordon SR, Kerr DA. Solitary fibrous tumor of the pancreas clinically mimicking a pancreatic neuroendocrine tumor: Cytologic pitfalls when a transgastric approach is utilized. *Diagn Cytopathol* 2021; **49**: E405-E409 [PMID: 34390624 DOI: 10.1002/dc.24834]

34 **Jones VM**, Wangsiricharoen S, Cornea V, Bocklage TJ, Ali SZ, Allison DB. Cytopathological characteristics of solitary fibrous tumour involving the pancreas by fine needle aspiration: Making an accurate preoperative diagnosis in an uncommon location. *Cytopathology* 2022; **33**: 222-229 [PMID: 34551176 DOI: 10.1111/cyt.13061]

35 **Liu W**, Wu S, Cai Y, Peng B. Total laparoscopic duodenum-preserving pancreatic head resection for solitary fibrous tumor: The first case report. *Asian J Surg* 2022; **45**: 651-652 [PMID: 34823990 DOI: 10.1016/j.asjsur.2021.11.010]

36 **Gold JS**, Antonescu CR, Hajdu C, Ferrone CR, Hussain M, Lewis JJ, Brennan MF, Coit DG. Clinicopathologic correlates of solitary fibrous tumors. *Cancer* 2002; **94**: 1057-1068 [PMID: 11920476]

37 **Yamashita H**, Fujino Y, Ohara T, Kakinoki K, Sugimoto T, Kajimoto K, Tominaga M. A rare case of metastatic solitary fibrous tumor of the pancreas manifesting as a cystic neoplasm: a case report. *Surg Case Rep* 2019; **5**: 142 [PMID: 31520184 DOI: 10.1186/s40792-019-0699-1]

38 **Thway K**, Ng W, Noujaim J, Jones RL, Fisher C. The Current Status of Solitary Fibrous Tumor: Diagnostic Features, Variants, and Genetics. *Int J Surg Pathol* 2016; **24**: 281-292 [PMID: 26811389 DOI: 10.1177/1066896915627485]

39 **Li J**, Li J, Xiong Y, Xu T, Xu J, Li Q, Yang G. Atypical/malignant solitary fibrous tumor of the pancreas with spleen vein invasion: Case report and literature review. *Medicine (Baltimore)* 2020; **99**: e19783 [PMID: 32332621 DOI: 10.1097/MD.0000000000019783]

40 **Krsková L**, Odintsov I, Fabián O, Hroudová P, Mrhalová M. Determination of biological behavior of solitary fibrous tumors: correlation of expression of Ki-67, TPX2 and TERT mRNA subunit level and NAB2-STAT6 fusion compared to morphological aspects of SFTs. *Neoplasma* 2022; **69**: 28-35 [PMID: 34818026 DOI: 10.4149/neo_2021_210511N642]

41 **Yoshida A**, Tsuta K, Ohno M, Yoshida M, Narita Y, Kawai A, Asamura H, Kushima R. STAT6 immunohistochemistry is helpful in the diagnosis of solitary fibrous tumors. *Am J Surg Pathol* 2014; **38**: 552-559 [PMID: 24625420 DOI: 10.1097/PAS.0000000000000137]

42 **Wu X**, Zhou S, Zhou X, Xu X, Wang L, Ruan Y, Lu J, Li H, Xu H, Ma X. Literature review of imaging, pathological diagnosis, and outcomes of metachronous lung and pancreatic metastasis of cecal cancer. *World J Surg Oncol* 2022; **20**: 341 [PMID: 36253824 DOI: 10.1186/s12957-022-02797-7]

43 **Zambo I**, Veselý K. [WHO classification of tumours of soft tissue and bone 2013: the main changes compared to the 3rd edition]. *Cesk Patol* 2014; **50**: 64-70 [PMID: 24758500]

44 **Demicco EG**, Wagner MJ, Maki RG, Gupta V, Iofin I, Lazar AJ, Wang WL. Risk assessment in solitary fibrous tumors: validation and refinement of a risk stratification model. *Mod Pathol* 2017; **30**: 1433-1442 [PMID: 28731041 DOI: 10.1038/modpathol.2017.54]

45 **Folpe AL**, Devaney K, Weiss SW. Lipomatous hemangiopericytoma: a rare variant of hemangiopericytoma that may be confused with liposarcoma. *Am J Surg Pathol* 1999; **23**: 1201-1207 [PMID: 10524520 DOI: 10.1097/00000478-199910000-00004]

46 **Sikri V**, Chawla R. Solitary fibrous tumour of the pleura. *Indian J Chest Dis Allied Sci* 2013; **55**: 167-169 [PMID: 24380226]

47 **Robinson LA**. Solitary fibrous tumor of the pleura. *Cancer Control* 2006; **13**: 264-269 [PMID: 17075563 DOI: 10.1177/107327480601300403]

World Journal of Clinical Cases

Submit a Manuscript: https://www.f6publishing.com

World J Clin Cases 2024 February 16; 12(5): 1004-1009

DOI: 10.12998/wjcc.v12.i5.1004

ISSN 2307-8960 (online)

CASE REPORT

Neuroimaging features in a patient with non-ketotic hyperglycaemic seizures: A case report

Jing Wu, Huijie Feng, Yaxiong Zhao, Junfeng Li, Ting Li, Kefeng Li

Specialty type: Neuroimaging

Provenance and peer review: Unsolicited article; Externally peer reviewed.

Peer-review model: Single blind

Peer-review report's scientific quality classification

Grade A (Excellent): 0
Grade B (Very good): B
Grade C (Good): C
Grade D (Fair): 0
Grade E (Poor): 0

P-Reviewer: Tuncyurek O, Cyprus; Yarmahmoodi F, Iran

Received: October 27, 2023
Peer-review started: October 27, 2023
First decision: November 28, 2023
Revised: December 27, 2023
Accepted: January 17, 2024
Article in press: January 17, 2024
Published online: February 16, 2024

Jing Wu, Huijie Feng, Yaxiong Zhao, Junfeng Li, Ting Li, Department of Radiology, Heping Hospital Affiliated to Changzhi Medical College, Changzhi 046000, Shanxi Province, China

Jing Wu, Huijie Feng, Yaxiong Zhao, Junfeng Li, Ting Li, Changzhi Key Lab of Functional Imaging for Brain Diseases, Heping Hospital Affiliated to Changzhi Medical College, Changzhi 046000, Shanxi Province, China

Kefeng Li, Faculty of Applied Sciences, Macao Polytechnic University, Macau 999078, China

Corresponding author: Kefeng Li, PhD, Associate Professor, Faculty of Applied Sciences, Macao Polytechnic University, R. de Luís Gonzaga Gomes, Macau 999078, China.
kefengl@mpu.edu.mo

Abstract

BACKGROUND

Non-ketotic hyperglycaemic (NKH) seizures are a rare neurological complication of diabetes caused by hyperglycaemia in non-ketotic and non-hyperosmotic states. The clinical characteristics of NKH seizures are atypical and lack unified diagnostic criteria, leading to potential misdiagnoses in the early stages of the disease.

CASE SUMMARY

This report presents a rare case of NKH seizures in a 52-year-old male patient with a history of type 2 diabetes mellitus. We performed comprehensive magnetic resonance imaging (MRI) studies at admission, 12 d post-admission, and 20 d post-discharge. The imaging techniques included contrast-enhanced head MRI, T2-weighted imaging (T2WI), fluid-attenuated inversion recovery (FLAIR), diffusion-weighted imaging, susceptibility-weighted imaging, magnetic resonance spectroscopy (MRS), and magnetic resonance venography. At the time of admission, T2WI and FLAIR of the cranial MRI showed that the left parieto-occipital cortex had gyrus-like swelling and high signal, and subcortical stripes had low signal. MRS showed a reduced N-acetylaspartate peak and increased creatine and choline peaks in the affected areas. A follow-up MRI 20 d later showed that the swelling and high signal of the left parieto-occipital cortex had disappeared, and the low signal of the subcortex had disappeared.

CONCLUSION

This case study provides valuable insights into the potential pathogenesis, diagnosis, and treatment of NKH seizures. The comprehensive MRI findings

highlight the potential utility of various MRI sequences in diagnosing and characterizing NKH seizures.

Key Words: Non-ketotic hyperglycaemia seizures; Magnetic resonance imaging; Magnetic resonance spectroscopy; Diabetes; Case report

Core Tip: This study presents a rare case of non-ketotic hyperglycaemic (NKH) seizures in a patient with type 2 diabetes. These seizures are a complication of diabetes, though they lack specific diagnostic criteria and are often misdiagnosed. In particular, the magnetic resonance imaging (MRI) findings of these manifestation have rarely been described in the literature, and previous reports are inconsistent. In this report, we describe the comprehensive findings in several MRI sequences, including T2-weighted images, fluid-attenuated inversion recovery, diffusion-weighted imaging, susceptibility-weighted imaging, and magnetic resonance spectroscopy and venography. We believe that our study makes a significant contribution to the literature because these findings can help elucidate the pathogenesis, diagnosis, and treatment of this rare condition. Further, we believe that this paper will be of interest to the readership of your journal because this case report expands the clinical knowledge on NKH seizures, a rare but severe complication of diabetes.

Citation: Wu J, Feng H, Zhao Y, Li J, Li T, Li K. Neuroimaging features in a patient with non-ketotic hyperglycaemic seizures: A case report. *World J Clin Cases* 2024; 12(5): 1004-1009
URL: https://www.wjgnet.com/2307-8960/full/v12/i5/1004.htm
DOI: https://dx.doi.org/10.12998/wjcc.v12.i5.1004

INTRODUCTION

Non-ketotic hyperglycaemia (NKH) is a rare clinical syndrome characterised by hyperglycaemia, serum hyperosmolarity, and intracellular dehydration with no ketoacidosis. NKH mainly affects patients with type 2 diabetes over 50 years of age and is often considered a complication of this metabolic disease in patients with poor glycaemic control or in undiagnosed patients as a first symptom[1].

NKH seizures are associated with various neurological manifestations, including epilepsy, headache, consciousness and vision alterations, and movement disorders. Magnetic resonance imaging (MRI) is a valuable tool for the accurate diagnosis of NKH seizures; however, findings from head imaging studies are inconsistent. Some researchers have suggested that unilateral subcortical hypointensities in T2-weighted imaging (T2WI) or fluid-attenuated inversion recovery (FLAIR) sequences are a characteristic MRI feature of NKH seizures, whereas others did not observe these findings[2,3]. Other MRI features reported in the literature include subcortical hypointense shadows on susceptibility-weighted imaging (SWI), focal enhancement of the pia mater and local cortex, and in arterial spin labelling sequences, enhancement of focal cerebral parenchyma perfusion[3-5]. Nevertheless, more extensive MRI evidence with multiple sequences is necessary to characterise and comprehensively understand the pathogenesis of NKH seizures.

Here, we present a rare case of NKH seizures in a patient. We also review the comprehensive MRI characteristics of this patient, including contrast-enhanced head MRI, T2WI, FLAIR, diffusion-weighted imaging (DWI), SWI, magnetic resonance spectroscopy (MRS), and magnetic resonance venography (MRV).

CASE PRESENTATION

Chief complaints

Dizziness for three days, aggravated with general convulsions for two hours.

History of present illness

A 52-year-old man with a one-year history of type 2 diabetes mellitus developed dizziness of unknown aetiology, accompanied by lethargy, poor mental status, and delayed reactions. The patient self-administered 'cold and flu capsules', although the dizziness symptoms persisted. On the second day, the patient experienced weakness and numbness in the right upper limb during work, accompanied by dizziness. This right upper extremity symptom manifested as weakness/difficulty in fine movements, such as holding chopsticks, with conserved lifting ability. The upper extremity and dizziness symptoms were not accompanied by altered consciousness or convulsions and resolved spontaneously after approximately one hour.

Three days later, the patient presented to the emergency room with worsening symptoms. During the consultation, the patient was in and out of consciousness, with delayed and inappropriate responses, subsequent involuntary lifting of the right upper limb, flexion and tonicity of the limbs with clonus, mouth foaming, upward gaze, and clenched teeth for more than 10 min. The symptoms were relieved with an intramuscular injection of sodium phenobarbital. Upon regaining full

consciousness, the patient was able to communicate and answer questions correctly.

The patient was admitted to the neurology department for further treatment. Admission vital signs and neurological examination were normal.

History of past illness

History of "diabetes mellitus" for 1 year, complaining of fair glycaemic control.

Personal and family history

No special notes.

Physical examination

Admission vital signs and neurological examination were normal.

Laboratory examinations

His admission blood glucose level was 329.4 mg/dL, and a cerebrospinal fluid sample showed a glucose level of 138.2 mg/dL, with negative tests for antibodies associated with autoimmune encephalitis and paraneoplastic syndrome. Blood glucose levels fluctuated between 129.6 and 351.0 mg/dL after admission.

Imaging examinations

A head MRI at admission showed a slight hyperintensity in the left parieto-occipital cortex and a subcortical hypointense line in T2WI and FLAIR images (Figure 1A and B). DWI revealed a limited diffusion-restricted signal in the same area and a reduced apparent diffusion coefficient (ADC map) (Figure 1C and D). MRS revealed a reduced N-acetylaspartate (NAA) peak and increased creatine and choline peaks in the left parietal-occipital cortex and subcortical areas, suggesting neuronal damage and metabolic encephalopathy (Figure 1E–H). Contrast-enhanced MRI showed swelling of the left parieto-occipital gyrus and localized soft meningeal enhancement in the parietal lobe (Figure 1I and 1J). No significant alterations were noted on SWI (Figure 1K) and MRV. Non-ketotic hyperglycaemia-associated epilepsy is difficult to identify and is even misdiagnosed in the emergency medical setting. It is distinguished from major acute infarction stroke, reversible posterior encephalopathy syndrome, encephalitis, and meningitis by the richness of cranial nuclear magnetic sequence manifestations in conjunction with clinical test indices. On day 5 of hospitalization, an electroencephalogram (EEG) revealed bilateral spike emanations in the frontal and central regions, asynchronous left and right sides, and multiple slow-wave activities in the left parietal, occipital, and temporal regions. These EEG alterations were consistent with the cortical swelling seen on MRI.

FINAL DIAGNOSIS

Non-ketotic hyperglycaemia-associated epilepsy.

TREATMENT

Following admission, the patient was treated with antiepileptic drugs *via* an intramuscular injection of 200 mg of phenobarbital sodium and antidiabetic therapy consisting of 10 mg of dapagliflozin taken orally once a day, 0.5 g of metformin hydrochloride extended-release tablets taken twice a day, and 4–6 IU of subcutaneous insulin given once a day in case of poor glycaemic control, as well as fluid supplementation to improve blood circulation.

OUTCOME AND FOLLOW-UP

MRI after 12 d of treatment showed alleviation of the subcortical hypointense T2 signal (Figure 1L). The hyperintensity observed on FLAIR images in the left parieto-occipital cortex was more pronounced than that seen on the MRI upon admission (Figure 1M). The performance of DWI and ADC did not change significantly from the images taken on admission (Figure 1N and O).

The patient did not experience any further seizures after admission and was discharged after 2 wk, continuing the diabetes treatment and blood glucose monitoring at home. A follow-up MRI 20 d later showed disappearance of the swelling and hyperintensity in the left parieto-occipital cortex and of the subcortical hypointensities seen on T2WI and FLAIR images (Figure 1P and Q).

DISCUSSION

Currently, no diagnostic criteria for NKH seizures have been established. Previous case studies show that blood glucose, osmolality, and haemoglobin A1c levels are often elevated in patients with NKH seizures. However, the degree of

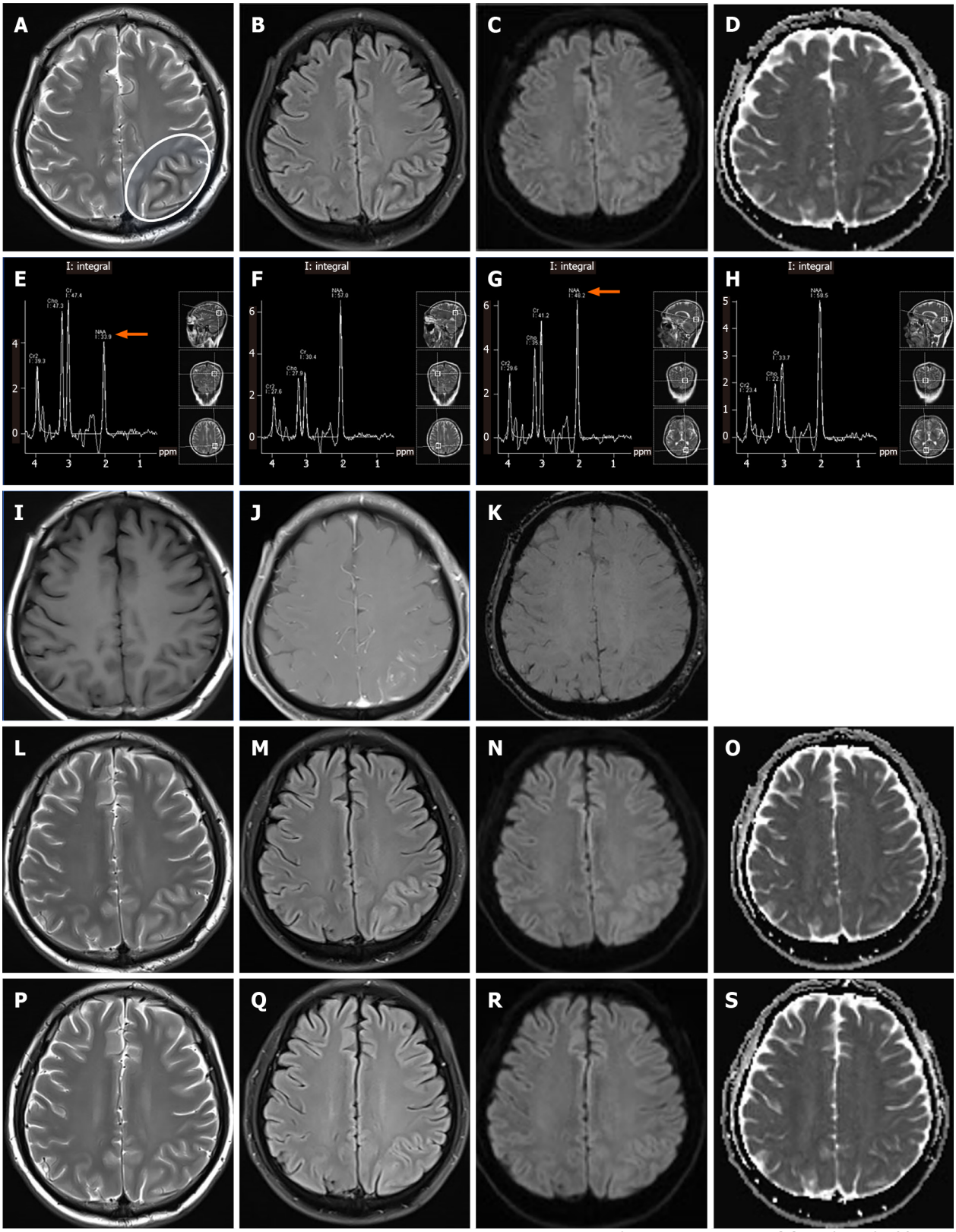

DOI: 10.12998/wjcc.v12.i5.1004

Figure 1 Head magnetic resonance imaging findings of a patient with non-ketotic hyperglycaemic seizures with hyperhomocysteinaemia. A-D: Images at admission, showing the left parieto-occipital cortex (white arrow) on (A) T2-weighted images (T2WI) and (B) fluid-attenuated inversion recovery (FLAIR) sequence with cortical swelling and hyperintense T2 signal. (C) Diffusion-weighted imaging (DWI) shows restricted diffusion in the left parieto-occipital cortex and (D) low signal in the apparent diffusion coefficient (ADC) map; E–H: Magnetic resonance spectroscopy (MRS) images on the day after admission, showing (E) decreased N-acetylaspartate (NAA) peaks (white arrows) in the left parieto-occipital subcortex, increased creatine (Cr) and choline (Cho) peak, and (F) no significant alterations in the right parieto-occipital subcortex. MRS also showed (G) decreased NAA peaks (white arrows) in the left parieto-occipital cortex, and increased Cr and Cho peaks, less evident than in the corresponding subcortex in panel (E). (H) The right parieto-occipital cortex showed no significant alterations; I–K: Contrast-enhanced magnetic resonance imaging (MRI) images on the day after admission, showing no significant alterations on (E) T1-weighted images, with swelling of the

left parieto-occipital gyrus and localized soft meningeal enhancement in the parietal lobe (J). No significant alterations were noted on susceptibility-weighted imaging (K); L–O: MRI findings after 12 d of treatment, showing alleviation of the subcortical hypointensities on (L) T2WI and (M) FLAIR images, with more pronounced hyperintensity in the left parieto-occipital cortex in the latter than at admission. (N) DWI and (O) ADC map showed no significant changes; P–S: Follow-up MRI images 20 d after discharge, showing normalisation of the left parieto-occipital cortex and subcortical areas on (P) T2WI and (Q) FLAIR images. (R) DWI and (S) ADC map showed no significant alterations.

elevation varies from case to case, with the majority of patients having only moderate hyperglycaemia, without significant hyperosmolality, and not meeting the diagnostic criteria for hyperosmolar hyperglycaemia syndrome (plasma glucose level of ≥ 600 mg/dL, serum osmolality of ≥ 320 mOsm/kg)[6]. This suggests that prolonged hyperglycaemia may lead to seizures rather than extreme hyperglycaemia, which is associated with an acute seizure[7].

In the present case, MRS revealed a decrease in NAA and an increase in creatine and choline in the affected cortical and subcortical regions compared to the contralateral regions. To our knowledge, these findings represent the first MRS report of non-ketotic hyperglycaemia-related epileptic brain lesions. NAA is a biomarker of neuronal density and survival, reflecting the functional status of neurones, whereas creatine is a biomarker of energy-dependent brain cell systems, which increases in low metabolic states. Choline is involved in cell membrane synthesis and metamorphosis, reflecting cell membrane renewal as a component of phospholipid metabolism[8]. Overall, these findings highlight the potential utility of MRS in the diagnosis and characterisation of NKH seizures.

Reversible subcortical T2WI/FLAIR hypointense areas are a specific manifestation of non-ketotic hyperglycaemia-related epilepsy, often attributed to iron deposition or free radicals[4]. The exact aetiology of this manifestation remains unclear; however, some patients present hypointensities in SWI sequences related to astrocyte dysfunction, which leads to iron deposition due to astrocyte involvement in the regulation of iron molecule inflow and outflow[9]. In the present case, no mineral-related hypointense alterations were found in the SWI sequence, suggesting that the short-term accumulation of free radicals due to axonal damage in excitatory neurones caused the lesions. This accumulation can cause T2 shortening effects, resulting in subcortical T2/FLAIR undersignalling[10].

Limited cortical diffusion signal and T2WI/FLAIR hyperintensities are common imaging signs of seizures. Decreased cortical diffusion signals reflect cytotoxic oedema, whereas T2WI/FLAIR cortical hyperintensity is associated with vasogenic oedema resulting from increased blood–brain barrier permeability. Vasogenic cerebral oedema is caused by increased capillary permeability due to damage and disruption of the blood–brain barrier, increased water exudation, and accumulation in the perivascular and intercellular spaces. The cerebral pia mater enhancement confirmed the altered permeability in the present case.

The current treatment of NKH seizures focuses on glycaemic control and maintaining stable blood glucose in an effort to prevent, reduce, and control seizures. However, the use of antiepileptic drugs remains controversial. Available case reports have found that most patients are poorly treated with antiepileptic drugs alone and that antiepileptic drugs, such as phenytoin sodium, cause insulin resistance and elevated blood glucose levels, leading to decreased antiepileptic effects and NKH-associated exacerbation of epilepsy[11]. The disease has a favourable prognosis; poor glycaemic control is the main cause of its recurrence. NKH seizures are difficult to recognize and can be misdiagnosed in the emergency medical setting due to a lack of awareness, making early and accurate recognition and appropriate treatment important.

CONCLUSION

We have reported a case of NHK-related seizures, focusing on detailed characteristics derived from various MRI sequences. This case study provides valuable insights into the pathogenesis, diagnostic processes, and potential treatment strategies for this rare condition. Our findings underscore the importance of comprehensive MRI analysis in managing complex neurological presentations associated with metabolic disorders, paving the way for future research in this field.

ACKNOWLEDGEMENTS

We are grateful to the patient and his family for their collaboration.

FOOTNOTES

Co-corresponding authors: Kefeng Li and Ting Li.

Author contributions: Wu J, Feng H, Zhao Y, and Li K conceived the article and wrote the manuscript draft; Wu J, Li J, and Li T were involved in the clinical care of the patient. Both Li T and Li K have played important and indispensable roles in the experimental design, data interpretation and manuscript preparation as the co-corresponding authors. Li T conceptualized, designed, and supervised the whole process of the project. Li K was instrumental and responsible for data re-analysis and re-interpretation, figure plotting, comprehensive literature search, preparation and submission of the current version of the manuscript. This collaboration between Li K and Li T is crucial for the publication of this manuscript and other manuscripts still in preparation. All authors critically reviewed the manuscript for intellectual content and edited the article.

Supported by Four "Batches" Innovation Project of Invigorating Medical Through Science and Technology of Shanxi Province, No. 2023XM016.

Informed consent statement: Informed consent for publication was obtained from the patient's guardian.

Conflict-of-interest statement: All the authors declare that they have no conflict of interest.

CARE Checklist (2016) statement: The authors have read the CARE Checklist (2016), and the manuscript was prepared and revised according to the CARE Checklist (2016).

Country/Territory of origin: China

ORCID number: Ting Li 0009-0004-7713-3319; Kefeng Li 0000-0002-7233-4347.

S-Editor: Liu JH
L-Editor: A
P-Editor: Yu HG

REFERENCES

1 **Hennis A**, Corbin D, Fraser H. Focal seizures and non-ketotic hyperglycaemia. *J Neurol Neurosurg Psychiatry* 1992; **55**: 195-197 [PMID: 1564479 DOI: 10.1136/jnnp.55.3.195]
2 **Licchetta L**, Ferri L, Morsillo F, Faustini-Fustini M, Toni F, Pondrelli F, Nonino F, Bisulli F, Tinuper P. Clinical characterization of non-ketotic hyperglycemia-related seizures: A systematic review and individual participant data meta-analysis. *Seizure* 2023; **106**: 50-57 [PMID: 36773573 DOI: 10.1016/j.seizure.2023.01.018]
3 **Peddawad D**. Epileptic manifestations, pathophysiology, and imaging characteristics of non-ketotic hyperglycaemia: a review of the literature and a report of two cases with irreversible cortical vision loss. *J Int Med Res* 2022; **50**: 3000605221081429 [PMID: 35301892 DOI: 10.1177/03000605221081429]
4 **Liu CJ**, Tsai HH, Ko KY, Lu CC, Yen RF. Ictal Phase Perfusion SPECT of Nonketotic Hyperglycemia-Induced Parieto-occipital Seizure. *Clin Nucl Med* 2017; **42**: e67-e68 [PMID: 27749417 DOI: 10.1097/RLU.0000000000001397]
5 **Sekar S**, Vinayagamani S, Thomas B, Kesavadas C. Arterial spin labeling hyperperfusion in seizures associated with non-ketotic hyperglycaemia: is it merely a post-ictal phenomenon? *Neurol Sci* 2021; **42**: 739-744 [PMID: 33047197 DOI: 10.1007/s10072-020-04815-6]
6 **Kitabchi AE**, Umpierrez GE, Murphy MB, Kreisberg RA. Hyperglycemic crises in adult patients with diabetes: a consensus statement from the American Diabetes Association. *Diabetes Care* 2006; **29**: 2739-2748 [PMID: 17130218 DOI: 10.2337/dc06-9916]
7 **Hung WL**, Hsieh PF, Lee YC, Chang MH. Occipital lobe seizures related to marked elevation of hemoglobin A1C: report of two cases. *Seizure* 2010; **19**: 359-362 [PMID: 20558093 DOI: 10.1016/j.seizure.2010.05.006]
8 **Najm IM**, Wang Y, Hong SC, Lüders HO, Ng TC, Comair YG. Temporal changes in proton MRS metabolites after kainic acid-induced seizures in rat brain. *Epilepsia* 1997; **38**: 87-94 [PMID: 9024189 DOI: 10.1111/j.1528-1157.1997.tb01082.x]
9 **Tsai JP**, Sheu JJ, Hsieh KL. Unusual Magnetic Resonance Imaging Abnormality in Nonketotic Hyperglycemia - related Epilepsia Partialis Continua. *Ann Indian Acad Neurol* 2018; **21**: 225-227 [PMID: 30258268 DOI: 10.4103/aian.AIAN_386_17]
10 **Paoletti M**, Bacila A, Pichiecchio A, Farina LM, Rognone E, Cremascoli R, Fanucchi S, Manni R, Bastianello S. Atypical postictal transient subcortical T2 hypointensity in a newly diagnosed diabetic patient with seizures. *Epileptic Disord* 2018; **20**: 209-213 [PMID: 29905159 DOI: 10.1684/epd.2018.0974]
11 **Tosur M**, Viau-Colindres J, Astudillo M, Redondo MJ, Lyons SK. Medication-induced hyperglycemia: pediatric perspective. *BMJ Open Diabetes Res Care* 2020; **8** [PMID: 31958298 DOI: 10.1136/bmjdrc-2019-000801]

World Journal of Clinical Cases

Submit a Manuscript: https://www.f6publishing.com

World J Clin Cases 2024 February 16; 12(5): 1010-1017

DOI: 10.12998/wjcc.v12.i5.1010

ISSN 2307-8960 (online)

CASE REPORT

Novel approach of ultrasound-guided lateral recess block for a patient with lateral recess stenosis: A case report

Jiao Yang, Xin-Ling Li, Qing-Bing Li

Specialty type: Integrative and complementary medicine

Provenance and peer review: Unsolicited article; Externally peer reviewed.

Peer-review model: Single blind

Peer-review report's scientific quality classification

Grade A (Excellent): 0
Grade B (Very good): 0
Grade C (Good): C
Grade D (Fair): 0
Grade E (Poor): 0

P-Reviewer: Gousheh M, Iran

Received: November 24, 2023
Peer-review started: November 24, 2023
First decision: December 18, 2023
Revised: January 2, 2024
Accepted: January 15, 2024
Article in press: January 15, 2024
Published online: February 16, 2024

Jiao Yang, Xin-Ling Li, Qing-Bing Li, Department of Rehabilitation Medicine Center, West China Hospital, Chengdu 610041, Sichuan Province, China

Jiao Yang, Xin-Ling Li, Qing-Bing Li, Key Laboratory of Rehabilitation Medicine in Sichuan Province, West China Hospital, Chengdu 610041, Sichuan Province, China

Corresponding author: Xin Ling Li, PhD, Assistant Professor, Department of Rehabilitation Medicine Center, West China Hospital, No. 37 Guoxue Alley, Wuhou District, Chengdu 610041, Sichuan Province, China. lilingxinlsh@163.com

Abstract

BACKGROUND

Ultrasound guide technology, which can provide real-time visualization of the needle tip and tissues and avoid many adverse events, is widely used in minimally invasive therapy. However, the studies on ultrasound-guided Lateral recess block (LRB) are limited, this is probably because there is no recognized standard method for ultrasound scanning. This study aimed to evaluate the effect of ultrasound-guided LRB in patients with lateral recess stenosis (LRS).

CASE SUMMARY

A 65-year-old patient complained of low back pain accompanied occasionally by pain and numbness in the left lower limb. Physical examination showed tenderness on the spinous process and paraspinal muscles from L1 to S1, extensor hallucis longus and tibialis anterior weakness (muscle strength: 4−), and a positive straight leg raising test in the left lower limb (60°). Magnetic resonance imaging showed L4–L5 disc degeneration with left LRS and nerve root entrapment. Subsequently, the patient was diagnosed with LRS. This patient was treated with a novel ultrasound-guided LRB approach. The patient's symptoms significantly improved without any complications at 1 wk postoperatively and at the 3-month follow-up.

CONCLUSION

This is the first report on the LRS treatment with ultrasound-guided LRB from the contralateral spinous process along the inner side of the articular process by out-plane technique. Further studies are expected to investigate the efficacy and safety of ultrasound-guided LRB for patients with LRS.

Key Words: Lateral recess stenosis; Ultrasound; Lateral recess block; Real-time

visualization; Low back pain; Case report

Core Tip: Lateral recess block (LRB) is a common treatment method for lateral recess stenosis (LRS). However, it is an unsatisfactory method because of its high risk of side effects. Ultrasound-guided technology is widely used in minimally invasive therapy, but only a few studies have reported its use in LRB, this is probably because there is no recognized standard method for ultrasound scanning. In order to explore the standard method for ultrasound-guided LRB, we reported a novel ultrasound-guided LRB approach in treating a patient with LRS whose symptoms significantly improved without any complications.

Citation: Yang J, Li XL, Li QB. Novel approach of ultrasound-guided lateral recess block for a patient with lateral recess stenosis: A case report. *World J Clin Cases* 2024; 12(5): 1010-1017
URL: https://www.wjgnet.com/2307-8960/full/v12/i5/1010.htm
DOI: https://dx.doi.org/10.12998/wjcc.v12.i5.1010

INTRODUCTION

Lateral recess stenosis (LRS) is a common type of lumbar spinal stenosis in elderly individuals[1,2]. In spinal anatomy, the lateral recess is the outermost region of the spinal canal bordered laterally by the pedicle, posteriorly by the superior articular facet and ligamentum flavum, and anteriorly by the vertebral body, endplate, and disc margin[3], which is considered stenotic when the anteroposterior measurement is < 4 mm[4]. Due to the close proximity within the spinal canal, stenosis in this region always leads to low back pain, numbness, neurogenic claudication and even urination-defecation impairment[2], which often affect mobility and walking ability, leading to a reduction in patients' quality of life[3,5]. Lateral recess block (LRB) is commonly used for this condition due to its immediate analgesic effect in approximately 50%–87% of patients[6,7]. To improve efficacy and accuracy, computed tomography (CT), X-ray, and ultrasound guidance are widely used in minimally invasive therapy[8]. However, the studies on ultrasound-guided LRB are limited, this is probably because there is no recognized standard method for ultrasound scanning.

We reported a successful case of a patient with LRS who underwent ultrasound-guided LRB. This case report may provide a new exploration of the standard method of ultrasound-guided LRB. This study followed the CARE Guidelines for consensus-based clinical case reporting guideline development[9].

CASE PRESENTATION

Chief complaints

A 65-year-old patient complained of low back pain accompanied occasionally by pain and numbness in the left lower limb for at least 10 years.

History of present illness

In the past 10 years, his symptoms did not significantly affect his life and work and were relieved after rest or massage therapy. However, his low back pain gradually worsened, and he developed persistent soreness, numbness, and intermittent claudication on the left lower limb, mainly at the lateral thigh, posterolateral, instep, and foot top. Consequently, his life and work were severely affected because his symptoms were unrelieved even after rest or massage.

History of past illness

His medical history was unremarkable.

Personal and family history

His family history was also unremarkable.

Physical examination

Physical examination showed tenderness on the spinous process and paraspinal muscles from L1 to S1, extensor hallucis longus and tibialis anterior weakness (muscle strength: 4^-), and a positive straight leg raising test in the left lower limb (60°). The visual analog scale (VAS) and Oswestry disability index (ODI) were 8 mm and 51%, respectively.

Laboratory examinations

No laboratory tests.

Imaging examinations

Magnetic resonance imaging (MRI) indicated L4–L5 disc degeneration with left LRS and nerve root entrapment (Figure 1).

FINAL DIAGNOSIS

Based on the clinical and imaging examination, the patient was diagnosed with LRS.

TREATMENT

Oral analgesics and physiotherapy did not benefit the patient. Therefore, we planned to perform left L4–L5 LRB under ultrasound guidance. We used a portable ultrasound imaging device (Lumify, Philips, Shanghai, China) with a 5-2 MHz frequency round probe. Before the procedure, the patient was placed in a prone position with a pillow under the lower abdomen to reduce lumbar lordosis in the operating room and supervised *via* a continuous electrocardiogram, and his blood pressure and pulse oximetry were supervised using a noninvasive monitor. After the involved lumbar intervertebral space between L4 and L5 was confirmed, the physician's hands, puncture sites, and ultrasound probe were sterilized. The physician stood on the left side of the patient. Subsequently, ultrasound-guided LRB was divided into four steps. First, the target L4 articular process was identified by locating the lumbosacral junction (L5-S1 gap; Figure 2) on paramedian sagittal scanning, and counting was performed cranially by numbering the lamina and transverse processes of the L5 and L4 vertebrae. Second, after marking the L4 vertebral level, the probe was rotated transversely to obtain the view of the L4 spinous process and interspinous process space between L4 and L5. Third, the probe was slightly moved toward the median line to obtain the view of the articular process, ligamentum flavum, and intraspinal anterior complex (posterior longitudinal ligament, dura mater and lumbar posterior margin) on median axis scanning. The puncture site was 0.8-1.0 cm away from the contralateral spinous process of L4 and L5 (Figure 3). Fourth, the puncture site was infiltrated using 1% lidocaine before insertion. Afterward, a needle was advanced along with the inner side of the articular process at 70°–80° guided by ultrasound in the out-plane technique. The lateral recess of L4 was the target of the needle tip. The needle was withdrawn to exclude vascular injection after the needle tip site was verified under ultrasound, and no blood or cerebrospinal fluid was aspirated. Hypoesthesia of the left medial malleolus was observed 5 min after injection of 2 mL of 0.25% lidocaine. Subsequently, 5 mL mixed injectate consisting of 1 mL triamcinolone, 4 mL 2% lidocaine, 1 mL mecobalamin and 14 mL 0.9% sodium chloride was injected into the lateral recess of L4. To display the needle trajectory more clearly, we used a diagram to illustrate the needle trajectory (Figure 4), but it was difficult to capture the ultrasonic image of the needle during the operation.

OUTCOME AND FOLLOW-UP

We carefully recorded the change in the patient's symptoms with VAS and ODI before and 30 min, 1 wk, 1 month, and 3 months postoperatively. The patient's symptoms greatly improved 1 wk postoperatively and at the 3-month follow-up (Table 1). The patient was satisfied with this treatment.

DISCUSSION

We reported a novel approach of ultrasound-guided LRB for LRS treatment. We preliminarily established that ultrasound-guided LRB from the contralateral spinous process along with the inner side of the articular process with the out-plane technique is an effective, accurate, and safe method in LRS treatment.

Surgery, a commonly used treatment method, showed superior outcomes[10]. However, its complications and less satisfaction with the results of surgery in the elderly population make it a difficult choice for clinicians[11]. Thus, nonsurgical treatment is appropriate for patients with mild to moderate symptoms. Some of the commonly used treatment strategies include medication, physical therapy, massage, conventional transforaminal epidural steroid injection (CTFESI), selected nerve root block (SNRB), and LRB[12-17]. Medication, physical therapy, and massage are unsatisfactory choices because of their short-term effect and high recurrence rate[15]. CTFESI and SNRB are widely used in LRS treatment[16]; However, the effective rate of SNRB for patients with LRS has not been satisfactory due to the stenosis pathology occurring in the intraspinal lateral recess but not in the intervertebral foramen outside the spinal canal [8]. Generally, the injectate includes local anesthetics and glucocorticoids. Local anesthetics can achieve analgesic effects by blocking neurological activity. Meanwhile, glucocorticoids reduce inflammation and the immune response by inhibiting prostaglandin synthesis, reducing nociceptor stimulation and sensitization, and decreasing inflammatory mediator release. In addition, it plays an indirect role in decompressing and increasing the blood supply to the nerve, which alleviates the patient's symptoms[18]. Therefore, accurate injection of the lateral recess is key to successful LRS treatment. The most common technique of SNRB is targeting the spinal nerve root[16], which is physically distant from the spinal nerve root to the lateral recess[2]. The injectate diffuses from the spinal nerve root to the lateral recess, resulting

Table 1 Evaluation of symptoms *via* visual analog scale and Oswestry Disability Index

Item	Pre-operation	30 min postoperation	1 wk postoperation	1 month postoperation	3 months postoperation
VAS	8	6	4	4	5
ODI, %	51	51	31	31	33

VAS: Visual analog scale; ODI: Oswestry Disability Index.

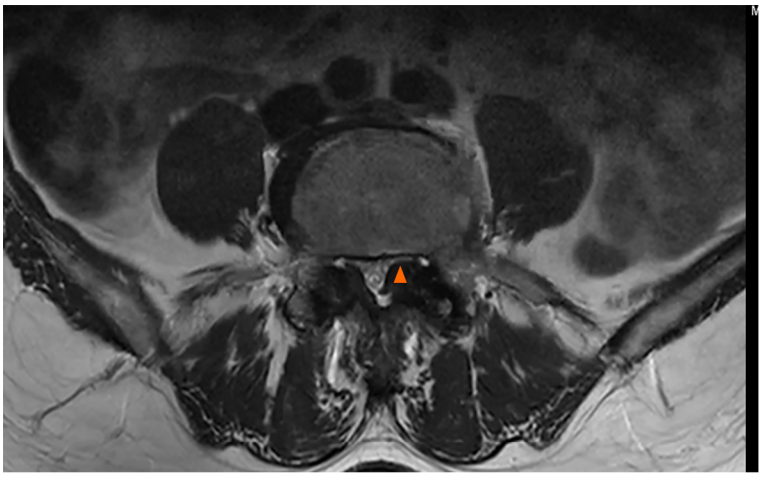

DOI: 10.12998/wjcc.v12.i5.1010

Figure 1 Preoperative magnetic resonance imaging shows lateral recess stenosis at L4–5 (asterisk).

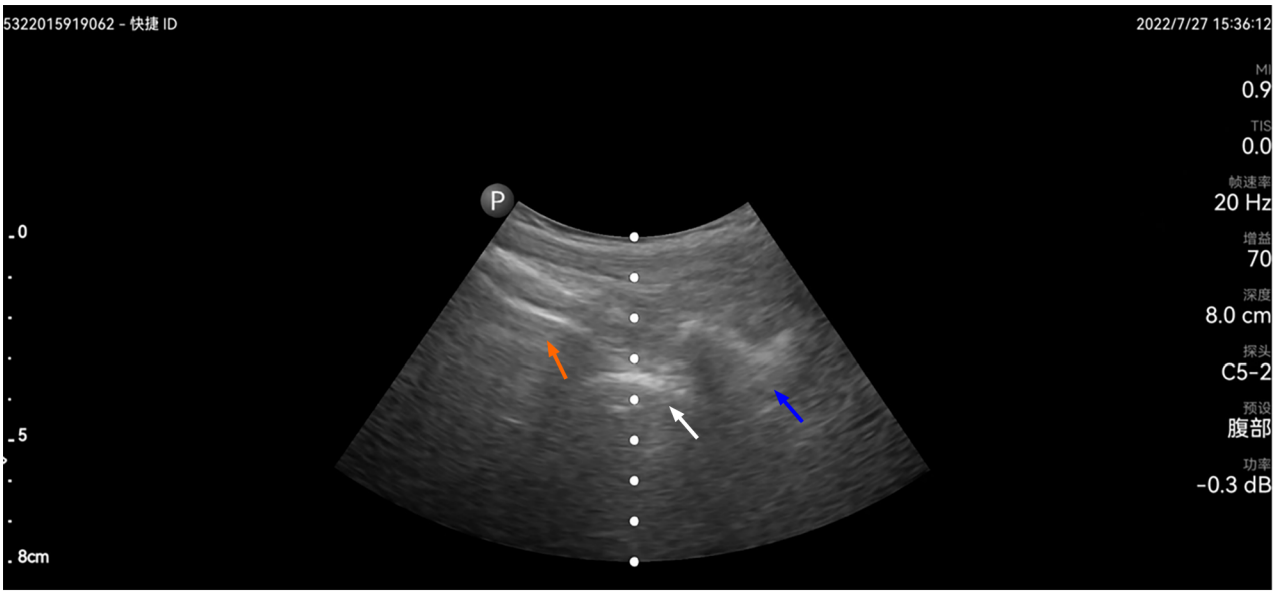

DOI: 10.12998/wjcc.v12.i5.1010

Figure 2 Ultrasound imaging shows the lumbosacral junction at L5–S1 (orange arrow) and the articular process of L5 (white arrow) and L4 (blue arrow) on paramedian sagittal scanning.

in a slow effect and weak efficacy, which leads to less satisfaction. Moreover, a retrospective study[7] reported that LRB was considerably safer, with a lower chance of nerve pricks[19] and intravascular dye spread than CTFESI. This study also revealed that a single LRB was significantly better than a single CTFESI in decreasing unilateral radiculopathy pain because the site of drug deposition was more proximal to the discovery interface.

LRB is effective in relieving pain and symptoms of nerve root entrapment[11,13]. However, the potential risk of subdural block, failure block, and intraspinal bleeding still makes it an entangled choice for many physicians[8]. CT, X-ray, and ultrasound guidance are widely used in minimally invasive therapy to improve efficacy, safety, and accuracy[8,

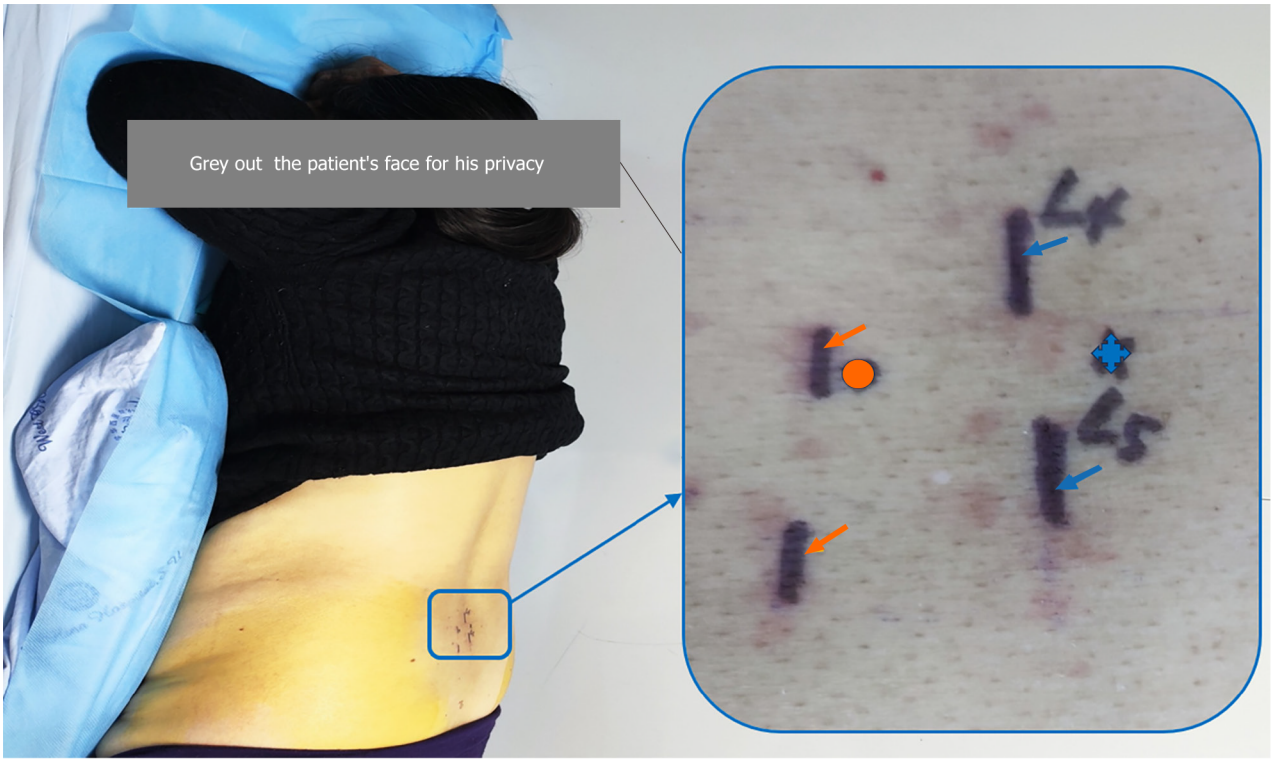

DOI: 10.12998/wjcc.v12.i5.1010

Figure 3 The position of patient on the bed during the procedure and the area of the procedure is marked and zoomed in to show a clearer picture, including spinal process of L4 and L5 (blue arrow), articular process of L4 and L5 (orange arrow), puncture site (blue asterisk) and body surface projection of target site (orange circle).

16]. Exposure to radiation during the procedure under CT or X-ray guidance may be a problem. Sacaklidir *et al*[20] reported that radiation exposure for 37.3–46.7s results in a radiation dose between 0.057 and 0.218 mGym^2. This is equivalent to 15–30 chest radiographs. Because of its real-time visualization of the needle tip and no radiation exposure, ultrasound-guided minimally invasive techniques have been widely adapted in clinical practice. Li *et al*[21] reported the efficacy of ultrasound-guided nerve blocks of the head and neck for chronic pain management. Takahashi *et al*[22] validated the efficacy of ultrasound-guided cervical nerve root block for frozen shoulder. However, only a few studies have reported ultrasound-guided LRB due to the lack of precise ultrasound scanning methods. Currently, no standard method of ultrasound-guided LRB exists. In our practice, we selected a new method. A previous study selected an injection point 0.8–1.0 cm away from the ipsilateral spinous process and then along the inner side of the articular pillar under ultrasound guidance[8]. This method increases the risk of total spinal paralysis caused by subdural block, particularly when LRS is associated with nerve root adhesion. In this case, the injection points were 0.8-1.0 cm away from the contralateral spinous process of L4 and L5. Then, the needle was advanced toward the inner side of the articular process at 70°–80° guided by ultrasound with the out-plane technique. This method increases the effectiveness, safety, and accuracy of surgery for patients and provides a new exploration into the standard method of ultrasound-guided LRB.

There are also some limitations in this study. It is difficult for us to capture the ultrasonic image of the needle during the operation. The lack of the ultrasonic image would decrease the illustration of this technology. Hence, we used a diagram to illustrate the needle trajectory in Figure 4. We expect that this image will help understand our needle trajectory more clearly. Moreover, we only reported one successful case, which may restrict the wide use of ultrasound-guided LRB. Further high-quality studies are expected to confirm the efficacy and safety of the use of ultrasound-guided LRB with this novel approach.

In conclusion, this study is the first report of the use of ultrasound-guided LRB from the contralateral spinous process along with the inner side of the articular process with the out-plane technique for LRS treatment, which was preliminarily proven to be effective, accurate, and safe. Further studies are needed to investigate the efficacy and safety of ultrasound-guided LRB for patients with LRS.

CONCLUSION

We reported a case of a patient with LRS who underwent ultrasound-guided LRB. This study is the first report of ultrasound-guided LRB from the contralateral spinous process along with the inner side of the articular process with the out-plane technique for LRS treatment. Further studies are expected to investigate the efficacy and safety of ultrasound-guided LRB for patients with LRS.

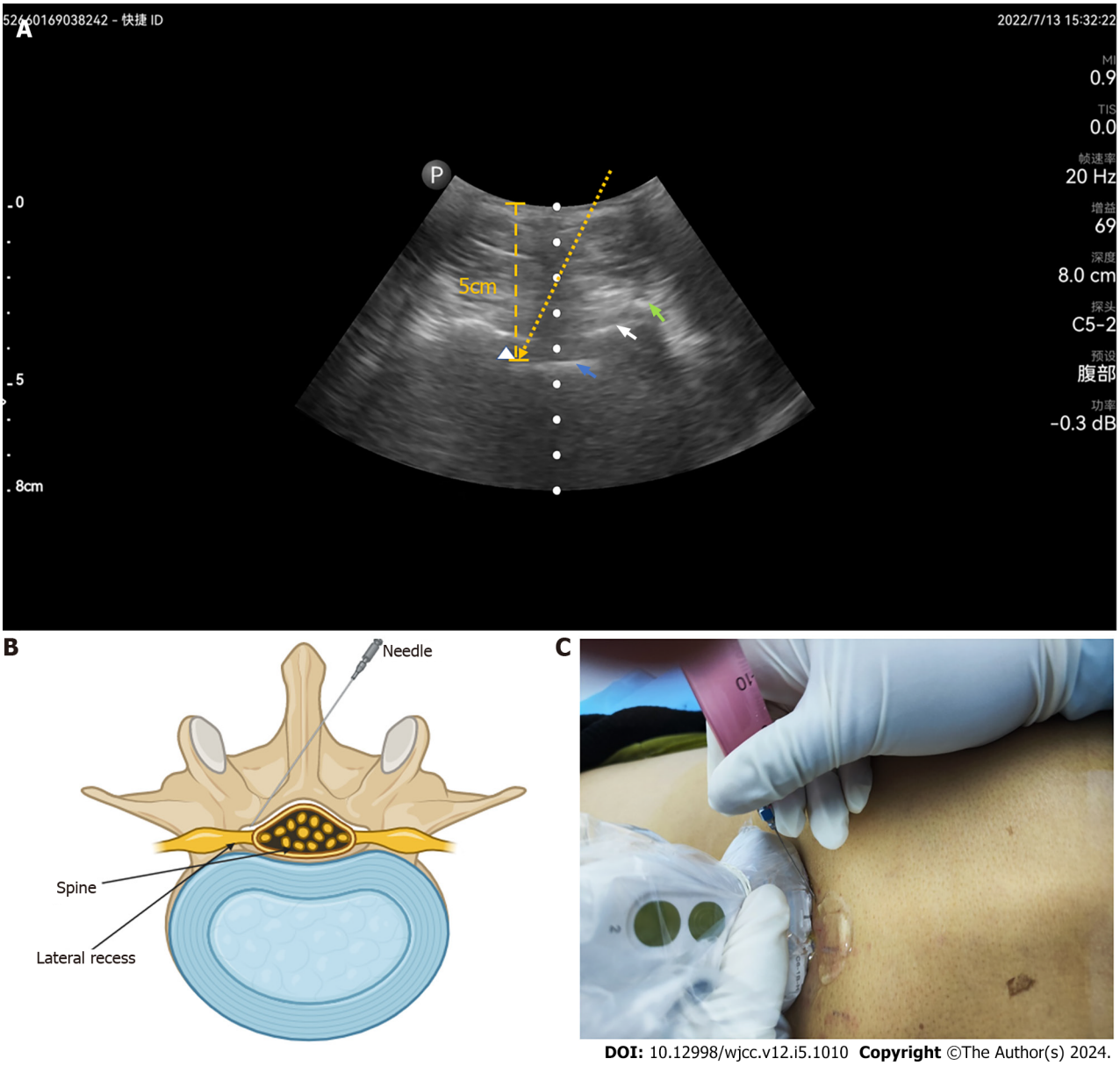

DOI: 10.12998/wjcc.v12.i5.1010

Figure 4 Needle trajectory during lateral recess steroid injection. A: Ultrasound image of needle trajectory, the lateral recess (white triangle), articular process (cyan arrow), ligamentum flavum (white arrow), and intraspinal anterior complex (blue arrow), needle direction (yellow arrow), depth from the target injection point into the skin (yellow line); B: Diagrammatic explanation of the needle trajectory; C: Picture of the right place of probe position and needle insertion.

ACKNOWLEDGEMENTS

We would like to thank the patient for agreeing to participate in this study.

FOOTNOTES

Author contributions: Li XL made substantial contributions to the study conception and design; Yang J was responsible for writing the original draft, reviewing, and editing; Li BQ contributed to the investigation and data curation; All authors approved the final version to be submitted.

Supported by the National Natural Science Foundation of China, No. 82305380; and The Postdoctoral Research Program, West China Hospital, Sichuan University, No. 2020HXBH018.

Informed consent statement: Informed written consent was obtained from the patient for publication of this report and any accompanying images.

Conflict-of-interest statement: All the authors declare that they have no conflict of interest to disclose.

CARE Checklist (2016) statement: The authors have read the CARE Checklist (2016), and the manuscript was prepared and revised according to the CARE Checklist (2016).

Country/Territory of origin: China

ORCID number: Jiao Yang 0000-0002-0323-2697; Xin-Ling Li 0000-0002-5644-7034; Qing-Bing Li 0000-0003-0360-3993.

S-Editor: Liu JH
L-Editor: A
P-Editor: Yu HG

REFERENCES

1 **Wang X**, Wu L, Zhao K, Chen D, Su B, Kong Y, Li J, Kang K, Si D. Trephine-based foraminoplasty in PTED treatment of lumbar lateral recess stenosis. *Adv Clin Exp Med* 2022; **31**: 359-367 [PMID: 35068091 DOI: 10.17219/acem/144638]
2 **Deer TR**, Grider JS, Pope JE, Lamer TJ, Wahezi SE, Hagedorn JM, Falowski S, Tolba R, Shah JM, Strand N, Escobar A, Malinowski M, Bux A, Jassal N, Hah J, Weisbein J, Tomycz ND, Jameson J, Petersen EA, Sayed D. Best Practices for Minimally Invasive Lumbar Spinal Stenosis Treatment 2.0 (MIST): Consensus Guidance from the American Society of Pain and Neuroscience (ASPN). *J Pain Res* 2022; **15**: 1325-1354 [PMID: 35546905 DOI: 10.2147/JPR.S355285]
3 **Lee BH**, Moon SH, Suk KS, Kim HS, Yang JH, Lee HM. Lumbar Spinal Stenosis: Pathophysiology and Treatment Principle: A Narrative Review. *Asian Spine J* 2020; **14**: 682-693 [PMID: 33108834 DOI: 10.31616/asj.2020.0472]
4 **Liu X**, Peng Y, Pei L, Zhu Y. Sufficient Lumbar Lateral Recess Decompression Acquired by Undercutting "Superior Articular Process Neck" Plus Intervertebral Disk Annuloplasty in Percutaneous Transforaminal Endoscopic Surgery. *Med Sci Monit* 2020; **26**: e921119 [PMID: 32243427 DOI: 10.12659/MSM.921119]
5 **Cheng X**, Zhang K, Sun X, Zhao C, Li H, Ni B, Zhao J. Clinical and radiographic outcomes of bilateral decompression *via* a unilateral approach with transforaminal lumbar interbody fusion for degenerative lumbar spondylolisthesis with stenosis. *Spine J* 2017; **17**: 1127-1133 [PMID: 28416439 DOI: 10.1016/j.spinee.2017.04.011]
6 **Thiengwittayaporn S**, Koompong P, Khamrailert S, Wetpiriyakul P. Comparison of Clinical Outcomes of Different Rates of Infusion in Caudal Epidural Steroid Injection: A Randomized Controlled Trial. *Asian Spine J* 2021; **15**: 244-251 [PMID: 32703925 DOI: 10.31616/asj.2019.0380]
7 **Jain A**, Agarwal A, Jain S, Waindeskar V. Comparison Between a Single Subpedicular Transforaminal Epidural Steroid Injection and Lateral Recess Steroid Injection in Reducing Paracentral Disc Herniation-Related Chronic Neuropathic Leg Pain: A Retrospective Study. *World Neurosurg* 2021; **149**: e392-e399 [PMID: 33578022 DOI: 10.1016/j.wneu.2021.02.011]
8 **Liang G**. Effect of ultrasound-guided lateral recess block in the treatment of patients with lumbar intervertebral disc herniation. *Hennan Medical Research* 2021; **30**: 1638-1640
9 **Gagnier JJ**, Kienle G, Altman DG, Moher D, Sox H, Riley D; CARE Group. The CARE guidelines: consensus-based clinical case reporting guideline development. *Headache* 2013; **53**: 1541-1547 [PMID: 24266334 DOI: 10.1111/head.12246]
10 **Lurie J**, Tomkins-Lane C. Management of lumbar spinal stenosis. *BMJ* 2016; **352**: h6234 [PMID: 26727925 DOI: 10.1136/bmj.h6234]
11 **Li X**, Liu T, Fan J, Zhang H, Yang C, Yin X, Gao H, Qian J, Sun S. Outcome of lumbar lateral recess stenosis with percutaneous endoscopic transforaminal decompression in patients 65 years of age or older and in younger patients. *Medicine (Baltimore)* 2020; **99**: e21049 [PMID: 32702846 DOI: 10.1097/MD.0000000000021049]
12 **Chen X**, Zheng Z, Lin J. Clinical Effectiveness of Conservative Treatments on Lumbar Spinal Stenosis: A Network Meta-Analysis. *Front Pharmacol* 2022; **13**: 859296 [PMID: 35734403 DOI: 10.3389/fphar.2022.859296]
13 **Kim HJ**, Kim JH, Park YS, Suk KS, Lee JH, Park MS, Moon SH. Comparative study of the efficacy of limaprost and pregabalin as single agents and in combination for the treatment of lumbar spinal stenosis: a prospective, double-blind, randomized controlled non-inferiority trial. *Spine J* 2016; **16**: 756-763 [PMID: 27045252 DOI: 10.1016/j.spinee.2016.02.049]
14 **Jang JH**, Lee WY, Kim JW, Cho KR, Nam SH, Park Y. Ultrasound-Guided Selective Nerve Root Block *versus* Fluoroscopy-Guided Interlaminar Epidural Block *versus* Fluoroscopy-Guided Transforaminal Epidural Block for the Treatment of Radicular Pain in the Lower Cervical Spine: A Retrospective Comparative Study. *Pain Res Manag* 2020; **2020**: 9103421 [PMID: 32617125 DOI: 10.1155/2020/9103421]
15 **Zhang Y**. Effects of lateral recess block on pain and functional recovery in patients with lumbar disc herniation. *Shiyong Zhongxiyi Jiehe Linchuang* 2020; **20**: 28-29
16 **Yue B**, Shen F, Ye ZF, Wang ZH, Yang HL, Jiang GQ. Accurate location and minimally invasive treatment of lumbar lateral recess stenosis with combined SNRB and PTED. *J Int Med Res* 2020; **48**: 300060519884817 [PMID: 31774009 DOI: 10.1177/0300060519884817]
17 **Schneider MJ**, Ammendolia C, Murphy DR, Glick RM, Hile E, Tudorascu DL, Morton SC, Smith C, Patterson CG, Piva SR. Comparative Clinical Effectiveness of Nonsurgical Treatment Methods in Patients With Lumbar Spinal Stenosis: A Randomized Clinical Trial. *JAMA Netw Open* 2019; **2**: e186828 [PMID: 30646197 DOI: 10.1001/jamanetworkopen.2018.6828]
18 **Guyot JP**. Lumbar Selective Nerve Root Block: Comparative Study Using Two Pharmacological Formulae. *Global Spine J* 2018; **8**: 374-377 [PMID: 29977722 DOI: 10.1177/2192568217728724]
19 **Kim HJ**, Park JH, Shin KM, Kang SS, Kim IS, Hong SJ, Song CK, Park JC, Yeom JS. The efficacy of transforaminal epidural steroid injection by the conventional technique in far-lateral herniation of lumbar disc. *Pain Physician* 2012; **15**: 415-420 [PMID: 22996853]

20 **Sacaklidir R**, Ozturk EC, Sencan S, Gunduz OH. Radiation Doses for Different Approaches of Fluoroscopy-Guided Epidural Injections: An Observational Clinical Study. *Pain Physician* 2022; **25**: E67-E72 [PMID: 35051153]

21 **Li J**, Szabova A. Ultrasound-Guided Nerve Blocks in the Head and Neck for Chronic Pain Management: The Anatomy, Sonoanatomy, and Procedure. *Pain Physician* 2021; **24**: 533-548 [PMID: 34793642]

22 **Takahashi R**, Kajita Y, Harada Y, Iwahori Y, Miyashita N, Deie M. Does the timing of shoulder manipulation under ultrasound-guided cervical nerve root block for frozen shoulder affect the clinical outcome? *J Orthop Sci* 2022; **27**: 122-125 [PMID: 33358448 DOI: 10.1016/j.jos.2020.11.002]

World Journal of Clinical Cases

Submit a Manuscript: https://www.f6publishing.com

World J Clin Cases 2024 February 16; 12(5): 1018-1024

DOI: 10.12998/wjcc.v12.i5.1018

ISSN 2307-8960 (online)

CASE REPORT

Ankylosing spondylitis coexisting with *Clonorchis sinensis* infection: A case report

Tian-Xin Yi, Wei Liu, Wen-Fei Leng, Xiao-Chuan Wang, Liang Luo

Specialty type: Medicine, research and experimental

Provenance and peer review: Unsolicited article; Externally peer reviewed.

Peer-review model: Single blind

Peer-review report's scientific quality classification

Grade A (Excellent): 0
Grade B (Very good): 0
Grade C (Good): C, C
Grade D (Fair): 0
Grade E (Poor): 0

P-Reviewer: Arumugam VA, India

Received: December 6, 2023
Peer-review started: December 6, 2023
First decision: December 21, 2023
Revised: January 4, 2024
Accepted: January 24, 2024
Article in press: January 24, 2024
Published online: February 16, 2024

Tian-Xin Yi, Wen-Fei Leng, Xiao-Chuan Wang, Department of Rheumatology, Traditional Chinese Medicine Hospital Dianjiang Chongqing, Chongqing 408300, China

Wei Liu, Department of Orthopaedic, Traditional Chinese Medicine Hospital Dianjiang Chongqing, Chongqing 408300, China

Liang Luo, Department of Chinese Medicine, The People's Hospital of Yubei District of Chongqing City, Chongqing 401120, China

Corresponding author: Liang Luo, MD, Attending Doctor, Department of Chinese Medicine, The People's Hospital of Yubei District of Chongqing City, No. 23 North Central Park Road, Yubei District, Chongqing 401120, China. luoliang202112@163.com

Abstract

BACKGROUND

Ankylosing spondylitis (AS) is a chronic immune-mediated inflammatory disease. The prevailing theory links AS onset to infections in susceptible individuals. Furthermore, infections may impair the immune responses. Numerous studies have investigated links between AS and various infections-bacterial, viral, fungal, and other microorganism infections. However, limited attention has been given to the association between AS and *Clonorchis sinensis* (*C. sinensis*) infection.

CASE SUMMARY

A 27-year-old male with a 10-yr history of AS presented to our hospital with inflammatory lower back pain as the primary manifestation. Ten years ago, the patient had achieved a stable condition after treatment with biological agents. However, he experienced a recurrence of lumbosacral pain with an unexplained cause 10 d before hospital admission. A lumbosacral magnetic resonance imaging (MRI) scan revealed bone marrow edema in the left sacroiliac joint, and laboratory indicators were elevated. Moreover, the presence of *C. sinensis* eggs was detected in the stool. The patient was prescribed praziquantel, resulting in the disappearance of *C. sinensis* eggs in subsequent routine stool tests and relief from lumbosacral pain. A follow-up MRI scan performed after 4 months revealed a reduction in bone marrow edema around the left sacroiliac joint.

CONCLUSION

C. sinensis infections could potentially trigger the exacerbation of AS. Clinicians should pay attention to investigating the presence of infections.

Key Words: Ankylosing spondylitis; *Clonorchis sinensis*; Parasites; Infection; Case report

Core Tip: This study explored the link between *Clonorchis sinensis* (*C. sinensis*) infection and ankylosing spondylitis (AS). While previous research extensively explored the association between AS and various infections, the association with *C. sinensis* received limited attention. The findings highlight the potential role of parasitic infections, particularly *C. sinensis*, in affecting AS disease activity. This study provides valuable insights into the less-explored aspects of AS etiology, emphasizing the need for further investigation into parasitic infections to comprehend and manage AS.

Citation: Yi TX, Liu W, Leng WF, Wang XC, Luo L. Ankylosing spondylitis coexisting with *Clonorchis sinensis* infection: A case report. *World J Clin Cases* 2024; 12(5): 1018-1024
URL: https://www.wjgnet.com/2307-8960/full/v12/i5/1018.htm
DOI: https://dx.doi.org/10.12998/wjcc.v12.i5.1018

INTRODUCTION

Ankylosing spondylitis (AS) is a chronic inflammatory and rheumatic disease resulting from an imbalance between innate and acquired immune responses[1]. While it can affect any part of the spine, its primary symptoms are persistent back pain and stiffness in the lower back and pelvis. The prevalence of AS per 10000 individuals is 23.8 in Europe, 31.9 in North America, 16.7 in Asia, 10.2 in Latin America, and 7.4 in Africa[2]. Infections commonly occur in the first 3 months and may act as potential triggers for the first symptoms of AS, often manifesting as gastrointestinal, urinary tract, and respiratory infections of microbiological origin[3,4].

Clonorchis sinensis (*C. sinensis*) infection is a severe parasitic disease affecting millions globally, especially prevalent in China, South Korea, the Far East of Russia, and Vietnam, with an estimated 15 million cases[5]. Transmission occurs through the consumption of undercooked freshwater fish containing metacercariae. Adult *C. sinensis* parasites then establish themselves within the human hepatobiliary system[6]. *C. sinensis* infection triggers the activation of sphingosine 1-phosphate receptor 2, leading to the injury and fibrosis of the hepatobiliary[7]. Recent research in a rat model found that *C. sinensis* infection increases the risk of hepatocellular carcinoma by stimulating hepatic progenitor cell proliferation[8]. Complications of *C. sinensis* infection include cholestasis, cholangitis, biliary system fibrosis, and in severe cases, the development of cholangiocarcinoma[9]. Consequently, the primary preventive measure is to abstain from consuming raw or undercooked freshwater fish. Praziquantel is the recommended and effective treatment for this infection[10].

While there is existing literature on the coexistence of AS and parasitic infections, there is limited research specifically addressing the simultaneous presence of AS and *C. sinensis* infection. This case report details a rare scenario of AS coexisting with *C. sinensis* infection, underscoring the potential impact of *C. sinensis* infection on AS disease activity.

CASE PRESENTATION

Chief complaints

A 27-year-old male patient with persistent lumbosacral pain for more than 10 yr had a recurrence 10 d before a hospital visit.

History of present illness

The patient, in his late twenties, reported experiencing lumbosacral pain for more than 10 years. The pain intensified while sitting or at rest but improved in the mornings. Throughout this period, there were no signs of heel pain, eye inflammation, symmetrical swelling, pain in small joints, psoriasis, sausage fingers/toes, facial erythema, photosensitivity, oral ulcer, alopecia, frequent urination, or urgency. Consequently, he was admitted to the Rheumatology Department at the Traditional Chinese Medicine Hospital of Dianjiang, Chongqing. Examinations conducted indicated a positive response to human leukocyte antigen B27, and magnetic resonance imaging (MRI) scans revealed localized edema around the bilateral sacroiliac joint bone marrow. Upon confirmation of AS, rheumatologists recommended a tailored treatment regimen. Subsequently, the patient managed his condition with subcutaneous administration of recombinant human tumor necrosis factor (TNF)-α receptor II: Immunoglobulin G Fc fusion protein, leading to a reduction in lumbosacral pain. Lumbosacral pain recurred 10 d before the patient's hospital admission without a clear cause. Despite orally taking aceclofenac at a dosage of 100 mg twice daily, the pain persisted and was not alleviate.

History of past illness
He had no notable past medical history.

Personal and family history
No significant medical findings were identified in the patient's personal history or family background.

Physical examination
The physical examination confirmed tenderness and percussive pain in the left sacroiliac joint. The Schober test recorded a value of 5 cm, with a finger-to-ground distance of 30 cm, a measured pillow wall distance of 0 cm, and a chest expansion of 4 cm. The physiological curvature of the spine was within the normal range, and no tenderness was detected within the cervical, thoracic, and lumbar spinous processes, vertebral bodies, and paravertebral bodies.

Laboratory examinations
Elevated levels of erythrocyte sedimentation rate (ESR) and C-reactive protein (CRP) indicated inflammation, while blood routine tests, liver and kidney functions, blood coagulation functions, and a routine urinalysis showed values within the normal range. Subsequent T-SPOT.TB and tumor marker tests were conducted to detect tuberculosis infection and prepare for the use of biological agents. The T-SPOT.TB result was negative, but alpha-fetoprotein levels were slightly elevated. However, routine stool examination revealed the presence of *C. sinensis* eggs (Figure 1).

Imaging examinations
The MRI scan of the sacroiliac joint displayed bone marrow edema in the left sacroiliac joint (Figure 2A and B). A subsequent colonoscopy indicated congestion in the descending colon, sigmoid colon, and rectum (Figure 3). No liver abnormalities were observed in the upper abdominal computed tomography.

FINAL DIAGNOSIS
Considering the patient's symptoms, physical examination, laboratory tests, and imaging results, the final diagnosis was AS coexisting with *C. sinensis* infection.

TREATMENT
Based on the patient's medical history, he had consumed uncooked freshwater fish the month before hospital admission. Therefore, praziquantel was administered orally at a dosage of 210 mg/kg/d, three times daily for 3 d.

OUTCOME AND FOLLOW-UP
One week later, a post-treatment fecal examination showed no *C. sinensis* eggs, and both ESR and CRP levels were normal. Notably, the lumbosacral pain had also subsided, and no *C. sinensis* eggs were detected in the three subsequent follow-up visits. The MRI indicated a reduction in bone marrow edema around the left sacroiliac joint after 4 months (Figure 2C and D).

DISCUSSION
The prevalence of AS in China is currently 0.29%, showing an upward trend. Sex-based differences in prevalence have been observed, with males exhibiting a prevalence rate 2.8 times higher than that of females[11]. The patient was diagnosed with AS 10 years ago and achieved a stable health condition following treatment with biologicals. Before the onset of backache, the patient ate uncooked freshwater fish, and *C. sinensis* eggs were detected. Both laboratory and imaging tests revealed an active AS disease. Concurrently, lumbosacral pain symptoms notably improved after insecticidal treatment, and relevant laboratory findings demonstrated improvement. Thus, there is speculation about the potential association between disease activity and *C. sinensis* infection.

Recent reviews have suggested that AS might coexist with various parasitic infections. Some researchers have reported the occurrence of AS alongside mucosal leishmaniasis, *Strongyloides stercoralis*, and *Toxocara canis*[12-14]. A study emphasized the potential risk of latent infection reactivation in individuals undergoing immunosuppressive anti-TNF treatment[12]. Additionally, another study supported a notable link between *C. sinensis* infection and immune suppression, influenced by gender dynamics[15]. Notably, AS patients with parasitic infection may undergo treatment using non-steroidal anti-inflammatory agents. However, administering corticosteroids is contraindicated until insecticidal treatment has been initiated[13].

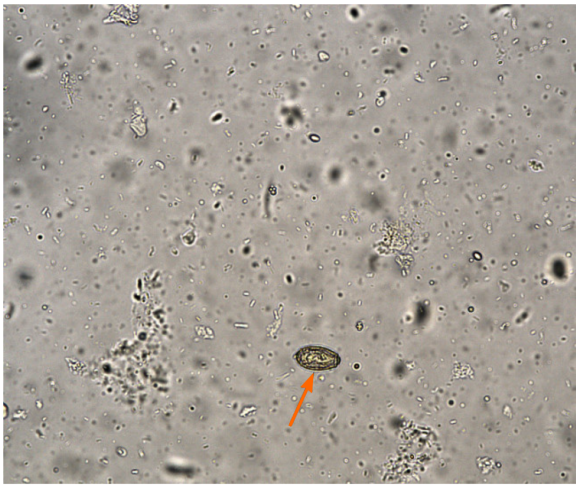

DOI: 10.12998/wjcc.v12.i5.1018

Figure 1 Routine stool examination. On September 29, 2022, the presence of *Clonorchis sinensis* eggs (arrow) was confirmed through microscopic examination of stool samples during hospitalization.

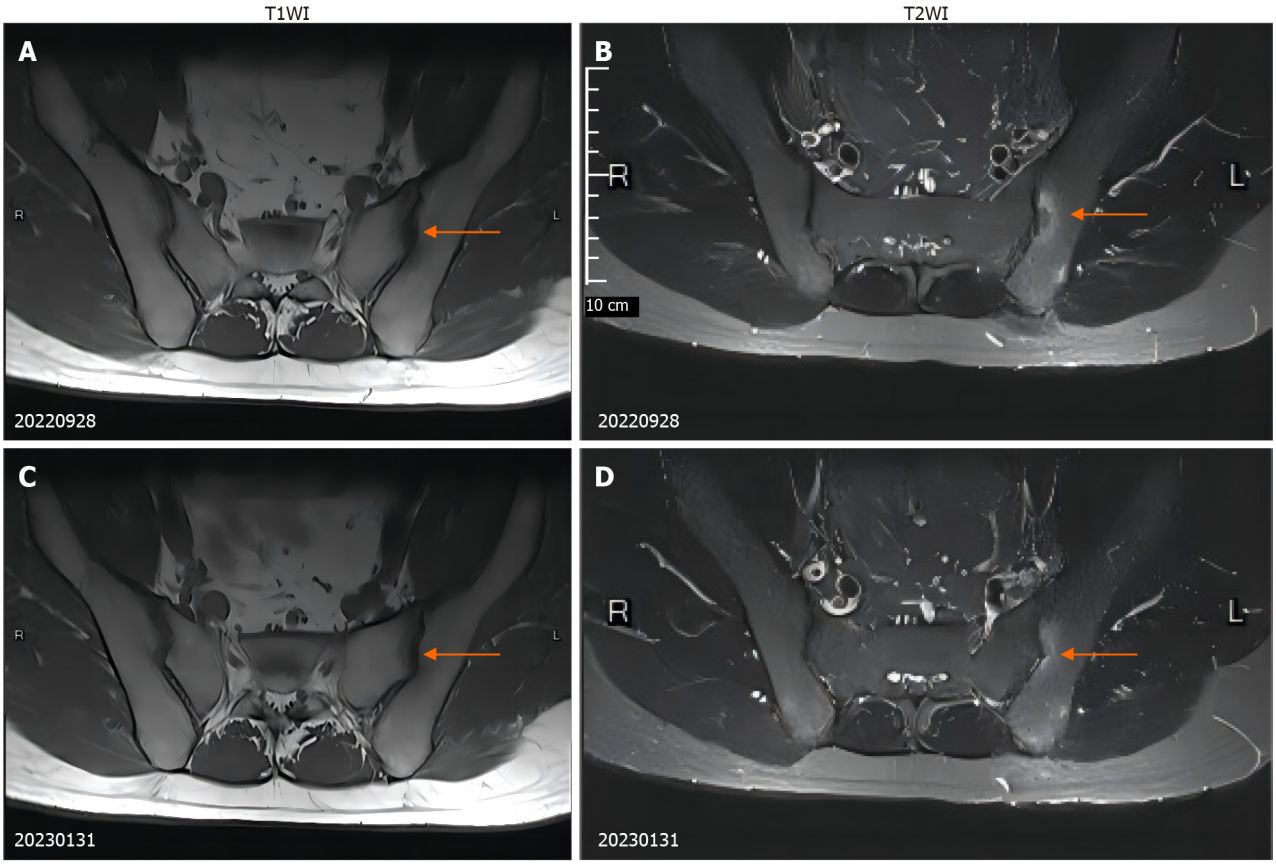

DOI: 10.12998/wjcc.v12.i5.1018

Figure 2 Magnetic resonance imaging of the sacroiliac joint. A: Axial T1-weighted magnetic resonance imaging (MRI) of the sacroiliac joint showing bone marrow edema in the left sacroiliac joint (September 28, 2022); B: T2-weighted MRI of the sacroiliac joint showing bone marrow edema in the left sacroiliac joint. The patient's condition at the time of admission indicates the presence of inflammation and edema in the left sacroiliac joint (September 28, 2022); C: Axial T1-weighted MRI of the sacroiliac joint showing a reduction in the area around the bone marrow edema in the left sacroiliac joint (January 31, 2023); D: T2-weighted MRI of the sacroiliac joint showing a reduction in the area around the bone marrow edema in the left sacroiliac joint. After treatment, follow-up at 4 months indicated a reduction in inflammation and edema of the sacroiliac joint (January 31, 2023).

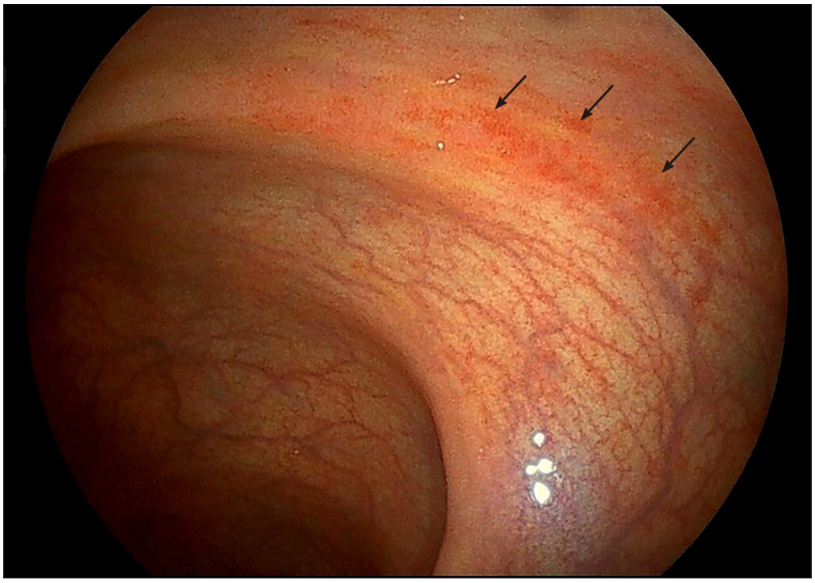

DOI: 10.12998/wjcc.v12.i5.1018

Figure 3 Colonoscopy image. On September 29, 2022, colonoscopy performed during hospitalization revealed scattered congestion in the descending colon, sigmoid colon, and rectum.

Microbial infections have shown a close correlation with autoimmune diseases, supported by evidence from clinical studies and animal experiments[16]. Earlier research indicated that *C. sinensis* might worsen arthritis progression, with this adverse effect potentially linked to changes in immune cell profiles and associated cytokine levels[17]. However, another study suggested that *C. sinensis*-induced protein could suppress new bone formation in a mouse model *in vivo* [18]. Notably, the role of *C. sinensis* infections in modulating arthritis symptoms is a multifaceted and complex phenomenon. Presently, it remains unclear whether there are differences in the pathogenic mechanisms of *C. sinensis* between humans and other animals. Hence, further research is crucial to explore this correlation.

This case report provided significant insights, an imbalance in the Th1/Th2 immune response might compromise the body's defense mechanisms against specific viral, bacterial, and parasitic pathogens, potentially heightening the risk of opportunistic infections[19]. Patients with rheumatic diseases are frequently treated with biologicals, such as anti-TNF, which increases susceptibility to opportunistic infections[20]. Therefore, rheumatologists must evaluate the patient's condition and manage the duration of biological treatment appropriately. Various microbial infections should be ruled out before initiating biologicals, particularly parasitic infections that might be overlooked due to improving environmental conditions. Early detection and treatment of these parasitic infections can significantly improve patient outcomes.

During the diagnosis of this case, some limitations were encountered. For instance, although colonoscopy suggested intestinal mucosal congestion, further pathological biopsies were not conducted. Given these limitations, advocating for continued monitoring of this patient through scheduled follow-up colonoscopy examinations is essential. If any signs of colonic abnormalities emerge during these assessments, then it is prudent to consider subsequent pathological biopsies for a more comprehensive evaluation.

CONCLUSION

Our findings suggest that *C. sinensis* infections could potentially trigger the exacerbation of AS. Clinicians should be mindful of the occurrence of *C. sinensis* infections, particularly in endemic areas when evaluating patients with rheumatic diseases. Despite providing significant insights, further studies are necessary to elucidate the mechanisms underlying the association between AS and *C. sinensis* infections.

ACKNOWLEDGEMENTS

We thank the colleagues in the laboratory at Traditional Chinese Medicine Hospital Dianjiang Chongqing for providing pictures of *C. sinensis* eggs.

FOOTNOTES

Co-first authors: Tian-Xin Yi and Wei Liu.

Author contributions: Yi TX and Liu W wrote the manuscript; Luo L summarized the case and revised the manuscript; Wang XC and Leng WF performed the data collection; all authors have read and approved the final manuscript.

Supported by Chongqing Municipal Health Commission's Key Discipline Construction Project of Traditional Chinese Medicine Bi Disease, Yu Traditional Chinese Medicine (2021), No. 16.

Informed consent statement: All study participants, or their legal guardian, provided informed written consent prior to study enrollment.

Conflict-of-interest statement: The authors have no conflict of interest to declare.

CARE Checklist (2016) statement: The authors have read the CARE Checklist (2016), and the manuscript was prepared and revised according to the CARE Checklist (2016).

Country/Territory of origin: China

ORCID number: Tian-Xin Yi 0009-0005-3353-8231; Wei Liu 0009-0002-8154-0801; Wen-Fei Leng 0009-0007-8070-8250; Xiao-Chuan Wang 0009-0000-5100-6021; Liang Luo 0000-0002-0231-8798.

S-Editor: Gao CC
L-Editor: A
P-Editor: Zhao S

REFERENCES

1 **Braun J**, Sieper J. Ankylosing spondylitis. *Lancet* 2007; **369**: 1379-1390 [PMID: 17448825 DOI: 10.1016/S0140-6736(07)60635-7]
2 **Dean LE**, Jones GT, MacDonald AG, Downham C, Sturrock RD, Macfarlane GJ. Global prevalence of ankylosing spondylitis. *Rheumatology (Oxford)* 2014; **53**: 650-657 [PMID: 24324212 DOI: 10.1093/rheumatology/ket387]
3 **Zochling J**, Bohl-Bühler MH, Baraliakos X, Feldtkeller E, Braun J. Infection and work stress are potential triggers of ankylosing spondylitis. *Clin Rheumatol* 2006; **25**: 660-666 [PMID: 16633712 DOI: 10.1007/s10067-005-0131-z]
4 **Zhang X**, Sun Z, Zhou A, Tao L, Chen Y, Shi X, Yin J, Ding G. Association Between Infections and Risk of Ankylosing Spondylitis: A Systematic Review and Meta-Analysis. *Front Immunol* 2021; **12**: 768741 [PMID: 34745144 DOI: 10.3389/fimmu.2021.768741]
5 **Qian MB**, Zhou XN. Clonorchis sinensis. *Trends Parasitol* 2021; **37**: 1014-1015 [PMID: 34229953 DOI: 10.1016/j.pt.2021.05.011]
6 **Qian MB**, Patel C, Palmeirim MS, Wang X, Schindler C, Utzinger J, Zhou XN, Keiser J. Efficacy of drugs against clonorchiasis and opisthorchiasis: a systematic review and network meta-analysis. *Lancet Microbe* 2022; **3**: e616-e624 [PMID: 35697047 DOI: 10.1016/S2666-5247(22)00026-X]
7 **Liu JX**, Liu M, Yu GZ, Zhao QQ, Wang JL, Sun YH, Koda S, Zhang B, Yu Q, Yan C, Tang RX, Jiang ZH, Zheng KY. Clonorchis sinensis infection induces hepatobiliary injury *via* disturbing sphingolipid metabolism and activating sphingosine 1-phosphate receptor 2. *Front Cell Infect Microbiol* 2022; **12**: 1011378 [PMID: 36339341 DOI: 10.3389/fcimb.2022.1011378]
8 **Qi Y**, Hu J, Liang J, Hu X, Ma N, Xiang B. Clonorchis sinensis infection contributes to hepatocellular carcinoma progression in rat. *Parasitol Res* 2022; **121**: 3403-3415 [PMID: 36266591 DOI: 10.1007/s00436-022-07699-x]
9 **Harrington D**, Lamberton PHL, McGregor A. Human liver flukes. *Lancet Gastroenterol Hepatol* 2017; **2**: 680-689 [PMID: 28786389 DOI: 10.1016/S2468-1253(17)30111-5]
10 **Singh S**, El-Sakkary N, Skinner DE, Sharma PP, Ottilie S, Antonova-Koch Y, Kumar P, Winzeler E, Poonam, Caffrey CR, Rathi B. Synthesis and Bioactivity of Phthalimide Analogs as Potential Drugs to Treat Schistosomiasis, a Neglected Disease of Poverty. *Pharmaceuticals (Basel)* 2020; **13** [PMID: 32028743 DOI: 10.3390/ph13020025]
11 **Zhao J**, Huang C, Huang H, Pan JK, Zeng LF, Luo MH, Liang GH, Yang WY, Liu J. Prevalence of ankylosing spondylitis in a Chinese population: a systematic review and meta-analysis. *Rheumatol Int* 2020; **40**: 859-872 [PMID: 32125505 DOI: 10.1007/s00296-020-04537-0]
12 **Nicodemo AC**, de Andrade HF, Muñoz Torres P, Amato VS. Secondary Prophylaxis with Liposomal Amphotericin B in a Patient with Mucosal Leishmaniasis Undergoing Immunobiological Therapy for Active Ankylosing Spondylitis. *Am J Trop Med Hyg* 2019; **101**: 402-403 [PMID: 31219006 DOI: 10.4269/ajtmh.19-0066]
13 **Richter J**, Müller-Stöver I, Strothmeyer H, Göbels K, Schmitt M, Häussinger D. Arthritis associated with Strongyloides stercoralis infection in HLA B-27-positive African. *Parasitol Res* 2006; **99**: 706-707 [PMID: 16738888 DOI: 10.1007/s00436-006-0225-9]
14 **Jiménez-Balderas FJ**, García-Jaimes J, Ríos R, Zonana-Nacach A, Tapia-Romero R, Villanueva N, Méndez-Samperio P, de-la-Rosa-Arana JL. Isolation of IgG antibodies to Toxocara in ankylosing spondylitis patients with acute anterior uveitis. *Korean J Ophthalmol* 2014; **28**: 207-212 [PMID: 24882953 DOI: 10.3341/kjo.2014.28.3.207]
15 **Kan S**, Li Q, Li HM, Yao YH, Du XY, Wu CY, Chen GJ, Guo XK, Qian MB, Wang ZJ. Clonorchis sinensis infection modulates key cytokines for essential immune response impacted by sex. *PLoS Negl Trop Dis* 2022; **16**: e0010726 [PMID: 36083861 DOI: 10.1371/journal.pntd.0010726]
16 **Verma A**, Sharda S, Rathi B, Somvanshi P, Pandey BD. Elucidating potential molecular signatures through host-microbe interactions for reactive arthritis and inflammatory bowel disease using combinatorial approach. *Sci Rep* 2020; **10**: 15131 [PMID: 32934294 DOI:

10.1038/s41598-020-71674-8]
17 **Li X**, Yang Y, Qin S, Kong F, Yan C, Cheng W, Pan W, Yu Q, Hua H, Zheng K, Tang R. The impact of Clonorchis sinensis infection on immune response in mice with type II collagen-induced arthritis. *BMC Immunol* 2020; **21**: 7 [PMID: 32066378 DOI: 10.1186/s12865-020-0336-6]
18 **Lee YJ**, Kim MJ, Jo S, Jin SH, Park PR, Park K, Song HC, Kim J, Kim JY, Shim SC, Kim TH, Hong SJ, Kang H, Kim TJ, Won EJ. Clonorchis sinensis-Derived Protein Attenuates Inflammation and New Bone Formation in Ankylosing Spondylitis. *Front Immunol* 2021; **12**: 615369 [PMID: 33717104 DOI: 10.3389/fimmu.2021.615369]
19 **Rostevanov IS**, Betesh-Abay B, Nassar A, Rubin E, Uzzan S, Kaplanski J, Biton L, Azab AN. Montelukast induces beneficial behavioral outcomes and reduces inflammation in male and female rats. *Front Immunol* 2022; **13**: 981440 [PMID: 36148246 DOI: 10.3389/fimmu.2022.981440]
20 **Byun JM**, Lee CK, Rhee SY, Kim HJ, Kim JW, Shim JJ, Jang JY. The risk of tuberculosis in Korean patients with inflammatory bowel disease receiving tumor necrosis factor-α blockers. *J Korean Med Sci* 2015; **30**: 173-179 [PMID: 25653489 DOI: 10.3346/jkms.2015.30.2.173]

World Journal of Clinical Cases

Submit a Manuscript: https://www.f6publishing.com

World J Clin Cases 2024 February 16; 12(5): 1025-1028

DOI: 10.12998/wjcc.v12.i5.1025

ISSN 2307-8960 (online)

CASE REPORT

Hematuria after nocturnal exercise of a man: A case report

Ming-Jian Bai, Song-Tao Yang, Xue-Kai Liu

Specialty type: Urology and nephrology

Provenance and peer review: Unsolicited article; Externally peer reviewed.

Peer-review model: Single blind

Peer-review report's scientific quality classification

Grade A (Excellent): 0
Grade B (Very good): B
Grade C (Good): 0
Grade D (Fair): 0
Grade E (Poor): 0

P-Reviewer: Shalaby MN, Egypt

Received: December 10, 2023
Peer-review started: December 10, 2023
First decision: December 18, 2023
Revised: December 28, 2023
Accepted: January 22, 2024
Article in press: January 22, 2024
Published online: February 16, 2024

Ming-Jian Bai, Xue-Kai Liu, Department of Clinical Laboratory, Aerospace Center Hospital, Beijing 100049, China

Song-Tao Yang, Department of Nephrology, Aerospace Center Hospital, Beijing 100049, China

Corresponding author: Xue-Kai Liu, MD, Doctor, Department of Clinical Laboratory, Aerospace Center Hospital, No. 15 Yuquan Road, Haidian District, Beijing 100049, China. 15101129780@163.com

Abstract

BACKGROUND

A man experienced multiple episodes of macroscopic hematuria following nocturnal exercise. Urinary stones and tumors were considered the two most likely causes. The patient had two hobbies: Consuming health care products in large quantities and engaging in late-night running.

CASE SUMMARY

Health care products contain a large amount of calcium phosphate, and we hypothesize that this could induce the formation of small phosphate stones. After exercise, the urinary system is abraded, resulting in bleeding. The patient was advised to stop using the health care products. Consequently, the aforementioned symptoms disappeared immediately. However, the patient resumed the above two habits one year later; correspondingly, the macroscopic hematuria reappeared.

CONCLUSION

This finding further confirmed the above inference and allowed for a new avenue to determine the cause of the patient's hematuria.

Key Words: Hematuria; Health care products; Exercise; Case report

Core Tip: If patients take a lot of healthcare products containing calcium phosphate, amorphous phosphate crystals may appear in urine. Once they do exercise, they may scratch the urethra and cause hematuria.

Citation: Bai MJ, Yang ST, Liu XK. Hematuria after nocturnal exercise of a man: A case report. *World J Clin Cases* 2024; 12(5): 1025-1028
URL: https://www.wjgnet.com/2307-8960/full/v12/i5/1025.htm
DOI: https://dx.doi.org/10.12998/wjcc.v12.i5.1025

INTRODUCTION

Multiple studies have shown that clinical hematuria is common after exercise[1], with 95-100% of the patients with clinical hematuria having it after exercise[2]. The degree of hematuria is related to the intensity of the exercise; for instance, contact sports can increase the risk of macroscopic hematuria. Exercise-related urological trauma is regarded as the leading cause of macroscopic hematuria, of which renal trauma accounts for 80% of cases. Here, we present the case of a patient with macroscopic hematuria who consumed a significant amount of health care products orally and favored exercise.

CASE PRESENTATION

Chief complaints

A 42-year-old man was admitted to the Emergency Department of our hospital on June 14, 2020 due to macroscopic hematuria after nocturnal exercise (Figure 1).

History of present illness

Upon reviewing the medical history, the patient experienced macroscopic hematuria three times after nocturnal exercise in the previous four years, and the hematuria was accompanied by lower abdominal pain. However, the actual cause of the disease had not been determined. Following a multidisciplinary team consultation, it was speculated that the nutcracker phenomenon, the very small stone traumatizing the mucosa, and urinary tract tumors were the three most likely causes of the patient's hematuria.

History of past illness

No special notes.

Personal and family history

No special notes.

Physical examination

No special notes.

Laboratory examinations

We conducted routine urine tests, Doppler ultrasound, computed tomography urography, and endoscopic examination of the urinary system. The results indicated that only the routine urine test was abnormal, revealing urine protein (+), occult blood (++), and a red blood cell count of 21587.0 cells/μL. Additionally, a significant number of amorphous phosphate crystals were observed under the microscope (Figure 1).

Imaging examinations

No obvious compression changes were observed in the left renal vein. The angle between the superior mesenteric artery and abdominal aorta was 41 degrees (Figure 2). At this point, hematuria caused by the nutcracker phenomenon and urologic neoplasms were essentially ruled out.

MULTIDISCIPLINARY EXPERT CONSULTATION

We re-inquired the patient again, with a focus on his lifestyle habits. The patient particularly enjoyed doing two things: taking large doses of health care products and exercising late at night. Upon reviewing the labels of the health care products, we identified calcium phosphate as one of the main components.

FINAL DIAGNOSIS

A hypothesis was formulated: the patient had orally consumed excessive amounts of health care products containing calcium phosphate, leading to the formation of tiny stones in the urine. These stones are not easily detected by imaging or

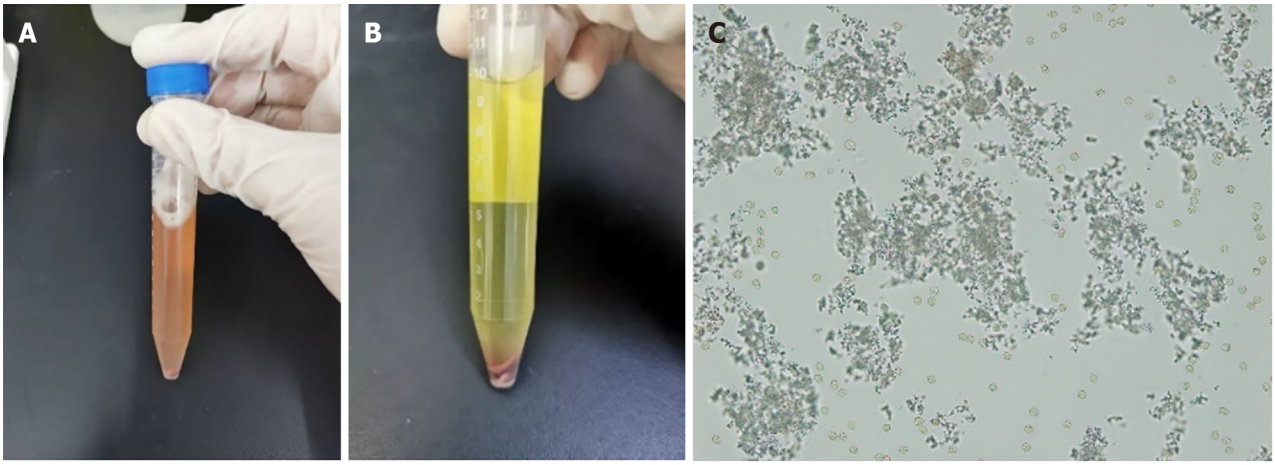

DOI: 10.12998/wjcc.v12.i5.1025

Figure 1 Urine test of the patient. A: Before centrifugation; B: After centrifugation (400 g × 5 min); C: Microscopic appearance (40 × 10 times).

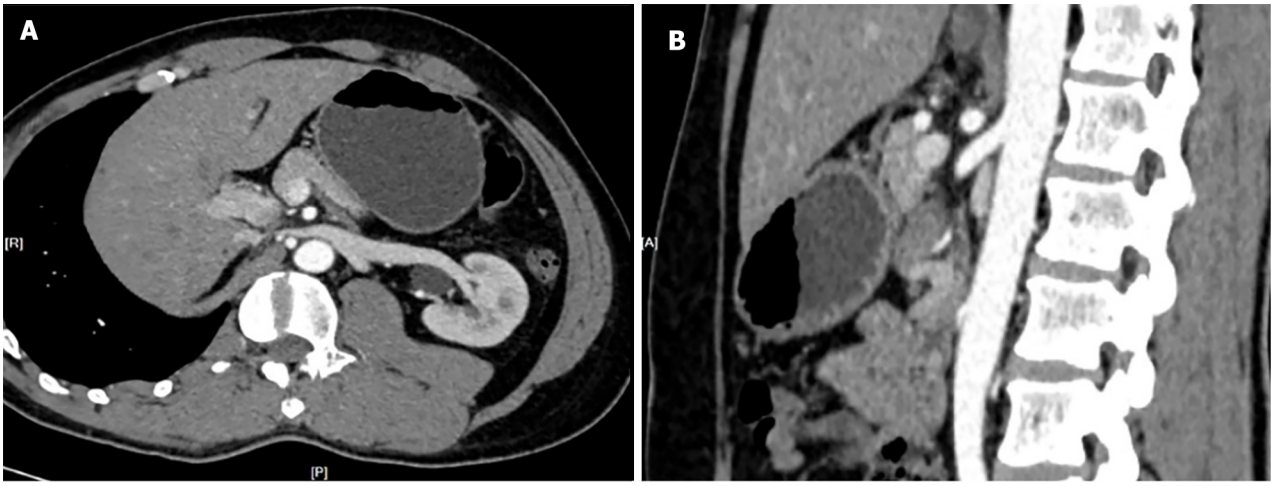

DOI: 10.12998/wjcc.v12.i5.1025

Figure 2 Computed tomography urography of the patient. A: Transverse plane; B: Sagittal plane.

endoscopy. Following nocturnal exercise, these tiny stones scratch the mucosa of the urinary system, resulting in bleeding and abdominal pain.

TREATMENT

Based on the above assumptions, the patient was advised to stop using the health care products after discharge.

OUTCOME AND FOLLOW-UP

Subsequently, the patient's hematuria disappeared. However, one year later, the patient consumed the aforementioned health care products in large quantities again, and his hematuria recurred after late-night exercise. It was then confirmed that the patient's hematuria was caused by the consumption of health care products containing calcium phosphate. The patient was again advised to stop using those health care products, at which point the patient's hematuria then disappeared.

DISCUSSION

Hematuria is a common phenomenon following exercise[1]. A previous study provided evidence of the relationship

between hypercalciuria and postglomerular hematuria in children[3]. Escribano *et al*[4] also discovered that hypercalciuria can lead to recurrent macroscopic or microscopic hematuria. Through follow-up, it was observed that the occurrence of hematuria after exercise was clearly associated with the patient's use of the aforementioned health care products. Consequently, we deduced the pathogenesis of this patient: the abundance of amorphous phosphate leads to the formation of crystals in the urine. These crystals may scratch the urethra during exercise, ultimately resulting in hematuria.

CONCLUSION

In conclusion, if patients consume a significant quantity of health care products containing calcium phosphate, amorphous phosphate crystals may appear in the urine. During exercise, these crystals may scratch the urethra, leading to hematuria. Therefore, the present case provides a new avenue for determining the cause of hematuria in clinical practice.

FOOTNOTES

Author contributions: Bai MJ wrote the manuscript; Yang ST was responsible for receiving patients; Liu XK was responsible for laboratory tests related to patients.

Informed consent statement: Informed written consent was obtained from the patient for publication.

Conflict-of-interest statement: All the authors declare that they have no conflict of interest.

CARE Checklist (2016) statement: The authors have read the CARE Checklist (2016), and the manuscript was prepared and revised according to the CARE Checklist (2016).

Country/Territory of origin: China

ORCID number: Xue-Kai Liu 0009-0008-2249-7528.

S-Editor: Liu JH
L-Editor: A
P-Editor: Yu HG

REFERENCES

1 **Akiboye RD**, Sharma DM. Haematuria in Sport: A Review. *Eur Urol Focus* 2019; **5**: 912-916 [PMID: 29500137 DOI: 10.1016/j.euf.2018.02.008]
2 **Mousavi M**, Sanavi S, Afshar R. Effects of continuous and intermittent trainings on exercise-induced hematuria and proteinuria in untrained adult females. *NDT Plus* 2011; **4**: 217-218 [PMID: 25984163 DOI: 10.1093/ndtplus/sfr011]
3 **Reusz G**, Szabó A. Hypercalciuria and postglomerular hematuria in children. The effects of thiazide on calcium excretion, urine saturation with respect to calcium-hydrogenphosphate and hematuria. *Acta Paediatr Hung* 1990; **30**: 63-71 [PMID: 2317387]
4 **Escribano J**, Balaguer A, Roqué i Figuls M, Feliu A, Ferre N. Dietary interventions for preventing complications in idiopathic hypercalciuria. *Cochrane Database Syst Rev* 2014; **2014**: CD006022 [PMID: 24519664 DOI: 10.1002/14651858.CD006022.pub4]

World Journal of Clinical Cases

Submit a Manuscript: https://www.f6publishing.com

World J Clin Cases 2024 February 16; 12(5): 1029-1032

DOI: 10.12998/wjcc.v12.i5.1029

ISSN 2307-8960 (online)

LETTER TO THE EDITOR

Response letter to "Acute cholangitis: Does malignant biliary obstruction *vs* choledocholithiasis etiology change the outcomes?" with imaging aspects

Sonay Aydin, Baris Irgul

Specialty type: Medicine, research and experimental

Provenance and peer review: Unsolicited article; Externally peer reviewed.

Peer-review model: Single blind

Peer-review report's scientific quality classification
Grade A (Excellent): 0
Grade B (Very good): B
Grade C (Good): C
Grade D (Fair): 0
Grade E (Poor): E

P-Reviewer: Dabbous H, Egypt; Salerno R, Italy; Wen XL, China

Received: October 26, 2023
Peer-review started: October 26, 2023
First decision: December 7, 2023
Revised: December 12, 2023
Accepted: January 24, 2024
Article in press: January 24, 2024
Published online: February 16, 2024

Sonay Aydin, Baris Irgul, Department of Radiology, Erzincan Binali Yildirim University, Erzincan 24100, Turkey

Corresponding author: Baris Irgul, MD, Research Assistant, Department of Radiology, Erzincan Binali Yildirim University, No. 32 Haci Ali Akin Street, Erzincan 24100, Turkey. barisirgul@gmail.com

Abstract

Radiological imaging findings may contribute to the differentiation of malignant biliary obstruction from choledocholithiasis in the etiology of acute cholangitis.

Key Words: Malignant biliary obstruction; Choledocholithiasis; Acute cholangitis; Dilated bile ducts; Magnetic resonance cholangiopancreatography; Endoscopic retrograde cholangiopancreatography

Core Tip: In malignant biliary obstructions, irregular walls, increased wall thickness, and blunt termination are seen in the choledochal duct. In choledocholithiasis, stones are seen in the lumen and the choledochal walls are regular.

Citation: Aydin S, Irgul B. Response letter to "Acute cholangitis: Does malignant biliary obstruction *vs* choledocholithiasis etiology change the outcomes?" with imaging aspects. *World J Clin Cases* 2024; 12(5): 1029-1032
URL: https://www.wjgnet.com/2307-8960/full/v12/i5/1029.htm
DOI: https://dx.doi.org/10.12998/wjcc.v12.i5.1029

TO THE EDITOR

We were intrigued by the paper "Acute cholangitis: Does malignant biliary obstruction *vs* choledocholithiasis etiology change the clinical presentation and outcomes?" by Tsou *et al*[1]. This study primarily examined laboratory data to dis-tinguish

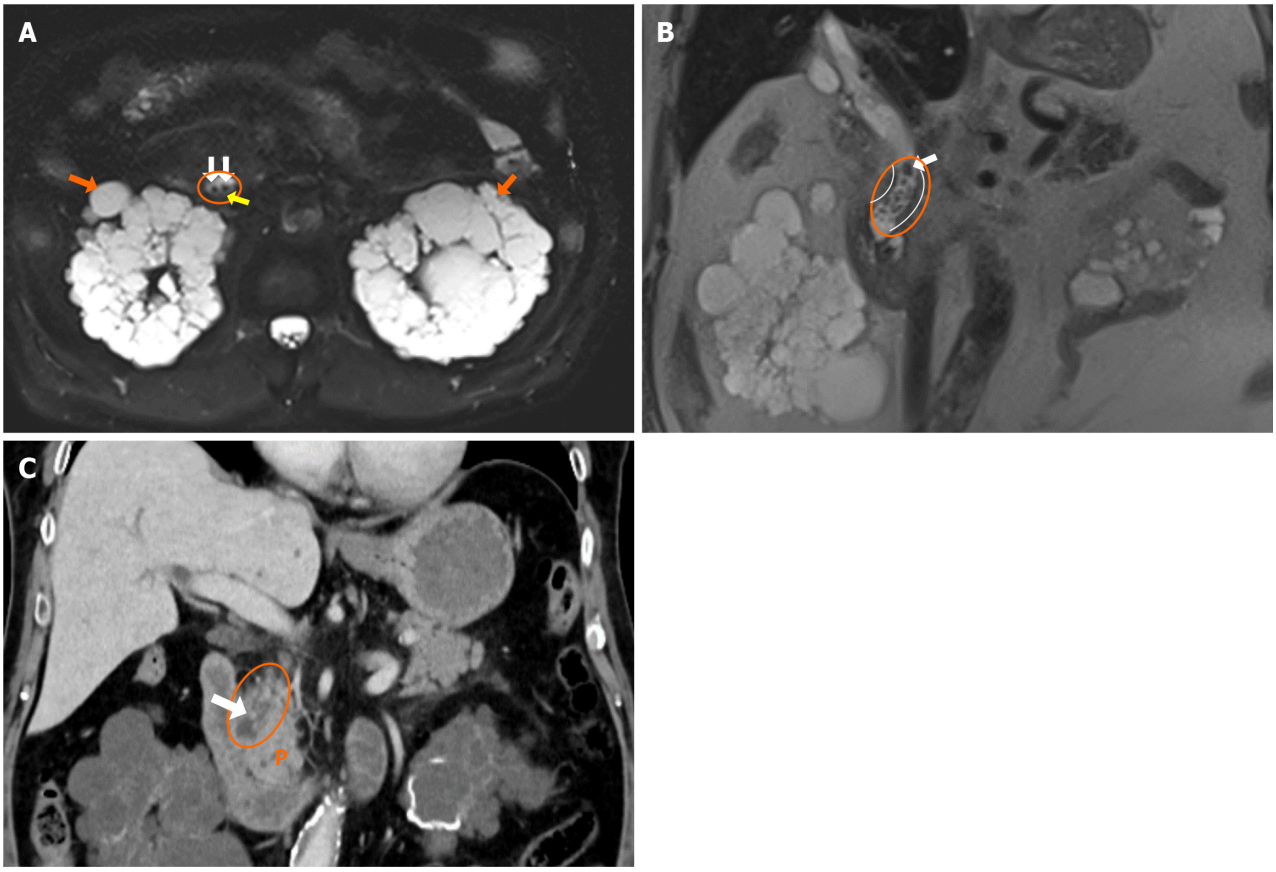

DOI: 10.12998/wjcc.v12.i5.1029

Figure 1 Choledochal obstruction caused by calculus. A: Fat-suppressed T2 WI shows calculus (white arrows) in the dilated choledochal duct (circle) and bile sludge (orange arrow). The patient also has autosomal dominant polycystic kidney disease (orange arrows); B: HASTE coronal image shows calculus (white arrow) in the dilated choledochal duct (circle) with smooth borders (curved lines); C: Coronal computed tomography image shows a dilated choledochal duct (circle) with calculus (white arrow) P: Pancreas.

between malignant biliary obstruction and obstruction caused by stones and underscored it's significance. However, the study did not investigate the role and significance of imaging in this differentiation. In this letter to the editor, we aim to highlight the crucial imaging indicators for the aforementioned differentiation.

In the current era of medical imaging, which offers a wide range of imaging techniques from basic radiographs to advanced magnetic resonance imaging (MRI) scans, the role of the radiologist is to assist the physician in choosing the appropriate imaging method and addressing important patient care issues. Ultrasound (US) is used as a preliminary method to screen for biliary obstruction, but it cannot accurately establish the severity and cause of obstructive jaundice. Therefore, further imaging with techniques like contrast enhanced computerized tomography and magnetic resonance cholangiopancreatography (MRCP) are necessary as they are more effective in providing accurate diagnostic information. MRCP has become the preferred method for examining biliary obstruction, with endoscopic retrograde cholangiopancreatography being reserved for patients who are more likely to require therapeutic intervention[2].

The Tokyo Guidelines are employed for the diagnosis of acute cholangitis. According to these criteria, acute cholangitis can be diagnosed based on signs of systemic inflammation, cholestasis, and imaging results[3]. Calculi and dilatation can be observed in the bile ducts on US and computed tomography (CT) scans due to the presence of stones in acute cholangitis caused by choledocholithiasis. MRCP scans reveal signal attenuation caused by the presence of calculi. The bile duct walls exhibit a rather slender and sleek shape[4] (Figure 1).

Acute cholangitis caused by malignant biliary obstructions is characterized by the enlargement of the biliary tract, which can be detected using US, CT, and MRCP, similar to the presentation in cases of choledocholithiasis. Furthermore, intraductal mass lesions are present, with extensive segments of contrasting bile duct walls that are uneven and thicker (> 1.5 mm). Additionally, blunt terminations in the bile ducts caused by distal tumoral lesions are visible[4] (Figure 2).

In conclusion, while certain imaging findings have been identified to distinguish between cancer and stone-induced blockages, there is currently no universally accepted approach or finding to definitively differentiate between the two. If a routinely used imaging modality like MRCP reveals any secondary finding that indicates malignant blockage, multiphase-dynamic CT/MRI is recommended for optimal evaluation of nearby organs such as the biliary system and pancreas. In addition, US is sufficient to explain the etiology of biliary obstructions such as stones. When the cause of obstruction cannot be found with US, second- and third-level imaging techniques such as CT, MRI, or endoscopic ultrasonography are needed; however, their unnecessary overuse should be avoided.

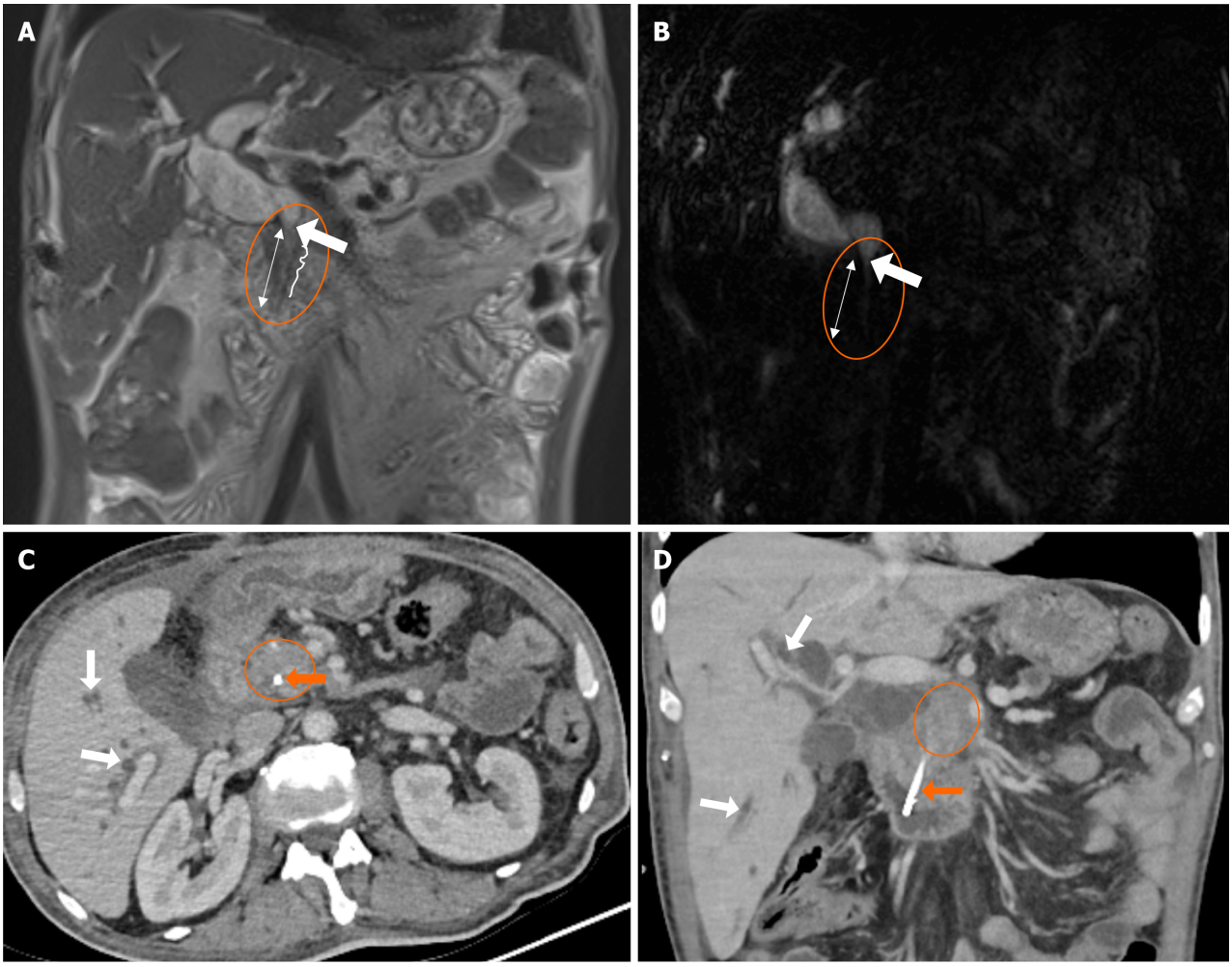

DOI: 10.12998/wjcc.v12.i5.1029

Figure 2 Choledochal involvement of a pancreatic mass. A and B: Coronal T2 WI and coronal magnetic resonance cholangiopancreatography images. The dilated choledochal duct (circle) abruptly narrows bluntly (white arrow) and continues narrowly in a long segment more distally (two-headed arrow). Contour irregularities (serrated lines) are seen on the distal walls of the choledochal duct; C and D: Post-treatment axial and coronal computed tomography images of the same patient show an irregularly bordered, hypodense, heterogeneous, solid mass lesion (circle) in the head of the pancreas, stent material extending from the duodenum to the pancreas (orange arrow), and dilated intrahepatic bile ducts (white arrow).

FOOTNOTES

Author contributions: Aydin S and Irgul B conceived and designed the analysis, collected the data, wrote the paper and performed the analysis.

Conflict-of-interest statement: All the authors report no relevant conflicts of interest for this article.

Country/Territory of origin: Turkey

ORCID number: Sonay Aydin 0000-0002-3812-6333; Baris Irgul 0000-0002-7551-8686.

S-Editor: Qu XL
L-Editor: Filipodia
P-Editor: Zhao S

REFERENCES

1 **Tsou YK**, Su YT, Lin CH, Liu NJ. Acute cholangitis: Does malignant biliary obstruction *vs* choledocholithiasis etiology change the clinical presentation and outcomes? *World J Clin Cases* 2023; **11**: 6984-6994 [PMID: 37946763 DOI: 10.12998/wjcc.v11.i29.6984]

2 **Joshi A**, Rajpal K, Kakadiya K, Bansal A. Role of CT and MRCP in Evaluation of Biliary Tract Obstruction. *Curr Radiol Rep* 2014; **72**: 2 [DOI: 10.1007/s40134-014-0072-x]

3 **Kiriyama S**, Kozaka K, Takada T, Strasberg SM, Pitt HA, Gabata T, Hata J, Liau KH, Miura F, Horiguchi A, Liu KH, Su CH, Wada K, Jagannath P, Itoi T, Gouma DJ, Mori Y, Mukai S, Giménez ME, Huang WS, Kim MH, Okamoto K, Belli G, Dervenis C, Chan ACW, Lau WY, Endo I, Gomi H, Yoshida M, Mayumi T, Baron TH, de Santibañes E, Teoh AYB, Hwang TL, Ker CG, Chen MF, Han HS, Yoon YS, Choi IS, Yoon DS, Higuchi R, Kitano S, Inomata M, Deziel DJ, Jonas E, Hirata K, Sumiyama Y, Inui K, Yamamoto M. Tokyo Guidelines 2018: diagnostic criteria and severity grading of acute cholangitis (with videos). *J Hepatobiliary Pancreat Sci* 2018; **25**: 17-30 [PMID: 29032610 DOI: 10.1002/jhbp.512]

4 **Choi SH**, Han JK, Lee JM, Lee KH, Kim SH, Lee JY, Choi BI. Differentiating malignant from benign common bile duct stricture with multiphasic helical CT. *Radiology* 2005; **236**: 178-183 [PMID: 15955859 DOI: 10.1148/radiol.2361040792]

World Journal of Clinical Cases

Submit a Manuscript: https://www.f6publishing.com

World J Clin Cases 2024 February 16; 12(5): 1033-1035

DOI: 10.12998/wjcc.v12.i5.1033

ISSN 2307-8960 (online)

LETTER TO THE EDITOR

Exploring multifaceted factors in chronic kidney disease risk: A comprehensive analysis of biochemistry, lifestyle, and inflammation in elderly Chinese individuals

Fernando Cardona

Specialty type: Biochemistry and molecular biology

Provenance and peer review: Unsolicited article; Externally peer reviewed.

Peer-review model: Single blind

Peer-review report's scientific quality classification

Grade A (Excellent): 0
Grade B (Very good): B
Grade C (Good): 0
Grade D (Fair): 0
Grade E (Poor): 0

P-Reviewer: Chiu H, Taiwan

Received: November 4, 2023
Peer-review started: November 4, 2023
First decision: December 31, 2023
Revised: December 31, 2023
Accepted: January 18, 2024
Article in press: January 18, 2024
Published online: February 16, 2024

Fernando Cardona, Unitat de Genètica Molecular, Instituto de Biomedicina de Valencia – CSIC, Valencia 46010, Spain

Fernando Cardona, Centro de investigación Biomédica en Red Enfermedades Neurodegenerativas (CIBERNED), Instituto de Salud Carlos III, Madrid 28029, Spain

Fernando Cardona, Departamento de Biotecnología, Escuela Técnica Superior de Ingeniería Agronómica y del Medio Natural (ETSIAMN), Univeristat Politècnica de Valencia, Valencia 46022, Spain

Corresponding author: Fernando Cardona, PhD, Assistant Lecturer, Research Assistant, Unitat de Genètica Molecular, Instituto de Biomedicina de Valencia – CSIC, C/Jaume Roig 11, Valencia 46010, Spain. fcardona@ibv.csic.es

Abstract

This letter praises a recent article in the *World Journal of Clinical Cases* (Roles of biochemistry data, lifestyle, and inflammation in identifying abnormal renal function in old Chinese), examining factors affecting abnormal renal function in elderly Chinese using advanced machine learning. It highlights the importance of uric acid, age, hemoglobin, body mass index, sport hours, and systolic blood pressure. The study's holistic approach, integrating lifestyle and inflammation, offers a nuanced understanding of chronic kidney disease risk factors. The letter suggests exploring mechanistic pathways of hyperuricemia, the link between anemia and renal function, and the connection between body mass index and estimated glomerular filtration rate. It advocates investigating physical activity's impact on renal health and the independent effects of blood pressure. The study significantly contributes to chronic kidney disease understanding, proposing avenues for further exploration and interventions. Commendations are extended to the authors and the journal.

Key Words: Biochemistry data; Lifestyle; Machine learning; Renal function

Core Tip: This letter commends a recent article in the *World Journal of Clinical Cases* that employs advanced machine learning to investigate factors affecting abnormal renal function in elderly Chinese individuals. The study emphasizes the significance of uric acid, age, hemoglobin, body mass index, sport hours, and systolic blood pressure. Its holistic approach, integrating lifestyle and inflammation, provides a nuanced understanding of chronic kidney disease risk factors. The letter proposes further exploration into mechanistic pathways of hyperuricemia, the link between anemia and renal function, and the association between body mass index and estimated glomerular filtration rate. Additionally, it advocates for investigating the impact of physical activity on renal health and the independent effects of blood pressure. The study contributes significantly to understanding chronic kidney disease, suggesting avenues for further research and interventions, and extends commendations to the authors and the journal.

Citation: Cardona F. Exploring multifaceted factors in chronic kidney disease risk: A comprehensive analysis of biochemistry, lifestyle, and inflammation in elderly Chinese individuals. *World J Clin Cases* 2024; 12(5): 1033-1035
URL: https://www.wjgnet.com/2307-8960/full/v12/i5/1033.htm
DOI: https://dx.doi.org/10.12998/wjcc.v12.i5.1033

TO THE EDITOR

I am writing to convey my appreciation for the recent article entitled "Roles of Biochemistry Data, Lifestyle, and Inflammation in Identifying Abnormal Renal Function in Elderly Chinese," which was recently published in the *World Journal of Clinical Cases*[1]. This study delves into the identification of factors associated with a low estimated glomerular filtration rate (L-eGFR) within a cohort of elderly Chinese individuals. The authors employed advanced machine learning techniques and their findings shed light on the significance of various risk factors, such as uric acid (UA), age, hemoglobin (Hb), body mass index (BMI), sport hours, and systolic blood pressure (SBP), in the identification of abnormal renal function.

The escalating incidence of chronic kidney disease (CKD) in recent years has raised considerable concerns, notably due to its substantial impact on patient mortality rates, rendering it a critical area of study. Given that the importance of UA has been highlighted for both diabetic[2] and non-diabetic patients[3], the article endeavors to offer a more comprehensive perspective on the risk factors for CKD. It extends beyond the traditional boundaries of research by incorporating lifestyle and inflammation markers into the analysis, and furthermore, employs cutting-edge machine learning methods, thereby presenting an innovative approach to identifying subjects with abnormal renal function.

One noteworthy aspect of the study is its inclusion of lifestyle and inflammation factors in addition to demographic and biochemistry data. This holistic approach provides a more comprehensive understanding of the intricate interplay of variables contributing to CKD. The utilization of machine learning techniques adds a layer of sophistication to the analysis, allowing for a more nuanced exploration of the data. This approach not only advances our understanding but also offers potential avenues for more personalized and effective interventions. These data both validate and advance previous results in this field, employing both linear and nonlinear relationships of risk factors for CKD in the elderly to develop a predictive model for early intervention in the health of the elderly[4].

The results presented in the article are indeed thought-provoking, particularly in accentuating the heightened significance of risk factors as we progress from Model 1 (incorporating demographic and biochemistry data) to Model 3 (including inflammatory markers). The study underscores the importance of inflammation markers and lifestyle factors in identifying individuals with abnormal renal function. Furthermore, Model 3 identifies UA as the most influential risk factor, followed by age, Hb, BMI, sport hours, and SBP. These findings not only provide new insights into the multifaceted nature of CKD risk factors but also raise questions about the potential mechanistic pathways underpinning these associations.

Nonetheless, I would like to propose further avenues for exploration and discussion. First, in light of the significance of UA in identifying L-eGFR, it would be intriguing to delve deeper into the mechanistic pathways through which hyperuricemia impacts renal function, especially concerning vascular obstruction and renal hypoperfusion. An emerging interpretation could entail an exploration of the interplay between UA and inflammation. Given the established links between hyperuricemia and vascular obstruction, investigating whether targeting UA levels could positively impact renal health, particularly in the context of CKD, would be of interest. Additionally, this raises the potential for designing interventions that not only focus on individual risk factors but also address their interactions.

Moreover, the study spotlights the role of hemoglobin levels as a significant risk factor for abnormal eGFR, eliciting questions about the causal relationship between anemia and renal function. It may be beneficial to investigate whether the management of anemia in elderly individuals could potentially impede the progression of CKD and contribute to the preservation of renal health, thereby opening avenues for interventions that address both conditions concurrently.

The connection between BMI and eGFR is intriguing, and the study's findings emphasize the necessity for further longitudinal research to elucidate this association, particularly given the escalating prevalence of obesity-related comorbidities. Given that prior works have linked BMI to kidney function[5] and UA to BMI[6], it would be constructive to investigate how the trajectory of BMI over time impacts renal function. This could provide insights into the potential benefits of weight management and offer more tailored recommendations for individuals at risk of CKD.

The importance of sport hours as a risk factor for L-eGFR underscores the potential role of physical activity in renal health. Future research could explore specific exercise regimens or interventions tailored to elderly individuals, aimed at improving renal function.

Lastly, the independent effects of SBP and diastolic blood pressure on eGFR warrant further investigation. Subsequent studies could help unveil the mechanisms underlying these effects and explore the potential for targeted interventions in blood pressure management.

As a constructive critique, the study appropriately underscores the significance of age, which has been substantiated by prior research on CKD. This may be because age is regarded as a static factor rather than a dynamic one. Gaining a deeper understanding of how age-related changes in renal function evolve over time could pave the way for interventions that are tailored to meet the specific needs of aging individuals.

In conclusion, the article makes a significant contribution to our comprehension of CKD risk factors in elderly Chinese individuals. It provides valuable insights into the intricate interplay of demographic, biochemistry, lifestyle, and inflammation factors in identifying individuals at risk of abnormal renal function. Its application of machine learning techniques and inclusion of a wide range of risk factors is commendable and enhances our understanding of CKD in the elderly Chinese population. To fully maximize the impact of these findings, future research could delve into the intricate interactions between risk factors, explore potential causal mechanisms, and design interventions that consider the evolving nature of these factors. Additionally, addressing the limitations and contemplating the potential for generalization to broader populations would further bolster the study's impact. I hope these suggested avenues for further research will contribute to the ongoing exploration of CKD risk factors and potential interventions.

I wish to extend my gratitude to the authors for their thought-provoking work and to your esteemed journal for publishing this crucial research.

FOOTNOTES

Author contributions: Cardona F is the sole author.

Conflict-of-interest statement: Fernando Cardona is not be in any situation which could give rise to a conflict of interest.

Country/Territory of origin: Spain

ORCID number: Fernando Cardona 0000-0001-7390-2265.

S-Editor: Liu JH
L-Editor: A
P-Editor: Yu HG

REFERENCES

1 **Chen CH**, Wang CK, Wang CY, Chang CF, Chu TW. Roles of biochemistry data, lifestyle, and inflammation in identifying abnormal renal function in old Chinese. *World J Clin Cases* 2023; **11**: 7004-7016 [PMID: 37946770 DOI: 10.12998/wjcc.v11.i29.7004]

2 **Zhou Q**, Ke S, Yan Y, Guo Y, Liu Q. Serum uric acid is associated with chronic kidney disease in elderly Chinese patients with diabetes. *Ren Fail* 2023; **45**: 2238825 [PMID: 37488934 DOI: 10.1080/0886022X.2023.2238825]

3 **Sturm G**, Kollerits B, Neyer U, Ritz E, Kronenberg F; MMKD Study Group. Uric acid as a risk factor for progression of non-diabetic chronic kidney disease? The Mild to Moderate Kidney Disease (MMKD) Study. *Exp Gerontol* 2008; **43**: 347-352 [PMID: 18294794 DOI: 10.1016/j.exger.2008.01.006]

4 **Chou YC**, Kuan JC, Yang T, Chou WY, Hsieh PC, Bai CH, You SL, Chen CH, Wei CY, Sun CA. Elevated uric acid level as a significant predictor of chronic kidney disease: a cohort study with repeated measurements. *J Nephrol* 2015; **28**: 457-462 [PMID: 25410145 DOI: 10.1007/s40620-014-0158-9]

5 **Russo D**, Morrone LF, Errichiello C, De Gregorio MG, Imbriaco M, Battaglia Y, Russo L, Andreucci M, Di Iorio BR. Impact of BMI on cardiovascular events, renal function, and coronary artery calcification. *Blood Purif* 2014; **38**: 1-6 [PMID: 25196674 DOI: 10.1159/000362862]

6 **Corso LML**, Wing RR, Tate DF, Espeland MA, Blanchard BE, McCaffery JM. Uric acid as a predictor of weight gain and cardiometabolic health in the Study of Novel Approaches to Weight Gain Prevention (SNAP) study. *Int J Obes (Lond)* 2022; **46**: 1556-1559 [PMID: 35501471 DOI: 10.1038/s41366-022-01131-1]

World Journal of Clinical Cases

Submit a Manuscript: https://www.f6publishing.com

World J Clin Cases 2024 February 16; 12(5): 1036-1038

DOI: 10.12998/wjcc.v12.i5.1036

ISSN 2307-8960 (online)

LETTER TO THE EDITOR

Transcranial direct current stimulation efficacy in trigeminal neuralgia

Theodoros Fasilis, Stylianos Gatzonis, Panayiotis Patrikelis, Stefanos Korfias, Athanasia Alexoudi

Specialty type: Neurosciences

Provenance and peer review: Unsolicited article; Externally peer reviewed.

Peer-review model: Single blind

Peer-review report's scientific quality classification

Grade A (Excellent): 0
Grade B (Very good): 0
Grade C (Good): C
Grade D (Fair): 0
Grade E (Poor): 0

P-Reviewer: Gupta L, Indonesia

Received: November 24, 2023
Peer-review started: November 24, 2023
First decision: December 18, 2023
Revised: December 27, 2023
Accepted: January 16, 2024
Article in press: January 16, 2024
Published online: February 16, 2024

Theodoros Fasilis, Stylianos Gatzonis, Panayiotis Patrikelis, Stefanos Korfias, Athanasia Alexoudi, 1st Department of Neurosurgery, National and Kapodistrian University of Athens, Athens 10676, Greece

Athanasia Alexoudi, Department of Neurology, Neurological Institute of Athens, Athens 10676, Greece

Corresponding author: Athanasia Alexoudi, MD, MSc, PhD, Academic Research, Research Fellow, Department of Neurosurgery, National and Kapodistrian University of Athens, Ipsilantou 45-47, Athens 10676, Greece. alexoudath@yahoo.gr

Abstract

Trigeminal neuralgia is a severe, disabling pain and its deafferentation remains a challenge for health providers. Transcranial direct current stimulation is a non-invasive stimulation technique which finds new utility in managing pain. Therefore, the introduction of alternative, non-invasive, safe, and effective methods should be considered in treating patients with trigeminal neuralgia unresponsive to conventional treatment.

Key Words: Trigeminal neuralgia; Patient-controlled intravenous analgesia; Neuromodulation; Transcranial direct current stimulation

Core Tip: Various drugs and surgical procedures have been utilized for the treatment of trigeminal neuralgia. The side effects of conventional treatments alongside with the refractoriness of the condition render numerous available approaches unsatisfactory. Mounting evidence suggest alternative, non-invasive, and safe methods such as patient-controlled intravenous analgesia with esketamine and transcranial direct current stimulation effective instruments in treating patients with trigeminal neuralgia unresponsive to conventional treatment.

Citation: Fasilis T, Gatzonis S, Patrikelis P, Korfias S, Alexoudi A. Transcranial direct current stimulation efficacy in trigeminal neuralgia. *World J Clin Cases* 2024; 12(5): 1036-1038
URL: https://www.wjgnet.com/2307-8960/full/v12/i5/1036.htm
DOI: https://dx.doi.org/10.12998/wjcc.v12.i5.1036

TO THE EDITOR

We read with interest a case report by Tao *et al*[1], who presented one patient with herpetic neuralgia after herpes zoster ophthalmicus who was treated with patient-controlled intravenous analgesia (PCIA) with esketamine. The procedure resulted in a significant pain relief without adverse reactions.

We support authors' statement that primary trigeminal neuralgia can achieve satisfactory curative effects through medical treatment and interventions like radiofrequency. However, people who suffer from side effects to oral medication or more complicated cases (such as neuralgia caused by varicella-zoster virus infection of the trigeminal nerve) are not satisfactorily managed and require more aggressive surgical treatments. Deep brain stimulation and motor cortex stimulation are off label, "last treatment option" techniques which may offer relief to trigeminal neuralgia that is otherwise refractory to pharmacological management and surgery[2,3]. Nevertheless, (PCIA) with esketamine could be an alternative, non-invasive, safe, and effective method.

We would like to suggest transcranial direct current stimulation (tDCS) as an additional potential effective method which could offer relief in intractable trigeminal neuralgia. A 51-year-old woman with idiopathic trigeminal neuralgia, was hospitalized towards modifying the therapeutic strategy and ameliorating the adverse events of medical treatment. She presented daily paroxysmal attacks with a mean duration of 1,5-2 h, reoccurring patterns of few minutes (up to 3-4 min) that created intense, needle-like pain on the dental, submental, and periocular areas of the right side of the face. Refractory period was not established, and she also reported night awakening with instant feeling of intense pain. She scored 9 in the visual analogue scale (VAS)[4]. Her medical history was unremarkable. Physical examination, imaging and laboratory investigations were normal. Peros medication (including carbamazepine) proved to be ineffective and was not tolerated.

Relying on current literature, we decided to apply tDCS[5,6]. The placement of the electrodes followed the Electroencephalography System 10-20 with the anode (+) occurring at the motor cortex and the cathode (-) at contralateral motor area-cortex and at the contralateral mastoid bone. The Sooma™ tDCS device was used, with the intensity settings for the active tDCS being at 2mA, lasting 30 min per session, with 30 s ramp up and down, for a total of 10 d (2 wk). The electrical conduction took place through 2 electrodes 5 cm × 5 cm (contact surface 25 cm^2). No severe adverse events were reported. Anodal tDCS for 10 d ameliorated the intensity of pain (the VAS score reduced from 9 to 2). During the post-stimulation period, the sleep and the quality of life were improved, as they were reflected in Short-Form (36) Health Survey (SF-36), Athens Insomnia Scale (AIS) (the SF-36 and the AIS scores changed from 32 to 60 and from 17 to 5, respectively)[7,8]. The patient displayed sustained efficacy with this management for 3 months.

A number of studies have demonstrated that anodal tDCS modulates the cortical excitability of the motor cortex. However, the effects of tDCS on cortical excitability can spread to distant cortical areas. The main mechanism of action of tDCS is the modulation of the membrane potential of neurons in the stimulated cortical area, mediated by N-methyl-D-aspartate receptors (NMDA-R). Nonetheless, it has been shown that the modulation of nicotinic receptors, BDNF polymorphisms and sex hormonal variations also affect brain plasticity[5].

The results described may provide additional evidence for the effectiveness of tDCS as a therapeutic instrument in treating patients with trigeminal neuralgia unresponsive to conventional treatment. The three-month efficacy reported is positive, however, studies with longer-term follow-up data to assess the sustainability of the tDCS intervention should be scheduled.

FOOTNOTES

Author contributions: Alexoudi A and Gatzonis S designed research; Fasilis T performed research; Alexoudi A and Fasilis T analyzed data; Alexoudi A wrote the letter; Korfias S and Patrikelis P, revised the letter.

Conflict-of-interest statement: All the authors declare no conflict of interest.

Country/Territory of origin: Greece

ORCID number: Athanasia Alexoudi 0000-0002-8137-8253.

S-Editor: Liu JH

L-Editor: A
P-Editor: Zheng XM

REFERENCES

1 **Tao JC**, Huang B, Luo G, Zhang ZQ, Xin BY, Yao M. Trigeminal extracranial thermocoagulation along with patient-controlled analgesia with esketamine for refractory postherpetic neuralgia after herpes zoster ophthalmicus: A case report. *World J Clin Cases* 2022; **10**: 4220-4225 [PMID: 35665100 DOI: 10.12998/wjcc.v10.i13.4220]

2 **Jones MR**, Urits I, Ehrhardt KP, Cefalu JN, Kendrick JB, Park DJ, Cornett EM, Kaye AD, Viswanath O. A Comprehensive Review of Trigeminal Neuralgia. *Curr Pain Headache Rep* 2019; **23**: 74 [PMID: 31388843 DOI: 10.1007/s11916-019-0810-0]

3 **Singleton WGB**, Ashida R, Patel NK. Deep Brain Stimulation for Facial Pain. *Prog Neurol Surg* 2020; **35**: 141-161 [PMID: 32906139 DOI: 10.1159/000509734]

4 **Delgado DA**, Lambert BS, Boutris N, McCulloch PC, Robbins AB, Moreno MR, Harris JD. Validation of Digital Visual Analog Scale Pain Scoring With a Traditional Paper-based Visual Analog Scale in Adults. *J Am Acad Orthop Surg Glob Res Rev* 2018; **2**: e088 [PMID: 30211382 DOI: 10.5435/JAAOSGlobal-D-17-00088]

5 **Hagenacker T**, Bude V, Naegel S, Holle D, Katsarava Z, Diener HC, Obermann M. Patient-conducted anodal transcranial direct current stimulation of the motor cortex alleviates pain in trigeminal neuralgia. *J Headache Pain* 2014; **15**: 78 [PMID: 25424567 DOI: 10.1186/1129-2377-15-78]

6 **Callai EMM**, Scarabelot VL, Fernandes Medeiros L, de Oliveira C, de Souza A, Macedo IC, Cioato SG, Finamor F, Caumo W, Quevedo ADS, Torres ILS. Transcranial direct current stimulation (tDCS) and trigeminal pain: A preclinical study. *Oral Dis* 2019; **25**: 888-897 [PMID: 30636099 DOI: 10.1111/odi.13038]

7 **Hays RD**, Sherbourne CD, Mazel RM. The RAND 36-Item Health Survey 1.0. *Health Econ* 1993; **2**: 217-227 [PMID: 8275167 DOI: 10.1002/hec.4730020305]

8 **Soldatos CR**, Dikeos DG, Paparrigopoulos TJ. Athens Insomnia Scale: validation of an instrument based on ICD-10 criteria. *J Psychosom Res* 2000; **48**: 555-560 [PMID: 11033374 DOI: 10.1016/s0022-3999(00)00095-7]

Published by **Baishideng Publishing Group Inc**
7041 Koll Center Parkway, Suite 160, Pleasanton, CA 94566, USA
Telephone: +1-925-3991568
E-mail: office@baishideng.com
Help Desk: https://www.f6publishing.com/helpdesk
https://www.wjgnet.com